EPILEPSY AND NEURODEVELOPMENTAL DISEASES

EDITED BY: Eleonora Palma, Eleonora Aronica and Erwin van Vliet
PUBLISHED IN: Frontiers in Cellular Neuroscience

frontiers Research Topics

frontiers

ISSN 1664-8714
ISBN 978-2-88966-165-7
DOI 10.3389/978-2-88966-165-7

About Frontiers

Frontiers is more than just an open-access publisher of scholarly articles: it is a pioneering approach to the world of academia, radically improving the way scholarly research is managed. The grand vision of Frontiers is a world where all people have an equal opportunity to seek, share and generate knowledge. Frontiers provides immediate and permanent online open access to all its publications, but this alone is not enough to realize our grand goals.

Frontiers Journal Series

The Frontiers Journal Series is a multi-tier and interdisciplinary set of open-access, online journals, promising a paradigm shift from the current review, selection and dissemination processes in academic publishing. All Frontiers journals are driven by researchers for researchers; therefore, they constitute a service to the scholarly community. At the same time, the Frontiers Journal Series operates on a revolutionary invention, the tiered publishing system, initially addressing specific communities of scholars, and gradually climbing up to broader public understanding, thus serving the interests of the lay society, too.

Dedication to Quality

Each Frontiers article is a landmark of the highest quality, thanks to genuinely collaborative interactions between authors and review editors, who include some of the world's best academicians. Research must be certified by peers before entering a stream of knowledge that may eventually reach the public - and shape society; therefore, Frontiers only applies the most rigorous and unbiased reviews.
Frontiers revolutionizes research publishing by freely delivering the most outstanding research, evaluated with no bias from both the academic and social point of view. By applying the most advanced information technologies, Frontiers is catapulting scholarly publishing into a new generation.

What are Frontiers Research Topics?

Frontiers Research Topics are very popular trademarks of the Frontiers Journals Series: they are collections of at least ten articles, all centered on a particular subject. With their unique mix of varied contributions from Original Research to Review Articles, Frontiers Research Topics unify the most influential researchers, the latest key findings and historical advances in a hot research area! Find out more on how to host your own Frontiers Research Topic or contribute to one as an author by contacting the Frontiers Editorial Office: researchtopics@frontiersin.org

EPILEPSY AND NEURODEVELOPMENTAL DISEASES

Topic Editors:
Eleonora Palma, Sapienza University of Rome, Italy
Eleonora Aronica, Amsterdam University Medical Center, Netherlands
Erwin van Vliet, University of Amsterdam, Netherlands

This topic has been realized in collaboration with Dr. Gabriele Ruffolo, Post Doctoral Researcher at the University of Rome (Sapienza) (ORCID ID: 0000-0002-6554-5496).

Citation: Palma, E., Aronica, E., van Vliet, E., eds. (2020). Epilepsy and Neurodevelopmental Diseases. Lausanne: Frontiers Media SA.
doi: 10.3389/978-2-88966-165-7

Table of Contents

frontiers in Cellular Neuroscience

EDITORIAL
published: 25 September 2020
doi: 10.3389/fncel.2020.00255

Editorial: Epilepsy and Neurodevelopmental Diseases

Gabriele Ruffolo[1,2], *Erwin A. Van Vliet*[3,4], *Eleonora Aronica*[4,5] *and Eleonora Palma*[1]*

[1] *Department of Physiology and Pharmacology, Istituto Pasteur-Fondazione Cenci Bolognetti, University of Rome Sapienza, Rome, Italy,* [2] *Istituto di Ricovero e Cura a Carattere Scientifico San Raffaele, Cassino, Italy,* [3] *Center for Neuroscience, Swammerdam Institute for Life Sciences, University of Amsterdam, Amsterdam, Netherlands,* [4] *Department of (Neuro)Pathology, Amsterdam UMC, University of Amsterdam, Amsterdam, Netherlands,* [5] *Stichting Epilepsie Instellingen Nederland, Heemstede, Netherlands*

Keywords: GABA, ion channels, brain immaturity, synaptic transmission, neurodevelopment, epilepsy

Editorial on the Research Topic

Epilepsy and Neurodevelopmental Diseases

The association between epilepsy and neurodevelopmental diseases is well-recognized and has gained significant attention in the field of neuroscience in recent years. One of the main reasons for this interest is the need for a better understanding of the events that lead to the development and maturation of the CNS. This is a fundamental and necessary basis for potential breakthrough strategies that could guide novel and more effective disease-modifying therapeutic approaches to neurodevelopmental syndromes that are frequently characterized by severe and drug-resistant epilepsy.

The perspective of such new therapeutic strategies is very promising. At the *state-of-the-art*, patients afflicted by these rare neurodevelopmental disorders mostly rely on "symptomatic" approaches that mitigate seizures and other major symptoms but do not target the underlying biological causes of the disease.

The study of this vast field of research is extremely complex and requires a multidisciplinary approach, from neuropathological to molecular and functional studies since even "simple" triggering events (e.g., a genetic mutation) during critical periods of brain development can lead to widespread effects on brain morphological and functional features.

This issue represents the concept of an integrated, interdisciplinary translational approach to epileptic syndromes of neurodevelopment. For instance, Rosch et al. thoroughly describe invertebrate animal models such as zebrafish and *drosophila* which can be used as tools to investigate the early stages of neurodevelopment. Even though these "simple" models are far from the complexity of the human brain, they offer superior manageability to mammalian models, allowing researchers to perform single-cell resolution studies on whole-brain imaging, thus tracking the effects of a pathogenic event from the "larval" stages to the mature brain.

Since the mechanisms by which an insult determines pathological events during neurodevelopment are not always univocal, they can be explored from different angles, using different methods and multidisciplinary perspectives in research design. For example, considering their pivotal role in neurotransmission, it is not surprising that many researchers have made efforts to characterize ion channels. Here, two original research articles by Levinson et al. and by Mao et al. followed this path.

The first by Levinson et al. supports the role of metabotropic $GABA_B$ receptors ($GABA_BRs$) in pediatric focal cortical dysplasia (FCD) and tuberous sclerosis complex (TSC) through an electrophysiological study of patients' brain slices. This research strengthened the hypothesis that there is significant participation of $GABA_BRs$ in synaptic inhibition in the aforementioned pathologies, highlighting the importance of studying possible therapeutic targets in a "comparative"

OPEN ACCESS

Edited and reviewed by:
Dirk M. Hermann, University of Duisburg-Essen, Germany

***Correspondence:**
Eleonora Palma
eleonora.palma@uniroma1.it

Specialty section:
This article was submitted to Cellular Neuropathology, a section of the journal Frontiers in Cellular Neuroscience

Received: *10 July 2020*
Accepted: *24 July 2020*
Published: *25 September 2020*

Citation:
Ruffolo G, Van Vliet EA, Aronica E and Palma E (2020) Editorial: Epilepsy and Neurodevelopmental Diseases. Front. Cell. Neurosci. 14:255. doi: 10.3389/fncel.2020.00255

fashion, since the permissive role of $GABA_BRs$ was observed in FCD and TSC, but not in non-dysplastic tissues.

The second study by Mao et al. reported two novel mutations in the *KCTN2* gene, encoding for $K_{Na}1.2$ subunit of the sodium-dependent voltage gated potassium channel K_{Na}. This protein frequently mutates in Epilepsy of Infancy with Migrating Focal Seizures (EIMFS) and this study deepened the knowledge of disease genetics and physiology, thus facilitating future studies of the mutated channel in cellular models.

The review by van Loo and Becker describes acquired and genetic channelopathies from an original point of view. This review makes clear that the direct malfunction of a channel protein is not the only problem, as many events precede the incorporation of the channel in the cellular membrane, such as regulation of mRNA transcription, micro-RNA interference, and epigenetic mechanisms such as DNA methylation.

In addition, another review by Fattorini et al. tackles the other relevant mechanisms that can modulate neurotransmission: neurotransmitter reuptake. The authors have reviewed recent findings on the localization of GAT-1 to underline the widespread distribution of the transporter in the CNS as an alternative to traditional ideas about its neuron-specific expression. This is an important contribution to a field that is continuously evolving.

The research article by Duy et al. proposed an interesting approach, aiming to restore an optimal function of KCC2 to enhance neuronal chloride extrusion, making neurons less prone to generate epileptic discharges. Such research also raises the question of whether similar strategies may prevent epileptogenesis and cognitive impairment when applied early during development.

The pathologic traits in the cytoarchitecture of the diseased brain are also explored in this issue. Liu et al. performed a proteomics study that described how the expression of Rho GTPases in hippocampal dentate granule cells may support the abnormal migratory activity observed in mesial temporal lobe epilepsy, determining granule cell dispersion. These dysmaturative processes reproduce events, characterizing early developmental stages, with detrimental consequences. These findings clearly show that the dysmaturation is not confined to the early stages of development but it is also a feature of adult mesial temporal lobe epilepsy. Liu et al. explored the impact of an early developmental dysregulation of the mechanistic target of rapamycin (mTOR) pathway, as a result of mutations of *STRADA* (pseudokinase STE20-related kinase adaptor alpha, an mTOR regulator), leading to a continuous overactivation of mTOR signaling. In particular, they studied the malfunction of *STRADA* with complementary techniques such as CRISPR-edited *Strada* mouse N2a cells and induced pluripotent stem cells (iPSCs). This study highlighted the novel contribution of this protein to pathologic hallmarks of mTORopathies such as increased cell size, neuronal hyperexcitability, and impaired cortical lamination.

The list of promising targets that require further investigation is much longer, as indicated in papers by Allocco et al. and Fassio et al.. The first research article defined a role for the impairment of Na^+/K^+ ATPase function in the pathogenesis of congenital hydrocephalus trough whole-exome sequencing, bioinformatics, and computational modeling. Indeed, these authors, by characterizing novel mutations of α3 subunit of Na^+/K^+ ATPase, have described, for the first time, a link between this protein and congenital hydrocephalus.

In their review, Fassio et al. highlighted the role of autophagy in neurodevelopment and epilepsy as a key process involved in neurogenesis, neuronal polarity, and synaptic function. Notably, these authors shed new light on this physiological mechanism, suggesting that defective autophagy may represent an additional therapeutic target for epileptic neurodevelopmental diseases.

In conclusion, this Research Topic combines different fields of neuroscience that analyze the correlation between epilepsy and neurodevelopment from different points of view. Therefore, as well as making significant contributions to research, this topic highlights the need for an integrated approach—from anatomy and pathology to molecular biology and electrophysiology—to speed-up the progress in this research field.

AUTHOR CONTRIBUTIONS

All authors listed have made a substantial, direct and intellectual contribution to the work, and approved it for publication.

Conflict of Interest: The authors declare the absence of any commercial or financial relationship that could be construed as a potential conflict of interest

frontiers in Cellular Neuroscience

BRIEF RESEARCH REPORT
published: 26 September 2019
doi: 10.3389/fncel.2019.00425

Recessive Inheritance of Congenital Hydrocephalus With Other Structural Brain Abnormalities Caused by Compound Heterozygous Mutations in *ATP1A3*

*August A. Allocco[1†], Sheng Chih Jin[2,3†], Phan Q. Duy[1†], Charuta G. Furey[1], Xue Zeng[2,3], Weilai Dong[2], Carol Nelson-Williams[2], Jason K. Karimy[1], Tyrone DeSpenza[1], Le T. Hao[1], Benjamin Reeves[1], Shozeb Haider[4], Murat Gunel[1,2], Richard P. Lifton[2,3] and Kristopher T. Kahle[1,5,6,7]**

[1] Department of Neurosurgery, School of Medicine, Yale University, New Haven, CT, United States, [2] Department of Genetics, School of Medicine, Yale University, New Haven, CT, United States, [3] Laboratory of Human Genetics and Genomics, The Rockefeller University, New York, NY, United States, [4] Department of Computational Chemistry, University College London School of Pharmacy, London, United Kingdom, [5] Department of Cellular and Molecular Physiology, School of Medicine, Yale University, New Haven, CT, United States, [6] NIH-Yale Centers for Mendelian Genomics, School of Medicine, Yale University, New Haven, CT, United States, [7] Yale Stem Cell Center, School of Medicine, Yale University, New Haven, CT, United States

OPEN ACCESS

Edited by:
Eleonora Palma,
Sapienza University of Rome, Italy

Reviewed by:
Antonio Gambardella,
University of Catanzaro, Italy
Ozgun Gokce,
Ludwig Maximilian University of Munich, Germany

***Correspondence:**
Kristopher T. Kahle
kristopher.kahle@yale.edu

[†] These authors have contributed equally to this work

Specialty section:
This article was submitted to Cellular Neuropathology, a section of the journal Frontiers in Cellular Neuroscience

Received: 24 June 2019
Accepted: 04 September 2019
Published: 26 September 2019

Citation:
Allocco AA, Jin SC, Duy PQ, Furey CG, Zeng X, Dong W, Nelson-Williams C, Karimy JK, DeSpenza T, Hao LT, Reeves B, Haider S, Gunel M, Lifton RP and Kahle KT (2019) Recessive Inheritance of Congenital Hydrocephalus With Other Structural Brain Abnormalities Caused by Compound Heterozygous Mutations in ATP1A3. Front. Cell. Neurosci. 13:425. doi: 10.3389/fncel.2019.00425

Background: *ATP1A3* encodes the α3 subunit of the Na^+/K^+ ATPase, a fundamental ion-transporting enzyme. Primarily expressed in neurons, *ATP1A3* is mutated in several autosomal dominant neurological diseases. To our knowledge, damaging recessive genotypes in *ATP1A3* have never been associated with any human disease. *Atp1a3* deficiency in zebrafish results in hydrocephalus; however, no known association exists between *ATP1A3* and human congenital hydrocephalus (CH).

Methods: We utilized whole-exome sequencing (WES), bioinformatics, and computational modeling to identify and characterize novel *ATP1A3* mutations in a patient with CH. We performed immunohistochemical studies using mouse embryonic brain tissues to characterize *Atp1a3* expression during brain development.

Results: We identified two germline mutations in *ATP1A3* (p. Arg19Cys and p.Arg463Cys), each of which was inherited from one of the patient's unaffected parents, in a single patient with severe obstructive CH due to aqueductal stenosis, along with open schizencephaly, type 1 Chiari malformation, and dysgenesis of the corpus callosum. Both mutations are predicted to be highly deleterious and impair protein stability. Immunohistochemical studies demonstrate robust *Atp1a3* expression in neural stem cells (NSCs), differentiated neurons, and choroid plexus of the mouse embryonic brain.

Conclusion: These data provide the first evidence of a recessive human phenotype associated with mutations in *ATP1A3*, and implicate impaired Na^+/K^+ ATPase function in the pathogenesis of CH.

Keywords: congenital hydrocephalus, *ATP1A3*, Na^+/K^+ ATPase, whole exome sequencing, genetics

INTRODUCTION

Congenital hydrocephalus (CH) is the most common reason for brain surgery in children and affects 1 in 1,000 newborns (Tully and Dobyns, 2014; Kahle et al., 2016). CH is characterized by ventriculomegaly, defined as dilation of cerebral ventricles, and thought to be secondary to impaired cerebrospinal fluid (CSF) homeostasis. Consequently, CH is treated by lifelong neurosurgical shunting with high complication rates and morbidity. The lack of satisfactory treatments highlights our incomplete understanding of CH pathogenesis (Kahle et al., 2016). There is a need to identify CH disease-causing genes, given that 40% of CH cases is estimated to have a genetic etiology (Haverkamp et al., 1999). Despite significant efforts to identify CH genes, including a recent whole-exome sequencing (WES) (Furey et al., 2018) study, the majority of CH cases remain idiopathic, underscoring the need for continued gene discovery.

ATP1A3 encodes the α3 subunit of the Na^+/K^+ ATPase, a fundamental enzyme that regulates ion homeostasis by maintaining ionic gradients across the plasma membrane (Clausen et al., 2017). *ATP1A3* is highly expressed in neurons of the adult rodent brain (McGrail et al., 1991; Pietrini et al., 1992; Bottger et al., 2011) and mutations in the gene have been implicated in three autosomal dominant Mendelian diseases, including alternating hemiplegia of childhood (AHC) type 2 (Rosewich et al., 2012), CAPOS syndrome (Demos et al., 2014), and Dystonia-12 (Anselm et al., 2009). Knockdown of *Atp1a3* in zebrafish (Doganli et al., 2013) results in hydrocephalus; however, no known association exists between *ATP1A3* and human CH.

Here, we present the first case of obstructive CH with aqueductal stenosis and other structural brain abnormalities associated with recessive compound heterozygous mutations in *ATP1A3*.

MATERIALS AND METHODS

Patient/Family Information

The patient is a 23-year-old Caucasian female of European descent. CH was diagnosed on prenatal ultrasound at 18 weeks gestation (**Figure 1A**). MR imaging captured immediately after delivery demonstrated marked asymmetric obstructive hydrocephalus secondary to aqueductal stenosis. The patient underwent ventriculoperitoneal shunt placement at birth with three subsequent surgical shunt revisions and was further diagnosed via MRI and computed tomography (**Figure 1B**) with craniosynostosis, open lip schizencephaly, type 1 Chiari malformation, dysgenesis of the corpus collosum, and learning disability. Routine genetic testing (FISH, microarray) was negative. The patient's mother reports two previous miscarriages. The mother reports a medical history of hyperthyroidism while the father reports a history of hypertension and anxiety. There are no known medical problems that run in the family on either the maternal or paternal side. The patient has one phenotypically normal sister. Institutional review board approval was obtained from the Yale University Human Investigative Committee, and all participants provided written informed consent.

Exome Sequencing and Analysis

To identify potential disease-causing variants in this patient, we performed WES on the affected individual and her parents. Targeted capture was performed using the xGEN Exome Research Panel v1.0 (IDT) followed by DNA sequencing on the Illumina HiSeq 4000 System. Sequence metrics are shown in **Supplementary Table S1**. Sequence reads were mapped to the reference genome (GRCh37) with BWA-MEM and further processed using the GATK Best Practices workflows (McKenna et al., 2010; Van der Auwera et al., 2013; 1000 Genomes Project Consortium, 2015) as previously described (Jin et al., 2017). Single nucleotide variants and small indels were called with GATK HaplotypeCaller and annotated using ANNOVAR (Wang et al., 2010), ExAC (v3), and gnomAD (v2.1.1) (Lek et al., 2016). The MetaSVM algorithm was used to predict deleteriousness of missense variants (Dong et al., 2015).

We filtered recessive variants for rare [minor allele frequency (MAF) $\leq 10^{-3}$ across ExAC and gnomAD] homozygous and compound heterozygous variants that exhibited high quality sequence reads. Only loss-of-function (LoF; including nonsense, frameshift, or canonical splice disruptions), D-Mis (MetaSVM-deleterious), and non-frameshift indels were considered potentially damaging to the disease. For dominant variants, we assessed for rare (MAF $\leq 2 \times 10^{-5}$) and damaging variants (LoF or D-Mis). Finally, false positive variants were excluded by *in silico* visualization followed by Sanger sequencing validation.

In silico Modeling

The sequence of the human α3 subunit of the Na^+/K^+ ATPase (*ATP1A3*) was taken from the Uniprot (P13637). The crystal structures of the Pig Sodium/potassium-transporting ATPase subunit α(PDB id 4RET and 3WGV) exhibit 86% sequence identity with human ATP1A3 (residues 1-1013). The structure of 4RET and 3WGV were used as templates to construct a homology model of the human ATP1A3 using MODELLER (Fiser and Sali, 2003). Conserved Arginine residues are present at the equivalent positions of R19 and R463 in both human and pigs. The spatial orientations of the side chains in the templates from pig were used to model the side chains of R19 and R463. A total of twenty models were built and subjected to restrained energy minimization to relieve any steric clashes between the side chains and the nucleic acid. The stereo-chemical parameters were analyzed using PROCHECK and PROSA (Wiederstein and Sippl, 2007) and the final model was chosen based on the on the basis of the lowest Cα RMSD value after superimposition on the template structure (0.9 Å). This lies within the permitted range for accurate homology model construction for sequence identity in the high range (>80%) (Fiser, 2010).The mutants, R19C and R463C, were constructed and the free energy of change calculated ($\Delta\Delta G$) *in silico* using the ICM mutagenesis program (Laskowski et al., 1993)[1].

Immunohistochemistry

WT mouse embryos of C57/BL6 background were harvested at embryonic day 15.5. Brains were dissected and fixed in 4%

[1]www.molsoft.com

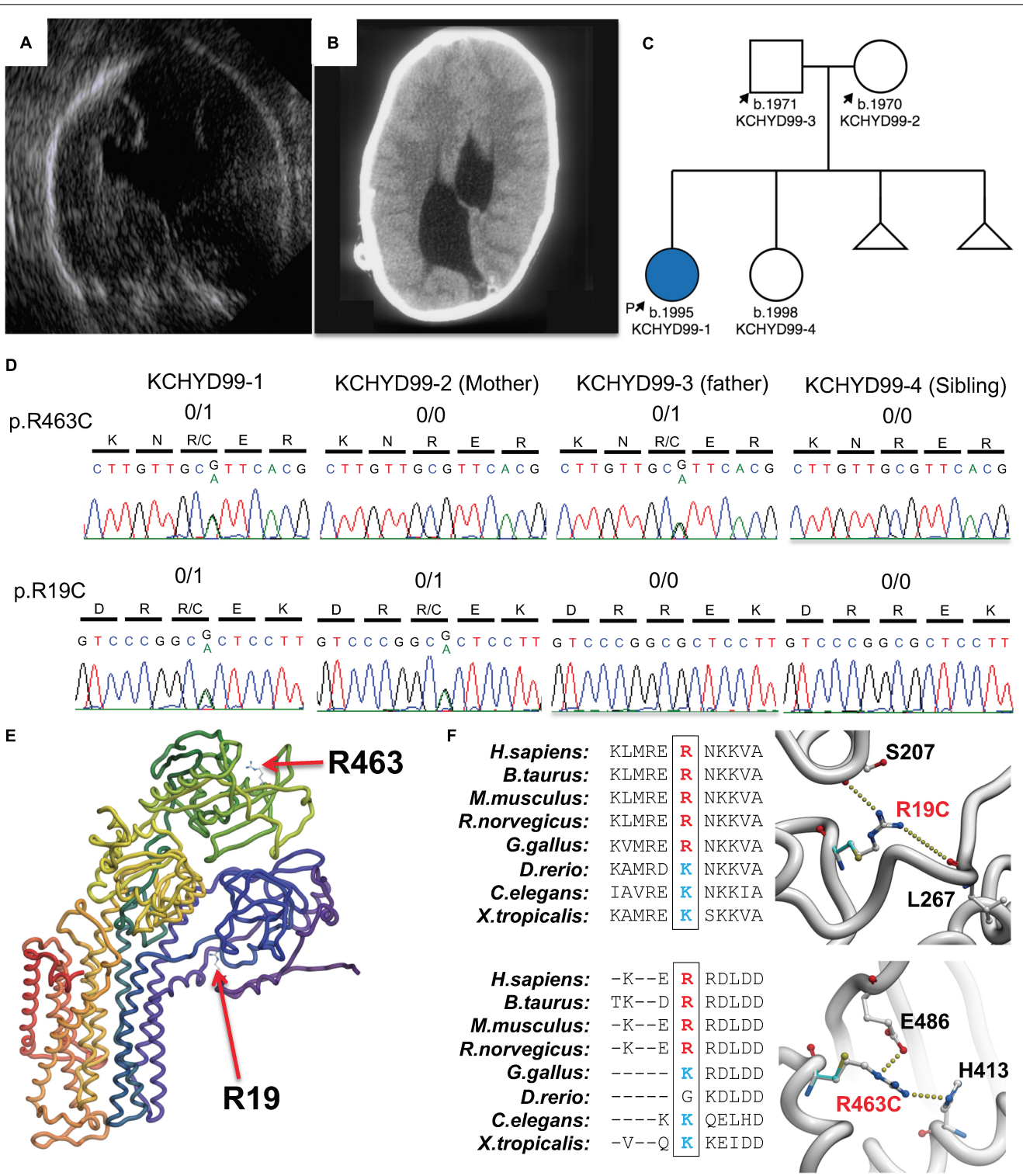

FIGURE 1 | Damaging, protein-altering compound heterozygous *ATP1A3* mutations in human congenital hydrocephalus and other structural brain defects. Pre-natal ultrasound **(A)** and postnatal computed tomography **(B)** images demonstrating asymmetric ventriculomegaly, agenesis of the corpus callosum, schizencephaly, and aqueductal stenosis. **(C)** Patient pedigree with affected individual denoted in blue. **(D)** DNA chromatograms depicting the maternally inherited c.G55A (p.R19C) and paternally inherited c.G1387A (p.R463C) compound heterozygous mutations in *ATP1A3*, encoding the α3 catalytic subunit of the Na^+/K^+ ATPase. **(E)** Mutation locations in canonically folded wild-type α3 subunits. **(F)** Evolutionary conservation across multiple species showing conserved positively charged amino acid side chain and hydrogen bonding by the positively charged side chains of Arg19 and Arg463 lost due to mutation of these residues.

PFA in PBS overnight at 4°C then cryoprotected in 30% sucrose in PBS for 48 h. Brains were then mounted in frozen OCT blocks and sectioned by cryostat at 25 μm in the coronal plane. Sections were mounted on microscope slides and stored in −80°C until use. To begin staining, slides containing brain sections were first thawed at room temperature, then washed in 0.5% PBST. Sections underwent antigen retrieval using citrate buffer, then washed in 0.5% PBST. Sections were blocked in 10% normal goat serum (NGS) in PBST at room temperature for 1 h, then incubated with primary antibodies diluted in 2.5% NGS in PBST at 4°C overnight. The primary antibodies were rabbit polyclonal anti-Atp1a3 (1:500 dilution) (Pietrini et al., 1992), mouse monoclonal anti-NeuN (1:250, MAB377, Millipore), and mouse monoclonal anti-Sox2 directly conjugated with Dylight 550 (1:250, MA1-014-D550, Invitrogen). Following primary antibody incubation, sections were washed and incubated with Alexa Fluor-conjugated secondary antibodies (1:500 in 2.5% NGS in PBST) for 1 h at room temperature. Following the final wash, slides were coverslipped with Prolong Gold Antifade mounting medium. For negative control, the primary antibody solution (containing anti-Atp1a3) was blocked with the immunizing peptide sequence (gdkkddsspkksc) (Pietrini et al., 1992). Images were acquired using the Zeiss LSM 880 confocal microscope or the Aperio digital scanner microscope. All experiments were done in accordance with the regulations set forth by the Yale University animal care and use committee.

RESULTS

Compound heterozygous mutations in *ATP1A3* were identified in the affected individual. A maternally inherited single nucleotide G to A variation was identified at cDNA NM_152296 position 55 in exon 2 (gnomAD MAF = 6.4×10^{-5}), corresponding to the amino acid substitution p. Arg19Cys in the α3 subunit. A paternally inherited single nucleotide G to A variation was identified at cDNA position 1387 in exon 11 (gnomAD MAF = 4.5×10^{-4}), corresponding to the amino acid substitution p.Arg463Cys in the α3 subunit (**Figures 1C,D**). *ATP1A3* is very intolerant to both loss-of-function mutations (pLI = 1) and missense variants (mis_z = 6.33) per gnomAD. No homozygous loss-of-function mutations or homozygous damaging missense mutations in *ATP1A3* have been reported in gnomAD. Both variants are predicted deleterious per MetaSVM. CADD scores for the p.Arg19Cys and p.Arg463Cys variants were 34 and 24.8, respectively. Conservation of positively charged amino acid residues (arginine and lysine) was observed across species (**Figure 1F**).

In silico modeling of p.Arg19Cys and p.Arg463Cys mutations shows disruptive effects on protein stability. The side chain of arg-19 forms interactions with the backbone atoms of Ser-207 and Leu-267. This interaction is lost when Arg-19 is mutated to a cysteine with a corresponding energy penalty ($\Delta\Delta G$ = 2.3 kcal/mole, **Figures 1E,F**). Similarly, the side chain of Arg-463 makes strong hydrogen bond interactions with the side chain of Glu-486 and His-413. These strong interactions are lost when Arg-463 is mutated to a Cys ($\Delta\Delta G$ = 3.2 kcal/mole, **Figures 1E,F**).

The association of *ATP1A3* mutations with CH and multiple other significant structural brain abnormalities implicate ATP1A3 in human brain development. Thus, we performed immunofluorescence studies in the embryonic mouse brain to characterize Atp1a3 expression. We stained histological brain sections collected from embryonic day 15.5 (E15.5) with an antibody against Atp1a3 (Pietrini et al., 1992) together with Sox2 [a marker of neural stem cells (NSCs)] (Ellis et al., 2004) and NeuN (a marker of differentiated neurons) (Mullen et al., 1992). Overall, Atp1a3 exhibits diffused and cytoplasmic expression throughout all cortical layers of the embryonic mouse brain (**Figure 2**). Co-localization studies showed that Atp1a3 is expressed in differentiated neurons at the cortical plate (CP) and in the NSCs at the ventricular zone (VZ) lining the lateral ventricles (**Figures 2E–N**). We also detected Atp1a3 expression in choroid plexus epithelial cells (**Figures 2O,P**). Furthermore, brain sections depicting the VZ and choroid plexus incubated with the Atp1a3 antibody blocked with the immunizing peptide showed minimal immuno-reactivity (**Figures 2Q,R**), demonstrating antibody specificity.

DISCUSSION

Atp1a3 expression is exclusive to neurons and highly expressed in inhibitory interneurons (Richards et al., 2007), where it plays a crucial role in electrophysiological functions including ion gradient maintenance (Arystarkhova et al., 2019), after hyperpolarization (Picton et al., 2017), and suppression of burst firing (Vaillend et al., 2002). Mice harboring loss of function mutations in *ATP1A3* exhibit increased seizure activity and neuronal hyperexcitability (Clapcote et al., 2009; Hunanyan et al., 2015) suggesting that *ATP1A3* is crucial to maintaining normal neurological function. Human mutations in *ATP1A3* have previously been discovered in a wide range of autosomal dominant neurological disorders (Heinzen et al., 2014), including encephalopathy with cerebellar ataxia (Sabouraud et al., 2019), AHC (Galaz-Montoya et al., 2019), rapid-onset dystonia Parkinsonism (ADP) (Anselm et al., 2009), cerebellar ataxia (Sabouraud et al., 2019), early-onset epilepsy (Ishihara et al., 2019), and autism spectrum disorder (Torres et al., 2018). Importantly, the majority of the mutations identified in AHC and RDP cluster in exons 8, 14, 17, and 18 (Rosewich et al., 2014), which are distinct from our variants (exon 2 and 11). To our knowledge, damaging recessive genotypes in *ATP1A3* have never been associated with any human disease.

We identified two germline mutations in *ATP1A3* (p. Arg19Cys and p.Arg463Cys), each of which was inherited from one of the patient's unaffected parents, in a single patient with severe obstructive CH due to aqueductal stenosis, along with open schizencephaly, type 1 Chiari malformation, and dysgenesis of the corpus callosum. Both mutations are predicted to be highly deleterious and impair protein stability. Consistent with our results, morpholino knockdown of *Atp1a3* causes ventriculomegaly in zebrafish (Doganli et al., 2013),

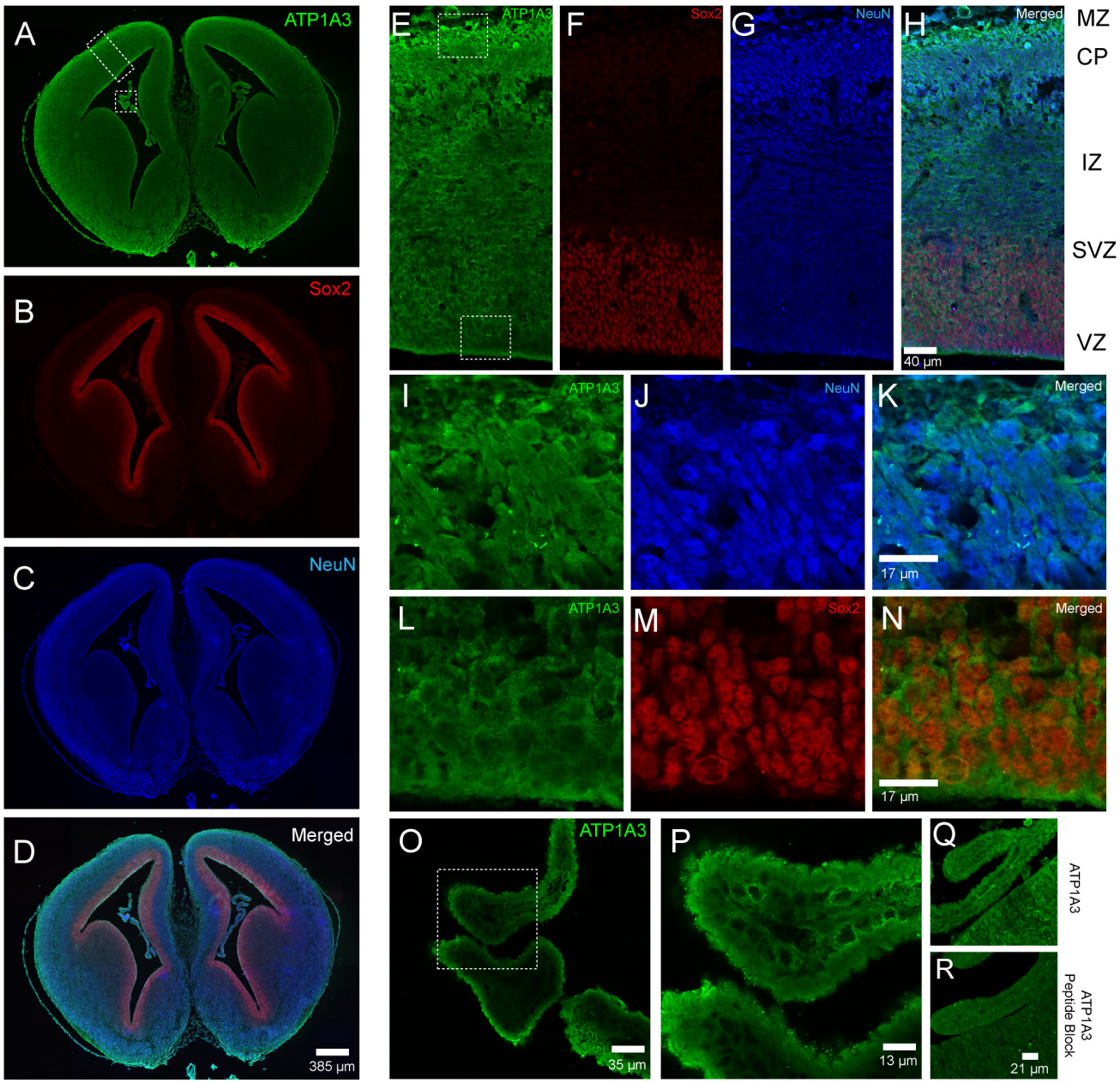

FIGURE 2 | Expression of Atp1a3 in the embryonic mouse brain at E15.5. Fluorescent images taken at low magnification showing expression of **(A)** Atp1a3, **(B)** Sox2, **(C)** NeuN, and **(D)** all channels merged in the embryonic mouse brain. Dotted boxes in panel A identify the cortex and the choroid plexus. High magnification cortical expression of **(E)** Atp1a3, **(F)** Sox2, **(G)** NeuN, and **(H)** all channels merged. MZ – marginal zone, CP – cortical plate, IZ – intermediate zone, SVZ – subventricular zone, VZ – ventricular zone. Dotted boxes in panel **(E)** shows the cortical plate and ventricular zone. **(I–K)** High magnification expression of Atp1a3 in NeuN$^+$ cells in the CP. **(L–N)** Expression of Atp1a3 in Sox2$^+$ cells in the ventricular zone. **(O,P)** High-magnification expression of Atp1a3 in the choroid plexus. **(Q)** Brain sections incubated with Atp1a3 primary antibody alone or **(R)** Atp1a3 primary antibody blocked with immunizing peptide.

recapitulating the hydrocephalus phenotype in our patient. Together, these data provide evidence for a recessive inheritance of CH with aqueductal stenosis caused by *ATP1A3* compound heterozygous mutations.

Extending from previous work demonstrating expression of Atp1a3 in mature neurons (McGrail et al., 1991; Pietrini et al., 1992; Bottger et al., 2011), we found Atp1a3 to also be expressed in NSCs, differentiated neurons, and choroid plexus epithelial cells of the mouse embryonic brain. Our findings suggest two separate but not necessarily mutually exclusive mechanisms whereby *ATP1A3* compound heterozygous mutations may cause ventriculomegaly. First, hydrocephalus is

classically thought to be a disorder of failed CSF homeostasis secondary to obstructed flow, increased secretion, or decreased absorption by the arachnoid villi (Kahle et al., 2016). The ion pump Na^+/K^+-ATPase is known to regulate CSF secretion in the choroid by maintaining an osmotic gradient of Na^+ that drives the movement of water into the cerebral ventricles (Masuzawa et al., 1984; Fisone et al., 1995; Speake et al., 2001). The Na^+/K^+-ATPase is composed of three subunits: α, β, and γ (Holm et al., 2016). The catalytic activity of Na^+/K^+-ATPase has been attributed to the α subunit, which binds ATP, Na^+, and K^+. Thus, α subunit dysfunction due to p. Arg19Cys and p.Arg463Cys mutations described in this study can impair CSF homeostasis and thus drive the development of hydrocephalus.

Second, our finding of Atp1a3 expression in embryonic NSCs suggests a novel role of *ATP1A3* in regulating neural development. Thus, mutations that disrupt ATPA13 function may impair NSC regulation and suggest dysregulation of neural development, rather than failed CSF homeostasis, to be the primary pathogenic driver of human CH. Indeed, multiple lines of evidence from animals (Huang et al., 2007; Lessard et al., 2007; Carter et al., 2012; Roy et al., 2019) and humans (Guerra et al., 2015; Rodriguez and Guerra, 2017; Furey et al., 2018) suggest abnormal NSC development to be a primary driver of CH pathogenesis. This potential impact on the general process of neural development may not only underpin ventriculomegaly but also other developmental anomalies (type 1 Chiari malformation, corpus callosum dysgenesis, and intellectual disability) observed in our patient. In addition, the notable lack of dystonic, epileptic, or motor deficits in this patient suggests that the spectrum of *ATP1A3* linked diseases may be broader than previously acknowledged.

In sum, our findings provide the first association of human CH with recessive mutations in *ATP1A3*, setting the stage for future studies to better understand the role of *ATP1A3* in brain development and the pathogenesis of human CH.

DATA AVAILABILITY STATEMENT

The datasets generated for this study can be found in the dbGAP: phs000744.

ETHICS STATEMENT

The studies involving human participants were reviewed and approved by Yale University Human Investigative Committee. The patients/participants provided their written informed consent to participate in this study.

AUTHOR CONTRIBUTIONS

AA designed the study, collected and analyzed the data, and wrote the manuscript. SJ and PD collected and analyzed the data, and wrote the manuscript. CF, CW, JK, TD, LH, and BR collected the data. XZ and WD collected and analyzed the data. SH analyzed the data. MG designed the study. RL designed the study and analyzed the data. KK designed the study, analyzed the data, and wrote the manuscript.

FUNDING

SJ was supported by the James Hudson Brown-Alexander Brown Coxe Postdoctoral Fellowship, an American Heart Association Postdoctoral Fellowship, and the National Heart, Lung, and Blood Institute of the National Institutes of Health under Award Number K99HL143036. PD was supported by the NIH Medical Scientist Training Program Grant T32GM007205. KK was supported by the NIH 1RO1NS109358-01, the Hydrocephalus Association, and the Rudi Schulte Research Institute.

ACKNOWLEDGMENTS

The authors would like to thank the family who participated in this study.

SUPPLEMENTARY MATERIAL

The Supplementary Material for this article can be found online at: https://www.frontiersin.org/articles/10.3389/fncel.2019.00425/full#supplementary-material

REFERENCES

1000 Genomes Project Consortium (2015). A global reference for human genetic variation. *Nature* 526, 68–74. doi: 10.1038/nature15393

Anselm, I. A., Sweadner, K. J., Gollamudi, S., Ozelius, L. J., and Darras, B. T. (2009). Rapid-onset dystonia-parkinsonism in a child with a novel atp1a3 gene mutation. *Neurology* 73, 400–401. doi: 10.1212/wnl.0b013e3181b04acd

Arystarkhova, E., Haq, I. U., Luebbert, T., Mochel, F., Saunders-Pullman, R., Bressman, S. B., et al. (2019). Factors in the disease severity of ATP1A3 mutations: impairment, misfolding, and allele competition. *Neurobiol. Dis.* 132:104577. doi: 10.1016/j.nbd.2019.104577

Bottger, P., Tracz, Z., Heuck, A., Nissen, P., Romero-Ramos, M., and Lykke-Hartmann, K. (2011). Distribution of Na/K-ATPase alpha 3 isoform, a sodium-potassium P-type pump associated with rapid-onset of dystonia parkinsonism (RDP) in the adult mouse brain. *J. Comp. Neurol.* 519, 376–404. doi: 10.1002/cne.22524

Carter, C. S., Vogel, T. W., Zhang, Q., Seo, S., Swiderski, R. E., Moninger, T. O., et al. (2012). Abnormal development of NG2+PDGFR-α+ neural progenitor cells leads to neonatal hydrocephalus in a ciliopathy mouse model. *Nat. Med.* 18, 1797–1804. doi: 10.1038/nm.2996

Clapcote, S. J., Duffy, S., Xie, G., Kirshenbaum, G., Bechard, A. R., Rodacker Schack, V., et al. (2009). Mutation I810N in the alpha3 isoform of Na+,K+-ATPase causes impairments in the sodium pump and hyperexcitability in the CNS. *Proc. Natl. Acad. Sci. U.S.A.* 106, 14085–14090. doi: 10.1073/pnas.0904817106

Clausen, M. V., Hilbers, F., and Poulsen, H. (2017). The Structure and Function of the Na,K-ATPase Isoforms in Health and Disease. *Front. Physiol.* 8:371. doi: 10.3389/fphys.2017.00371

Demos, M. K., van Karnebeek, C. D., Ross, C. J., Adam, S., Shen, Y., Zhan, S. H., et al. (2014). A novel recurrent mutation in ATP1A3 causes CAPOS syndrome. *Orphanet J. Rare Dis.* 9:15. doi: 10.1186/1750-1172-9-15

Doganli, C., Beck, H. C., Ribera, A. B., Oxvig, C., and Lykke-Hartmann, K. (2013). alpha3Na+/K+-ATPase deficiency causes brain ventricle dilation and abrupt embryonic motility in zebrafish. *J. Biol. Chem.* 288, 8862–8874. doi: 10.1074/jbc.M112.421529

Dong, C., Wei, P., Jian, X., Gibbs, R., Boerwinkle, E., Wang, K., et al. (2015). Comparison and integration of deleteriousness prediction methods for nonsynonymous SNVs in whole exome sequencing studies. *Hum. Mol. Genet.* 24, 2125–2137. doi: 10.1093/hmg/ddu733

Ellis, P., Fagan, B. M., Magness, S. T., Hutton, S., Taranova, O., Hayashi, S., et al. (2004). SOX2, a persistent marker for multipotential neural stem cells derived from embryonic stem cells, the embryo or the adult. *Dev. Neurosci.* 26, 148–165. doi: 10.1159/000082134

Fiser, A. (2010). Template-based protein structure modeling. *Methods Mol. Biol.* 673, 73–94. doi: 10.1007/978-1-60761-842-3_6

Fiser, A., and Sali, A. (2003). Modeller: generation and refinement of homology-based protein structure models. *Methods Enzymol.* 374, 461–491. doi: 10.1016/s0076-6879(03)74020-8

Fisone, G., Snyder, G. L., Fryckstedt, J., Caplan, M. J., Aperia, A., and Greengard, P. (1995). Na+,K(+)-ATPase in the choroid plexus. Regulation by serotonin/protein kinase C pathway. *J. Biol. Chem.* 270, 2427–2430. doi: 10.1074/jbc.270.6.2427

Furey, C. G., Choi, J., Jin, S. C., Zeng, X., Timberlake, A. T., Nelson-Williams, C., et al. (2018). De Novo Mutation in Genes Regulating Neural Stem Cell Fate in Human Congenital Hydrocephalus. *Neuron* 99:302-314.e4. doi: 10.1016/j.neuron.2018.06.019

Galaz-Montoya, C. I., Alcaraz-Estrada, S., Garcia-Montano, L. A., Zenteno, J. C., and Pina-Aguilar, R. E. (2019). A recurrent de novo mutation in ATP1A3 gene in a Mexican patient with alternating hemiplegia of childhood detected by massively parallel sequencing. *Bol. Med. Hosp. Infant. Mex.* 76, 49–53. doi: 10.24875/BMHIM.18000099

Guerra, M. M., Henzi, R., Ortloff, A., Lichtin, N., Vío, K., Jiménez, A. J., et al. (2015). Cell Junction Pathology of Neural Stem Cells Is Associated With Ventricular Zone Disruption, Hydrocephalus, and Abnormal Neurogenesis. *J. Neuropathol. Exp. Neurol.* 74, 653–671. doi: 10.1097/NEN.0000000000000203

Haverkamp, F., Wolfle, J., Aretz, M., Kramer, A., Hohmann, B., Fahnenstich, H., et al. (1999). Congenital hydrocephalus internus and aqueduct stenosis: aetiology and implications for genetic counselling. *Eur. J. Pediatr.* 158, 474–478. doi: 10.1007/s004310051123

Heinzen, E. L., Arzimanoglou, A., Brashear, A., Clapcote, S. J., Gurrieri, F., Goldstein, D. B., et al. (2014). Distinct neurological disorders with ATP1A3 mutations. *Lancet Neurol.* 13, 503–514. doi: 10.1016/S1474-4422(14)70011-0

Holm, R., Toustrup-Jensen, M. S., Einholm, A. P., Schack, V. R., Andersen, J. P., and Vilsen, B. (2016). Neurological disease mutations of alpha3 Na(+),K(+)-ATPase: structural and functional perspectives and rescue of compromised function. *Biochim. Biophys. Acta* 1857, 1807–1828. doi: 10.1016/j.bbabio.2016.08.009

Huang, X., Litingtung, Y., and Chiang, C. (2007). Ectopic sonic hedgehog signaling impairs telencephalic dorsal midline development: implication for human holoprosencephaly. *Hum. Mol. Genet.* 16, 1454–1468. doi: 10.1093/hmg/ddm096

Hunanyan, A. S., Fainberg, N. A., Linabarger, M., Arehart, E., Leonard, A. S., Adil, S. M., et al. (2015). Knock-in mouse model of alternating hemiplegia of childhood: behavioral and electrophysiologic characterization. *Epilepsia* 56, 82–93. doi: 10.1111/epi.12878

Ishihara, N., Inagaki, H., Miyake, M., Kawamura, Y., Yoshikawa, T., and Kurahashi, H. (2019). A case of early onset life-threatening epilepsy associated with a novel ATP1A3 gene variant. *Brain Dev.* 41, 285–291. doi: 10.1016/j.braindev.2018.10.008

Jin, S. C., Homsy, J., Zaidi, S., Lu, Q., Morton, S., DePalma, S. R., et al. (2017). Contribution of rare inherited and de novo variants in 2,871 congenital heart disease probands. *Nat. Genet.* 49, 1593–1601. doi: 10.1038/ng.3970

Kahle, K. T., Kulkarni, A. V., Limbrick, D. D. Jr., and Warf, B. C. (2016). Hydrocephalus in children. *Lancet* 387, 788–799.

Laskowski, R. A., MacArthur, M. W., Moss, D. S., and Thornton, J. M. (1993). PROCHECK: a program to check the stereochemical quality of protein structures. *J. Appl. Cryst.* 26, 283–291. doi: 10.1107/s0021889892009944

Lek, M., Karczewski, K. J., Minikel, E. V., Samocha, K. E., Banks, E., Fennell, T., et al. (2016). Aggregation, Analysis of protein-coding genetic variation in 60,706 humans. *Nature* 536, 285–291. doi: 10.1038/nature19057

Lessard, J., Wu, J. I., Ranish, J. A., Wan, M., Winslow, M. M., Staahl, B. T., et al. (2007). An essential switch in subunit composition of a chromatin remodeling complex during neural development. *Neuron* 55, 201–215. doi: 10.1016/j.neuron.2007.06.019

Masuzawa, T., Ohta, T., Kawamura, M., Nakahara, N., and Sato, F. (1984). Immunohistochemical localization of Na+, K+-ATPase in the choroid plexus. *Brain Res.* 302, 357–362. doi: 10.1016/0006-8993(84)90250-6

McGrail, K. M., Phillips, J. M., and Sweadner, K. J. (1991). Immunofluorescent localization of three Na,K-ATPase isozymes in the rat central nervous system: both neurons and glia can express more than one Na,K-ATPase. *J. Neurosci.* 11, 381–391. doi: 10.1523/jneurosci.11-02-00381.1991

McKenna, A., Hanna, M., Banks, E., Sivachenko, A., Cibulskis, K., Kernytsky, A., et al. (2010). The genome analysis toolkit: a mapreduce framework for analyzing next-generation DNA sequencing data. *Genome Res.* 20, 1297–1303. doi: 10.1101/gr.107524.110

Mullen, R. J., Buck, C. R., and Smith, A. M. (1992). NeuN, a neuronal specific nuclear protein in vertebrates. *Development* 116, 201–211.

Picton, L. D., Nascimento, F., Broadhead, M. J., Sillar, K. T., and Miles, G. B. (2017). Sodium Pumps Mediate Activity-Dependent Changes in Mammalian Motor Networks. *J. Neurosci.* 37, 906–921. doi: 10.1523/JNEUROSCI.2005-16.2016

Pietrini, G., Matteoli, M., Banker, G., and Caplan, M. J. (1992). Isoforms of the Na,K-ATPase are present in both axons and dendrites of hippocampal neurons in culture. *Proc. Natl. Acad. Sci. U.S.A.* 89, 8414–8418. doi: 10.1073/pnas.89.18.8414

Richards, K. S., Bommert, K., Szabo, G., and Miles, R. (2007). Differential expression of Na+/K+-ATPase alpha-subunits in mouse hippocampal interneurones and pyramidal cells. *J. Physiol.* 585, 491–505. doi: 10.1113/jphysiol.2007.144733

Rodriguez, E. M., and Guerra, M. M. (2017). Neural Stem Cells and Fetal-Onset Hydrocephalus. *Pediatr. Neurosurg.* 52, 446–461. doi: 10.1159/000453074

Rosewich, H., Ohlenbusch, A., Huppke, P., Schlotawa, L., Baethmann, M., Carrilho, I., et al. (2014). The expanding clinical and genetic spectrum of ATP1A3-related disorders. *Neurology* 82, 945–955. doi: 10.1212/WNL.0000000000000212

Rosewich, H., Thiele, H., Ohlenbusch, A., Maschke, U., Altmuller, J., Frommolt, P., et al. (2012). Heterozygous de-novo mutations in ATP1A3 in patients with alternating hemiplegia of childhood: a whole-exome sequencing gene-identification study. *Lancet Neurol.* 11, 764–773. doi: 10.1016/S1474-4422(12)70182-5

Roy, A., Murphy, R. M., Deng, M., MacDonald, J. W., Bammler, T. K., Aldinger, K. A., et al. (2019). PI3K-Yap activity drives cortical gyrification and hydrocephalus in mice. *eLife* 8:e45961. doi: 10.7554/eLife.45961

Sabouraud, P., Riquet, A., Spitz, M. A., Deiva, K., Nevsimalova, S., Mignot, C., et al. (2019). Relapsing encephalopathy with cerebellar ataxia are caused by variants involving p.Arg756 in ATP1A3. *Eur. J. Paediatr. Neurol.* 23, 448–455. doi: 10.1016/j.ejpn.2019.02.004

Speake, T., Whitwell, C., Kajita, H., Majid, A., and Brown, P. D. (2001). Mechanisms of CSF secretion by the choroid plexus. *Microsc. Res. Tech.* 52, 49–59. doi: 10.1002/1097-0029(20010101)52:1<49::aid-jemt7>3.0.co;2-c

Torres, A., Brownstein, C. A., Tembulkar, S. K., Graber, K., Genetti, C., Kleiman, R. J., et al. (2018). De novo ATP1A3 and compound heterozygous NLRP3 mutations in a child with autism spectrum disorder, episodic fatigue and somnolence, and muckle-wells syndrome. *Mol. Genet. Metab. Rep.* 16, 23–29. doi: 10.1016/j.ymgmr.2018.06.001

Tully, H. M., and Dobyns, W. B. (2014). Infantile hydrocephalus: a review of epidemiology, classification and causes. *Eur. J. Med. Genet.* 57, 359–368. doi: 10.1016/j.ejmg.2014.06.002

Vaillend, C., Mason, S. E., Cuttle, M. F., and Alger, B. E. (2002). Mechanisms of neuronal hyperexcitability caused by partial inhibition of Na+-K+-ATPases in the rat CA1 hippocampal region. *J. Neurophysiol.* 88, 2963–2978. doi: 10.1152/jn.00244.2002

Van der Auwera, G. A., Carneiro, M. O., Hartl, C., Poplin, R., Del Angel, G., Levy-Moonshine, A., et al. (2013). From FastQ data to high confidence variant calls: the Genome Analysis Toolkit best practices pipeline. *Curr. Protoc. Bioinformatics* 43, 11101–111033. doi: 10.1002/0471250953.bi1110s43

Wang, K., Li, M., and Hakonarson, H. (2010). ANNOVAR: functional annotation of genetic variants from high-throughput sequencing data. *Nucleic Acids Res.* 38:e164. doi: 10.1093/nar/gkq603

Wiederstein, M., and Sippl, M. J. (2007). ProSA-web: interactive web service for the recognition of errors in three-dimensional structures of proteins. *Nucleic Acids Res.* 35, W407–W410.

Conflict of Interest: The authors declare that the research was conducted in the absence of any commercial or financial relationships that could be construed as a potential conflict of interest.

frontiers in Cellular Neuroscience

MINI REVIEW
published: 15 November 2019
doi: 10.3389/fncel.2019.00515

Identification of KCC2 Mutations in Human Epilepsy Suggests Strategies for Therapeutic Transporter Modulation

Phan Q. Duy[1,2], *Wyatt B. David*[1] *and Kristopher T. Kahle*[1,3,4,5,6]*

[1]*Department of Neurosurgery, Yale University School of Medicine, New Haven, CT, United States,* [2]*Medical Scientist Training Program, Yale University School of Medicine, New Haven, CT, United States,* [3]*Department of Genetics, Yale University School of Medicine, New Haven, CT, United States,* [4]*Departments of Pediatrics and Cellular & Molecular Physiology, Yale University School of Medicine, New Haven, CT, United States,* [5]*Yale-Rockefeller NIH Centers for Mendelian Genomics, Yale University, New Haven, CT, United States,* [6]*Yale Stem Cell Center, Yale School of Medicine, New Haven, CT, United States*

Epilepsy is a common neurological disorder characterized by recurrent and unprovoked seizures thought to arise from impaired balance between neuronal excitation and inhibition. Our understanding of the neurophysiological mechanisms that render the brain epileptogenic remains incomplete, reflected by the lack of satisfactory treatments that can effectively prevent epileptic seizures without significant drug-related adverse effects. Type 2 K^+-Cl^- cotransporter (KCC2), encoded by *SLC12A5*, is important for chloride homeostasis and neuronal excitability. KCC2 dysfunction attenuates Cl^- extrusion and impairs GABAergic inhibition, and can lead to neuronal hyperexcitability. Converging lines of evidence from human genetics have secured the link between KCC2 dysfunction and the development of epilepsy. Here, we review KCC2 mutations in human epilepsy and discuss potential therapeutic strategies based on the functional impact of these mutations. We suggest that a strategy of augmenting KCC2 activity by antagonizing its critical inhibitory phosphorylation sites may be a particularly efficacious method of facilitating Cl^- extrusion and restoring GABA inhibition to treat medication-refractory epilepsy and other seizure disorders.

Keywords: KCC2, SLC125A, epilepsy, seizure, neuronal excitability, neurodevelopment

OPEN ACCESS

Edited by:
Eleonora Aronica,
University Medical Center Amsterdam, Netherlands

Reviewed by:
Francesco Ferrini,
University of Turin, Italy
Quentin Chevy,
Cold Spring Harbor Laboratory, United States

***Correspondence:**
Kristopher T. Kahle
kristopher.kahle@yale.edu

Received: *12 July 2019*
Accepted: *01 November 2019*
Published: *15 November 2019*

Citation:
Duy PQ, David WB and Kahle KT (2019) Identification of KCC2 Mutations in Human Epilepsy Suggests Strategies for Therapeutic Transporter Modulation. Front. Cell. Neurosci. 13:515. doi: 10.3389/fncel.2019.00515

INTRODUCTION

A seizure is a transient increase in the brain's electrical activity that may be triggered by a variety of factors, including medications (Chen et al., 2016), metabolic alterations (Imad et al., 2015), and infections (Zoons et al., 2008). When seizures arise spontaneously, they are considered to be epileptic. Epilepsy is the most common serious brain disorder worldwide (World Health Organization, 2019) characterized by recurrent and unprovoked seizures that can cause loss of consciousness and/or abnormal motor behavior depending on the afflicted brain region (Stafstrom and Carmant, 2015). The disorder affects 0.5% of the general population (Sander and Shorvon, 1996) and is associated with increased rates of mortality (Zieliński, 1974), cognitive impairment (Aldenkamp, 2006), and psychosocial dysfunction (Pershad and Siddiqui, 1992) at an annual cost to the US economy of $12 billion (Begley et al., 2000).

Epilepsy is classically thought to arise from an imbalance between neuronal excitation and inhibition, leading to a hyperexcitable state that is prone to seizure activity. Antiepileptic drugs (AEDs) are the mainstay therapy for epilepsy that aim to restore this balance in neuronal excitability by either suppressing excitatory neurotransmission or augmenting inhibition. Despite decades of medical research and development of novel third-generation AEDs, a third to a half of epilepsy patients on medications continue to have seizures (medication refractory epilepsy; Kwan and Brodie, 2000; Shorvon and Luciano, 2007; Cascino, 2008). Furthermore, AEDs often exert significant drug-related adverse effects, including dizziness, nausea, fatigue, depression, learning and memory impairments, and ataxia (Perucca and Meador, 2005). The lack of a truly satisfactory AED reflects our incomplete understanding of epileptogenesis, the set of pathogenic alterations that render neuronal networks hyperexcitable and thus vulnerable to pathological seizure activity. There is an urgent clinical need for novel insights into cellular and molecular mechanisms of epileptogenesis in order to develop more efficacious AEDs that can achieve seizure freedom with minimal or no side effects.

Human genetic studies have associated mutations in the neuron-specific type 2 K^+/Cl^- cotransporter KCC2 with the development of epilepsy (Kahle et al., 2014; Puskarjov et al., 2014; Stödberg et al., 2015; Saitsu et al., 2016; Saito et al., 2017; Till et al., 2019). Preclinical studies suggest that modulation of KCC2 activity by targeting critical regulatory domains may be exploited to suppress seizure activity (Moore et al., 2018), highlighting the key role of KCC2 in the regulation of neuronal excitability in physiological and epileptogenic states. In this article, we review the KCC2 mutations that are associated with the development of epilepsy in humans. We also discuss the therapeutic ramifications of these findings and postulate that KCC2 may be a potentially powerful therapeutic target for the development of novel AEDs to treat refractory epilepsy.

Type 2 K^+-Cl^- COTRANSPORTER (KCC2) IN CHLORIDE HOMEOSTASIS AND SYNAPTIC INHIBITION

Neuronal excitability describes the propensity of a postsynaptic neuron to generate an action potential, a rapid rise and fall in membrane potential that occurs when the neuron reaches a threshold level of membrane depolarization. Consequently, neuronal excitability is governed by a dynamic balance between excitatory and inhibitory inputs. Excitatory inputs are depolarizing and thus raise the neuronal membrane potential towards the threshold, whereas inhibitory inputs are hyperpolarizing and lower the potential away from threshold. In the central nervous system, neuronal inhibition occurs primarily *via* activation of ligand-gated γ-aminobutyric acid (GABA) type A receptors ($GABA_A$Rs) that are highly permeable to Cl^-, and to a lesser extent, HCO_3^- (Kaila and Voipio, 1987). Ligand binding to $GABA_A$Rs on the postsynaptic neuron opens a central pore to trigger a hyperpolarizing Cl^- influx that lowers the probability of action potential being generated by neuron. The strength of synaptic inhibition is thus dependent on a low intra-neuronal concentration of Cl^-, which provides the basis for an electrochemical gradient that permits passive movement of Cl^- through the plasma membrane upon $GABA_A$R activation.

The electroneutral K^+/Cl^- cotransporter KCC2 (encoded by *SLC12A5*) is a key determinant of Cl^- homeostasis in neurons of the central nervous system (Kahle and Delpire, 2016; Moore et al., 2017). Under normal physiological settings, KCC2 uses the outwardly directed K^+ gradient generated by the N^+-K^+ ATPase pump to extrude Cl^- against its electrochemical gradient from neuronal cells in humans and thus maintains low intra-neuronal Cl^- concentrations required for hyperpolarizing GABAergic currents. In a likely over-simplified but useful scheme, intra-neuronal Cl^- concentrations are high during early brain development secondary to low KCC2 activity (Li et al., 2002; Stein et al., 2004) and high influx of Cl^- *via* Na^+-K^+-Cl^- cotransporter 1 (NKCC1; Plotkin et al., 1997; Yamada et al., 2004) in young neurons, leading to membrane depolarization following ligand binding to $GABA_A$R (Ben-Ari et al., 1989). As the brain matures, NKCC1 activity is downregulated whereas KCC2 activity is upregulated (Plotkin et al., 1997; Stein et al., 2004), leading to hyperpolarizing GABAergic responses, though recent data shows that the expression changes of these molecules vary within the heterogeneous neuronal populations within the brain (Sedmak et al., 2016). Although other KCC isoforms exist, KCC2 is unique in that its expression is primarily localized to central nervous system neurons (Williams et al., 1999; Payne et al., 2003) and it remains constitutively active even under isotonic conditions (Khirug et al., 2005; Mercado et al., 2006). Importantly, at least in the setting of normal neurophysiology, KCC2 is able to remove extra Cl^- introduced by GABAergic neurotransmission and thus recover low intracellular Cl^- levels in neurons (Kaila et al., 2014; Doyon et al., 2016). These properties indicate that KCC2 is a major extruder of Cl^- in mature neurons that establishes the inwardly directed Cl^- electrochemical gradient across the plasma membrane necessary for the emergence and maintenance of inhibitory hyperpolarizing responses upon activation of $GABA_A$Rs.

KCC2 MUTATIONS AND HUMAN EPILEPSY

The importance of KCC2 in maintaining the strength of synaptic inhibition highlights its potential involvement in epilepsy, a disorder of neuronal hyperexcitability that has been thought to arise from failed neuronal inhibition. Preclinical studies in multiple organisms show that genetic KCC2 deficiency results in diminished Cl^- extrusion, neuronal hyperexcitability, and epileptic seizures (Hübner et al., 2001; Hekmat-Scafe et al., 2006; Tanis et al., 2009). Accordingly, downregulation of KCC2 levels is observed in human idiopathic epilepsy (Huberfeld et al., 2007). Recent studies have now demonstrated the presence of KCC2 mutations in human epilepsy patients, providing strong evidence for the role

TABLE 1 | KCC2 (SLC12A5) mutations in human epilepsy.

Exon	NT change	AA change	Type	Inheritance	Phenotype	Ethnicity	Reference
21	c.2855G>A	p.R952H	Missense	AD	IGE; Febrile Seizures	French Canadian; Australian	Kahle et al. (2014) and Puskarjov et al. (2014)
23	c.3145C>T	p.R1049C	Missense	AD	IGE	French Canadian	Kahle et al. (2014)
9	c.1277T>C	p.L426P	Missense	AR, compound heterozygous	EIMFS	Swedish	Stödberg et al. (2015)
13	c.1625G>A	p.G551D	Missense				
8	c.932T>A	p.L331H	Missense	AR, homozygous	EIMFS	Pakistani	Stödberg et al. (2015)
3	c.279 + 1G>C	p.E50_Q93del	Deletion	AR, compound heterozygous	EIMFS	Japanese	Saitsu et al. (2016)
6	c.572C>T	p.A191V	Missense				
8	c.967T>C	p.S323P	Missense	AR, compound heterozygous	EIMFS	Malaysian	Saitsu et al. (2016)
10	c.1243A>G	p.M415V	Missense				
8	c.953G>C	p.W318S	Deletion	AR, compound heterozygous	EIMFS	Japanese	Saitsu et al. (2016)
18	c.2242_2244del	p.S748del	Missense				
9	c.1196C>T	p.S399L	Missense	AR, compound heterozygous	EIMFS	Japanese	Saito et al. (2017)
20	c.2639G>T	p.R880L	Missense				
11	c.1417G>A	p.V473I	Missense	AD	IGE	Hungarian	Till et al. (2019)

AA, amino acid; AD, autosomal dominant; AR, autosomal recessive; EIMFS, epilepsy of infancy with migrating focal seizures; IGE, idiopathic generalized epilepsy; NT, nucleotide.

of KCC2 in seizure disorders. All of the KCC2 mutations discovered in human epilepsy thus far are summarized in **Table 1**.

Idiopathic Generalized Epilepsy 14 (OMIM# 616685, Autosomal Dominant)

Kahle et al. (2014) used a targeted DNA-sequencing approach to screen the cytoplasmic C-terminal region of SLC12A5 which is an important regulatory region of transporter function. They identified two different heterozygous missense variants in *SLC12A5* (R952H, 606726.0004 and R1049C, 606726.0005) that were enriched among individuals of French Canadian origin with idiopathic generalized epilepsy-14 (EIG14; 616685) compared to controls. Both variants exhibited reduced Cl^- extrusion capacity, although unlike the R952H variant, the R1049C variant exhibited normal surface expression with decreased intrinsic cotransporter activity. Both variants also showed decreased phosphorylation of the serine 940 (S940) residue (Kahle et al., 2014), which normally promotes KCC2 activity (Lee et al., 2011). The overall effect impaired the function of KCC2. The variants were inherited from an unaffected parent in several cases, consistent with incomplete penetrance, consistent with other large genomic studies of human idiopathic generalized epilepsy (Mefford et al., 2011). Puskarjov et al. (2014) reported the R952H mutation in an Australian family with early childhood onset of febrile seizures. Segregation of the variant in this kindred was difficult because of uncertain phenotyping, but there was some evidence of incomplete penetrance. Electrophysiological and biochemical assays suggest that the R952H variant exhibits impaired Cl^- extrusion likely due to reduced surface expression. Overexpression of this variant in KCC2-deficient mouse cortical neurons failed to rescue defects in dendritic spine development, suggesting a potential role of the R952H variant in formation and maturation of cortical dendritic spines. Puskarjov et al. (2014) suggested that the decrease in KCC2-dependent hyperpolarizing inhibition would promote seizures, and that decreased dendritic spine formation could lead to desynchronization of overall excitability. Importantly, the function of KCC2 in the dendritic spine does not depend on transporter function but rather involves interactions between KCC2 and other proteins (Llano et al., 2015). The most recent study has identified a new missense KCC2 variant, V473I, that causes IGE in a Hungarian patient who is heterozygous for the mutation (Till et al., 2019).

Early Infantile Epileptic Encephalopathy 34 (OMIM# 616645, Autosomal Recessive)

The strongest genetic evidence for KCC2 dysfunction in epilepsy is demonstrated by studies of patients in families with a severe infantile epilepsy syndrome termed epilepsy of infancy with migrating focal seizures (EIMFS; Stödberg et al., 2015; Saitsu et al., 2016; Saito et al., 2017). To date, nine probands with monogenetic KCC2-related EIMFS have been reported. By whole-exome sequencing of two unrelated families, Stödberg et al. (2015) discovered that affected children with EIMFS harbored biallelic *SLC12A5* loss-of-function mutations. Two affected children from a consanguineous family harbored the homozygous mutation L311H that localizes to an extracellular loop. The L426P (localizing to a transmembrane domain) and G551D (localizing to an intracellular loop) variants were found as compound heterozygous mutations in two affected children from another family. All of the KCC2 mutations identified by Stödberg et al. (2015) resulted in diminished Cl^- extrusion and reduced cell surface expression. Follow-up studies identified eight additional recessive KCC2 mutations that cause EIMFS (Saitsu et al., 2016; Saito et al., 2017), including the E50_Q93del variant that causes skipping of exon 3 and the S749del variant that causes an amino acid deletion (Saitsu et al., 2016). Functional characterization of some of these EIFM-causing KCC2 mutations (E50_Q93del, A191V, S323P, M415V) suggested that they attenuated neuronal Cl^- extrusion without altering cell surface expression and distribution (Saitsu et al., 2016). It is important to note that all of the

homozygous or compound heterozygous EIMFS patients inherited KCC2 mutations from unaffected heterozygous parents, in contrast to the R952H and R1049 variants that were sufficient to cause epilepsy disorders in heterozygous individuals (Kahle et al., 2014; Puskarjov et al., 2014). The reasons underlying these phenotypic differences are not understood, although some have hypothesized that mutations located in different KCC2 domains exert different effects on functional activity that underlie variations in phenotypic manifestations (Kahle et al., 2016a).

AUGMENTING KCC2 ACTIVITY TO RESTORE SYNAPTIC INHIBITION AS A THERAPEUTIC AVENUE FOR EPILEPSY

The presence of KCC2 mutations in human epilepsy indicates that accumulation of intracellular Cl^- secondary to KCC2 dysfunction may be responsible for driving neuronal hyperexcitability underlying the development of epilepsy syndromes. The association between loss-of-function KCC2 mutations and epilepsy also suggests that augmenting KCC2 activity to enhance Cl^- extrusion may confer the opposite effect of rendering neuronal cells more resistant to seizures, representing a potentially powerful therapeutic avenue for idiopathic epilepsy. Indeed, high levels of neural activity due to seizures may promote the intracellular accumulation of Cl^- that exceeds the normal Cl^- extrusion capacity of KCC2, leading to GABAergic depolarizing currents and loss of synaptic inhibition that underlie epileptogenesis (Ellender et al., 2014; Magloire et al., 2019). Augmenting KCC2 function could theoretically extrude excessive Cl^- and restore neuronal inhibition in hyperexcitable states.

Targeting critical phosphorylation sites of KCC2 regulation is one promising strategy to enhance KCC2 function for therapeutic benefit. KCC2 activity is bidirectionally regulated at key phosphorylation sites: S940 phosphorylation increases KCC2 function (Lee et al., 2011), whereas phosphorylation of T906 and T1007 inhibits its function (Rinehart et al., 2009). Dephosphorylation of T906 and T1007 upregulates Cl^- extrusion from neurons (Friedel et al., 2015; Titz et al., 2015; Heubl et al., 2017). To test the hypothesis that increasing KCC2 activity is anticonvulsant *in vivo*, Moore et al. (2018) generated knock-in mice in which threonines 906 and 1007 were substituted for alanines (KCC2-T906A/T1007A) to genetically prevent phospho-dependent inactivation, resulting in higher basal neuronal Cl^- extrusion (Moore et al., 2018). Strikingly, KCC2-T906A/T1007A mice exhibited profound resistance to chemoconvulsant-induced seizures without altered basal neuronal excitability. These findings suggest that modulation of KCC2 phosphorylation sites may be leveraged to strengthen synaptic inhibition for therapeutic benefit in epilepsy syndromes. For clinical translation, KCC2 function could be enhanced by inhibition of the upstream with no lysine (WNK) and Ste20-related proline-alanine kinase (WNK-SPAK) cascade that normally inhibits KCC2 function by promoting T906 and T1007 phosphorylation (Kahle et al., 2005, 2014, 2016b; Friedel et al., 2015; Kahle and Delpire, 2016; Heubl et al., 2017). Indeed, small molecule inhibitors of the WNK-SPAK pathway are being developed (Yamada et al., 2016). In addition to targeting the WNK/SPAK pathway, other pharmacological strategies to enhance KCC2 activity are also being investigated. A large screening of molecules to identify putative KCC2 agonists was first proposed by Gagnon et al. (2013). Another screening was recently carried out to detect small molecules capable of enhancing KCC2 expression levels (Tang et al., 2019). The ability to augment KCC2 function *via* different pharmacological approaches will enable flexibility in the selection of the ideal KCC2 modulator that is tailored to the underlying epileptogenic process.

Although efforts to identify KCC2 modulators reflect its promise as a druggable target in epilepsy, there remain several caveats. First, it is unclear which pharmacological approach or combination of approaches to enhance KCC2 activity would rescue the defects in expression and function due to KCC2 mutations observed in epilepsy syndromes. Second, it remains uncertain whether there may be unintended adverse effects that arise from increased KCC2 activity. Indeed, a major shortcoming of current AEDs is not only their inability to prevent seizures in a large population of patients but also their association with drug-related side effects such as cognitive disturbance (Park and Kwon, 2008). Potentiating KCC2 activity does not alter basal neuronal excitability (Moore et al., 2018), and a previously identified KCC2 activator (CLP257) produces analgesia without motor side effects often seen with other analgesics (Gagnon et al., 2013). While these preliminary findings suggest that enhancing KCC2 may be a safe therapeutic avenue to prevent seizures without altering the function of healthy neurons, more systematic studies are still needed to fully characterize potential side effects of the approach before clinical translation.

CONCLUSION

Epilepsy is a common brain disorder characterized by recurrent and unprovoked seizures thought to be caused by neuronal hyperexcitability. A third to half of epilepsy patients continue to have seizures despite medications (Kwan and Brodie, 2000; Shorvon and Luciano, 2007; Cascino, 2008), underscoring the clinical need for the identification of novel therapeutic targets. KCC2 functions as a major Cl^- extruder in mature neurons to establish an inwardly-directed electrochemical gradient of Cl^- necessary for the maintenance of fast synaptic inhibition. In the settings of diminished KCC2 activity secondary to risk factor and causal mutations in human epilepsy patients, intracellular Cl^- concentrations accumulate, leading to impaired hyperpolarizing responses that render neurons hyperexcitable. In contrast, increasing KCC2 function by overexpression or modulation of key phosphorylation sites confers an anticonvulsant effect. Altogether, the presence of KCC2 mutations in

epilepsy coupled with preclinical proof-of-principle for KCC2 as a therapeutic target motivates a rich stream of future studies to further investigate the mechanistic roles of KCC2 in epileptogenesis and how manipulation of KCC2 activity can be leveraged pharmacologically for therapeutic benefit in epilepsy syndromes and conditions of hyperexcitation.

AUTHOR CONTRIBUTIONS

PD, WD and KK reviewed the literature and wrote the manuscript.

FUNDING

This work was supported by 1R01NS109358-01 (to KK), 1R01NS111029-01A1 (to KK), the Simons Foundation (to KK), the March of Dimes Foundation (to KK), and National Institutes of Health (NIH) Medical Scientist Program Training Grant T32GM007205 (to PD).

ACKNOWLEDGMENTS

We thank all members of the Kahle lab for their help and support.

REFERENCES

Aldenkamp, A. P. (2006). Cognitive impairment in epilepsy: state of affairs and clinical relevance. *Seizure* 15, 219–220. doi: 10.1016/j.seizure.2006.02.010

Begley, C. E., Famulari, M., Annegers, J. F., Lairson, D. R., Reynolds, T. F., Coan, S., et al. (2000). The cost of epilepsy in the united states: an estimate from population-based clinical and survey data. *Epilepsia* 41, 342–351. doi: 10.1111/j.1528-1157.2000.tb00166.x

Ben-Ari, Y., Cherubini, E., Corradetti, R., and Gaiarsa, J. L. (1989). Giant synaptic potentials in immature rat CA3 hippocampal neurones. *J. Physiol.* 416, 303–325. doi: 10.1113/jphysiol.1989.sp017762

Cascino, G. D. (2008). When drugs and surgery don't work. *Epilepsia* 49, 79–84. doi: 10.1111/j.1528-1167.2008.01930.x

Chen, H.-Y., Albertson, T. E., and Olson, K. R. (2016). Treatment of drug-induced seizures. *Br. J. Clin. Pharmacol.* 81, 412–419. doi: 10.1111/bcp.12720

Doyon, N., Vinay, L., Prescott, S. A., and De Koninck, Y. (2016). Chloride regulation: a dynamic equilibrium crucial for synaptic inhibition. *Neuron* 89, 1157–1172. doi: 10.1016/j.neuron.2016.02.030

Ellender, T. J., Raimondo, J. V., Irkle, A., Lamsa, K. P., and Akerman, C. J. (2014). excitatory effects of parvalbumin-expressing interneurons maintain hippocampal epileptiform activity via synchronous afterdischarges. *J. Neurosci.* 34, 15208–15222. doi: 10.1523/JNEUROSCI.1747-14.2014

Friedel, P., Kahle, K. T., Zhang, J., Hertz, N., Pisella, L. I., Buhler, E., et al. (2015). WNK1-regulated inhibitory phosphorylation of the KCC2 cotransporter maintains the depolarizing action of GABA in immature neurons. *Sci. Signal.* 8:ra65. doi: 10.1126/scisignal.aaa0354

Gagnon, M., Bergeron, M. J., Lavertu, G., Castonguay, A., Tripathy, S., Bonin, R. P., et al. (2013). Chloride extrusion enhancers as novel therapeutics for neurological diseases. *Nat. Med.* 19, 1524–1528. doi: 10.1038/nm.3356

Hekmat-Scafe, D. S., Lundy, M. Y., Ranga, R., and Tanouye, M. A. (2006). Mutations in the K^+/Cl^- cotransporter gene *kazachoc (Kcc)* increase seizure susceptibility in *Drosophila*. *J. Neurosci.* 26, 8943–8954. doi: 10.1523/JNEUROSCI.4998-05.2006

Heubl, M., Zhang, J., Pressey, J. C., Al Awabdh, S., Renner, M., Gomez-Castro, F., et al. (2017). $GABA_A$ receptor dependent synaptic inhibition rapidly tunes KCC2 activity via the Cl^--sensitive WNK1 kinase. *Nat. Commun.* 8:1776. doi: 10.1038/s41467-017-01749-0

Huberfeld, G., Wittner, L., Clemenceau, S., Baulac, M., Kaila, K., Miles, R., et al. (2007). Perturbed chloride homeostasis and GABAergic signaling in human temporal lobe epilepsy. *J. Neurosci.* 27, 9866–9873. doi: 10.1523/JNEUROSCI.2761-07.2007

Hübner, C. A., Stein, V., Hermans-Borgmeyer, I., Meyer, T., Ballanyi, K., and Jentsch, T. J. (2001). Disruption of KCC2 reveals an essential role of K-Cl cotransport already in early synaptic inhibition. *Neuron* 30, 515–524. doi: 10.1016/s0896-6273(01)00297-5

Imad, H., Zelano, J., and Kumlien, E. (2015). Hypoglycemia and risk of seizures: a retrospective cross-sectional study. *Seizure* 25, 147–149. doi: 10.1016/j.seizure.2014.10.005

Kahle, K. T., and Delpire, E. (2016). Kinase-KCC2 coupling: Cl^- rheostasis, disease susceptibility, therapeutic target. *J. Neurophysiol.* 115, 8–18. doi: 10.1152/jn.00865.2015

Kahle, K. T., Khanna, A. R., Duan, J., Staley, K. J., Delpire, E., and Poduri, A. (2016a). The KCC2 cotransporter and human epilepsy: getting excited about inhibition. *Neuroscientist* 22, 555–562. doi: 10.1177/1073858416645087

Kahle, K. T., Schmouth, J.-F., Lavastre, V., Latremoliere, A., Zhang, J., Andrews, N., et al. (2016b). Inhibition of the kinase WNK1/HSN2 ameliorates neuropathic pain by restoring GABA inhibition. *Sci. Signal.* 9:ra32. doi: 10.1126/scisignal.aad0163

Kahle, K. T., Merner, N. D., Friedel, P., Silayeva, L., Liang, B., Khanna, A., et al. (2014). Genetically encoded impairment of neuronal KCC2 cotransporter function in human idiopathic generalized epilepsy. *EMBO Rep.* 15, 766–774. doi: 10.15252/embr.201438840

Kahle, K. T., Rinehart, J., de Los Heros, P., Louvi, A., Meade, P., Vazquez, N., et al. (2005). WNK3 modulates transport of Cl^- in and out of cells: implications for control of cell volume and neuronal excitability. *Proc. Natl. Acad. Sci. U S A* 102, 16783–16788. doi: 10.1073/pnas.0508307102

Kaila, K., Price, T. J., Payne, J. A., Puskarjov, M., and Voipio, J. (2014). Cation-chloride cotransporters in neuronal development, plasticity and disease. *Nat. Rev. Neurosci.* 15, 637–654. doi: 10.1038/nrn3819

Kaila, K., and Voipio, J. (1987). Postsynaptic fall in intracellular PH induced by GABA-activated bicarbonate conductance. *Nature* 330, 163–165. doi: 10.1038/330163a0

Khirug, S., Huttu, K., Ludwig, A., Smirnov, S., Voipio, J., Rivera, C., et al. (2005). Distinct properties of functional KCC2 expression in immature mouse hippocampal neurons in culture and in acute slices. *Eur. J. Neurosci.* 21, 899–904. doi: 10.1111/j.1460-9568.2005.03886.x

Kwan, P., and Brodie, M. J. (2000). Early identification of refractory epilepsy. *N. Engl. J. Med.* 342, 314–319. doi: 10.1056/NEJM200002033420503

Lee, H. H. C., Deeb, T. Z., Walker, J. A., Davies, P. A., and Moss, S. J. (2011). NMDA receptor activity downregulates KCC2 resulting in depolarizing $GABA_A$ receptor-mediated currents. *Nat. Neurosci.* 14, 736–743. doi: 10.1038/nn.2806

Li, H., Tornberg, J., Kaila, K., Airaksinen, M. S., and Rivera, C. (2002). Patterns of cation-chloride cotransporter expression during embryonic rodent CNS development. *Eur. J. Neurosci.* 16, 2358–2370. doi: 10.1046/j.1460-9568.2002.02419.x

Llano, O., Smirnov, S., Soni, S., Golubtsov, A., Guillemin, I., Hotulainen, P., et al. (2015). KCC2 regulates actin dynamics in dendritic spines via interaction with β-PIX. *J. Cell Biol.* 209, 671–686. doi: 10.1083/jcb.201411008

Magloire, V., Cornford, J., Lieb, A., Kullmann, D. M., and Pavlov, I. (2019). KCC2 overexpression prevents the paradoxical seizure-promoting action of somatic inhibition. *Nat. Commun.* 10:1225. doi: 10.1038/s41467-019-08933-4

Mefford, H. C., Yendle, S. C., Hsu, C., Cook, J., Geraghty, E., McMahon, J. M., et al. (2011). Rare copy number variants are an important cause of epileptic encephalopathies. *Ann. Neurol.* 70, 974–985. doi: 10.1002/ana.22645

Mercado, A., Broumand, V., Zandi-Nejad, K., Enck, A. H., and Mount, D. B. (2006). A C-terminal domain in KCC2 confers constitutive K^+-Cl^- cotransport. *J. Biol. Chem.* 281, 1016–1026. doi: 10.1074/jbc.M509972200

Moore, E. Y., Deeb, T. Z., Chadchankar, H., Brandon, N. J., and Moss, S. J. (2018). Potentiating KCC2 activity is sufficient to limit the onset and severity of seizures. *Proc. Natl. Acad. Sci. U S A* 115, 10166–10171. doi: 10.1073/pnas.1810134115

Moore, Y. E., Kelley, M. R., Brandon, N. J., Deeb, T. Z., and Moss, S. J. (2017). Seizing control of KCC2: a new therapeutic target for epilepsy. *Trends Neurosci.* 40, 555–571. doi: 10.1016/j.tins.2017.06.008

Park, S.-P., and Kwon, S.-H. (2008). Cognitive effects of antiepileptic drugs. *J. Clin. Neurol.* 4, 99–106. doi: 10.3988/jcn.2008.4.3.99

Payne, J. A., Rivera, C., Voipio, J., and Kaila, K. (2003). Cation-chloride co-transporters in neuronal communication, development and trauma. *Trends Neurosci.* 26, 199–206. doi: 10.1016/s0166-2236(03)00068-7

Pershad, D., and Siddiqui, R. S. (1992). Psychosocial dysfunction in adults with epilepsy. *Int. J. Rehabil. Res.* 15, 258–261. doi: 10.1097/00004356-199209000-00012

Perucca, E., and Meador, K. J. (2005). Adverse effects of antiepileptic drugs. *Acta Neurol. Scand. Suppl.* 181, 30–35. doi: 10.1111/j.1600-0404.2005.00506.x

Plotkin, M. D., Snyder, E. Y., Hebert, S. C., and Delpire, E. (1997). Expression of the Na-K-2Cl cotransporter is developmentally regulated in postnatal rat brains: a possible mechanism underlying GABA's excitatory role in immature brain. *J. Neurobiol.* 33, 781–795. doi: 10.1002/(sici)1097-4695(19971120)33:6<781::aid-neu6>3.0.co;2-5

Puskarjov, M., Seja, P., Heron, S. E., Williams, T. C., Ahmad, F., Iona, X., et al. (2014). A variant of KCC2 from patients with febrile seizures impairs neuronal Cl^- extrusion and dendritic spine formation. *EMBO Rep.* 15, 723–729. doi: 10.1002/embr.201438749

Rinehart, J., Maksimova, Y. D., Tanis, J. E., Stone, K. L., Hodson, C. A., Zhang, J., et al. (2009). Sites of regulated phosphorylation that control K-Cl cotransporter activity. *Cell* 138, 525–536. doi: 10.1016/j.cell.2009.05.031

Saito, T., Ishii, A., Sugai, K., Sasaki, M., and Hirose, S. (2017). A *de novo* missense mutation in SLC12A5 found in a compound heterozygote patient with epilepsy of infancy with migrating focal seizures. *Clin. Genet.* 92, 654–658. doi: 10.1111/cge.13049

Saitsu, H., Watanabe, M., Akita, T., Ohba, C., Sugai, K., Ong, W. P., et al. (2016). Impaired neuronal KCC2 function by biallelic SLC12A5 mutations in migrating focal seizures and severe developmental delay. *Sci. Rep.* 6:30072. doi: 10.1038/srep30072

Sander, J. W., and Shorvon, S. D. (1996). Epidemiology of the epilepsies. *J. Neurol. Neurosurg. Psychiatry* 61, 433–443. doi: 10.1136/jnnp.61.5.433

Sedmak, G., Jovanov-Miloševic, N., Puskarjov, M., Ulamec, M., Krušlin, B., Kaila, K., et al. (2016). Developmental expression patterns of KCC2 and functionally associated molecules in the human brain. *Cereb. Cortex* 26, 4574–4589. doi: 10.1093/cercor/bhv218

Shorvon, S., and Luciano, A. L. (2007). Prognosis of chronic and newly diagnosed epilepsy: revisiting temporal aspects. *Curr. Opin. Neurol.* 20, 208–212. doi: 10.1097/wco.0b013e3280555175

Stafstrom, C. E., and Carmant, L. (2015). Seizures and epilepsy: an overview for neuroscientists. *Cold Spring Harb. Perspect. Med.* 5:a022426. doi: 10.1101/cshperspect.a022426

Stein, V., Hermans-Borgmeyer, I., Jentsch, T. J., and Hübner, C. A. (2004). Expression of the KCl cotransporter KCC2 parallels neuronal maturation and the emergence of low intracellular chloride. *J. Comp. Neurol.* 468, 57–64. doi: 10.1002/cne.10983

Stödberg, T., McTague, A., Ruiz, A. J., Hirata, H., Zhen, J., Long, P., et al. (2015). Mutations in SLC12A5 in epilepsy of infancy with migrating focal seizures. *Nat. Commun.* 6:8038. doi: 10.1038/ncomms9038

Tang, X., Drotar, J., Li, K., Clairmont, C. D., Brumm, A. S., Sullins, A. J., et al. (2019). Pharmacological enhancement of KCC2 gene expression exerts therapeutic effects on human rett syndrome neurons and Mecp2 mutant mice. *Sci. Transl. Med.* 11:eaau0164. doi: 10.1126/scitranslmed.aau0164

Tanis, J. E., Bellemer, A., Moresco, J. J., Forbush, B., and Koelle, M. R. (2009). The potassium chloride cotransporter KCC-2 coordinates development of inhibitory neurotransmission and synapse structure in caenorhabditis elegans. *J. Neurosci.* 29, 9943–9954. doi: 10.1523/JNEUROSCI.1989-09.2009

Till, Á., Szalai, R., Hegyi, M., Kövesdi, E., Büki, G., Hadzsiev, K., et al. (2019). A rare form of ion channel gene mutation identified as underlying cause of generalized epilepsy. *Orv. Hetil.* 160, 835–838. doi: 10.1556/650.2019.31404

Titz, S., Sammler, E. M., and Hormuzdi, S. G. (2015). Could tuning of the inhibitory tone involve graded changes in neuronal chloride transport? *Neuropharmacology* 95, 321–331. doi: 10.1016/j.neuropharm.2015.03.026

Williams, J. R., Sharp, J. W., Kumari, V. G., Wilson, M., and Payne, J. A. (1999). The neuron-specific K-Cl cotransporter, KCC2. Antibody development and initial characterization of the protein. *J. Biol. Chem.* 274, 12656–12664. doi: 10.1074/jbc.274.18.12656

World Health Organization. (2019). "Neurological disorders, including epilepsy," in *Mental Health Home*. Available online at: https://www.who.int/mental_health/management/neurological/en/.

Yamada, J., Okabe, A., Toyoda, H., Kilb, W., Luhmann, H. J., and Fukuda, A. (2004). Cl^- uptake promoting depolarizing GABA actions in immature rat neocortical neurones is mediated by NKCC1. *J. Physiol.* 557, 829–841. doi: 10.1113/jphysiol.2004.062471

Yamada, K., Zhang, J.-H., Xie, X., Reinhardt, J., Xie, A. Q., LaSala, D., et al. (2016). Discovery and characterization of allosteric WNK kinase inhibitors. *ACS Chem. Biol.* 11, 3338–3346. doi: 10.1021/acschembio.6b00511

Zieliński, J. J. (1974). Epilepsy and mortality rate and cause of death. *Epilepsia* 15, 191–201. doi: 10.1111/j.1528-1157.1974.tb04941.x

Zoons, E., Weisfelt, M., de Gans, J., Spanjaard, L., Koelman, J. H. T. M., Reitsma, J. B., et al. (2008). Seizures in adults with bacterial meningitis. *Neurology* 70, 2109–2115. doi: 10.1212/01.wnl.0000288178.91614.5d

Conflict of Interest: The authors declare that the research was conducted in the absence of any commercial or financial relationships that could be construed as a potential conflict of interest.

frontiers in Cellular Neuroscience

MINI REVIEW
published: 13 December 2019
doi: 10.3389/fncel.2019.00556

Functional Genomics of Epilepsy and Associated Neurodevelopmental Disorders Using Simple Animal Models: From Genes, Molecules to Brain Networks

*Richard Rosch[1,2,3], Dominic R. W. Burrows[1], Laura B. Jones[4], Colin H. Peters[4], Peter Ruben[4] and Éric Samarut[5,6]**

[1] MRC Centre for Neurodevelopmental Disorders, Institute of Psychiatry, Psychology and Neuroscience, King's College London, London, United Kingdom, [2] Department of Paediatric Neurology, Great Ormond Street Hospital, NHS Foundation Trust, London, United Kingdom, [3] Department of Bioengineering, University of Pennsylvania, Philadelphia, PA, United States, [4] Department of Biomedical Physiology and Kinesiology, Simon Fraser University, Burnaby, BC, Canada, [5] Department of Neurosciences, Research Center of the University of Montreal Hospital Center (CRCHUM), Université de Montréal, Montreal, QC, Canada, [6] Modelis Inc., Montreal, QC, Canada

OPEN ACCESS

Edited by:
Eleonora Aronica, University Medical Center Amsterdam, Netherlands

Reviewed by:
Michel Joseph Roux, INSERM U964 Institut de Génétique et de Biologie Moléculaire et Cellulaire (IGBMC), France
Dilja Krueger-Burg, University Medical Center Göttingen, Germany

***Correspondence:**
Éric Samarut
eric.samarut@umontreal.ca

Specialty section:
This article was submitted to Cellular Neuropathology, a section of the journal Frontiers in Cellular Neuroscience

Received: *20 September 2019*
Accepted: *02 December 2019*
Published: *13 December 2019*

Citation:
Rosch R, Burrows DRW, Jones LB, Peters CH, Ruben P and Samarut É (2019) Functional Genomics of Epilepsy and Associated Neurodevelopmental Disorders Using Simple Animal Models: From Genes, Molecules to Brain Networks. Front. Cell. Neurosci. 13:556. doi: 10.3389/fncel.2019.00556

The genetic diagnosis of patients with seizure disorders has been improved significantly by the development of affordable next-generation sequencing technologies. Indeed, in the last 20 years, dozens of causative genes and thousands of associated variants have been described and, for many patients, are now considered responsible for their disease. However, the functional consequences of these mutations are often not studied *in vivo,* despite such studies being central to understanding pathogenic mechanisms and identifying novel therapeutic avenues. One main roadblock to functionally characterizing pathogenic mutations is generating and characterizing *in vivo* mammalian models carrying clinically relevant variants in specific genes identified in patients. Although the emergence of new mutagenesis techniques facilitates the production of rodent mutants, the fact that early development occurs internally hampers the investigation of gene function during neurodevelopment. In this context, functional genomics studies using simple animal models such as flies or fish are advantageous since they open a dynamic window of investigation throughout embryonic development. In this review, we will summarize how the use of simple animal models can fill the gap between genetic diagnosis and functional and phenotypic correlates of gene function *in vivo*. In particular, we will discuss how these simple animals offer the possibility to study gene function at multiple scales, from molecular function (i.e., ion channel activity), to cellular circuit and brain network dynamics. As a result, simple model systems offer alternative avenues of investigation to model aspects of the disease phenotype not currently possible in rodents, which can help to unravel the pathogenic substratum *in vivo.*

Keywords: epilepsy, neurodevelopmental disorder, brain disorder, zebrafish, *Drosophila*

FROM PHENOTYPE TO GENOTYPE: THE ERA OF GENETICS IN THE FIELD OF NEURODEVELOPMENTAL DISORDERS

Investigating the genetic basis of childhood epilepsy and neurodevelopmental disorders over the last two decades has revealed the unexpected role of a number of key genes in guiding normal brain development and emergent brain dynamics (Myers and Mefford, 2015). Facilitated by the increasing affordability of genomic technologies, genes affecting synaptic function have been identified as causative in a diverse range of epilepsy syndromes and other neurodevelopmental disorders such that many are now considered "synaptopathies" (Grant, 2012). Interestingly, many non-synaptic genes have also been identified as risk factors in various neurodevelopmental disorders. For these genes, the underlying pathogenic mechanisms are puzzling as they are not necessarily known to regulate synaptic activity directly. Taken together, a better understanding of the functional consequences of the wide spectrum of neurodevelopmental genetic mutations is required, for which *in vivo* systems are particularly useful.

Severe *de novo* Mutations and Genomic Alterations in Neurodevelopmental Disorders

Genetic insights have been particularly transformative in our understanding of some of the most severe disorders of neurodevelopment, known now as developmental and epileptic encephalopathies (DEEs) (Scheffer et al., 2016). DEEs usually occur as isolated cases in families, yet in a large proportion of cases, causative *de novo* mutations in single genes can now be identified from clinical genetic diagnostics (Epi et al., 2013; Oates et al., 2018). The most common genes and their functional effects are illustrated in **Figure 1**. Affordable technology that allows the identification of even small structural genomic alterations [i.e., copy number variations (CNVs)] was key to investigating the genetic basis for common neurodevelopmental disorders. Beginning with transformative studies of people living with autistic spectrum disorders (ASD) (Sebat et al., 2007; Pinto et al., 2010), we have come to understand that individually rare CNVs account for a significant proportion of the incidence not only of autism, but intellectual disability (Cooper et al., 2011), "idiopathic" generalized epilepsies (Mefford et al., 2010; Addis et al., 2016) and schizophrenia (Stefansson et al., 2008; Marshall et al., 2017), particularly where there is overlap between these conditions. Interestingly, genes identified from genome-wide association studies of particular disorders often overlap across disorder categories (Fromer et al., 2014; International League Against Epilepsy Consortium on Complex Epilepsies, 2014; Schizophrenia Working Group of the Psychiatric Genomics Consortium, 2014; Turner et al., 2017), suggesting that many of the genes have a broad neurodevelopmental role that may result in a range of recognizable syndromes or phenotypes.

Genotype-Phenotype Correlations

The increasing ability to make genetic diagnoses at the level of individual patients carries the promise of allowing the development of targeted therapies informed by underlying pathomechanisms. However, with increasing diagnosis, the phenotypic spectrum widens and linking genotypes to phenotypes is becoming more and more challenging. Indeed, mutations in the same gene (or even identical same genetic mutations) may cause very different phenotypes in different patients. For example, up to 50% of patients with *de novo* mutations in known epilepsy genes do not have seizures (Deciphering Developmental Disorders, 2017). Another example is the spectrum of epileptic phenotypes caused by different mutations affecting the same GABA receptor gene (*GABRA*1). This spectrum ranges from some of the most severe developmental DEEs of infancy, to juvenile onset treatable generalized epilepsy syndromes (Johannesen et al., 2016). Some variability in the mapping between affected genes and phenotype can be explained by differences in specific mutations' effects (even at the level of the same gene) on protein function (Ben-Shalom et al., 2017). This genotype-phenotype relation may be addressed in the future by increasing efforts to investigate the functional effects of individual genes as well as individual mutations *in vivo* through translational research (Scheffer et al., 2016). This gene has been described as both an epilepsy, and an autism gene but also emerges in a range of other neurodevelopmental contexts suggesting potentially shared mechanisms. Understanding the contribution of the genetic alteration to the various phenotypes is essential to now attempt and translate these broad insights into novel, targeted therapies.

FROM GENE MUTATION TO MOLECULAR DYSFUNCTION (TEMPORAL MICROSCALE)

In the light of the difficulties in relating newly diagnosed genetic variants with their underlying functional consequences, and because of the unclear correlation between phenotype and genotype we described above, there is a need for *in vivo* models to explore the functional effects of specific genetic alterations. In particular, epilepsy has been studied using multiple model organisms, most traditionally rodents (Seyfried and Glaser, 1985; Yu et al., 2006). Although rat and mouse models have been foundational to the field, recent research has expanded to include non-mammalian models such as round worms, zebrafish, and fruit flies (Baraban, 2007; Cunliffe et al., 2015).

Drosophila melanogaster has become an increasingly popular model organism in epilepsy research due to its small size, short generation time, and the relative ease of stock maintenance and mutant isolation (Bier, 2005; Song and Tanouye, 2008; Cunliffe et al., 2015). These factors, in addition to the large percentage of conserved human disease genes in *Drosophila* (Fortini et al., 2000; Rubin et al., 2000; Bier, 2005), result in it being an extremely cost-effective model system for epilepsy research (Baraban, 2007; Song and Tanouye, 2008; Cunliffe et al., 2015).

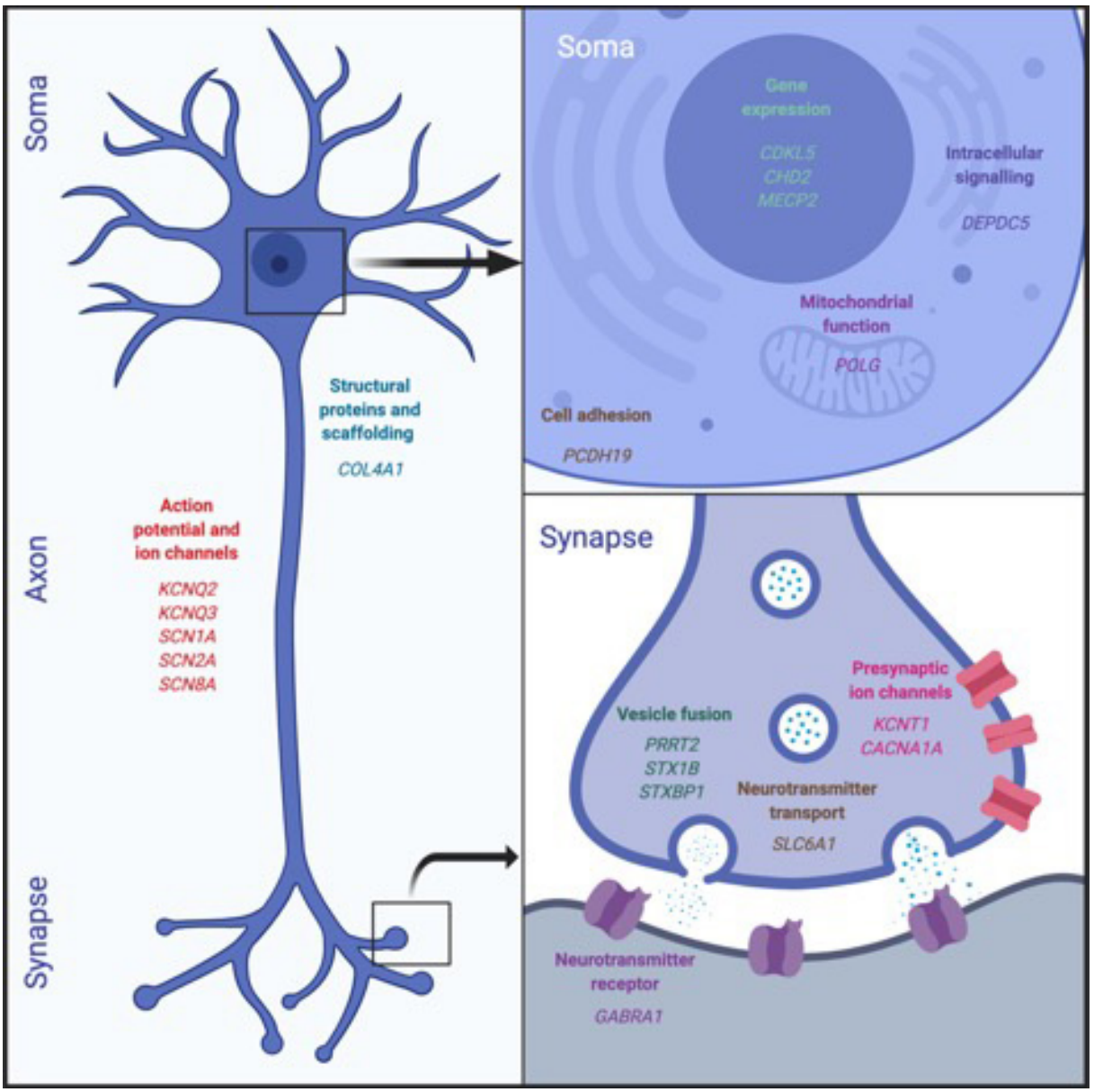

FIGURE 1 | Epilepsy genes. This figure illustrates the functional classes of the most commonly identified genetic mutations in children with DDEs. These affect a broad range of neuronal functions, ranging from gene expression and intracellular signaling to neurotransmission.

Developments in genome editing technology have facilitated the introduction of human disease-causing mutations into the corresponding genes of *Drosophila*, resulting in the improved ability to characterize gene-phenotype relationships as well as to perform high-throughput *in vivo* drug testing (Stilwell et al., 2006). These techniques have advanced the identification of disease-specific epilepsy treatments (Griffin et al., 2018). One example is the study of Dravet syndrome (DS), a severe form of infant-onset febrile epilepsy that is often co-morbid with other developmental disorders. DS patients are typically pharmaco-resistant (Chiron, 2011; Dravet, 2011; Griffin et al., 2018), with many common antiepileptic drugs even aggravating their seizures (Guerrini et al., 1998; Chiron, 2011; Nissenkorn et al., 2019). Thus, there exists a demand for increased therapeutic treatment options, an issue that is further complicated by the multitude of different DS-causing mutations (Meng et al., 2015; Schutte et al., 2016). Electrophysiology research has revealed that these mutations exhibit considerable variation in their channel characteristics ("channotype"), ranging from gain-of-function to loss-of-function effects (Escayg and Goldin, 2010; Meng et al., 2015; Peters et al., 2016). Elucidating the molecular variations behind this functional heterogeneity can inform drug selection for preliminary pharmacological testing, which can in turn provide *in vivo* validation for electrophysiology results.

Combining these two techniques can therefore be a powerful approach to better understanding and treating DS, serving as informative steps on the pathway to clinical drug testing.

A common mutation target for generating DS models is the *Drosophila para* gene, encoding the voltage-gated sodium channels and corresponding to the human *SCN1A* gene in which many DS-causing mutations have been identified (Dravet, 2011). The *Drosophila para* gene is edited using CRISPR-cas9 to reproduce specific human *DS* causing mutations in *SCN1A,* whilst also introducing a marker mutation (e.g., eye color). In these flies, transient seizure-like behaviors [falling into their backs or sides and beginning to twitch their legs and wings, sometimes accompanied by abdominal curling (Sun et al., 2012; Schutte et al., 2016; Griffin et al., 2018)] can be induced by hyperthermia (**Supplementary Video S1**). Once a model organism line is validated, potential drug therapies can be assessed by mixing the therapeutic target of interest into liquified cornmeal food and allowing the flies to feed on it before subsequent seizure assays (Sun et al., 2012). Thus, modeling epilepsy with *Drosophila* enables researchers to use a simple model to shed light on the functional characterization of genetic data and to perform large-scale screenings of antiepileptic drug candidates, providing a cost-effective form of preclinical testing.

Danio rerio (zebrafish) is another model appropriate for linking genotype to phenotype in patient models of neurodevelopmental disorders. A major reason for this is the phylogenetic proximity of this vertebrate model, the high homology of the zebrafish and human genomes (∼80% homology), and the ease of genetic manipulation in the zebrafish. In fact, genetic modification in zebrafish is highly efficient, allowing comprehensive *in vivo* studies even of neurodevelopmental disorders with complex genetic backgrounds. One example is a recent study in which 132 schizophrenia risk variants were generated using CRISPR-Cas9 (Thyme et al., 2019). A wide array of zebrafish models have also been developed across epilepsy genes, and genes associated with broader neurodevelopmental phenotypes [e.g., *scn1lab* (Baraban et al., 2013), *gabrg2* (Liao et al., 2019), *GABRA1* (Samarut et al., 2018), *mecp2* (Pietri et al., 2013), *grin2*a/b (Thyme et al., 2019), and others]. Importantly, despite different brain anatomy and physiology to mammalian counterparts, various zebrafish models exhibit phenotypes analogous to corresponding rodent models and clinical phenotypes. In particular a zebrafish model of DS carrying a loss-of-function mutation in the *scn1lab* gene, exhibits spontaneous electrographic abnormalities reminiscent of seizures (Baraban et al., 2013). Such recordings, obtained from field electrodes placed in the midbrain of agar immobilized larval zebrafish, appear as brief, small amplitude inter-ictal like events and prolonged, multi-spike ictal-like discharges which are qualitatively comparable to epileptiform discharges in patients and mammalian epilepsy models. Furthermore, *GABRA1*$^{-/-}$ and *gabrg2*$^{-/-}$ larvae, both modeling mutations reported in common epilepsy syndromes (Wallace et al., 2001; Johannesen et al., 2016), exhibit reflexive seizure-like events in response to light stimulation, reported as convulsive motor abnormalities and abnormal brain synchrony (**Supplementary Video S2**; Samarut et al., 2018; Liao et al., 2019).

It is, however, important to note that zebrafish lack a cortex and therefore qualitative homologies between zebrafish and human epilepsy (a putative cortical pathology) may be more useful for broad functional characterizations of genetic epilepsies, while specific seizure subtypes may be better modeled by more complex model organisms systems. Nonetheless, given that common anti-epileptic drugs correct electrographic, and motor abnormalities in these zebrafish models, the underlying neuropathology is likely to be conserved in genetic models (Baraban et al., 2013; Samarut et al., 2018; Liao et al., 2019). Finally, zebrafish larvae are also highly amenable to high-throughput behavioral drug screens, which have already identified novel drugs for the treatment of DS, thus closing the loop from fish tank to bedside (Griffin et al., 2018).

Therefore the larval zebrafish can provide realistic models of a wide array of neurodevelopmental disorders which may open alternative avenues for investigation at scales not possible in its mammalian counterparts making them complementary models.

FROM GENE MUTATION TO BRAIN NETWORK PERTURBATION (TEMPORAL MACROSCALE)

As discussed above, in order to translate an improved genetic understanding of neurodevelopmental disorders into novel therapies, a detailed understanding of pathomechanisms is required. Simple animal models can enable the characterization of the functional consequences of genetic mutations at multiple different scales, ranging from single-cell behavior to whole-brain dynamics, and allow this translation much more rapidly and at times more comprehensively than in mammalian models.

The utility of simple model systems for bridging this gap is particularly evident in epilepsy. Given that seizures are an emergent property of microcircuits, understanding the effect of specific genetic mutations at a network level is necessary to explain the emergence of clinical phenotypes. At this juncture, the larval zebrafish is a particularly appealing model for studying brain network dynamics due to its amenability to whole brain imaging at single-cell resolution, allowing identification of abnormal dynamics at multiple scales (Ahrens et al., 2013). The larval fish at 7 days-post-fertilization has a small, simple brain (100,000 cells, <1 mm^3) but is capable of a variety of complex behaviors whose brain dynamics can be monitored accurately (**Figure 2**). Various genetic lines of pigment deficient larval zebrafish have been developed which enable unrestricted optical access into the developing brain (Antinucci and Hindges, 2016). Furthermore, the development of various transgenic reporters of cellular activity, such as GCaMP and RGECO enable the imaging of calcium dynamics in single cells and whole brain networks during behavior, using fluorescence microscopy (**Figure 2**; Walker et al., 2013; Wolf et al., 2017; Chen et al., 2018). In fact, various transgenic lines have also been developed to monitor specifically GABA (Marvin et al., 2019) or glutamate (Marvin et al., 2013) signaling *in vivo*. Given that these cellular reporters have been utilized to characterize neuronal function across brain scales [from synapses to cell populations and brain

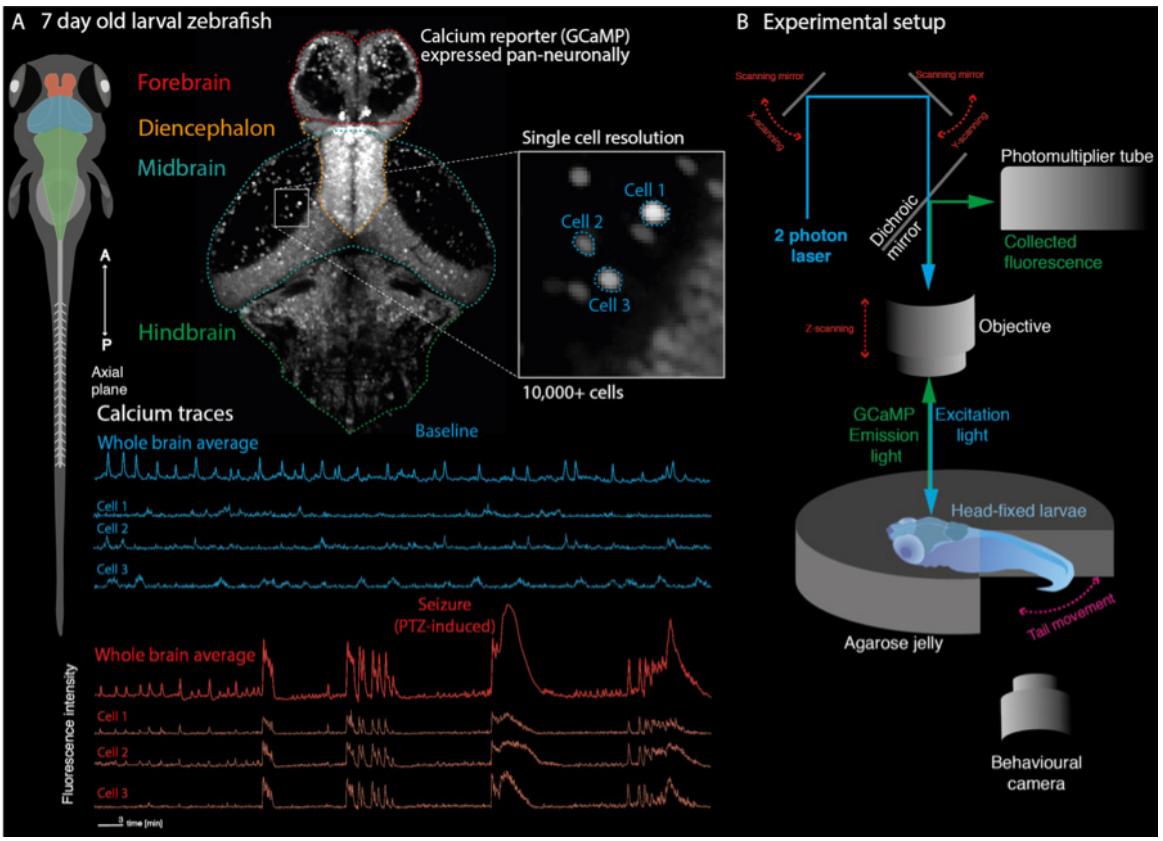

FIGURE 2 | Recording whole-brain dynamics at single-cell resolution in zebrafish models of neurodevelopmental disorders. **(A)** Larval zebrafish at 7 days post fertilization are freely behaving and have all the major anatomical subdivisions of the vertebrate brain (left). Transgenic lines expressing genetically encoded calcium indicators in neurons can be used to record neuronal function through fluorescence signals. Because of their small size, the whole brain can be captured at single cell resolution (top). This allows recording of whole brain dynamics alongside single-cell behavior (bottom). **(B)** Zebrafish larvae can be embedded in transparent agarose, allowing *in vivo* imaging using fluorescence microscopy (shown here is a two-photon microscopy setup). Depending on the experimental paradigm, behavioral output can further be tracked using recordings of tail movements in tail free set ups. This allows e.g., linking of convulsive movements and brain hypersynchrony to identify epileptic seizures in the zebrafish.

networks (Walker et al., 2013; Boulanger-Weill et al., 2017; Betzel, 2018)], functional imaging of zebrafish genetic models may provide a unique window into the multi-scale functional consequences of upstream channel abnormalities. Thus, it may provide an explanatory bridge between gene mutation and whole brain clinical phenotypes.

While at present, the majority of zebrafish functional imaging studies have characterized acute, induced seizures using the GABA-A antagonist pentelynetetrazole (PTZ), a variety of useful network features have been identified which may provide insight into future genetic models. Multiple studies have reported increased functional connectivity across local and distributed brain regions during seizure events (**Figure 2A**; Diaz Verdugo et al., 2019; Liu and Baraban, 2019), in accordance with reports of increased phase locking in EEG recordings during seizures (Meisel et al., 2012).

Importantly, single cell-level information can be harnessed from functional imaging data to explain seizure network dynamics. For example, zebrafish imaging suggests that seizures emerge as cellular ensembles, which are composed of more spatially distant cells than pre-seizure (Diaz Verdugo et al., 2019; Liu and Baraban, 2019). Furthermore, the role of cell subtypes in the emergence of network abnormalities may be probed with the application of double transgenic larval zebrafish, expressing calcium reporters and specific cellular subtype reporters (Lyons et al., 2003; Xi et al., 2011; Shimizu et al., 2015). Such approaches have demonstrated that astrocytes facilitate widespread neuronal synchrony during generalized seizures, thereby enabling seizure state transitions (Diaz Verdugo et al., 2019). Identifying critical cell subpopulations in this way in genetic epilepsies has the potential to identify novel treatment targets in patients. Interestingly, model-based approaches which are widely used to explain network phenomena in EEG data can also be applied to calcium imaging data to test causal mechanisms underlying network features of seizures (Rosch et al., 2018). Such approaches have shown that acute seizures are caused by parameter changes in local excitation-inhibition balance, and alterations in timescales of excitatory and inhibitory connectivity. In this way the cellular mechanisms underlying observed network features in functional imaging data can be uncovered, to provide a

conceptual bridge to explaining EEG phenomena during seizures, such as hypersynchrony and transitions between network states. As more genetic lines become available (Baraban et al., 2013; Samarut et al., 2018; Swaminathan et al., 2018; Liao et al., 2019), such imaging approaches may be harnessed to link gene mutation with network perturbation.

Flies have also become convenient models to perform neuronal cell recording in the adult brain (*ex vivo*) that can be studies in the context of genetic and/or pharmacological manipulations (Gu and O'dowd, 2007; Roemmich et al., 2018). As an example, electrophysiological studies carried out in adult flies that were genetically modified to mimic DS were pioneers in showing the link between pathological missense mutations and disturbances of sodium ion current activity at the receptor level (Sun et al., 2012; Schutte et al., 2014). These cellular experimentations in a genuine *in vivo* context are very advantageous in order to unravel the basic cellular mechanisms of brain circuit function and malfunction. They can also be suitable for evaluating the mechanism of action of candidate therapies against neurodevelopmental disorders that were first identified through behavioral assays.

Remarkably, the larval zebrafish is also a suitable model for longitudinal studies of neural development. Indeed, the transparency of the embryo allows one to follow *in vivo* organogenesis, in particular the observation of central nervous system structures with a single-cell resolution. Moreover, there is a large repertoire of available transgenic lines expressing fluorescent reporters in different neural cell populations such as post-mitotic neurons (huc/elavl3^{+}) (Park et al., 2000), GABAergic interneurons (dlx5/6^{+}) (Zerucha et al., 2000), glutamatergic neurons (vglut2a^{+}) (Kimura et al., 2006) or oligodendrocytes (olig2^{+}) (Shin et al., 2003). This is of a particular interest in the context of neurodevelopmental disorders for which one can expect defects in brain wiring to occur during early neurodevelopment. In this context, the accessibility of the zebrafish embryo from the earliest stages of development is an advantage compared to mammals in which the embryos develops *in utero*. The use of larval zebrafish has proven particularly useful in modeling several human neurological disorders with a developmental component such as ASD or epileptic encephalopathy. For example, using specific transgenic lines identifying excitatory versus inhibitory neuronal networks, Hoffman et al. (2016) revealed a specific deficit of GABAergic neuronal population networks in the forebrain of zebrafish larvae mutant for *CNTNAP2*, an ASD-related gene. Another zebrafish model of ASD (shank3b$^{-/-}$) displays a reduction in the overall brain neuronal content as revealed by a transgenic line expressing a fluorescent protein in post-mitotic neurons (Liu et al., 2018). Interestingly, the development of these neuronal populations can be followed over time and the defects can therefore be monitored throughout neurodevelopment. More recently, two genetic models of epilepsy [idiopathic generalized epilepsy: *GABRA1*$^{-/-}$ (Samarut et al., 2018), and focal epilepsy: depdc5$^{-/-}$ (Swaminathan et al., 2018)] have been generated. These models depict relevant phenotypes to the human disorders, but more interestingly, they demonstrated impaired GABAergic synaptic network branching in the mutant larval brains identifying a potential pathomechanism. In this way, zebrafish genetic models can be harnessed to further understand the developmental component of these diseases and in so doing, at least partially, account for the pathogenicity of the mutations tested.

As a result, simple models like flies and zebrafish appear to be an amenable model to (i) mimic human genetic condition associated with neurological disorders, (ii) investigate the consequence at the neuronal network activity level through *in vivo* calcium imaging, and (iii) unravel neurodevelopmental defects associated with the disorder.

CONCLUSION: SIMPLE MODELS AS GENETIC AVATARS OF HUMAN PATIENTS FOR A SYSTEMIC APPROACH (FROM GENE TO PHYSIOLOGY)

In the current context of fast-evolving accessibility to genetic diagnosis, more and more genetic basis of neurological disorders are being unraveled. They opened the door to a new challenges that is the translation of this genetic data into functional read-out. Can we predict the functional consequence of a specific mutation in a particular gene? What are the effects of a specific mutation on the activity of the protein? at the level of the neuronal network? At the scale of whole neurodevelopment? These puzzling questions necessitate the use of fast and complementary *in vivo* approaches. In this review, we are discussing how simple animal models can be employed to bridge the gap between genetic diagnosis and functional studies. Considering the fast development of mutagenesis techniques that now allow to mimic a specific genetic mutation in these simple models, plus their relative low-cost of housing as well as their fast generation time, they represent a model of choice to study neurodevelopmental disorders in an integrated fashion and at multiple scales. Thanks to their versatility, these simple animal models can unravel the basic pathomechanims of gene mutations and therefore open new avenues for therapy development. As mentioned previously, they are also convenient for standardize procedures, in particular for high-throughput screening of small molecules. Interestingly, they are also very convenient for genetic manipulation. Indeed, by microinjecting molecular tools in the one-cell stage embryo, it is possible to either knockdown [with morpholinos or CRISPRi (Long et al., 2015)], knockout [by CRISPR/Cas9 genome editing (Hwang et al., 2013)] or overexpress [by CRISPRa (Long et al., 2015) or by injecting *in vitro* transcribed messenger RNAs or transposon plasmids for transgenesis] the expression of a gene of interest. As a result, these simple animal models can also serve as tools to test genetic-derived therapeutic strategies through restorative functional assays after modulating the expression of candidate genes.

AUTHOR CONTRIBUTIONS

RR, DB, LJ, PR, and ÉS wrote the manuscript. CP performed the *Drosophila* recording. ÉS performed the fish recording.

FUNDING

This work is supported by the Rare Disease Model and Mechanism Network, the Rare Disease Foundation and Dravet Canada. RR is supported by a Sir Henry Wellcome Fellowship (Wellcome Trust, United Kingdom; Grant Number 209164/Z/17/Z). DB is supported by the Medical Research Council and the Sackler Institute for Translational Neurodevelopment.

SUPPLEMENTARY MATERIAL

The Supplementary Material for this article can be found online at: https://www.frontiersin.org/articles/10.3389/fncel.2019.00556/full#supplementary-material

VIDEO S1 | Temperature-induced seizures in *Drosophila* with a mutation in the *Para* gene, analogous to *SCN1A*. To introduce the human A1273V mutation into the corresponding location on *Drosophila's* para gene (A1356V), we used the *Drosophila* CRISPR-Cas9 system developed by a set of labs at Brown and University of Wisconsin https://flycrispr.org/about/ (citation). We designed 2 RNA ides and a donor vector with mutated template DNA for homology-directed repair as well as insertion of a DsRed eye reporter in the subsequent intron. Embryo injections and genetic crosses were performed by the company BestGene, Inc. (Chino Hills, CA, United States).

VIDEO S2 | Light-induced seizures in zebrafish with a mutation in the *GABRA1* gene. As described previously in Samarut et al. (2018). Infrared camera recording of 5, 5 wpf *GABRA1*$^{+/+}$(top, $n = 4$), ±(middle, $n = 4$), and −/− (bottom, $n = 4$) embryos maintained in a 12-well plate, using a DanioVision recording chamber. Light was switched on about 5 s after the video started (see icon on the top left corner). Immediately after light turning on, the −/− juveniles underwent a first phase of tonic-like seizures lasting few seconds and during wish they convulsed heavily and lost their posture. After a short pause, they underwent a second clonic-like phase that lasted up to 1 min and during which they swam quickly in circle (the "whirlpool" phenotype).

REFERENCES

Addis, L., Rosch, R. E., Valentin, A., Makoff, A., Robinson, R., Everett, K. V., et al. (2016). Analysis of rare copy number variation in absence epilepsies. *Neurol. Genet.* 2:e56. doi: 10.1212/NXG.0000000000000056

Ahrens, M. B., Orger, M. B., Robson, D. N., Li, J. M., and Keller, P. J. (2013). Whole-brain functional imaging at cellular resolution using light-sheet microscopy. *Nat. Methods* 10, 413–420. doi: 10.1038/nmeth.2434

Antinucci, P., and Hindges, R. (2016). A crystal-clear zebrafish for in vivo imaging. *Sci. Rep.* 6:29490. doi: 10.1038/srep29490

Baraban, S. C. (2007). Emerging epilepsy models: insights from mice, flies, worms and fish. *Curr. Opin. Neurol.* 20, 164–168. doi: 10.1097/wco.0b013e328042bae0

Baraban, S. C., Dinday, M. T., and Hortopan, G. A. (2013). Drug screening in Scn1a zebrafish mutant identifies clemizole as a potential Dravet syndrome treatment. *Nat. Commun.* 4:2410. doi: 10.1038/ncomms3410

Ben-Shalom, R., Keeshen, C. M., Berrios, K. N., An, J. Y., Sanders, S. J., and Bender, K. J. (2017). Opposing effects on NaV1.2 function underlie differences between SCN2A variants observed in individuals with autism spectrum disorder or infantile seizures. *Biol. Psychiatry* 82, 224–232. doi: 10.1016/j.biopsych.2017.01.009

Betzel, R. (2018). Organizing principles of whole-brain functional connectivity in zebrafish larvae. *bioRxiv* [Preprint]. doi: 10.1101/496414

Bier, E. (2005). *Drosophila*, the golden bug, emerges as a tool for human genetics. *Nat. Rev. Genet.* 6, 9–23. doi: 10.1038/nrg1503

Boulanger-Weill, J., Candat, V., Jouary, A., Romano, S. A., Perez-Schuster, V., and Sumbre, G. (2017). Functional interactions between newborn and mature neurons leading to integration into established neuronal circuits. *Curr. Biol.* 27:e1705. doi: 10.1016/j.cub.2017.05.029

Chen, X., Mu, Y., Hu, Y., Kuan, A. T., Nikitchenko, M., Randlett, O., et al. (2018). Brain-wide organization of neuronal activity and convergent sensorimotor transformations in larval Zebrafish. *Neuron* 100:e875. doi: 10.1016/j.neuron.2018.09.042

Chiron, C. (2011). Current therapeutic procedures in dravet syndrome. *Dev. Med. Child Neurol.* 53(Suppl. 2), 16–18. doi: 10.1111/j.1469-8749.2011.03967.x

Cooper, G. M., Coe, B. P., Girirajan, S., Rosenfeld, J. A., Vu, T. H., Baker, C., et al. (2011). A copy number variation morbidity map of developmental delay. *Nat. Genet.* 43, 838–846. doi: 10.1038/ng.909

Cunliffe, V. T., Baines, R. A., Giachello, C. N., Lin, W. H., Morgan, A., Reuber, M., et al. (2015). Epilepsy research methods update: understanding the causes of epileptic seizures and identifying new treatments using non-mammalian model organisms. *Seizure* 24, 44–51. doi: 10.1016/j.seizure.2014.09.018

Deciphering Developmental Disorders, S. (2017). Prevalence and architecture of de novo mutations in developmental disorders. *Nature* 542, 433–438. doi: 10.1038/nature21062

Diaz Verdugo, C., Myren-Svelstad, S., Aydin, E., Van Hoeymissen, E., Deneubourg, C., Vanderhaeghe, S., et al. (2019). Glia-neuron interactions underlie state transitions to generalized seizures. *Nat. Commun.* 10:3830. doi: 10.1038/s41467-019-11739-z

Dravet, C. (2011). The core Dravet syndrome phenotype. *Epilepsia* 52(Suppl. 2), 3–9. doi: 10.1111/j.1528-1167.2011.02994.x

Epi, K. C., Epilepsy Phenome Genome, P., Allen, A. S., Berkovic, S. F., Cossette, P., Delanty, N., et al. (2013). De novo mutations in epileptic encephalopathies. *Nature* 501, 217–221. doi: 10.1038/nature12439

Escayg, A., and Goldin, A. L. (2010). Sodium channel SCN1A and epilepsy: mutations and mechanisms. *Epilepsia* 51, 1650–1658. doi: 10.1111/j.1528-1167.2010.02640.x

Fortini, M. E., Skupski, M. P., Boguski, M. S., and Hariharan, I. K. (2000). A survey of human disease gene counterparts in the *Drosophila* genome. *J. Cell Biol.* 150, F23–F30.

Fromer, M., Pocklington, A. J., Kavanagh, D. H., Williams, H. J., Dwyer, S., Gormley, P., et al. (2014). De novo mutations in schizophrenia implicate synaptic networks. *Nature* 506, 179–184. doi: 10.1038/nature12929

Grant, S. G. (2012). Synaptopathies: diseases of the synaptome. *Curr. Opin. Neurobiol.* 22, 522–529. doi: 10.1016/j.conb.2012.02.002

Griffin, A., Hamling, K. R., Hong, S., Anvar, M., Lee, L. P., and Baraban, S. C. (2018). Preclinical animal models for dravet syndrome: seizure phenotypes, comorbidities and drug screening. *Front. Pharmacol.* 9:573. doi: 10.3389/fphar.2018.00573

Gu, H., and O'dowd, D. K. (2007). Whole cell recordings from brain of adult *Drosophila*. *J. Vis. Exp.* 2007:248.

Guerrini, R., Dravet, C., Genton, P., Belmonte, A., Kaminska, A., and Dulac, O. (1998). Lamotrigine and seizure aggravation in severe myoclonic epilepsy. *Epilepsia* 39, 508–512. doi: 10.1111/j.1528-1157.1998.tb01413.x

Hoffman, E. J., Turner, K. J., Fernandez, J. M., Cifuentes, D., Ghosh, M., Ijaz, S., et al. (2016). Estrogens suppress a behavioral phenotype in zebrafish mutants of the autism risk gene. *CNTNAP2. Neuron* 89, 725–733. doi: 10.1016/j.neuron.2015.12.039

Hwang, W. Y., Fu, Y., Reyon, D., Maeder, M. L., Tsai, S. Q., Sander, J. D., et al. (2013). Efficient genome editing in zebrafish using a CRISPR-Cas system. *Nat. Biotechnol.* 31, 227–229. doi: 10.1038/nbt.2501

International League Against Epilepsy Consortium on Complex Epilepsies (2014). Genetic determinants of common epilepsies: a meta-analysis of genome-wide association studies. *Lancet Neurol.* 13, 893–903. doi: 10.1016/s1474-4422(14)70171-1

Johannesen, K., Marini, C., Pfeffer, S., Moller, R. S., Dorn, T., Niturad, C. E., et al. (2016). Phenotypic spectrum of GABRA1: from generalized epilepsies to severe epileptic encephalopathies. *Neurology* 87, 1140–1151. doi: 10.1212/WNL.0000000000003087

Kimura, Y., Okamura, Y., and Higashijima, S. (2006). alx, a zebrafish homolog of Chx10, marks ipsilateral descending excitatory interneurons that participate in the regulation of spinal locomotor circuits. *J. Neurosci.* 26, 5684–5697. doi: 10.1523/jneurosci.4993-05.2006

Liao, M., Kundap, U., Rosch, R. E., Burrows, D. R. W., Meyer, M. P., Ouled Amar Bencheikh, B., et al. (2019). Targeted knockout of GABA-A receptor gamma 2 subunit provokes transient light-induced reflex seizures in zebrafish larvae. *Dis. Model. Mech.* 12:dmm040782. doi: 10.1242/dmm.040782

Liu, C. X., Li, C. Y., Hu, C. C., Wang, Y., Lin, J., Jiang, Y. H., et al. (2018). CRISPR/Cas9-induced shank3b mutant zebrafish display autism-like behaviors. *Mol. Autism.* 9:23. doi: 10.1186/s13229-018-0204-x

Liu, J., and Baraban, S. C. (2019). Network properties revealed during multi-scale calcium imaging of seizure activity in Zebrafish. *eNeuro* 6, ENEURO.0041-19.2019.

Long, L., Guo, H., Yao, D., Xiong, K., Li, Y., Liu, P., et al. (2015). Regulation of transcriptionally active genes via the catalytically inactive Cas9 in *C. elegans* and *D. rerio*. *Cell Res.* 25, 638–641. doi: 10.1038/cr.2015.35

Lyons, D. A., Guy, A. T., and Clarke, J. D. (2003). Monitoring neural progenitor fate through multiple rounds of division in an intact vertebrate brain. *Development* 130, 3427–3436. doi: 10.1242/dev.00569

Marshall, C. R., Howrigan, D. P., Merico, D., Thiruvahindrapuram, B., Wu, W., Greer, D. S., et al. (2017). Contribution of copy number variants to schizophrenia from a genome-wide study of 41,321 subjects. *Nat. Genet.* 49, 27–35. doi: 10.1038/ng.3725

Marvin, J. S., Borghuis, B. G., Tian, L., Cichon, J., Harnett, M. T., Akerboom, J., et al. (2013). An optimized fluorescent probe for visualizing glutamate neurotransmission. *Nat. Methods* 10, 162–170. doi: 10.1038/nmeth.2333

Marvin, J. S., Shimoda, Y., Magloire, V., Leite, M., Kawashima, T., Jensen, T. P., et al. (2019). A genetically encoded fluorescent sensor for in vivo imaging of GABA. *Nat. Methods* 16, 763–770. doi: 10.1038/s41592-019-0471-2

Mefford, H. C., Muhle, H., Ostertag, P., Von Spiczak, S., Buysse, K., Baker, C., et al. (2010). Genome-wide copy number variation in epilepsy: novel susceptibility loci in idiopathic generalized and focal epilepsies. *PLoS Genet.* 6:e1000962. doi: 10.1371/journal.pgen.1000962

Meisel, C., Storch, A., Hallmeyer-Elgner, S., Bullmore, E., and Gross, T. (2012). Failure of adaptive self-organized criticality during epileptic seizure attacks. *PLoS Comput. Biol.* 8:e1002312. doi: 10.1371/journal.pcbi.1002312

Meng, H., Xu, H. Q., Yu, L., Lin, G. W., He, N., Su, T., et al. (2015). The SCN1A mutation database: updating information and analysis of the relationships among genotype, functional alteration, and phenotype. *Hum. Mutat.* 36, 573–580. doi: 10.1002/humu.22782

Myers, C. T., and Mefford, H. C. (2015). Advancing epilepsy genetics in the genomic era. *Genome Med.* 7:91. doi: 10.1186/s13073-015-0214-7

Nissenkorn, A., Almog, Y., Adler, I., Safrin, M., Brusel, M., Marom, M., et al. (2019). In vivo, in vitro and in silico correlations of four de novo SCN1A missense mutations. *PLoS One* 14:e0211901. doi: 10.1371/journal.pone.0211901

Oates, S., Tang, S., Rosch, R., Lear, R., Hughes, E. F., Williams, R. E., et al. (2018). Incorporating epilepsy genetics into clinical practice: a 360 degrees evaluation. *NPJ Genom. Med.* 3:13. doi: 10.1038/s41525-018-0052-9

Park, H. C., Kim, C. H., Bae, Y. K., Yeo, S. Y., Kim, S. H., Hong, S. K., et al. (2000). Analysis of upstream elements in the HuC promoter leads to the establishment of transgenic zebrafish with fluorescent neurons. *Dev. Biol.* 227, 279–293. doi: 10.1006/dbio.2000.9898

Peters, C., Rosch, R. E., Hughes, E., and Ruben, P. C. (2016). Temperature-dependent changes in neuronal dynamics in a patient with an SCN1A mutation and hyperthermia induced seizures. *Sci. Rep.* 6:31879. doi: 10.1038/srep31879

Pietri, T., Roman, A. C., Guyon, N., Romano, S. A., Washbourne, P., Moens, C. B., et al. (2013). The first mecp2-null zebrafish model shows altered motor behaviors. *Front. Neural. Circuits* 7:118. doi: 10.3389/fncir.2013.00118

Pinto, D., Pagnamenta, A. T., Klei, L., Anney, R., Merico, D., Regan, R., et al. (2010). Functional impact of global rare copy number variation in autism spectrum disorders. *Nature* 466, 368–372. doi: 10.1038/nature09146

Roemmich, A. J., Schutte, S. S., and O'dowd, D. K. (2018). Ex vivo whole-cell recordings in adult *Drosophila* brain. *Bio. Protoc.* 8:e2467. doi: 10.21769/BioProtoc.2467

Rosch, R. E., Hunter, P. R., Baldeweg, T., Friston, K. J., and Meyer, M. P. (2018). Calcium imaging and dynamic causal modelling reveal brain-wide changes in effective connectivity and synaptic dynamics during epileptic seizures. *PLoS Comput. Biol.* 14:e1006375. doi: 10.1371/journal.pcbi.1006375

Rubin, G. M., Yandell, M. D., Wortman, J. R., Gabor Miklos, G. L., Nelson, C. R., Hariharan, I. K., et al. (2000). Comparative genomics of the eukaryotes. *Science* 287, 2204–2215. doi: 10.1126/science.287.5461.2204

Samarut, E., Swaminathan, A., Riche, R., Liao, M., Hassan-Abdi, R., Renault, S., et al. (2018). Gamma-Aminobutyric acid receptor alpha 1 subunit loss of function causes genetic generalized epilepsy by impairing inhibitory network neurodevelopment. *Epilepsia* 59, 2061–2074. doi: 10.1111/epi.14576

Scheffer, I. E., French, J., Hirsch, E., Jain, S., Mathern, G. W., Moshe, S. L., et al. (2016). Classification of the epilepsies: new concepts for discussion and debate-Special report of the ILAE Classification Task Force of the Commission for Classification and Terminology. *Epilepsia Open* 1, 37–44. doi: 10.1002/epi4.5

Schizophrenia Working Group of the Psychiatric Genomics Consortium (2014). Biological insights from 108 schizophrenia-associated genetic loci. *Nature* 511, 421–427. doi: 10.1038/nature13595

Schutte, R. J., Schutte, S. S., Algara, J., Barragan, E. V., Gilligan, J., Staber, C., et al. (2014). Knock-in model of Dravet syndrome reveals a constitutive and conditional reduction in sodium current. *J. Neurophysiol.* 112, 903–912. doi: 10.1152/jn.00135.2014

Schutte, S. S., Schutte, R. J., Barragan, E. V., and O'dowd, D. K. (2016). Model systems for studying cellular mechanisms of SCN1A-related epilepsy. *J. Neurophysiol.* 115, 1755–1766. doi: 10.1152/jn.00824.2015

Sebat, J., Lakshmi, B., Malhotra, D., Troge, J., Lese-Martin, C., Walsh, T., et al. (2007). Strong association of de novo copy number mutations with autism. *Science* 316, 445–449.

Seyfried, T. N., and Glaser, G. H. (1985). A review of mouse mutants as genetic models of epilepsy. *Epilepsia* 26, 143–150. doi: 10.1111/j.1528-1157.1985.tb05398.x

Shimizu, Y., Ito, Y., Tanaka, H., and Ohshima, T. (2015). Radial glial cell-specific ablation in the adult Zebrafish brain. *Genesis* 53, 431–439. doi: 10.1002/dvg.22865

Shin, J., Park, H. C., Topczewska, J. M., Mawdsley, D. J., and Appel, B. (2003). Neural cell fate analysis in zebrafish using olig2 BAC transgenics. *Methods Cell Sci.* 25, 7–14. doi: 10.1023/b:mics.0000006847.09037.3a

Song, J., and Tanouye, M. A. (2008). From bench to drug: human seizure modeling using *Drosophila*. *Prog. Neurobiol.* 84, 182–191. doi: 10.1016/j.pneurobio.2007.10.006

Stefansson, H., Rujescu, D., Cichon, S., Pietilainen, O. P., Ingason, A., Steinberg, S., et al. (2008). Large recurrent microdeletions associated with schizophrenia. *Nature* 455, 232–236.

Stilwell, G. E., Saraswati, S., Littleton, J. T., and Chouinard, S. W. (2006). Development of a *Drosophila* seizure model for in vivo high-throughput drug screening. *Eur. J. Neurosci.* 24, 2211–2222.

Sun, L., Gilligan, J., Staber, C., Schutte, R. J., Nguyen, V., O'dowd, D. K., et al. (2012). A knock-in model of human epilepsy in *Drosophila* reveals a novel cellular mechanism associated with heat-induced seizure. *J. Neurosci.* 32, 14145–14155. doi: 10.1523/JNEUROSCI.2932-12.2012

Swaminathan, A., Hassan-Abdi, R., Renault, S., Siekierska, A., Riche, R., Liao, M., et al. (2018). Non-canonical mTOR-independent role of DEPDC5 in regulating GABAergic network development. *Curr. Biol.* 28:e1925. doi: 10.1016/j.cub.2018.04.061

Thyme, S. B., Pieper, L. M., Li, E. H., Pandey, S., Wang, Y., Morris, N. S., et al. (2019). Phenotypic landscape of schizophrenia-associated genes defines candidates and their shared functions. *Cell* 177:e420. doi: 10.1016/j.cell.2019.01.048

Turner, T. N., Coe, B. P., Dickel, D. E., Hoekzema, K., Nelson, B. J., Zody, M. C., et al. (2017). Genomic patterns of De Novo mutation in simplex Autism. *Cell* 171:e712. doi: 10.1016/j.cell.2017.08.047

Walker, A. S., Burrone, J., and Meyer, M. P. (2013). Functional imaging in the zebrafish retinotectal system using RGECO. *Front. Neural. Circuits* 7:34. doi: 10.3389/fncir.2013.00034

Wallace, R. H., Marini, C., Petrou, S., Harkin, L. A., Bowser, D. N., Panchal, R. G., et al. (2001). Mutant GABA(A) receptor gamma2-subunit in childhood absence epilepsy and febrile seizures. *Nat. Genet.* 28, 49–52. doi: 10.1038/ng0501-49

Wolf, S., Dubreuil, A. M., Bertoni, T., Bohm, U. L., Bormuth, V., Candelier, R., et al. (2017). Sensorimotor computation underlying phototaxis in zebrafish. *Nat. Commun.* 8:651. doi: 10.1038/s41467-017-00310-3

Xi, Y., Yu, M., Godoy, R., Hatch, G., Poitras, L., and Ekker, M. (2011). Transgenic zebrafish expressing green fluorescent protein in dopaminergic neurons of the ventral diencephalon. *Dev. Dyn.* 240, 2539–2547. doi: 10.1002/dvdy.22742

Yu, F. H., Mantegazza, M., Westenbroek, R. E., Robbins, C. A., Kalume, F., Burton, K. A., et al. (2006). Reduced sodium current in GABAergic interneurons in a mouse model of severe myoclonic epilepsy in infancy. *Nat. Neurosci.* 9, 1142–1149. doi: 10.1038/nn1754

Zerucha, T., Stühmer, T., Hatch, G., Park, B. K., Long, Q., Yu, G., et al. (2000). A highly conserved enhancer in the Dlx5/Dlx6 intergenic region is the site of cross-regulatory interactions between Dlx genes in the embryonic forebrain. *J. Neurosci.* 20, 709–721. doi: 10.1523/jneurosci.20-02-00709.2000

Conflict of Interest: ÉS is a co-founder of Modelis Inc.

The remaining authors declare that the research was conducted in the absence of any commercial or financial relationships that could be construed as a potential conflict of interest.

frontiers in Cellular Neuroscience

MINI REVIEW
published: 14 January 2020
doi: 10.3389/fncel.2019.00587

Transcriptional Regulation of Channelopathies in Genetic and Acquired Epilepsies

Karen M. J. van Loo and Albert J. Becker*

Department of Neuropathology, Section for Translational Epilepsy Research, University of Bonn Medical Center, Bonn, Germany

Epilepsy is a common neurological disorder characterized by recurrent uncontrolled seizures and has an idiopathic "*genetic*" etiology or a symptomatic "*acquired*" component. Genetic studies have revealed that many epilepsy susceptibility genes encode ion channels, including voltage-gated sodium, potassium and calcium channels. The high prevalence of ion channels in epilepsy pathogenesis led to the causative concept of "ion channelopathies," which can be elicited by specific mutations in the coding or promoter regions of genes in *genetic* epilepsies. Intriguingly, expression changes of the same ion channel genes by augmentation of specific transcription factors (TFs) early after an insult can underlie *acquired* epilepsies. In this study, we review how the transcriptional regulation of ion channels in both *genetic* and *acquired* epilepsies can be controlled, and compare these epilepsy "ion channelopathies" with other neurodevelopmental disorders.

Keywords: genetic and acquired epilepsies, ion channels, channelopathies, transcriptional regulation, neurodevelopmental disorders

OPEN ACCESS

Edited by:
Eleonora Aronica,
University Medical Center Amsterdam, Netherlands

Reviewed by:
Hee Jung Chung,
University of Illinois at Urbana-Champaign, United States
Darrin Brager,
University of Texas at Austin, United States

****Correspondence:***
Karen M. J. van Loo
karen.van_loo@ukb.uni-bonn.de

Received: *12 September 2019*
Accepted: *23 December 2019*
Published: *14 January 2020*

Citation:
van Loo KMJ and Becker AJ (2020) Transcriptional Regulation of Channelopathies in Genetic and Acquired Epilepsies. Front. Cell. Neurosci. 13:587. doi: 10.3389/fncel.2019.00587

INTRODUCTION

Epilepsy is a severe chronic brain disorder characterized by recurrent seizure activity due to aberrant neuronal network activity (Fisher et al., 2014; Fisher, 2015). Despite many years of research, the underlying mechanisms that orchestrate seizure activity are still not fully understood. This is also reflected in the fact that treatment strategies for epilepsy with antiepileptic drugs (AEDs) are insufficient in about one-third of epilepsy patients (Kwan and Sander, 2004). This relatively high level of pharmacoresistance, together with the often severe side effects of AEDs, asks for a better understanding of its etiology and pathogenesis (Löscher et al., 2013).

Nowadays, it is generally accepted that both genetic as well as environmental factors, such as head trauma, brain tumors, brain infection, stroke, autoimmune diseases, status epilepticus (SE) and hippocampal sclerosis (Engel, 1996; Bien and Elger, 2007; Bien et al., 2007; Liu et al., 2016; Pitkänen et al., 2016; Vezzani et al., 2016) can play a role in the etiopathogenesis of epilepsy. Epilepsies with such a causal injury to the central nervous system (CNS) are called *acquired* or *symptomatic* epilepsies, whereas those lacking a clear predisposing cause, are called *idiopathic* or *genetic* epilepsies (Shorvon, 2011).

In the last decades, enormous progress has been made in the discovery of epilepsy genes, resulting in a current list of approximately 1,000 epilepsy-associated genes (reviewed by Wang et al., 2017). Since many of the genes annotated on this list are ion channels, the theory was born that epilepsy is a disease of "ion channelopathies" (Wallace et al., 1998; Reid et al., 2009). Ion channels are pore-forming membrane proteins involved in maintaining ion homeostasis and the generation

and propagation of neuronal action potentials. A disturbance in the neuronal ionic flow might result in hyperexcitability, which can form the basis for seizure activity (Raimondo et al., 2015). In general, ion channels can be divided into two main groups, depending on their mode of activation (Brenowitz et al., 2017). Voltage-gated ion channels are activated by changes in membrane potential and ligand-gated ion channels are opened in response to specific ligands binding to the extracellular domain of the ion channel (Alexander et al., 2015a,b).

In this study, we focus on the transcriptional mechanisms involved in channelopathy-induced epilepsy. We review how the expression of ion channel genes can be affected and compare these mechanisms between *genetic* and *acquired* epilepsies. In addition, we also summarize how these transcriptional mechanisms can play a role in the etiopathogenesis of other neurodevelopmental disorders.

VOLTAGE-GATED AND LIGAND-GATED ION CHANNELS IN GENETIC EPILEPSIES

For decades, scientists try to unravel the molecular background of epilepsies. In 1995, the first epilepsy-associated ion channel was identified; a mutation in a strongly conserved amino acid residue in the acetylcholine receptor alpha 4 subunit (CHRNA4) correlated with autosomal dominant nocturnal frontal lobe epilepsy (ADNFLE; Steinlein et al., 1995). After this first discovery, many other ion channels were reported to be linked to epilepsy, including genes belonging to the voltage-gated sodium, potassium, calcium and hyperpolarization-activated cyclic nucleotide-gated (HCN) channels. Besides the voltage-gated ion channels, also several ligand-gated ion channel genes were identified as epilepsy-associated genes, including ionotropic glutamate receptors, $GABA_A$ receptors and nicotinic acetylcholine receptors (**Table 1**; reviewed by Lerche et al., 2013; Wang et al., 2017; Wei et al., 2017; Oyrer et al., 2018).

Currently, it is thought that *genetic* epilepsy can be the result of: (i) rare variants with high penetrance (also known as monogenic or "common-disease-rare-variant model") or of (ii) common variants with low penetrance (also known as polygenic or "common-disease-common-variants model"; Reich and Lander, 2001; Gibson, 2012; Saint Pierre and Génin, 2014). Such rare variants (or mutations) can nowadays be identified by deep sequencing approaches (e.g., exome sequencing or whole-genome sequencing; Dunn et al., 2018), whereas for the identification of common variants (also known as single nucleotide polymorphisms, SNPs), genome-wide association studies are indispensable in large cohorts of patients and controls (International League Against Epilepsy Consortium on Complex Epilepsies, 2018). However, common variants are often difficult to link unequivocally to disease, since these variants contribute only minimally and might also require an additional environmental factor for a pathological outcome.

In epilepsy, both rare as well as common variants have been identified in ion channel genes. Mutations in the sodium channel *SCN1A*, probably the most studied and best-documented epilepsy gene, can cause a spectrum of epilepsy syndromes including Dravet syndrome and genetic (generalized) epilepsy with febrile Seizures Plus (GEFS+; Brunklaus and Zuberi, 2014), whereas a common variant within an intron of the same gene (rs7587026), was found to associate with mesial temporal lobe epilepsy (mTLE; Kasperaviciute et al., 2013).

Mostly, *genetic* channelopathies are the result of variants within the coding region of the gene. Both missense mutations (mutations causing an amino acid change), as well as nonsense mutations (mutations causing a premature stop codon), can underlie epilepsy pathogenesis by inducing a loss-of-function (LOF) or a gain-of-function (GOF) channelopathy. In addition, also deletions and duplications of (part of) the gene can strongly affect normal channel function (Borlot et al., 2017; Monlong et al., 2018). Since the focus of this review is on the transcriptional regulation of ion channels, listing all genetic variants within the coding regions of ion channel genes is beyond the scope of this article (for reviews, see Deng et al., 2014; Wei et al., 2017; Zhang et al., 2019).

TRANSCRIPTIONAL REGULATION OF GENETIC ION CHANNELOPATHIES

Genetic epilepsies can also be the result of a genetic variant positioned in the promoter region, a splice site, or a regulatory region of the gene. How can variants outside the coding region induce a channelopathy? For *SCN1A* for example, a microdeletion in the 5'-promoter region was found in patients with Dravet syndrome (Nakayama et al., 2010), and another heterozygous mutation in the promoter region (h1u-1962 T >G) was identified in a patient with partial epilepsy and febrile seizures (Gao et al., 2017). Functional analysis of this *SCN1A* h1u-1962 T >G variant revealed a reduction of *SCN1A* promoter activity by 42.1% compared to the wild-type variant (Gao et al., 2017), explaining the relatively mild phenotypical impairment caused by this non-coding variant when compared with effects caused by *SCN1A* coding variants that can result in *null* expression.

A genetic variant can also be located at a splice site, resulting in alternative splicing of the ion channel gene. This process allows a single gene to produce alternative ion channels with different functional characteristics. In particular, for *SCN1A* many alternative splicing mutations have been identified in epilepsy pathogenesis (Lossin, 2009; Thompson et al., 2011; Carvill et al., 2018; **Table 1**).

If a genetic variant is located within the binding site of an activating or repressing transcription factor (TF) or a repressor, it may result in altered regulation of the transcriptional machinery. For example, four different haplotypes, consisting of 13 SNPs located in the 5' region of the *GABRB3* gene were found to segregate with childhood absence epilepsy (CAE; Urak et al., 2006). The *GABRB3* gene encodes the β3 subunit of the $GABA_A$ receptor which mediates phasic (synaptic) and tonic (perisynaptic) inhibition (Farrant and Nusser, 2005; Hirose, 2014). Functional analysis of these haplotypes revealed a reduced transcriptional activity of the *GABRB3*-haplotype-2 promoter (overrepresented in CAE) compared to the *GABRB3*-haplotype-1 promoter

TABLE 1 | Transcriptional channelopathies implicated in epilepsies.

Gene*	Protein	Transcriptional mechanisms	Impact	References
Sodium channels				
Scn1a	$Na_v1.1$	Genetic variants in the promoter region	LOF	Nakayama et al. (2010) and Gao et al. (2017)
		Differential TF-binding	LOF	Dong et al. (2014)
		Epigenetic control mechanisms	LOF	Schuster et al. (2019)
		Alternative splicing	LOF	Lossin (2009) and Schlachter et al. (2009)
Scn1b	$Na_v\beta1$			
Scn2a	$Na_v1.2$	Differential TF-binding	LOF	Xiang et al. (2018)
Scn3a	$Na_v1.3$	Epigenetic control mechanisms	GOF	Li et al. (2015) and Tan et al. (2017)
Scn8a	$Na_v1.6$	Epigenetic control mechanisms	GOF	Liu et al. (2017)
Scn9a	$Na_v1.7$	Differential TF-binding	GOF	Diss et al. (2008)
Potassium channels				
Kcna1	$K_v1.1$	Regulation by miRNAs	LOF	Sosanya et al. (2013)
Kcna2	$K_v1.2$			
Kcnb1	$K_v2.1$			
Kcnc1	$K_v3.1$			
Kcnd2	$K_v4.2$	Differential TF-binding	LOF	Gross et al. (2016) and Tiwari et al. (2019)
		Regulation by miRNAs	LOF	Yao et al. (2016)
Kcnd3	$K_v4.3$			
Kcnh2	$K_v11.1$			
Kcnh3	$K_v12.2$			
Kcnh5	$K_v10.2$			
Kcnj10	Kir4.1	Epigenetic control mechanisms	LOF, GOF	Nwaobi et al. (2014) and Zhang et al. (2018)
Kcnk10	K2P10.1	Regulation by miRNAs	GOF	Haenisch et al. (2016)
Kcnq2	$K_v7.2$	Differential TF-binding	LOF	Mucha et al. (2010)
		Alternative splicing	LOF	de Haan et al. (2006)
Kcnq3	$K_v7.3$	Differential TF-binding	LOF	Mucha et al. (2010)
Kcnv2	$K_v8.2$			
Kcnma1	$K_{ca}1.1$			
Kcnt1	$K_{ca}4.1$			
Kctd7	Kctd-7			
Calcium channels				
Cacna1a	$Ca_v2.1$			
Cacna1g	$Ca_v3.1$			
Cacna1h	$Ca_v3.2$	Alternative splicing	GOF	Powell et al. (2009)
		Differential TF-binding	GOF	van Loo et al. (2012, 2015)
Cacna2d2	$Ca_v\alpha2\delta$-2			
Cacna2d4	$Ca_v\alpha2\delta$-4	Differential TF-binding	GOF	van Loo et al. (2019)
Cacnb4	$Ca_v\beta4$			
Chloride channels				
Clcn2	Clc-2	Alternative splicing	LOF	Bertelli et al. (2007)
Clcn4	Clc-4	Alternative splicing	LOF	Palmer et al. (2018)
$GABA_A$ receptors				
Gabra1	$GABA_A\alpha1$	Differential TF-binding	LOF	Hu et al. (2008), Lund et al. (2008)
		Epigenetic control mechanisms	LOF	Bohnsack et al. (2017)
Gabra4	$GABA_A\alpha4$	Differential TF-binding	GOF	Roberts et al. (2005)
Gabra6	$GABA_A\alpha6$			
Gabrb1	$GABA_A\beta1$	Differential TF-binding	LOF	Li et al. (2018)
Gabrb2	$GABA_A\beta2$			
Gabrb3	$GABA_A\beta3$	Genetic variants in the promoter region	LOF	Urak et al. (2006)
		Differential TF-binding	LOF	Tanaka et al. (2012a)
		Epigenetic control mechanisms	LOF	Tanaka et al. (2012a,b)
Gabrd	$GABA_A\delta$			
Gabrg2	$GABA_A\gamma2$	Alternative splicing	LOF	Kananura et al. (2002)
Ionotropic glutamate receptors				
Gria2	GluA2	Epigenetic control mechanisms	LOF	Machnes et al. (2013) and Kiese et al. (2017)
Grin1	GluN1			
Grin2a	GluN2A	Epigenetic control mechanisms	GOF	Kiese et al. (2017)
		Regulation by miRNAs	GOF	Alsharafi et al. (2016)
Grin2b	GuN2B	Epigenetic control mechanisms	LOF	Parrish et al. (2013)
		Alternative splicing	undetermined	Smigiel et al. (2016)
Grin2d	GluN2D			

(Continued)

TABLE 1 | Continued

Gene*	Protein	Transcriptional mechanisms	Impact	References
Nicotinic acetylcholine receptors				
Chrna2	nAChRα2			
Chrna4	nAChRα4			
Chrna7	nAChRα7			
Chrnb2	nAChRβ2			
Hyperpolarization-activated cyclic nucleotide-gated channels				
Hcn1	Hcn1	Epigenetic control mechanisms	LOF	McClelland et al. (2011)
Hcn2	Hcn2			
Hcn4	Hcn4			

**Epilepsy genes based on Online Mendelian Inheritance in Man (OMIM) database, Wang et al. (2017), Wei et al. (2017) and Oyrer et al. (2018). LOF, Loss-of-function; GOF, Gain-of-function; TF, Transcription Factor; miRNA, microRNA.*

(overrepresented in controls). The difference in expression could be explained by reduced binding of the TF N-Oct3 to the *GABRB3*-haplotype-2 promoter, resulting in decreased expression of the *GABRB3* gene (Urak et al., 2006). The reduced β3 levels observed in CAE patients might cause a loss of inhibitory properties of the receptor, eventually causing seizure activity.

ION CHANNELS IN ACQUIRED EPILEPSIES

Acquired epilepsies are epilepsies, which are on the consequence of an environmental factor. These epilepsies can be: (i) completely dependent on environmental factors; or (ii) can be caused by an interaction of environmental factor(s) with a predisposition genome. In the latter case, the presence of common susceptibility variants (e.g., SNPs or CNVs) can lower the threshold of the environmental factor for inducing an epileptic outcome. Most of our current knowledge of *acquired* epilepsy pathogenesis comes from the use of animal models, in which insults causing TLE can be mimicked in rodents using approaches like traumatic brain injury, kindling, or by applying one of the chemo-convulsants pilocarpine or kainic acid to induce SE (reviewed by Jefferys et al., 2016; Lévesque et al., 2016; Becker, 2018; Nirwan et al., 2018). Numerous studies using animal models for TLE have provided valuable information on epilepsy pathogenesis, resulting in a list of several channels involved in *acquired* epilepsies, including but not limited to HCN channels (Chen et al., 2001; Shah et al., 2004; Marcelin et al., 2009; Jung et al., 2011; Arnold et al., 2019), the A-type potassium channel $K_v4.2$ (Bernard et al., 2004; Monaghan et al., 2008), $K_{ir}2$ channels (Young et al., 2009), small-conductance (SK) calcium-activated potassium channels (Oliveira et al., 2010), big potassium channels (BK-channels; Pacheco Otalora et al., 2008; Shruti et al., 2008), persistent sodium channels (Agrawal et al., 2003; Chen et al., 2011), the T-type calcium channel $Ca_V3.2$ (Su et al., 2002; Becker et al., 2008) and the calcium channel subunit α2δ4 (van Loo et al., 2019).

TRANSCRIPTIONAL REGULATION OF ACQUIRED ION CHANNELOPATHIES

Currently, one of the main questions in epilepsy research is how the expression of ion channel genes in *acquired* epilepsies can be regulated. The transcriptional regulation of ion channels in *acquired* epilepsy can occur for example *via* differential expression of transcriptional activators or repressors. After a brain insult, a transient increase of activity-regulated TFs is evident (e.g., *Egr-4*, *Fos*, *Jun* and *Arc*), which can as a consequence dysregulate the transcriptional machinery of many genes, including ion channel genes (Herdegen et al., 1993; Beer et al., 1998; Herdegen and Leah, 1998; Honkaniemi and Sharp, 1999). To date, several transcriptional mechanisms have already been identified in the context of channelopathies and epilepsy pathogenesis (**Table 1**).

For $Ca_V3.2$, we recently performed an in-depth promoter analysis, examining the molecular mechanisms involved in the transcriptional augmentation of this channel early after pilocarpine-induced SE (Becker et al., 2008). Here, we observed a highly-sophisticated mechanism of transcriptional regulation: the increase of $Ca_V3.2$ expression was found to be mediated by metal-regulatory transcription factor 1 (MTF1) upon a rise in intracellular zinc ($[Zn^{2+}]_i$); denoted as the Zn^{2+}-MTF1-$Ca_V3.2$ cascade (van Loo et al., 2015). A rise in $[Zn^{2+}]_i$, often seen after a transient insult to the brain (Assaf and Chung, 1984; Zhao et al., 2014), can activate MTF1, which then binds to metal-responsive elements within the *$Ca_V3.2$* promoter region. Consequently, this results in increased $Ca_V3.2$ expression, a larger T-type current and increased burst-firing behavior (van Loo et al., 2015). In this way, the Zn^{2+}-MTF1-$Ca_V3.2$ cascade can enhance hippocampal network excitability, resulting in seizure activity. Besides the Zn^{2+}-MTF1-$Ca_V3.2$ cascade, also other TFs were found to control $Ca_V3.2$ expression, including Egr1 and RE1-silencing transcription factor (REST; van Loo et al., 2012). Such a multifactorial regulation by several TFs, thought to be a general phenomenon of ion channel regulation, severely complicates pharmacological intervention.

EPIGENETIC CONTROL OF ACQUIRED ION CHANNELOPATHIES

The transcription of ion channels in *acquired* epilepsies can also be regulated at the epigenetic level: both DNA methylation at cytosine residues, as well as changes in histone modifications (e.g., acetylation or methylation) can strongly affect the transcriptional machinery (reviewed by Hauser et al., 2018). Methylation of DNA generally occurs at cytosines within the 5'-cytosine-guanine-3' context (CpG). Gene promoters often contain large clusters of CpGs (referred to as CpG islands), which are mostly hypomethylated and are linked to transcriptional activation. An increase in DNA methylation may cause reduced transcriptional activity due to physical inhibition of TF binding to their cognate DNA binding motif, or by binding of repressor proteins known as methyl-CpG binding domain proteins (MBDs) to the methylated DNA. In the latter case, MBDs can recruit histone deacetylases (HDAC1 and HDAC2) to the methylated DNA, resulting in the silencing of the corresponding gene (Clouaire and Stancheva, 2008). To date, several epilepsy-channelopathies have been described to be caused by an epigenetic control mechanism (**Table 1**).

REGULATION OF ACQUIRED ION CHANNELOPATHIES BY microRNAs

The transcriptional machinery of ion channels in *acquired* epilepsies can also be influenced by small non-coding RNAs, such as microRNAs (miRNAs). miRNAs are 22 nucleotides noncoding RNAs that can regulate gene expression by associating with the RNA-induced silencing complex (RISC). The RISC complex then uses the miRNA as a template for recognizing the complementary mRNA of the ion channel gene (Ranganathan and Sivasankar, 2014). The main function of miRNAs appears to be the regulation at the post-transcriptional level: either by hindering protein translation or by enhancing mRNA degradation. Nowadays, it is also debated that miRNAs can have a nuclear function by modulating gene expression directly at the transcriptional level (reviewed by Catalanotto et al., 2016). Numerous miRNAs have been identified in relation to epilepsy pathogenesis (reviewed by Reschke and Henshall, 2015; Henshall et al., 2016; Shao and Chen, 2017; Tiwari et al., 2018), and also several ion channels appear to be under control of miRNAs, including $K_v1.1$, $K_v4.2$, Kcnk10 and Grin2a (Sosanya et al., 2013; Alsharafi et al., 2016; Gross et al., 2016; Haenisch et al., 2016; Tiwari et al., 2019; **Table 1**).

TRANSCRIPTIONAL REGULATION OF CHANNELOPATHIES IN NEURODEVELOPMENTAL DISORDERS

To date, it is generally accepted that ion channelopathies are not unique for epilepsy pathogenesis, but have gained considerable attention for the pathogenesis of several neurodevelopmental disorders, including pathology aspects of autism spectrum disorders (ASDs), schizophrenia, bipolar disorder, major depressive disorder and migraine (reviewed by Imbrici et al., 2013; Schmunk and Gargus, 2013; Albury et al., 2017). Seizures have been noted as a comorbidity feature of neurodevelopmental disorders (Hyde and Weinberger, 1997; Canitano, 2007; Mula et al., 2008; Liao et al., 2018; Salpekar and Mula, 2018; Strasser et al., 2018), which overall may point to the emergence of a functionally impaired neuronal network. For many neurodevelopmental disorders, several genetic variations (both rare mutations as well as common variants) in the coding regions of ion channel genes have been identified and reviewed elsewhere (Imbrici et al., 2013; Schmunk and Gargus, 2013; Daghsni et al., 2018; Weiss and Zamponi, 2019). Interestingly, also the mechanisms described above to be involved in the transcriptional regulation of ion channels in epilepsy pathogenesis, have been observed in the regulation of ion channels in other neurodevelopmental diseases. For example, transcriptional regulation by presence of genetic variants within the promoter region was observed for *Grin2a* and *Grin2b* and resulted in schizophrenia pathogenesis (Miyatake et al., 2002; Itokawa et al., 2003; Liu et al., 2015); alternative splicing was documented for *Gabrb2*, *Grin2b* and *Gabra3* and resulted in mental retardation and ASD (Zhao et al., 2009; Endele et al., 2010; O'Roak et al., 2012; Piton et al., 2013); differential expression of TFs was observed for *Scn10a*, *Kcnq1*, *Cacna1c*, and *Grin1* in schizophrenia and other psychiatric disorders (Rannals et al., 2016; Billingsley et al., 2018; Page et al., 2018); epigenetic control mechanisms were described for *Gabrb2*, *Gabrb3*, *Gria*, and *Chrna7* in ASD, schizophrenia and Rett syndrome (Samaco et al., 2005; Yasui et al., 2011; Kordi-Tamandani et al., 2013; Zong et al., 2017) and regulation by miRNAs was observed for *Cacna1c*, *Cacnb1*, *Grin2b* and NMDAR in schizophrenia and ASD (Kocerha et al., 2009; Guan et al., 2014; Cammaerts et al., 2015; Zhang et al., 2015; Kichukova et al., 2017).

Many of these "transcriptional channelopathies" apparently are rather specific, since they are mostly associated with only one individual neurodevelopmental disorder. However, a few examples exist, in which a comparable transcriptional regulatory mechanism has been observed for channelopathies in epilepsy and other neurodevelopmental disorders, hinting at an explanation for the comorbidity seen between the different disorders. One such example is the *GABRB3* gene, an important neurodevelopmental gene and besides epilepsy also associated with Angelman syndrome, Rett syndrome and ASD (Tanaka et al., 2012b). Differential expression of *GABRB3* in CAE can be caused by genetic variants within the promoter region (Urak et al., 2006). Interestingly, one of these variants is also associated with schizophrenia and heroin dependence (Chen et al., 2014b; Liu et al., 2019), whereas other genetic variants within the same regulatory region are correlated with ASD (Chen et al., 2014a).

Another example of comparable transcriptional control mechanisms in epilepsy and neurodevelopmental disorders was observed for the NMDAR gene *Grin2b*. The expression of *Grin2b* was significantly decreased in the kainic acid-induced SE model and correlated with increased DNA methylation levels at specific CpGs located within the *Grin2b* locus. Additionally,

interfering with the DNA methylation levels prior to SE using a DNA-methyltransferase inhibitor, prevented the *Grin2b* DNA methylation increase after SE and resulted in augmented *Grin2b* mRNA and protein expression (Parrish et al., 2013).

Such a glutamatergic hypofunction caused by an epigenetic control mechanism in *Grin2b* in the epilepsy model can also contribute to the pathophysiology of other neurodevelopmental disorders (Coyle et al., 2002; Lau and Zukin, 2007). Recently, it was reported that in a mouse model for schizophrenia, *Grin2b* expression was also under control of epigenetic control mechanisms. Here, the reduction in *Grin2b* expression was caused by an increase in H3K27me3 and REST at the *Grin2b* promoter (Gulchina et al., 2017). We may thus assume that different neurodevelopmental disorders are associated with a channelopathy with similar underlying transcriptional mechanisms.

Although we see comparable transcriptional mechanisms, no large overlap exists between the individual regulatory players in epilepsy pathogenesis and other neurodevelopmental disorders. Of course, this can also be explained by the fact that most specific mechanisms simply have not been analyzed in all neurodevelopmental disorders, or not in an analogous manner, making a direct comparison at the moment impossible. Further studies will reveal whether the altered diseases-associated expression of more proteins is based on a (partly) general underlying transcriptional phenomenon, possibly explaining the comorbidity between epilepsy and other neurodevelopmental disorders.

FUTURE PERSPECTIVES

In this study, we reviewed the mechanisms involved in the transcriptional regulation of channelopathies in *genetic* and *acquired* epilepsies. Although a large amount of data exists, our understanding of transcriptional mechanisms governing ion channel expression is far from complete and requires further detailed investigation, not only for epilepsy pathogenesis, but also for other neurodevelopmental disorders. A better understanding of the underlying mechanisms might result in the development of novel drugs and may provide opportunities for better-individualized treatment strategies.

AUTHOR CONTRIBUTIONS

Both authors contributed to the writing and editing of the manuscript.

FUNDING

This work was supported by the Deutsche Forschungsgemeinschaft (SFB 1089: KL, AB), FOR 2715 (AB), BMBF (EraNet DeCipher to AB), the European Union's Seventh Framework Programme (FP7/2007–2013) under grant agreement n°602102 (EPITARGET; AB), Else Kröner-Fresenius-Foundation 'Promotionskolleg NeuroImmunology' (AB) as well as the BONFOR program of the University of Bonn Medical Center.

REFERENCES

Agrawal, N., Alonso, A., and Ragsdale, D. S. (2003). Increased persistent sodium currents in rat entorhinal cortex layer V neurons in a post-status epilepticus model of temporal lobe epilepsy. *Epilepsia* 44, 1601–1604. doi: 10.1111/j.0013-9580.2003.23103.x

Albury, C. L., Stuart, S., Haupt, L. M., and Griffiths, L. R. (2017). Ion channelopathies and migraine pathogenesis. *Mol. Genet. Genomics* 292, 729–739. doi: 10.1007/s00438-017-1317-1

Alexander, S. P., Catterall, W. A., Kelly, E., Marrion, N., Peters, J. A., Benson, H. E., et al. (2015a). The concise guide to PHARMACOLOGY 2015/16: voltage-gated ion channels. *Br. J. Pharmacol.* 172, 5904–5941. doi: 10.1111/bph.13349

Alexander, S. P., Peters, J. A., Kelly, E., Marrion, N., Benson, H. E., Faccenda, E., et al. (2015b). The concise guide to PHARMACOLOGY 2015/16: ligand-gated ion channels. *Br. J. Pharmacol.* 172, 5870–5903. doi: 10.1111/bph.13350

Alsharafi, W. A., Xiao, B., and Li, J. (2016). MicroRNA-139–5p negatively regulates NR2A-containing NMDA receptor in the rat pilocarpine model and patients with temporal lobe epilepsy. *Epilepsia* 57, 1931–1940. doi: 10.1111/epi.13568

Arnold, E. C., McMurray, C., Gray, R., and Johnston, D. (2019). Epilepsy-induced reduction in hcn channel expression contributes to an increased excitability in dorsal, but not ventral, hippocampal CA1 neurons. *eNeuro* 6:ENEURO.0036-19.2019. doi: 10.1523/eneuro.0036-19.2019

Assaf, S. Y., and Chung, S. H. (1984). Release of endogenous Zn^{2+} from brain tissue during activity. *Nature* 308, 734–736. doi: 10.1038/308734a0

Becker, A. J. (2018). Review: animal models of acquired epilepsy: insights into mechanisms of human epileptogenesis. *Neuropathol. Appl. Neurobiol.* 44, 112–129. doi: 10.1111/nan.12451

Becker, A. J., Pitsch, J., Sochivko, D., Opitz, T., Staniek, M., Chen, C. C., et al. (2008). Transcriptional upregulation of $Ca_v3.2$ mediates epileptogenesis in the pilocarpine model of epilepsy. *J. Neurosci.* 28, 13341–13353. doi: 10.1523/JNEUROSCI.1421-08.2008

Beer, J., Mielke, K., Zipp, M., Zimmermann, M., and Herdegen, T. (1998). Expression of c-jun, junB, c-fos, fra-1 and fra-2 mRNA in the rat brain following seizure activity and axotomy. *Brain Res.* 794, 255–266. doi: 10.1016/s0006-8993(98)00233-9

Bernard, C., Anderson, A., Becker, A., Poolos, N. P., Beck, H., and Johnston, D. (2004). Acquired dendritic channelopathy in temporal lobe epilepsy. *Science* 305, 532–535. doi: 10.1126/science.1097065

Bertelli, M., Cecchin, S., Lapucci, C., de Gemmis, P., Danieli, D., d'Amore, E. S., et al. (2007). Quantification of chloride channel 2 (CLCN2) gene isoforms in normal versus lesion- and epilepsy-associated brain tissue. *Biochim. Biophys. Acta* 1772, 15–20. doi: 10.1016/j.bbadis.2006.10.015

Bien, C. G., and Elger, C. E. (2007). Limbic encephalitis: a cause of temporal lobe epilepsy with onset in adult life. *Epilepsy Behav.* 10, 529–538. doi: 10.1016/j.yebeh.2007.03.011

Bien, C. G., Urbach, H., Schramm, J., Soeder, B. M., Becker, A. J., Voltz, R., et al. (2007). Limbic encephalitis as a precipitating event in adult-onset temporal lobe epilepsy. *Neurology* 69, 1236–1244. doi: 10.1212/01.wnl.0000276946.08412.ef

Billingsley, K. J., Manca, M., Gianfrancesco, O., Collier, D. A., Sharp, H., Bubb, V. J., et al. (2018). Regulatory characterisation of the schizophrenia-associated CACNA1C proximal promoter and the potential role for the transcription factor EZH2 in schizophrenia aetiology. *Schizophr. Res.* 199, 168–175. doi: 10.1016/j.schres.2018.02.036

Bohnsack, J. P., Patel, V. K., and Morrow, A. L. (2017). Ethanol exposure regulates gabra1 expression *via* histone deacetylation at the promoter in cultured cortical neurons. *J. Pharmacol. Exp. Ther.* 363, 1–11. doi: 10.1124/jpet.117.242446

Borlot, F., Regan, B. M., Bassett, A. S., Stavropoulos, D. J., and Andrade, D. M. (2017). Prevalence of pathogenic copy number variation in adults with pediatric-onset epilepsy and intellectual disability. *JAMA Neurol.* 74, 1301–1311. doi: 10.1001/jamaneurol.2017.1775

Brenowitz, S., Duguid, I., and Kammermeier, P. J. (2017). Ion channels: history, diversity, and impact. *Cold Spring Harb. Protoc.* 2017:pdb.top092288. doi: 10.1101/pdb.top092288

Brunklaus, A., and Zuberi, S. M. (2014). Dravet syndrome—from epileptic encephalopathy to channelopathy. *Epilepsia* 55, 979–984. doi: 10.1111/epi.12652

Cammaerts, S., Strazisar, M., Smets, B., Weckhuysen, S., Nordin, A., De Jonghe, P., et al. (2015). Schizophrenia-associated MIR204 regulates noncoding RNAs and affects neurotransmitter and ion channel gene sets. *PLoS One* 10:e0144428. doi: 10.1371/journal.pone.0144428

Canitano, R. (2007). Epilepsy in autism spectrum disorders. *Eur. Child Adolesc. Psychiatry* 16, 61–66. doi: 10.1007/s00787-006-0563-2

Carvill, G. L., Engel, K. L., Ramamurthy, A., Cochran, J. N., Roovers, J., Stamberger, H., et al. (2018). Aberrant inclusion of a poison exon causes dravet syndrome and related SCN1A-associated genetic epilepsies. *Am. J. Hum. Genet.* 103, 1022–1029. doi: 10.1016/j.ajhg.2018.10.023

Catalanotto, C., Cogoni, C., and Zardo, G. (2016). MicroRNA in control of gene expression: an overview of nuclear functions. *Int. J. Mol. Sci.* 17:E1712. doi: 10.3390/ijms17101712

Chen, K., Aradi, I., Thon, N., Eghbal-Ahmadi, M., Baram, T. Z., and Soltesz, I. (2001). Persistently modified h-channels after complex febrile seizures convert the seizure-induced enhancement of inhibition to hyperexcitability. *Nat. Med.* 7, 331–337. doi: 10.1038/85480

Chen, C. H., Huang, C. C., Cheng, M. C., Chiu, Y. N., Tsai, W. C., Wu, Y. Y., et al. (2014a). Genetic analysis of *GABRB3* as a candidate gene of autism spectrum disorders. *Mol. Autism* 5:36. doi: 10.1186/2040-2392-5-36

Chen, C. H., Huang, C. C., and Liao, D. L. (2014b). Association analysis of GABRB3 promoter variants with heroin dependence. *PLoS One* 9:e102227. doi: 10.1371/journal.pone.0102227

Chen, S., Su, H., Yue, C., Remy, S., Royeck, M., Sochivko, D., et al. (2011). An increase in persistent sodium current contributes to intrinsic neuronal bursting after status epilepticus. *J. Neurophysiol.* 105, 117–129. doi: 10.1152/jn.00184.2010

Clouaire, T., and Stancheva, I. (2008). Methyl-CpG binding proteins: specialized transcriptional repressors or structural components of chromatin? *Epigenomes* 65, 1509–1522. doi: 10.1007/s00018-008-7324-y

Coyle, J. T., Tsai, G., and Goff, D. C. (2002). Ionotropic glutamate receptors as therapeutic targets in schizophrenia. *Curr. Drug Targets CNS Neurol. Disord.* 1, 183–189. doi: 10.2174/1568007024606212

Daghsni, M., Rima, M., Fajloun, Z., Ronjat, M., Brusés, J. L., M'Rad, R., et al. (2018). Autism throughout genetics: perusal of the implication of ion channels. *Brain Behav.* 8:e00978. doi: 10.1002/brb3.978

de Haan, G. J., Pinto, D., Carton, D., Bader, A., Witte, J., Peters, E., et al. (2006). A novel splicing mutation in KCNQ2 in a multigenerational family with BFNC followed for 25 years. *Epilepsia* 47, 851–859. doi: 10.1111/j.1528-1167.2006.00552.x

Deng, H., Xiu, X., and Song, Z. (2014). The molecular biology of genetic-based epilepsies. *Mol. Neurobiol.* 49, 352–367. doi: 10.1007/s12035-013-8523-6

Diss, J. K., Calissano, M., Gascoyne, D., Djamgoz, M. B., and Latchman, D. S. (2008). Identification and characterization of the promoter region of the Nav1.7 voltage-gated sodium channel gene (SCN9A). *Mol. Cell. Neurosci.* 37, 537–547. doi: 10.1016/j.mcn.2007.12.002

Dong, Z. F., Tang, L. J., Deng, G. F., Zeng, T., Liu, S. J., Wan, R. P., et al. (2014). Transcription of the human sodium channel SCN1A gene is repressed by a scaffolding protein RACK1. *Mol. Neurobiol.* 50, 438–448. doi: 10.1007/s12035-014-8633-9

Dunn, P., Albury, C. L., Maksemous, N., Benton, M. C., Sutherland, H. G., Smith, R. A., et al. (2018). Next generation sequencing methods for diagnosis of epilepsy syndromes. *Front. Genet.* 9:20. doi: 10.3389/fgene.2018.00020

Endele, S., Rosenberger, G., Geider, K., Popp, B., Tamer, C., Stefanova, I., et al. (2010). Mutations in GRIN2A and GRIN2B encoding regulatory subunits of NMDA receptors cause variable neurodevelopmental phenotypes. *Nat. Genet.* 42, 1021–1026. doi: 10.1038/ng.677

Engel, J. Jr. (1996). Introduction to temporal lobe epilepsy. *Epilepsy Res.* 26, 141–150. doi: 10.1016/s0920-1211(96)00043-5

Farrant, M., and Nusser, Z. (2005). Variations on an inhibitory theme: phasic and tonic activation of $GABA_A$ receptors. *Nat. Rev. Neurosci.* 6, 215–229. doi: 10.1038/nrn1625

Fisher, R. S. (2015). Redefining epilepsy. *Curr. Opin. Neurol.* 28, 130–135. doi: 10.1097/WCO.0000000000000174

Fisher, R. S., Acevedo, C., Arzimanoglou, A., Bogacz, A., Cross, J. H., Elger, C. E., et al. (2014). ILAE official report: a practical clinical definition of epilepsy. *Epilepsia* 55, 475–482. doi: 10.1111/epi.12550

Gao, Q. W., Hua, L. D., Wang, J., Fan, C. X., Deng, W. Y., Li, B., et al. (2017). A point mutation in SCN1A 5' genomic region decreases the promoter activity and is associated with mild epilepsy and seizure aggravation induced by antiepileptic drug. *Mol. Neurobiol.* 54, 2428–2434. doi: 10.1007/s12035-016-9800-y

Gibson, G. (2012). Rare and common variants: twenty arguments. *Nat. Rev. Genet.* 13, 135–145. doi: 10.1038/nrg3118

Gross, C., Yao, X., Engel, T., Tiwari, D., Xing, L., Rowley, S., et al. (2016). MicroRNA-mediated downregulation of the potassium channel Kv4.2 contributes to seizure onset. *Cell Rep.* 17, 37–45. doi: 10.1016/j.celrep.2016.08.074

Guan, F., Zhang, B., Yan, T., Li, L., Liu, F., Li, T., et al. (2014). MIR137 gene and target gene CACNA1C of miR-137 contribute to schizophrenia susceptibility in Han Chinese. *Schizophr. Res.* 152, 97–104. doi: 10.1016/j.schres.2013.11.004

Gulchina, Y., Xu, S. J., Snyder, M. A., Elefant, F., and Gao, W. J. (2017). Epigenetic mechanisms underlying NMDA receptor hypofunction in the prefrontal cortex of juvenile animals in the MAM model for schizophrenia. *J. Neurochem.* 143, 320–333. doi: 10.1111/jnc.14101

Haenisch, S., von Ruden, E. L., Wahmkow, H., Rettenbeck, M. L., Michler, C., Russmann, V., et al. (2016). miRNA-187–3p-mediated regulation of the KCNK10/TREK-2 potassium channel in a rat epilepsy model. *ACS Chem. Neurosci.* 7, 1585–1594. doi: 10.1021/acschemneuro.6b00222

Hauser, R. M., Henshall, D. C., and Lubin, F. D. (2018). The epigenetics of epilepsy and its progression. *Neuroscientist* 24, 186–200. doi: 10.1177/1073858417705840

Henshall, D. C., Hamer, H. M., Pasterkamp, R. J., Goldstein, D. B., Kjems, J., Prehn, J. H. M., et al. (2016). MicroRNAs in epilepsy: pathophysiology and clinical utility. *Lancet Neurol.* 15, 1368–1376. doi: 10.1016/S1474-4422(16)30246-0

Herdegen, T., and Leah, J. D. (1998). Inducible and constitutive transcription factors in the mammalian nervous system: control of gene expression by Jun, Fos and Krox, and CREB/ATF proteins. *Brain Res. Rev.* 28, 370–490. doi: 10.1016/s0165-0173(98)00018-6

Herdegen, T., Sandkuhler, J., Gass, P., Kiessling, M., Bravo, R., and Zimmermann, M. (1993). JUN, FOS, KROX and CREB transcription factor proteins in the rat cortex: basal expression and induction by spreading depression and epileptic seizures. *J. Comp. Neurol.* 333, 271–288. doi: 10.1002/cne.903330212

Hirose, S. (2014). Mutant $GABA_A$ receptor subunits in genetic (idiopathic) epilepsy. *Prog. Brain Res.* 213, 55–85. doi: 10.1016/b978-0-444-63326-2.00003-x

Honkaniemi, J., and Sharp, F. R. (1999). Prolonged expression of zinc finger immediate-early gene mRNAs and decreased protein synthesis following kainic acid induced seizures. *Eur. J. Neurosci.* 11, 10–17. doi: 10.1046/j.1460-9568.1999.00401.x

Hu, Y., Lund, I. V., Gravielle, M. C., Farb, D. H., Brooks-Kayal, A. R., and Russek, S. J. (2008). Surface expression of $GABA_A$ receptors is transcriptionally controlled by the interplay of cAMP-response element-binding protein and its binding partner inducible cAMP early repressor. *J. Biol. Chem.* 283, 9328–9340. doi: 10.1074/jbc.m705110200

Hyde, T. M., and Weinberger, D. R. (1997). Seizures and schizophrenia. *Schizophr. Bull.* 23, 611–622. doi: 10.1093/schbul/23.4.611

Imbrici, P., Camerino, D. C., and Tricarico, D. (2013). Major channels involved in neuropsychiatric disorders and therapeutic perspectives. *Front. Genet.* 4:76. doi: 10.3389/fgene.2013.00076

International League Against Epilepsy Consortium on Complex Epilepsies. (2018). Genome-wide mega-analysis identifies 16 loci and highlights diverse biological mechanisms in the common epilepsies. *Nat. Commun.* 9:5269. doi: 10.1038/s41467-018-07524-z

Itokawa, M., Yamada, K., Yoshitsugu, K., Toyota, T., Suga, T., Ohba, H., et al. (2003). A microsatellite repeat in the promoter of the N-methyl-D-aspartate receptor 2A subunit (GRIN2A) gene suppresses transcriptional activity and correlates with chronic outcome in schizophrenia. *Pharmacogenetics* 13, 271–278. doi: 10.1097/00008571-200305000-00006

Jefferys, J., Steinhäuser, C., and Bedner, P. (2016). Chemically-induced TLE models: topical application. *J. Neurosci. Methods* 260, 53–61. doi: 10.1016/j.jneumeth.2015.04.011

Jung, S., Warner, L. N., Pitsch, J., Becker, A. J., and Poolos, N. P. (2011). Rapid loss of dendritic HCN channel expression in hippocampal pyramidal neurons following status epilepticus. *J. Neurosci.* 31, 14291–14295. doi: 10.1523/jneurosci.1148-11.2011

Kananura, C., Haug, K., Sander, T., Runge, U., Gu, W., Hallmann, K., et al. (2002). A splice-site mutation in GABRG2 associated with childhood absence epilepsy and febrile convulsions. *Arch. Neurol.* 59, 1137–1141. doi: 10.1001/archneur.59.7.1137

Kasperaviciute, D., Catarino, C. B., Matarin, M., Leu, C., Novy, J., Tostevin, A., et al. (2013). Epilepsy, hippocampal sclerosis and febrile seizures linked by common genetic variation around SCN1A. *Brain* 136, 3140–3150. doi: 10.1093/brain/awt233

Kichukova, T. M., Popov, N. T., Ivanov, I. S., and Vachev, T. I. (2017). Profiling of circulating serum MicroRNAs in children with autism spectrum disorder using stem-loop qRT-PCR assay. *Folia Med.* 59, 43–52. doi: 10.1515/folmed-2017-0009

Kiese, K., Jablonski, J., Hackenbracht, J., Wrosch, J. K., Groemer, T. W., Kornhuber, J., et al. (2017). Epigenetic control of epilepsy target genes contributes to a cellular memory of epileptogenesis in cultured rat hippocampal neurons. *Acta Neuropathol. Commun.* 5:79. doi: 10.1186/s40478-017-0485-x

Kocerha, J., Faghihi, M. A., Lopez-Toledano, M. A., Huang, J., Ramsey, A. J., Caron, M. G., et al. (2009). MicroRNA-219 modulates NMDA receptor-mediated neurobehavioral dysfunction. *Proc. Natl. Acad. Sci. U S A* 106, 3507–3512. doi: 10.1073/pnas.0805854106

Kordi-Tamandani, D. M., Dahmardeh, N., and Torkamanzehi, A. (2013). Evaluation of hypermethylation and expression pattern of GMR2, GMR5, GMR8 and GRIA3 in patients with schizophrenia. *Gene* 515, 163–166. doi: 10.1016/j.gene.2012.10.075

Kwan, P., and Sander, J. W. (2004). The natural history of epilepsy: an epidemiological view. *J. Neurol. Neurosurg. Psychiatry* 75, 1376–1381. doi: 10.1136/jnnp.2004.045690

Lau, C. G., and Zukin, R. S. (2007). NMDA receptor trafficking in synaptic plasticity and neuropsychiatric disorders. *Nat. Rev. Neurosci.* 8, 413–426. doi: 10.1038/nrn2153

Lerche, H., Shah, M., Beck, H., Noebels, J., Johnston, D., and Vincent, A. (2013). Ion channels in genetic and acquired forms of epilepsy. *J. Physiol.* 591, 753–764. doi: 10.1113/jphysiol.2012.240606

Lévesque, M., Avoli, M., and Bernard, C. (2016). Animal models of temporal lobe epilepsy following systemic chemoconvulsant administration. *J. Neurosci. Methods* 260, 45–52. doi: 10.1016/j.jneumeth.2015.03.009

Li, Z., Cogswell, M., Hixson, K., Brooks-Kayal, A. R., and Russek, S. J. (2018). Nuclear respiratory factor 1 (NRF-1) controls the activity dependent transcription of the GABA-A receptor β 1 subunit gene in neurons. *Front. Mol. Neurosci.* 11:285. doi: 10.3389/fnmol.2018.00285

Li, H. J., Wan, R. P., Tang, L. J., Liu, S. J., Zhao, Q. H., Gao, M. M., et al. (2015). Alteration of Scn3a expression is mediated *via* CpG methylation and MBD2 in mouse hippocampus during postnatal development and seizure condition. *Biochim. Biophys. Acta* 1849, 1–9. doi: 10.1016/j.bbagrm.2014.11.004

Liao, J., Tian, X., Wang, H., and Xiao, Z. (2018). Epilepsy and migraine-Are they comorbidity? *Genes Dis.* 5, 112–118. doi: 10.1016/j.gendis.2018.04.007

Liu, R., Dang, W., Du, Y., Zhou, Q., Liu, Z., and Jiao, K. (2015). Correlation of functional GRIN2A gene promoter polymorphisms with schizophrenia and serum D-serine levels. *Gene* 568, 25–30. doi: 10.1016/j.gene.2015.05.011

Liu, Y., Ding, M., Liu, Y. P., Zhang, X. C., Xing, J. X., Xuan, J. F., et al. (2019). Functional analysis of haplotypes and promoter activity at the 5′ region of the human GABRB3 gene and associations with schizophrenia. *Mol. Genet. Genomic Med.* 7:e652. doi: 10.1002/mgg3.652

Liu, Y., Lai, S., Ma, W., Ke, W., Zhang, C., Liu, S., et al. (2017). CDYL suppresses epileptogenesis in mice through repression of axonal Nav1.6 sodium channel expression. *Nat. Commun.* 8:355. doi: 10.1038/s41467-017-00368-z

Liu, S., Yu, W., and Lu, Y. (2016). The causes of new-onset epilepsy and seizures in the elderly. *Neuropsychiatr. Dis. Treat.* 12, 1425–1434. doi: 10.2147/ndt.s107905

Löscher, W., Klitgaard, H., Twyman, R. E., and Schmidt, D. (2013). New avenues for anti-epileptic drug discovery and development. *Nat. Rev. Drug Discov.* 12, 757–776. doi: 10.1038/nrd4126

Lossin, C. (2009). A catalog of SCN1A variants. *Brain Dev.* 31, 114–130. doi: 10.1016/j.braindev.2008.07.011

Lund, I. V., Hu, Y., Raol, Y. H., Benham, R. S., Faris, R., Russek, S. J., et al. (2008). BDNF selectively regulates $GABA_A$ receptor transcription by activation of the JAK/STAT pathway. *Sci. Signal.* 1:ra9. doi: 10.1126/scisignal.1162396

Machnes, Z. M., Huang, T. C., Chang, P. K., Gill, R., Reist, N., Dezsi, G., et al. (2013). DNA methylation mediates persistent epileptiform activity *in vitro* and *in vivo*. *PLoS One* 8:e76299. doi: 10.1371/journal.pone.0076299

Marcelin, B., Chauviere, L., Becker, A., Migliore, M., Esclapez, M., and Bernard, C. (2009). h channel-dependent deficit of theta oscillation resonance and phase shift in temporal lobe epilepsy. *Neurobiol. Dis.* 33, 436–447. doi: 10.1016/j.nbd.2008.11.019

McClelland, S., Flynn, C., Dube, C., Richichi, C., Zha, Q., Ghestem, A., et al. (2011). Neuron-restrictive silencer factor-mediated hyperpolarization-activated cyclic nucleotide gated channelopathy in experimental temporal lobe epilepsy. *Ann. Neurol.* 70, 454–464. doi: 10.1002/ana.22479

Miyatake, R., Furukawa, A., and Suwaki, H. (2002). Identification of a novel variant of the human NR2B gene promoter region and its possible association with schizophrenia. *Mol. Psychiatry* 7, 1101–1106. doi: 10.1038/sj.mp.4001152

Monaghan, M. M., Menegola, M., Vacher, H., Rhodes, K. J., and Trimmer, J. S. (2008). Altered expression and localization of hippocampal A-type potassium channel subunits in the pilocarpine-induced model of temporal lobe epilepsy. *Neuroscience* 156, 550–562. doi: 10.1016/j.neuroscience.2008.07.057

Monlong, J., Girard, S. L., Meloche, C., Cadieux-Dion, M., Andrade, D. M., Lafreniere, R. G., et al. (2018). Global characterization of copy number variants in epilepsy patients from whole genome sequencing. *PLoS Genet.* 14:e1007285. doi: 10.1371/journal.pgen.1007285

Mucha, M., Ooi, L., Linley, J. E., Mordaka, P., Dalle, C., Robertson, B., et al. (2010). Transcriptional control of KCNQ channel genes and the regulation of neuronal excitability. *J. Neurosci.* 30, 13235–13245. doi: 10.1523/jneurosci.1981-10.2010

Mula, M., Schmitz, B., Jauch, R., Cavanna, A., Cantello, R., Monaco, F., et al. (2008). On the prevalence of bipolar disorder in epilepsy. *Epilepsy Behav.* 13, 658–661. doi: 10.1016/j.yebeh.2008.08.002

Nakayama, T., Ogiwara, I., Ito, K., Kaneda, M., Mazaki, E., Osaka, H., et al. (2010). Deletions of SCN1A 5′ genomic region with promoter activity in Dravet syndrome. *Hum. Mutat.* 31, 820–829. doi: 10.1002/humu.21275

Nirwan, N., Vyas, P., and Vohora, D. (2018). Animal models of status epilepticus and temporal lobe epilepsy: a narrative review. *Rev. Neurosci.* 29, 757–770. doi: 10.1515/revneuro-2017-0086

Nwaobi, S. E., Lin, E., Peramsetty, S. R., and Olsen, M. L. (2014). DNA methylation functions as a critical regulator of Kir4.1 expression during CNS development. *Glia* 62, 411–427. doi: 10.1002/glia.22613

Oliveira, M. S., Skinner, F., Arshadmansab, M. F., Garcia, I., Mello, C. F., Knaus, H. G., et al. (2010). Altered expression and function of small-conductance (SK) Ca^{2+}-activated K^+ channels in pilocarpine-treated epileptic rats. *Brain Res.* 1348, 187–199. doi: 10.1016/j.brainres.2010.05.095

O'Roak, B. J., Vives, L., Fu, W., Egertson, J. D., Stanaway, I. B., Phelps, I. G., et al. (2012). Multiplex targeted sequencing identifies recurrently mutated genes in autism spectrum disorders. *Science* 338, 1619–1622. doi: 10.1126/science.1227764

Oyrer, J., Maljevic, S., Scheffer, I. E., Berkovic, S. F., Petrou, S., and Reid, C. A. (2018). Ion channels in genetic epilepsy: from genes and mechanisms to disease-targeted therapies. *Pharmacol. Rev.* 70, 142–173. doi: 10.1124/pr.117.014456

Pacheco Otalora, L. F., Hernandez, E. F., Arshadmansab, M. F., Francisco, S., Willis, M., Ermolinsky, B., et al. (2008). Down-regulation of BK channel expression in the pilocarpine model of temporal lobe epilepsy. *Brain Res.* 1200, 116–131. doi: 10.1016/j.brainres.2008.01.017

Page, S. C., Hamersky, G. R., Gallo, R. A., Rannals, M. D., Calcaterra, N. E., Campbell, M. N., et al. (2018). The schizophrenia- and autism-associated gene, transcription factor 4 regulates the columnar distribution of layer 2/3 prefrontal pyramidal neurons in an activity-dependent manner. *Mol. Psychiatry* 23, 304–315. doi: 10.1038/mp.2017.37

Palmer, E. E., Stuhlmann, T., Weinert, S., Haan, E., Van Esch, H., Holvoet, M., et al. (2018). *De novo* and inherited mutations in the X-linked gene CLCN4 are associated with syndromic intellectual disability and behavior and seizure disorders in males and females. *Mol. Psychiatry* 23, 222–230. doi: 10.1038/mp.2016.135

Parrish, R. R., Albertson, A. J., Buckingham, S. C., Hablitz, J. J., Mascia, K. L., Davis Haselden, W., et al. (2013). Status epilepticus triggers early and late alterations in brain-derived neurotrophic factor and NMDA glutamate receptor Grin2b DNA methylation levels in the hippocampus. *Neuroscience* 248, 602–619. doi: 10.1016/j.neuroscience.2013.06.029

Pitkänen, A., Roivainen, R., and Lukasiuk, K. (2016). Development of epilepsy after ischaemic stroke. *Lancet Neurol.* 15, 185–197. doi: 10.1016/s1474-4422(15)00248-3

Piton, A., Jouan, L., Rochefort, D., Dobrzeniecka, S., Lachapelle, K., Dion, P. A., et al. (2013). Analysis of the effects of rare variants on splicing identifies alterations in $GABA_A$ receptor genes in autism spectrum disorder individuals. *Eur. J. Hum. Genet.* 21, 749–756. doi: 10.1038/ejhg.2012.243

Powell, K. L., Cain, S. M., Ng, C., Sirdesai, S., David, L. S., Kyi, M., et al. (2009). A Cav3.2 T-type calcium channel point mutation has splice-variant-specific effects on function and segregates with seizure expression in a polygenic rat model of absence epilepsy. *J. Neurosci.* 29, 371–380. doi: 10.1523/JNEUROSCI.5295-08.2009

Raimondo, J. V., Burman, R. J., Katz, A. A., and Akerman, C. J. (2015). Ion dynamics during seizures. *Front. Cell Neurosci.* 9:419. doi: 10.3389/fncel.2015.00419

Ranganathan, K., and Sivasankar, V. (2014). MicroRNAs - biology and clinical applications. *J. Oral Maxillofac. Pathol.* 18, 229–234. doi: 10.4103/0973-029x.140762

Rannals, M. D., Hamersky, G. R., Page, S. C., Campbell, M. N., Briley, A., Gallo, R. A., et al. (2016). Psychiatric risk gene transcription factor 4 regulates intrinsic excitability of prefrontal neurons *via* repression of SCN10a and KCNQ1. *Neuron* 90, 43–55. doi: 10.1016/j.neuron.2016.02.021

Reich, D. E., and Lander, E. S. (2001). On the allelic spectrum of human disease. *Trends Genet.* 17, 502–510. doi: 10.1016/s0168-9525(01)02410-6

Reid, C. A., Berkovic, S. F., and Petrou, S. (2009). Mechanisms of human inherited epilepsies. *Prog. Neurobiol.* 87, 41–57. doi: 10.1016/j.pneurobio.2008.09.016

Reschke, C. R., and Henshall, D. C. (2015). microRNA and epilepsy. *Adv. Exp. Med. Biol.* 888, 41–70. doi: 10.1007/978-3-319-22671-2_4

Roberts, D. S., Raol, Y. H., Bandyopadhyay, S., Lund, I. V., Budreck, E. C., Passini, M. A., et al. (2005). Egr3 stimulation of GABRA4 promoter activity as a mechanism for seizure-induced up-regulation of $GABA_A$ receptor α4 subunit expression. *Proc. Natl. Acad. Sci. U S A* 102, 11894–11899. doi: 10.1073/pnas.0501434102

Saint Pierre, A., and Génin, E. (2014). How important are rare variants in common disease? *Brief. Funct. Genomics* 13, 353–361. doi: 10.1093/bfgp/elu025

Salpekar, J. A., and Mula, M. (2018). Common psychiatric comorbidities in epilepsy: how big of a problem is it? *Epilepsy Behav.* 98, 293–297. doi: 10.1016/j.yebeh.2018.07.023

Samaco, R. C., Hogart, A., and LaSalle, J. M. (2005). Epigenetic overlap in autism-spectrum neurodevelopmental disorders: MECP2 deficiency causes reduced expression of UBE3A and GABRB3. *Hum. Mol. Genet.* 14, 483–492. doi: 10.1093/hmg/ddi045

Schlachter, K., Gruber-Sedlmayr, U., Stogmann, E., Lausecker, M., Hotzy, C., Balzar, J., et al. (2009). A splice site variant in the sodium channel gene SCN1A confers risk of febrile seizures. *Neurology* 72, 974–978. doi: 10.1212/01.wnl.0000344401.02915.00

Schmunk, G., and Gargus, J. J. (2013). Channelopathy pathogenesis in autism spectrum disorders. *Front. Genet.* 4:222. doi: 10.3389/fgene.2013.00222

Schuster, J., Laan, L., Klar, J., Jin, Z., Huss, M., Korol, S., et al. (2019). Transcriptomes of Dravet syndrome iPSC derived GABAergic cells reveal dysregulated pathways for chromatin remodeling and neurodevelopment. *Neurobiol. Dis.* 132:104583. doi: 10.1016/j.nbd.2019.104583

Shah, M. M., Anderson, A. E., Leung, V., Lin, X., and Johnston, D. (2004). Seizure-induced plasticity of h channels in entorhinal cortical layer III pyramidal neurons. *Neuron* 44, 495–508. doi: 10.1016/j.neuron.2004.10.011

Shao, Y., and Chen, Y. (2017). Pathophysiology and clinical utility of non-coding RNAs in epilepsy. *Front. Mol. Neurosci.* 10:249. doi: 10.3389/fnmol.2017.00249

Shorvon, S. D. (2011). The etiologic classification of epilepsy. *Epilepsia* 52, 1052–1057. doi: 10.1111/j.1528-1167.2011.03041.x

Shruti, S., Clem, R. L., and Barth, A. L. (2008). A seizure-induced gain-of-function in BK channels is associated with elevated firing activity in neocortical pyramidal neurons. *Neurobiol. Dis.* 30, 323–330. doi: 10.1016/j.nbd.2008.02.002

Smigiel, R., Kostrzewa, G., Kosinska, J., Pollak, A., Stawinski, P., Szmida, E., et al. (2016). Further evidence for GRIN2B mutation as the cause of severe epileptic encephalopathy. *Am. J. Med. Genet. A* 170, 3265–3270. doi: 10.1002/ajmg.a.37887

Sosanya, N. M., Huang, P. P., Cacheaux, L. P., Chen, C. J., Nguyen, K., Perrone-Bizzozero, N. I., et al. (2013). Degradation of high affinity HuD targets releases Kv1.1 mRNA from miR-129 repression by mTORC1. *J. Cell Biol.* 202, 53–69. doi: 10.1083/jcb.201212089

Steinlein, O. K., Mulley, J. C., Propping, P., Wallace, R. H., Phillips, H. A., Sutherland, G. R., et al. (1995). A missense mutation in the neuronal nicotinic acetylcholine receptor α 4 subunit is associated with autosomal dominant nocturnal frontal lobe epilepsy. *Nat. Genet.* 11, 201–203. doi: 10.1038/ng1095-201

Strasser, L., Downes, M., Kung, J., Cross, J. H., and De Haan, M. (2018). Prevalence and risk factors for autism spectrum disorder in epilepsy: a systematic review and meta-analysis. *Dev. Med. Child Neurol.* 60, 19–29. doi: 10.1111/dmcn.13598

Su, H., Sochivko, D., Becker, A., Chen, J., Jiang, Y., Yaari, Y., et al. (2002). Upregulation of a T-type Ca^{2+} channel causes a long-lasting modification of neuronal firing mode after status epilepticus. *J. Neurosci.* 22, 3645–3655. doi: 10.1523/jneurosci.22-09-03645.2002

Tan, N. N., Tang, H. L., Lin, G. W., Chen, Y. H., Lu, P., Li, H. J., et al. (2017). Epigenetic downregulation of Scn3a expression by valproate: a possible role in its anticonvulsant activity. *Mol. Neurobiol.* 54, 2831–2842. doi: 10.1007/s12035-016-9871-9

Tanaka, M., Bailey, J. N., Bai, D., Ishikawa-Brush, Y., Delgado-Escueta, A. V., and Olsen, R. W. (2012a). Effects on promoter activity of common SNPs in 5′ region of GABRB3 exon 1A. *Epilepsia* 53, 1450–1456. doi: 10.1111/j.1528-1167.2012.03572.x

Tanaka, M., DeLorey, T. M., Delgado-Escueta, A., and Olsen, R. W. (2012b). "GABRB3, Epilepsy and Neurodevelopment," in *Jasper's Basic Mechanisms of the Epilepsies*, eds J. L. Noebels, M. Avoli, M. A. Rogawski, R. W. Olsen, and A. V. Delgado-Escueta (Bethesda, MD: Oxford University Press), 887–899.

Thompson, C. H., Kahlig, K. M., and George, A. L. Jr. (2011). SCN1A splice variants exhibit divergent sensitivity to commonly used antiepileptic drugs. *Epilepsia* 52, 1000–1009. doi: 10.1111/j.1528-1167.2011.03040.x

Tiwari, D., Brager, D. H., Rymer, J. K., Bunk, A. T., White, A. R., Elsayed, N. A., et al. (2019). MicroRNA inhibition upregulates hippocampal A-type potassium current and reduces seizure frequency in a mouse model of epilepsy. *Neurobiol. Dis.* 130:104508. doi: 10.1016/j.nbd.2019.104508

Tiwari, D., Pearlso, K., and Gross, C. (2018). MicroRNA-induced silencing in epilepsy: opportunities and challenges for clinical application. *Dev. Dyn.* 247, 94–110. doi: 10.1002/dvdy.24582

Urak, L., Feucht, M., Fathi, N., Hornik, K., and Fuchs, K. (2006). A GABRB3 promoter haplotype associated with childhood absence epilepsy impairs transcriptional activity. *Hum. Mol. Genet.* 15, 2533–2541. doi: 10.1093/hmg/ddl174

van Loo, K. M. J., Rummel, C. K., Pitsch, J., Muller, J. A., Bikbaev, A. F., Martinez-Chavez, E., et al. (2019). Calcium channel subunit α2δ4 is regulated by early growth response 1 and facilitates epileptogenesis. *J. Neurosci.* 39, 3175–3187. doi: 10.1523/jneurosci.1731-18.2019

van Loo, K. M., Schaub, C., Pernhorst, K., Yaari, Y., Beck, H., Schoch, S., et al. (2012). Transcriptional regulation of T-type calcium channel CaV3.2: bi-directionality by early growth response 1 (Egr1) and repressor element 1 (RE-1) protein-silencing transcription factor (REST). *J. Biol. Chem.* 287, 15489–15501. doi: 10.1074/jbc.m111.310763

van Loo, K. M., Schaub, C., Pitsch, J., Kulbida, R., Opitz, T., Ekstein, D., et al. (2015). Zinc regulates a key transcriptional pathway for epileptogenesis *via* metal-regulatory transcription factor 1. *Nat. Commun.* 6:8688. doi: 10.1038/ncomms9688

Vezzani, A., Fujinami, R. S., White, H. S., Preux, P. M., Blumcke, I., Sander, J. W., et al. (2016). Infections, inflammation and epilepsy. *Acta Neuropathol.* 131, 211–234. doi: 10.1007/s00401-015-1481-5

Wallace, R. H., Wang, D. W., Singh, R., Scheffer, I. E., George, A. L. Jr., Phillips, H. A., et al. (1998). Febrile seizures and generalized epilepsy associated with a mutation in the Na^+-channel β1 subunit gene SCN1B. *Nat. Genet.* 19, 366–370. doi: 10.1038/1252

Wang, J., Lin, Z. J., Liu, L., Xu, H. Q., Shi, Y. W., Yi, Y. H., et al. (2017). Epilepsy-associated genes. *Seizure* 44, 11–20. doi: 10.1016/j.seizure.2016.11.030

Wei, F., Yan, L. M., Su, T., He, N., Lin, Z. J., Wang, J., et al. (2017). Ion channel genes and epilepsy: functional alteration, pathogenic potential and mechanism of epilepsy. *Neurosci. Bull.* 33, 455–477. doi: 10.1007/s12264-017-0134-1

Weiss, N., and Zamponi, G. W. (2019). Genetic T-type calcium channelopathies. *J. Med Genet.* 57, 1–10. doi: 10.1136/jmedgenet-2019-106163

Xiang, J., Wen, F., Zhang, L., and Zhou, Y. (2018). FOXD3 inhibits SCN2A gene transcription in intractable epilepsy cell models. *Exp. Neurol.* 302, 14–21. doi: 10.1016/j.expneurol.2017.12.012

Yao, J. J., Zhao, Q. R., Liu, D. D., Chow, C. W., and Mei, Y. A. (2016). Neuritin up-regulates Kv4.2 α-subunit of potassium channel expression and affects neuronal excitability by regulating the calcium-calcineurin-NFATc4 signaling pathway. *J. Biol. Chem.* 291, 17369–17381. doi: 10.1074/jbc.m115.708883

Yasui, D. H., Scoles, H. A., Horike, S., Meguro-Horike, M., Dunaway, K. W., Schroeder, D. I., et al. (2011). 15q11.2–13.3 chromatin analysis reveals epigenetic regulation of CHRNA7 with deficiencies in Rett and autism brain. *Hum. Mol. Genet.* 20, 4311–4323. doi: 10.1093/hmg/ddr357

Young, C. C., Stegen, M., Bernard, R., Muller, M., Bischofberger, J., Veh, R. W., et al. (2009). Upregulation of inward rectifier K^+ (Kir2) channels in dentate gyrus granule cells in temporal lobe epilepsy. *J. Physiol.* 587, 4213–4233. doi: 10.1113/jphysiol.2009.170746

Zhang, Y., Fan, M., Wang, Q., He, G., Fu, Y., Li, H., et al. (2015). Polymorphisms in MicroRNA Genes and genes involving in NMDAR signaling and schizophrenia: a case-control study in chinese han population. *Sci. Rep.* 5:12984. doi: 10.1038/srep12984

Zhang, S. P., Zhang, M., Tao, H., Luo, Y., He, T., Wang, C. H., et al. (2018). Dimethylation of Histone 3 Lysine 9 is sensitive to the epileptic activity and affects the transcriptional regulation of the potassium channel Kcnj10 gene in epileptic rats. *Mol. Med. Rep.* 17, 1368–1374. doi: 10.3892/mmr.2017.7942

Zhang, S., Zhu, Y., Cheng, J., and Tao, J. (2019). *Ion Channels in Epilepsy: Blasting Fuse for Neuronal Hyperexcitability*. IntechOpen. 1–12. doi: 10.5772/intechopen.83698

Zhao, Y., Pan, R., Li, S., Luo, Y., Yan, F., Yin, J., et al. (2014). Chelating intracellularly accumulated zinc decreased ischemic brain injury through reducing neuronal apoptotic death. *Stroke* 45, 1139–1147. doi: 10.1161/strokeaha.113.004296

Zhao, C., Xu, Z., Wang, F., Chen, J., Ng, S. K., Wong, P. W., et al. (2009). Alternative-splicing in the exon-10 region of $GABA_A$ receptor β2. subunit gene: relationships between novel isoforms and psychotic disorders. *PLoS One* 4:e6977. doi: 10.1371/journal.pone.0006977

Zong, L., Zhou, L., Hou, Y., Zhang, L., Jiang, W., Zhang, W., et al. (2017). Genetic and epigenetic regulation on the transcription of *GABRB2*: Genotype-dependent hydroxymethylation and methylation alterations in schizophrenia. *J. Psychiatr. Res.* 88, 9–17. doi: 10.1016/j.jpsychires.2016.12.019

Conflict of Interest: The authors declare that the research was conducted in the absence of any commercial or financial relationships that could be construed as a potential conflict of interest.

The handling Editor declared a past co-authorship with one of the authors AB.

frontiers in Cellular Neuroscience

ORIGINAL RESEARCH
published: 24 January 2020
doi: 10.3389/fncel.2020.00001

The Epilepsy of Infancy With Migrating Focal Seizures: Identification of *de novo* Mutations of the *KCNT2* Gene That Exert Inhibitory Effects on the Corresponding Heteromeric $K_{Na}1.1/K_{Na}1.2$ Potassium Channel

Xiao Mao[1,2†], Nadine Bruneau[3†], Quwen Gao[4†], Hélène Becq[3], Zhengjun Jia[1,2], Hui Xi[1,2], Li Shu[1,2], Hua Wang[1,2], Pierre Szepetowski[3]* and Laurent Anikszteijn[3]**

[1]Hunan Provincial Maternal and Child Health Care Hospital, Changsha, China, [2]NHC Key Laboratory of Birth Defects Research, Prevention and Treatment, Changsha, China, [3]INSERM, Aix-Marseille University, INMED, UMR1249, Marseille, France, [4]Department of Epilepsy, General Hospital of Southern Theater Command, Guangzhou, China

OPEN ACCESS

Edited by:
Eleonora Palma,
Sapienza University of Rome, Italy

Reviewed by:
Amy McTague,
University College London,
United Kingdom
Terence Hébert,
McGill University, Canada

***Correspondence:**
Hua Wang
wanghua_213@hotmail.com
Pierre Szepetowski
pierre.szepetowski@inserm.fr
Laurent Anikszteijn
laurent.anikszteijn@inserm.fr

†These authors have contributed equally to this work

Received: 11 July 2019
Accepted: 06 January 2020
Published: 24 January 2020

Citation:
Mao X, Bruneau N, Gao Q, Becq H, Jia Z, Xi H, Shu L, Wang H, Szepetowski P and Anikszteijn L (2020) The Epilepsy of Infancy With Migrating Focal Seizures: Identification of de novo Mutations of the KCNT2 Gene That Exert Inhibitory Effects on the Corresponding Heteromeric $K_{Na}1.1/K_{Na}1.2$ Potassium Channel. Front. Cell. Neurosci. 14:1. doi: 10.3389/fncel.2020.00001

The epilepsy of infancy with migrating focal seizures (EIMFS; previously called Malignant migrating partial seizures of infancy) are early-onset epileptic encephalopathies (EOEE) that associate multifocal ictal discharges and profound psychomotor retardation. EIMFS have a genetic origin and are mostly caused by *de novo* mutations in the *KCNT1* gene, and much more rarely in the *KCNT2* gene. *KCNT1* and *KCNT2* respectively encode the $K_{Na}1.1$ (Slack) and $K_{Na}1.2$ (Slick) subunits of the sodium-dependent voltage-gated potassium channel K_{Na}. Functional analyses of the corresponding mutant homomeric channels *in vitro* suggested gain-of-function effects. Here, we report two novel, *de novo* truncating mutations of *KCNT2*: one mutation is frameshift (p.L48Qfs43), is situated in the N-terminal domain, and was found in a patient with EOEE (possibly EIMFS); the other mutation is nonsense (p.K564*), is located in the C-terminal region, and was found in a typical EIMFS patient. Using whole-cell patch-clamp recordings, we have analyzed the functional consequences of those two novel *KCNT2* mutations on reconstituted $K_{Na}1.2$ homomeric and $K_{Na}1.1/K_{Na}1.2$ heteromeric channels in transfected chinese hamster ovary (CHO) cells. We report that both mutations significantly impacted on K_{Na} function; notably, they decreased the global current density of heteromeric channels by ∼25% (p.K564*) and ∼55% (p.L48Qfs43). Overall our data emphasize the involvement of *KCNT2* in EOEE and provide novel insights into the role of heteromeric K_{Na} channel in the severe *KCNT2*-related epileptic phenotypes. This may have important implications regarding the elaboration of future treatment.

Keywords: epilepsy of infancy with migrating focal seizures, K_{Na} channels, KCNT genes, epilepsy, encephalopathy

INTRODUCTION

Channelopathies represent an important cause of neurological disorders (Kumar et al., 2016). Dysfunction of potassium channels has notably been involved in various types of epileptic encephalopathies, including epilepsy of infancy with migrating focal seizures (EIMFS), previously known as malignant migrating partial seizures of infancy. EIMFS are rare, neonatal epilepsies characterized by onset before the age of 6 months, and usually during the first weeks of life, by continuous migrating polymorphous focal seizures with corresponding multifocal ictal electroencephalographic (EEG) discharges associated with progressive deterioration of psychomotor development (Coppola et al., 1995). EIMFS have a genetic origin and can be caused by *de novo* mutations in the *KCNT1* gene encoding the $K_{Na}1.1$ subunit (Slack or Slo2.2) of K_{Na} channels (Barcia et al., 2012; Ishii et al., 2013; McTague et al., 2013; Rizzo et al., 2016). More recently, two pathogenic mutations in the *KCNT2* gene encoding the $K_{Na}1.2$ subunit (Slick or Slo2.1) have been reported (Gururaj et al., 2017; Ambrosino et al., 2018). K_{Na} channels are voltage-gated potassium channels that are activated by an increase of cytoplasmic Na^+ concentration. They contribute to the slow afterhyperpolarization that follows a train of the action potential in several neuronal populations of the brain (Stafstrom et al., 1985; Kim and McCormick, 1998; Budelli et al., 2009; Hage and Salkoff, 2012; Kaczmarek, 2013; Kaczmarek et al., 2016). These subunits co-assemble to form homo or tetra-heteromeric K_{Na} channels. Each subunit is composed of six transmembrane segments and of two intracellular N and C terminal domains (**Figure 1**). These two subunits display structural differences notably regarding their distal C-terminal region, their electrophysiological properties, their responses to neuromodulators, and their sensitivities to changes in cell volume (Bhattacharjee et al., 2003; Santi et al., 2006; Kaczmarek, 2013; Tejada et al., 2017). The C terminal part contains consensus sites for Na^+ within the RCK2 (regulator of conductance of K^+) domain and interaction sites for cytoplasmic proteins (e.g., protein kinase C). In $K_{Na}1.2$ but not $K_{Na}1.1$, the C-terminus also harbors a binding site for ATP, which function remains elusive (Bhattacharjee et al., 2003; Berg et al., 2007; Kaczmarek, 2013; Garg and Sanguinetti, 2014; Kaczmarek et al., 2016; Gururaj et al., 2017). In heterologous cells, functional analysis of mutant channels associated with EIMFS mostly revealed gain of function effects: potassium current was increased in cells expressing homomeric $K_{Na}1.1$ channels harboring either of the p.Val271Phe, p.Gly288Ser, p.Arg398Gln, p.Arg428Gln, p.Arg474His, p.Met516Val, p.Lys629Asn, p.Ile760Met, p.Pro924Leu or p.Ala934Thr missense mutations, and in cells expressing homomeric $K_{Na}1.2$ channels harboring either of the p.Arg190His or p.Arg190Pro missense mutations (Barcia et al., 2012; Rizzo et al., 2016; Villa and Combi, 2016; Ambrosino et al., 2018). A change in channel function has also been described in cells expressing the $K_{Na}1.2$ subunit harboring the p.Phe240Leu missense mutation: the mutant channel lost its selectivity to K^+ ions and gained permissiveness to Na^+ ions (Gururaj et al., 2017).

Here, we have used exome sequencing to identify two novel *de novo* nonsense and frameshift mutations of the *KCNT2* gene in two patients with ascertained EIMFS and with EIMFS-like early-onset epileptic encephalopathies (EOEE), respectively. We have investigated the functional consequences of the two mutations in heterologous cells expressing heteromeric channels and showed that both mutations reduced whole-cell potassium current. Therefore, EIMFS may be caused not only by an increase but also by a decrease in the function of K_{Na}.

MATERIALS AND METHODS

Patients

The two patients with *KCNT2* mutations were recruited at Hunan Provincial Maternal and Child Health Care Hospital. Leukocyte DNA was extracted from peripheral blood stored in EDTA tubes by the phenol-chloroform method. Clinical information was collected by experienced neurologists. Patients' parents had informed consents and the study was approved by the Ethics Committee of Hunan Provincial Maternal and Child Health Care Hospital.

Exome Sequencing

Patients' DNAs were analyzed by next-generation sequencing with the whole-exome sequencing (WES) approach. DNA fragments were sequenced on the HiSeq2500 system (Illumina, San Diego, CA, USA) with a mean depth of 100×. A preliminary processing of WES data (data alignment and filter) followed pipelines as previously reported (Wang et al., 2011).

The annotated data by ANNOVAR (version 20160201; Wang et al., 2011) was used for further data analyses. Public databases (1000Genome, ESP6500, ExAC, dbSNP, and gnomAD) were used to filter known variants with minor allele frequencies (MAFs) over 0.001. Bioinformatics software (PolyPhen, SIFT, CADD or Mutation Taster) were used to predict the pathogenicity of single-nucleotide variations (SNVs). The loss-of-function variants (nonsense variants, frameshift variants, and splicing variants) and predicted pathogenic SNVs were retained. ACMG guidelines were finally used to evaluate the pathogenicity of the variants (Richards et al., 2015).

Sanger sequencing was performed on patients' DNA to validate the findings of WES and on parents' DNA to study familial inheritance. Sequencing primers were designed according to the sequences of the detected variants and polymerase chain reaction amplification was carried out for Sanger sequencing.

Constructs and Site-Directed Mutagenesis

The human *KCNT1* cDNA construct (Genecopoeia EX-Y5001-M02, thereafter designated as pKCNT1) was used for the expression of wild-type human $K_{Na}1.1$ subunit (NM_020822). Two human *KCNT2* cDNA constructs (Genecopoeia EX-Y5628-M61and EX-Y5628-M83, thereafter designated as pKCNT2-ires-GFP and pKCNT2-ires-mCherry, respectively) were used for expression of mutant or wild-type human $K_{Na}1.2$ subunits (NM_198503) coupled with internal ribosome

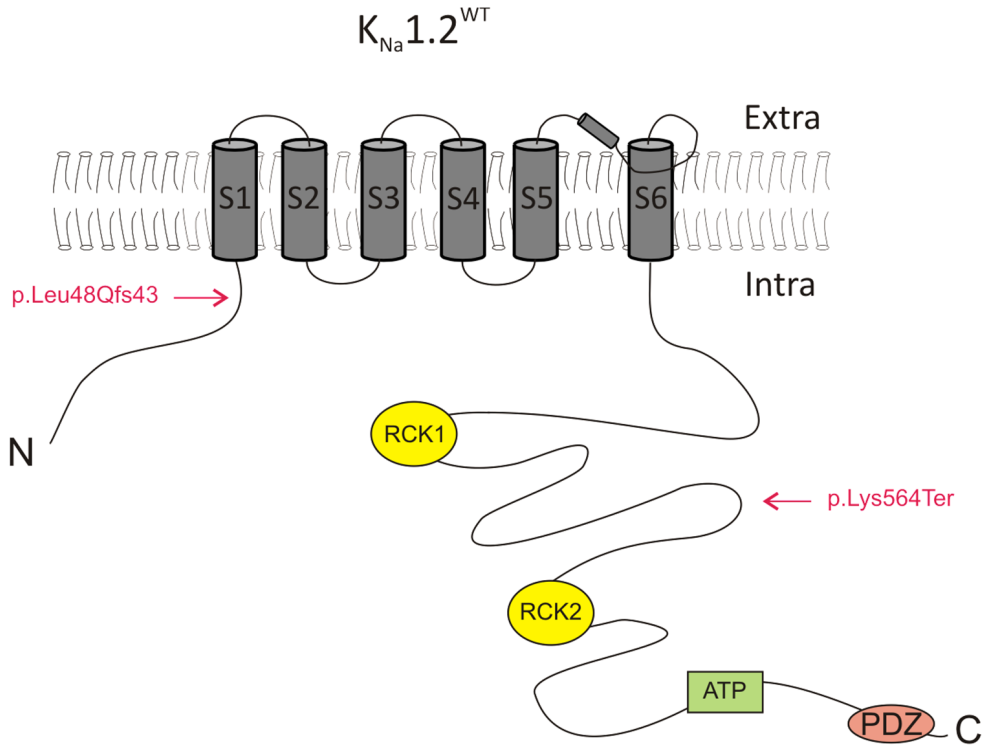

FIGURE 1 | Schematic representation of the $K_{Na}1.2$ subunit. The location of the two mutations identified in the present study (p.K564* and p.L48Qfs43) is indicated. ATP, adenosine triphosphate binding domain; Extra, extracellular milieu; Intra, intracellular milieu. RCK1 and RCK2, regulator of conductance of K^+ domains 1 and 2.

entry site (IRES)-driven independent expression of eGFP (green fluorescent protein) or mcherry protein, respectively.

Mutant *KCNT2* constructs were generated from their wild-type counterpart by using QuikChange Lightning Site-Directed Mutagenesis Kit according to the manufacturer's protocol (Agilent Technologies) and the following forward and reverse primers: *KCNT2-A1690T*: 5′-tctctgctg gtcttggttttaaaatgctgaattctcttctttg and 5′-caaagaagagaattcagc attttaaaaccaagaccagcagaga ($K_{Na}1.2^{K564*}$); *KCNT2-del143-144*: 5′-cttgatctctggttttttatgaaaaataatttgtctttctttaaatgtattttcattcat atag and 5′-ctatatgaatgaaaatacatttaaagaaagacaaattatttttcataaaaaac cagagatcaag($K_{Na}1.2^{L48Qfs43}$). *KCNT2* sequences from wild-type and mutant constructs were all verified by Sanger sequencing (GATC Biotech).

Cell Cultures and Transfections

Chinese hamster ovary (CHO) cells were cultured at 37°C in a humidified atmosphere with 5% CO_2 with an F-12 Nutrient Mixture (Life Technologies) supplemented with 10% FBS (Fetal Bovine Serum) and 100 units/ml antibiotics/antimycotics (Life Technologies). These cells were transiently transfected using the Neon® Transfection System (Life Technologies) according to the manufacturer's protocol. Briefly, 10^5 cells in suspension were transfected with a total amount of 2 μg of DNA. Non-recombinant pcDNA3.1 was added if necessary and concentrations were adjusted to get a total amount of 2 μg of DNA. Electroporation configuration was 1,400 V, 1 pulse, 20 ms. Cells were transiently co-transfected with pKCNT1 and either of pKCNT2-Mutant-ires-GFP or pKCNT2-WT-ires-mCherry or both (see below). Following electroporation, cells were cultured on pre-coated glass coverslips and maintained at 37°C and 5% CO_2 with a complete medium for 2 days before recordings. Combinations of plasmids used in this study are shown in **Table 1**. The eGFP and mCherry fluorescent dyes were used to ascertain the efficacy of transfection assays and select cells for recordings.

Electrophysiology

CHO cells were perfused at 1–2 ml/min with the following solution (in mM): 135 NaCl, 3.5 KCl, 5 $NaHCO_3$, 0.5 NaH_2PO_4, 1 $MgCl_2$, 1.5 $CaCl_2$, 10 HEPES, 10 glucose, and pH 7.3 adjusted with NaOH. Whole-cell patch-clamp recordings were performed with microelectrodes (borosilicate glass capillaries GC 150F-15, Harvard apparatus) filled with a solution containing (in mM): 135 KCl, 0.1 $CaCl_2$, 1.1 EGTA, 10 HEPES, 3 Mg^{2+}ATP, 0.3 Na^+GTP, 4 phosphocreatine, pH 7.3 adjusted with KOH and a resistance of 4–6 MΩ. In some experiments, ATP and GTP were omitted from the internal pipette solution. Data were sampled at 10 kHz and filtered with a cut-off frequency of 3 kHz using an EPC-10 amplifier (HEKA Electronik). An hyperpolarizing voltage step of 10 mV during 500 ms followed by incremental depolarizing voltage steps command of 10 mV was applied from a holding potential of −90 mV and up to +110 mV in order to analyze current densities and the conductance–voltage

TABLE 1 | Biophysical properties of currents recorded in chinese hamster ovary (CHO) cells transfected with the following plasmid combinations.

	Transfected plasmid (μg)	*n*	Current density @+60 mV	$V_{1/2}$ (mV)	k (mV/efold)
peGFP + pcDNA3.1	1 + 1	9	30.8 ± 4.2		
Homozygous configurations					
KCNT2-ires-GFP + pcDNA3.1 ($K_{Na}1.2^{WT}$)	1 + 1	12	46.7 ± 5.6 (without ATP)		
KCNT2-ires-GFP + pcDNA3.1 ($K_{Na}1.2^{WT}$)	1 + 1	6	50.8 ± 12.1 (with ATP)		
KCNT2-A1690T-ires-GFP + pcDNA3.1 ($K_{Na}1.2^{K564*}$)	1 + 1	10	31.9 ± 4.4		
KCNT2-del143-144-ires-GFP + pcDNA3.1 ($K_{Na}1.2^{L48Qfs43}$)	1 + 1	10	24.6 ± 3.9		
KCNT2-ires-mcherry + KCNT2-A1690T-ires-GFP ($K_{Na}1.2^{WT}$ + $K_{Na}1.2^{K564*}$)	1 + 1	11	34.5 ± 6.9		
KCNT2-ires-mcherry + KCNT2-del143-144-ires-GFP ($K_{Na}1.2^{WT}$ + $K_{Na}1.2^{L48Qfs43}$)	1 + 1	10	26.0 ± 4.2		
KCNT1 + pcDNA3.1 + peGFP ($K_{Na}1.1$)	1 + 0.5 + 0.5	25	371.8 ± 39.7	10.7 ± 3.3	42.9 ± 3.3
Heterozygous configurations					
KCNT1 + KCNT2-ires-GFP ($K_{Na}1.1$ + $K_{Na}1.2^{WT}$)	1 + 1	21	629.4 ± 63.5	−1.3 ± 5.1	44.6 ± 5.2
KCNT1 + KCNT2-A1690T-ires-GFP ($K_{Na}1.1^{WT}$ + $K_{Na}1.2^{K564*}$)	1 + 1	18	405.8 ± 46.0	6.8 ± 4.2	33.8 ± 3.1
KCNT1 + KCNT2-del143-144-ires-GFP ($K_{Na}1.1^{WT}$ + $K_{Na}1.2^{L48Qfs43}$)	1 + 1	19	369.8 ± 51.1	−6.5 ± 4.3	42.7 ± 3.7
KCNT1 + KCNT2-ires-mcherry + KCNT2-A1690T-ires-GFP ($K_{Na}1.1$ + $K_{Na}1.2^{WT}$ + $K_{Na}1.2^{K564*}$)	1 + 0.5 + 0.5	18	496.3 ± 54.7	4.7 ± 5.61	41.0 ± 3.5
KCNT1 + KCNT2-ires-mcherry + KCNT2-del143-144-ires-GFP ($K_{Na}1.1$ + $K_{Na}1.2^{WT}$ + $K_{Na}1.2^{L48Qfs43}$)	1 + 0.5 + 0.5	14	332.8 ± 39.8	7.9 ± 4.3	33.1 ± 3.3

n, number of recorded cells. Values of voltage for half-maximal activation of potassium channel ($V_{1/2}$) and of slope factor (k) of conductance/voltage relationships are indicated.

(G–V) relationships. Current densities (expressed in pA/pF) were calculated by measuring current amplitude at the end of the voltage step divided by the capacitance (Cm). G values were obtained from peak amplitudes of the slow outward current divided by the driving force for K^+ ions with E_K ∼−93 mV and normalized to the maximal conductance. Plotted points were fitted with a Boltzmann function: G/Gmax = 1/[1 + exp(V1/2 − Vm)/k] to yield the voltage for half-maximum activation (V_{half}) and the slope factor (k) values. Currents were analyzed using Origin 8.0 software. Analyses were performed after offline leak current subtraction. Membrane potentials were corrected for liquid junction potential (∼5 mV).

Statistical Analyses

Data are represented as means ± SEM. Two-way ANOVA with Tukey's correction for multiple testing or Kruskal–Wallis test were used to assess statistical significance; *adjusted $p < 0.05$; **adjusted $p < 0.01$; ***adjusted $p < 0.001$.

RESULTS

Identification of Two Novel *de novo* KCNT2 Defects in Patients With Early-Onset Epileptic Encephalopathies

Patient A, female, was born at 42 weeks of gestation after normal pregnancy and delivery. She is the first child of healthy non-consanguineous parents. At 2 months of age, she started to have seizures characterized by twitches of the eyelids, tonic elevation of a single limb or both limbs, and perioral cyanosis. The seizures usually lasted several minutes and occurred in clusters with an increasing frequency of more than 20 seizures per day at 3 months. Neurologic examination revealed generalized hypotonia and severe neurologic impairment with the poor visual following. Seizures were refractory to various antiepileptic drugs including valproate, lamotrigine and levetiracetam. Brain magnetic resonance imaging (MRI) was normal. EEG showed a symmetric slow background pattern, multifocal spikes and seizures arising from different regions independently and migrating from one hemisphere to the other at times (**Figure 2A**).

DNA from patient A were screened by WES and analyzed by Clinical Sequencing Analyzer (CSA of WuXiNextCODE). After applying filtering methods, Sanger sequencing was performed to exclude false-positive and examine inheritance. We identified a *de novo* nonsense variant p.K564* (NM_198503.2:c.1690A>T; ClinVar accession number: VCV000695093.1) in *KCNT2* which was absent from controls in ExAC, gnomAD, 1000 Genomes, ESP6500 and dbSNP databases, and compound heterozygous variants in *ABCC2* (NM_000392.3:c.1018C>A and c.1313T>G). No other variant of interest was identified in other genes including known epilepsy genes. Pathogenic variants in *ABCC2* can cause Dubin-Johnson syndrome, a benign autosomal recessive disorder characterized by hyperbilirubinemia with no clinical feature shared with our patients. In the course of the present study, Gururaj

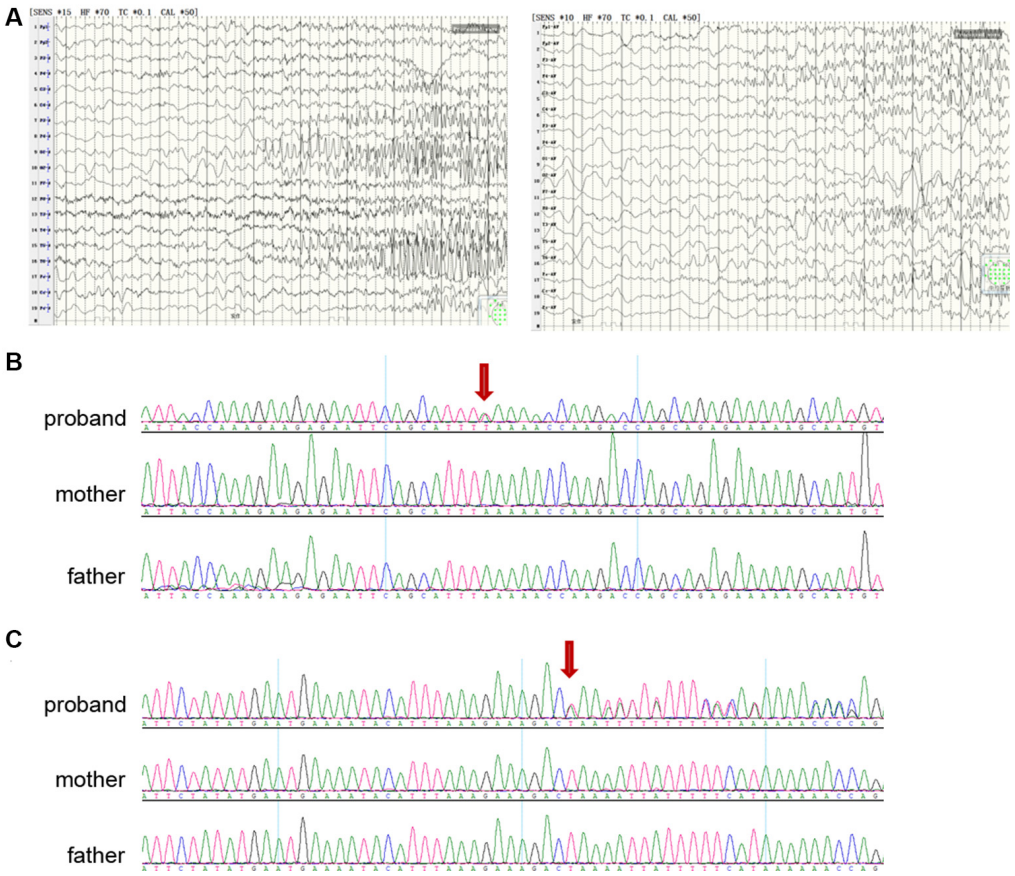

FIGURE 2 | Clinical and genetic data. **(A)** Electroencephalographic (EEG) of a proband with epilepsy of infancy with migrating focal seizures (EIMFS; patient A), showing seizures arising from different hemispheres (left: left occipital lobe; right: right frontal lobe). **(B)** Sanger sequencing showing (red arrow) nonsense variant p.K564* (NM_198503.2:c.1690A>T) in *KCNT2* in the proband (patient A) and not in the parents. **(C)** Sanger sequencing showing (red arrow) frameshift variant p.L48Qfs43 (NM_198503.2:c.143-144 delTA) in *KCNT2* in the proband (patient B) and not in the parents.

et al. (2017) and Ambrosino et al. (2018) identified two *de novo KCNT2* missense variants in patients with epileptic encephalopathy. Despite the fact that the *KCNT2* gene would not be highly intolerant to loss-of-function mutations, as a few nonsense variants have been detected in control individuals and the pLI score (the probability of being loss of function intolerant) is at 0.67 only (see the ExAC database at: http://exac.broadinstitute.org/), we considered the *de novo* nonsense variant p.K564* as the most plausible genetic cause (**Figure 2B**).

We then searched additional *KCNT2* variants in our in-house WES database of a cohort of more than 200 patients with early-onset epileptic encephalopathy (EOEE). We found a *de novo* frameshift variant p.L48Qfs43 (NM_198503.2:c.143-144 delTA; ClinVar accession number: VCV000695094.1) in *KCNT2* in an EOEE patient (Patient B) and validated this variant by Sanger sequencing (**Figure 2C**). This frameshift variant was absent from controls in control databases and no other variant of interest was found in known causative epilepsy genes including EIMFS. Patient B is a 29 years old female who showed mild intellectual disability and seizures. According to her parents and to the medical records, the patient began to have seizure attacks when she was 4 months old. Seizures were mainly focal and migrating, which likely corresponded to EIMFS. However, due to the fact that this is an aged case and considering the relatively low medical level in China almost 30 years ago, diagnosis cannot be firmly ascertained.

Functional Analysis of Wild Type and Mutant Homomeric Human $K_{Na}1.2$ Channels

To investigate the functional consequences of the $K_{Na}1.2$ (*KCNT2*) mutations, CHO cells were first transfected with plasmids encoding the wild type $K_{Na}1.2$ ($K_{Na}1.2^{WT}$) subunit. Two days later, cells were recorded with a KCl filled pipette solution that did not contain ATP, as this nucleotide which binds the C-terminal domain of $K_{Na}1.2$ inhibits channel activity (Bhattacharjee et al., 2003; but see Berg et al., 2007; Garg and Sanguinetti, 2014; Gururaj et al., 2017). We observed that whole-cell current density was slightly but significantly higher than in cells transfected with control plasmid encoding GFP only

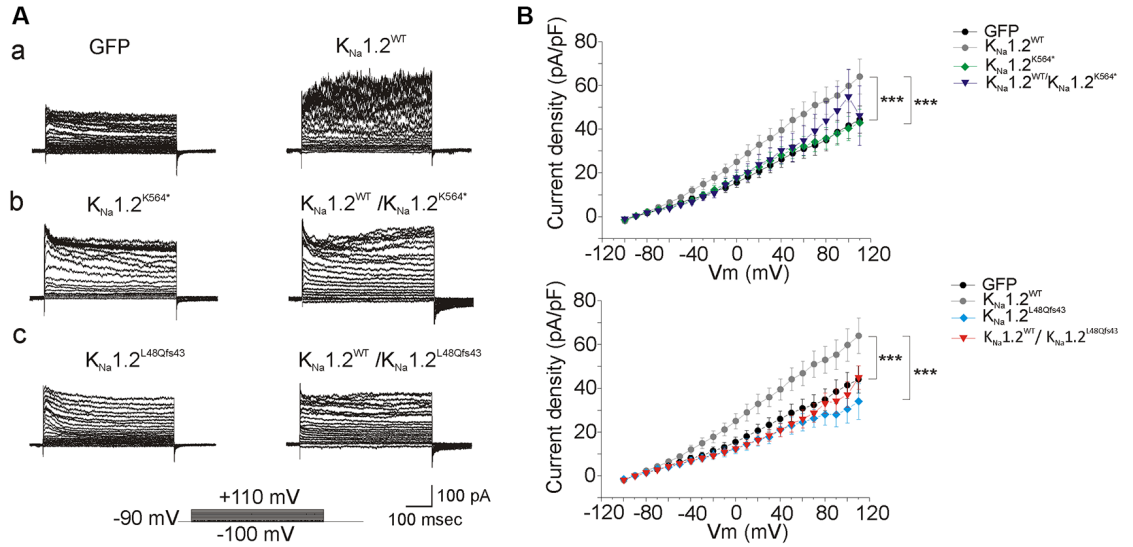

FIGURE 3 | Functional analysis of homomeric wild type and mutant human $K_{Na}1.2$ channels in chinese hamster ovary (CHO) cells. **(A)** Current response to 10 milliVolts (mV) voltage steps command from −90 mV to +110 mV for 500 ms in cells transfected with plasmids encoding: (a) green fluorescent protein (GFP, left traces), wild-type $K_{Na}1.2$ ($K_{Na}1.2^{WT}$, right traces) subunits; (b) the mutant p.K564* ($K_{Na}1.2^{K564*}$, left traces), both $K_{Na}1.2^{WT}$ and $K_{Na}1.2^{K564*}$ subunits (right traces); (c) the mutant p.L48Qfs43 ($K_{Na}1.2^{L48Qfs43}$, left traces), both $K_{Na}1.2^{WT}$ and $K_{Na}1.2^{L48Qfs43}$ subunits (right traces). **(B)** Upper graph: current density expressed in picoAmperes/picofarads (pA/pF) measured at membrane potentials (Vm) as indicated in abscissa, in cells transfected with plasmids encoding GFP, $K_{Na}1.2^{WT}$, $K_{Na}1.2^{K564*}$, both $K_{Na}1.2^{WT}$, and $K_{Na}1.2^{K564*}$ subunits. Bottom graph: same measurements in cells transfected with plasmids encoding GFP, $K_{Na}1.2^{WT}$, $K_{Na}1.2^{L48Qfs43}$, both $K_{Na}1.2^{WT}$ and $K_{Na}1.2^{L48Qfs43}$ subunits. Corresponding symbols are shown on the right of each graph. Two-way ANOVA with Tukey's correction for multiple comparisons. ***$p < 0.001$.

(n = 12 and 9 cells respectively, **Figure 3**, **Table 1**). Values were close to those reported recently in HEK cells (Ambrosino et al., 2018). Similar recordings with pipette solution containing ATP yielded the same results (n = 6 cells, **Table 1**). This suggested that low expression of $K_{Na}1.2$ channel-mediated current in CHO cells is independent of the presence or absence of ATP.

CHO cells were then transfected with plasmids encoding either the human $K_{Na}1.2$ p.K564* ($K_{Na}1.2^{K564*}$; n = 10 cells) or the $K_{Na}1.2$ p.L48Qfs43 ($K_{Na}1.2^{L48Qfs43}$; n = 10 cells) mutant subunits. p.K564* is a nonsense mutation localized in the C-terminal part of $K_{Na}1.2$ and situated between the RCK1 and RCK2 domains (**Figure 1**). This mutation leads to a truncated protein lacking the RCK2 domain and the ATP and PDZ binding sites. p.L48Qfs43 is a frameshift mutation localized in the N-terminal domain of the protein. This mutation leads to a protein composed of the N-terminal domain and the first transmembrane segment S1. For both mutations, depolarizing voltage steps elicited significantly smaller currents compared to cells transfected with $K_{Na}1.2^{WT}$ plasmids (n = 12 cells), and responses were similar to those obtained in cells expressing only GFP. Same results were obtained in cells co-transfected with plasmids encoding $K_{Na}1.2^{WT}$ and $K_{Na}1.2^{K564*}$ subunits (n = 11 cells), or $K_{Na}1.2^{WT}$ and $K_{Na}1.2^{L48Qfs43}$ subunits (n = 10 cells, **Figure 3**). Although the current mediated by $K_{Na}1.2^{WT}$ was very small, these data suggested that in contrast with other previously reported *KCNT2* mutations (Ambrosino et al., 2018), p.K564* and p.L48Qfs43 decreased $K_{Na}1.2$-mediated currents.

Functional Analysis of Wild Type and Mutants Heteromeric $K_{Na}1.1/K_{Na}1.2$ Channels

Immunohistochemical studies performed in rodent brain have shown that $K_{Na}1.1$ and $K_{Na}1.2$ subunits exhibited distinct expression patterns but could also co-localize (Bhattacharjee et al., 2005; Chen et al., 2009; Rizzi et al., 2016). Moreover, biochemical and electrophysiological studies performed in heterologous cells have demonstrated that rat $K_{Na}1.1$ and rat $K_{Na}1.2$ subunits can form heteromeric channels (Chen et al., 2009). The co-assembly of the two subunits enhances channel expression to the plasma membrane, leading to the global current density that is higher than with $K_{Na}1.1$ or $K_{Na}1.2$ alone (Chen et al., 2009). We thus decided to study if the same properties would also characterize the human K_{Na} subunits, and if so, to analyze the impact of the two pathogenic mutations in this heteromeric condition.

To this aim, CHO cells were first transfected with plasmid encoding $K_{Na}1.1$ and recorded with a KCl filled pipette solution containing ATP. These cells responded to depolarizing voltage steps by large outwardly rectifying currents (n = 25 cells, **Figures 4A,B**). Currents were abolished in cells superfused with bepridil 10 μM (n = 5 cells), or in cells recorded with a Na^+-free internal pipette solution (n = 5 cells, **Figures 4A,B**). These data confirmed that the outward rectifying current was mediated by activation of the Na^+-dependent potassium K_{Na} channels. Boltzmann analysis of the conductance/voltage curve showed that V_{half} was at 10.7 ± 3.3 mV, a mean value close to the one

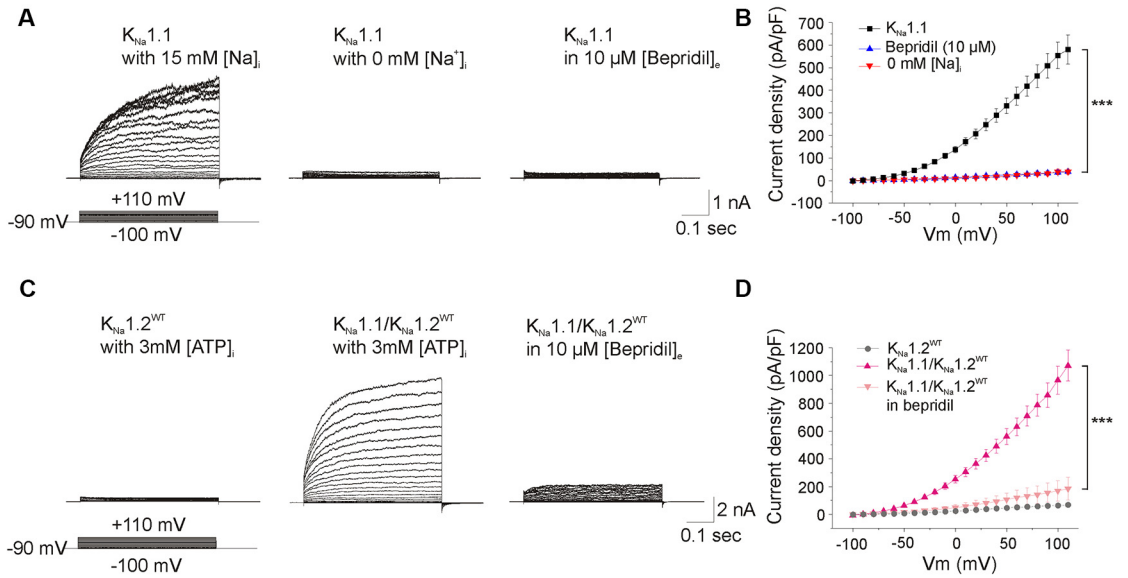

FIGURE 4 | Functional analysis of $K_{Na}1.1$ and heteromeric $K_{Na}1.1/K_{Na}1.2$ channels. **(A)** Current traces evoked by voltage steps in cells expressing $K_{Na}1.1$ subunit and recorded with pipette solution containing either 15 mM Na^+ (left traces), or no Na^+ (middle traces), or 15 mM Na^+ and an extracellular medium containing 10 µM bepridil (right traces). **(B)** Current densities measured in the three recording conditions as in **(A)**. **(C)** Current traces recorded with pipette solution containing 3 mM ATP/0.3 mM GTP in cells expressing the $K_{Na}1.2^{WT}$ subunit (left traces), both $K_{Na}1.1$ and $K_{Na}1.2^{WT}$ subunits (middle traces) and both $K_{Na}1.1$ and $K_{Na}1.2^{WT}$ subunits in the presence of 10 µM bepridil in the extracellular medium (right traces). **(D)** Current densities measured in the three conditions as depicted in **(C)**. Two-way ANOVA with Tukey's correction for multiple comparisons. ***$p < 0.001$.

reported previously (Rizzo et al., 2016), and the slope factor was at 42.9 ± 3.3 mV/e fold (n = 17 cells; **Table 1**), a mean value higher than the one reported by the same authors but which indicated the low voltage sensitivity of K_{Na} channels (Salkoff et al., 2006).

CHO cells were then transfected with plasmids encoding the $K_{Na}1.1$ and $K_{Na}1.2^{WT}$ subunits (n = 21 cells). We observed that whole-cell current was almost twice higher than that generated by $K_{Na}1.1$ alone (n = 25 cells, **Figures 4C,D**), without any significant change in V_{half} and in the slope factor of the conductance/voltage relationship (**Figure 5**, **Table 1**). This current was also dramatically reduced by bepridil 10 µM (n = 5 cells). Thus, like for rat $K_{Na}1.1$ and rat $K_{Na}1.2$, the two human subunits might co-assemble in CHO cells to form heteromeric channels with larger currents.

We then evaluated the consequences of each of the two mutant $K_{Na}1.2$ subunits on heteromeric $K_{Na}1.1/K_{Na}1.2$ channels, either in a homozygous state, or in a heterozygous state to mimic the patient's situation. In cells co-transfected with $K_{Na}1.1$ and $K_{Na}1.2^{K564*}$ plasmids (homozygous mutant state, n = 18 cells), the level of whole-cell current was lower as compared to the wild-type situation, and was similar to the current recorded in cells expressing $K_{Na}1.1$ only (**Figures 5A,B**). The reduction of global current density was not associated with any significant change in the conductance-voltage relationship (n = 15 cells). In cells co-transfected with $K_{Na}1.1/K_{Na}1.2^{WT}/K_{Na}1.2^{K564*}$ plasmids (heterozygous mutant state, n = 18 cells), the level of whole-cell current was significantly increased as compared with cells expressing $K_{Na}1.1$ channels only and was significantly decreased as compared with cells expressing heteromeric wild-type $K_{Na}1.1/K_{Na}1.2^{WT}$ channels (**Figures 5B–D**, **Table 1**).

As with the p.K564* mutation, whole-cell current measured in cells co-transfected with $K_{Na}1.1$ and mutant $K_{Na}1.2^{L48Qfs43}$ plasmids (homozygous mutant state, n = 19 cells, **Figures 6A,B**) was identical to the current measured in cells transfected with $K_{Na}1.1$ plasmid only (n = 25 cells), again without any significant change in the conductance/voltage relationship. Interestingly, currents measured in cells co-transfected with $K_{Na}1.1/K_{Na}1.2^{WT}/K_{Na}1.2^{L48Qfs43}$ plasmids (n = 14 cells) were identical to currents measured in cells expressing $K_{Na}1.1$ only (**Figures 6B–D**, **Table 1**). This indicated a possible dominant-negative effect for p.L48Qfs43.

DISCUSSION

Here, we report two patients diagnosed as EIMFS and EIMFS-like EOEE, respectively, and carrying two novel *de novo* variants in the *KCNT2* gene. Patient A in our study fulfilled the diagnostic criterion for EIMFS (Coppola et al., 1995) including age at the onset before 6 months of age, migrating focal motor seizures, seizures refractory to antiepileptic drugs, and severe psychomotor delay. EEG of patient A also showed the typical "jumping" areas at onset between two hemispheres. According to the clinical manifestations and the EEGs, diagnosis of EIMFS in patient A can be ascertained. We also diagnosed patient B as probably having EIMFS, based on the age at onset and characteristics of her seizure attacks.

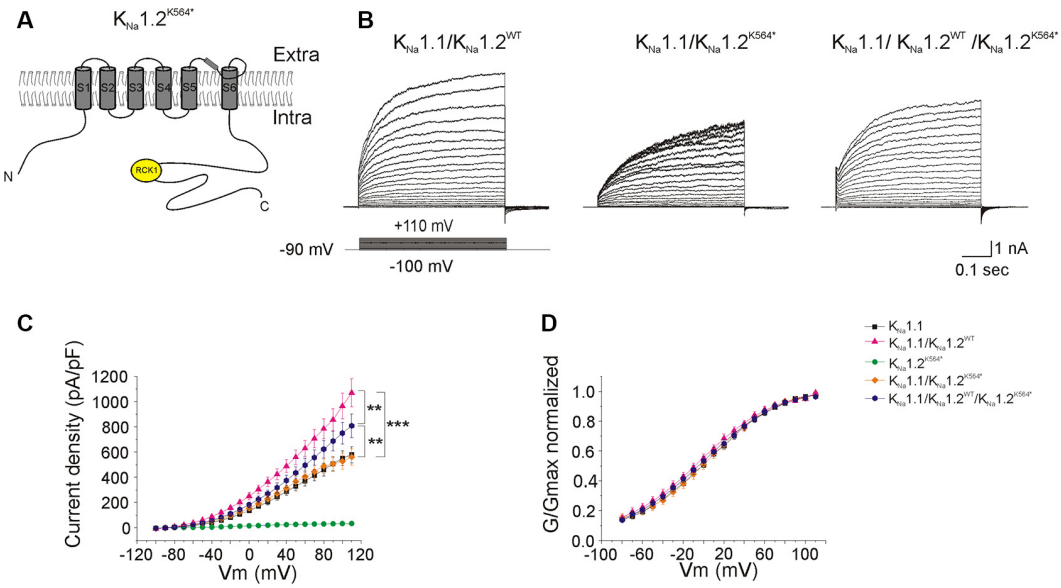

FIGURE 5 | Functional consequences of the p.K564* mutation on heteromeric channels. **(A)** Schematic representation of the expected $K_{Na}1.2^{K564*}$ mutant subunit. The nonsense mutation locates in the C-terminal part of the protein between the RCK1 and RCK2 domains, leading to a predicted truncated protein. **(B)** Representative current responses to depolarizing voltage steps in CHO cells transfected with $K_{Na}1.1$ + $K_{Na}1.2^{WT}$ (left traces); $K_{Na}1.1$ + $K_{Na}1.2^{K564*}$ (middle traces); $K_{Na}1.1$ + $K_{Na}1.2^{WT}$ + $K_{Na}1.2^{K564*}$ (right traces) plasmids. **(C)** Current densities measured in these three conditions but also including $K_{Na}1.1$ and $K_{Na}1.2^{WT}$ for comparison. **(D)** Conductance-voltage relationship of wild type homomeric $K_{Na}1.1$; wild type heteromeric $K_{Na}1.1$ + $K_{Na}1.2$; heteromeric mutant $K_{Na}1.1$ + $K_{Na}1.2^{K564*}$ and heteromeric mutant $K_{Na}1.1$ + $K_{Na}1.2^{WT}$+ $K_{Na}1.2^{K564*}$ channels normalized. Two-way ANOVA with Tukey's correction for multiple comparison. $^{***}p < 0.001$; $^{**}p < 0.01$.

EIMFS is a severe, drug-resistant, early-onset epilepsy encephalopathy in which variants in the *KCNT1*, *SCN1A*, *SCN8A*, *SCN2A*, *PLCB1*, *KCNT1*, *SLC25A22*, *TBC1D24* and *SLC12A5* genes as well as 16p11.2 duplication have been reported. While *de novo* gain of function *KCNT1* ($K_{Na}1.1$) variants are the most common cause of EIMFS (Bedoyan et al., 2010; Carranza Rojo et al., 2011; Barcia et al., 2012; Poduri et al., 2012, 2013; Ishii et al., 2013; McTague et al., 2013; Milh et al., 2013; Ohba et al., 2014; Howell et al., 2015; Stödberg et al., 2015; Rizzo et al., 2016; Villa and Combi, 2016), it was recently reported that *de novo* mutations in the *KCNT2* ($K_{Na}1.2$) gene also caused EOEE, including EIMFS. Two gain-of-function *KCNT2* mutations were identified in a patient with West syndrome that evolved to a Lennox-Gastaut syndrome, and in a patient with EIMFS, respectively (Ambrosino et al., 2018). A third *KCNT2* mutation leading to $K_{Na}1.2$ channels that were no more selective for K^+ ions and that became permeable to Na^+ ions was identified in a patient with multi-focal epileptogenic activity or hypsarrhythmia (Gururaj et al., 2017). Here, we have identified in two patients with EIMFS and EIMFS-like phenotypes, two novel *de novo* mutations in *KCNT2* ($K_{Na}1.2$), respectively localized in the N-terminal (p.L48Qfs43) and C-terminal (p.K564*) domains of the protein and which both led to significantly reduced activity of heteromeric K_{Na} channels *in vitro*. To reach this conclusion, we have analyzed the macroscopic current in CHO cells co-transfected with wild type and mutant $K_{Na}1.2$ subunits, notably in the heterozygous configuration to mimic the patient's situation. To the best of our knowledge, the functional impact of $K_{Na}1.2$ pathogenic mutations on currents generated by human heteromeric K_{Na} channels had never been tested in such a configuration, although immunohistochemical studies performed in adult rodent brain provided evidence that $K_{Na}1.1$ and $K_{Na}1.2$ subunits can co-localize and potentially form heteromeric channels (Bhattacharjee et al., 2005; Chen et al., 2009; Rizzi et al., 2016). K_{Na} channels are also very likely to be formed by homomeric $K_{Na}1.1$ or $K_{Na}1.2$ subunits in another large subset of neuronal cells. Here, we observed that human $K_{Na}1.2^{WT}$ produced a very small current either in the presence or absence of ATP. The same difficulty to detect current in CHO cells was mentioned by Gururaj et al. (2017). In cells co-transfected with $K_{Na}1.1$ and $K_{Na}1.2$ plasmids, the current was larger as compared to cells transfected either with $K_{Na}1.1$ or with $K_{Na}1.2$ plasmids alone, indicating that both subunits are expressed and would co-assemble to form a heteromeric channel. It is possible that in spite of the internal dialysis due to whole-cell recording, the endogenous concentration of ATP in CHO cells is high enough to exert its inhibitory effect on the $K_{Na}1.2$ subunit (Bhattacharjee et al., 2003)—although the action of ATP has been challenged in other studies (Berg et al., 2007; Garg and Sanguinetti, 2014; Gururaj et al., 2017). Another possibility is that the intracellular concentration of Na^+ (15 mM) is not high enough to activate the channel. The reliable current was observed in HEK cells expressing human $K_{Na}1.2$ subunit but with a patch pipette solution containing 70 mM Na^+ concentration (Berg et al., 2007). In fact, $K_{Na}1.2$ channels might be less sensitive to $[Na^+]_i$ than $K_{Na}1.1$ (Bhattacharjee et al., 2003; Kaczmarek,

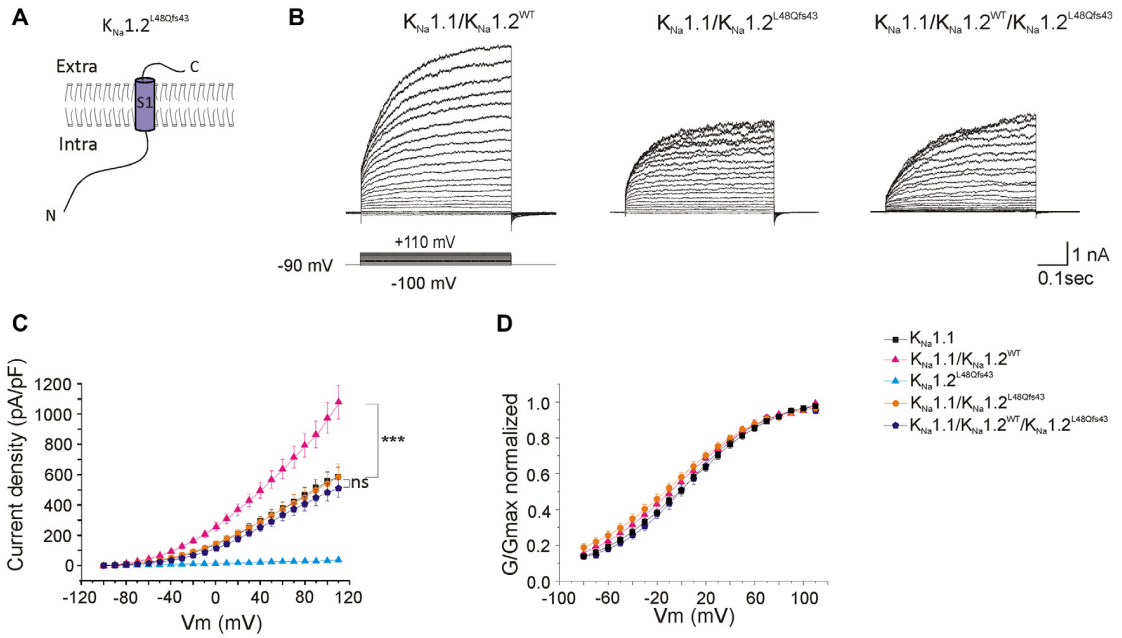

FIGURE 6 | Functional consequences of the p.L48Qfs43 mutation on heteromeric channels. **(A)** Schematic representation of the expected $K_{Na}1.2^{L48Qfs43}$ mutant subunit. The frameshift mutation locates in the N-terminal part of the protein, leading to predicted protein composed of the N-terminal domain and of transmembrane segment S1. **(B)** Representative current responses to depolarizing voltage steps in CHO cells transfected with $K_{Na}1.1$ + $K_{Na}1.2^{WT}$ (left traces); $K_{Na}1.1$ + $K_{Na}1.2^{L48Qfs43}$ (middle traces); $K_{Na}1.1$ + $K_{Na}1.2^{WT}$+ $K_{Na}1.1^{L48Qfs43}$ (right traces) plasmids. **(C)** Current densities measured in these three conditions but also including $K_{Na}1.1$ and $K_{Na}1.2^{WT}$ for comparison. Corresponding symbols are indicated on the top of the graph. **(D)** Conductance-voltage relationship of wild type homomeric $K_{Na}1.1$; wild type heteromeric $K_{Na}1.1$ + $K_{Na}1.2$; heteromeric mutant $K_{Na}1.1$ + $K_{Na}1.2^{L48Qfs43}$ and heteromeric mutant $K_{Na}1.1$ + $K_{Na}1.2^{WT}$+ $K_{Na}1.2^{L48Qfs43}$ channels normalized. Two-way ANOVA with Tukey's correction for multiple comparisons. $^{***}p < 0.001$; ns, not significant.

2013). The small current produced by human $K_{Na}1.2$ contrasts with the large whole-cell current produced in the same cells by rat $K_{Na}1.2$ subunit (Gururaj et al., 2017). There are slight differences in amino acids sequence between the rat and human $K_{Na}1.2$ subunits (∼2%; Bhattacharjee et al., 2003): some of these amino acids may be instrumental for the functional discrepancy between rat and human $K_{Na}1.2$ subunit, as shown for the rodent and human Kv7.3 subunit of Kv7 potassium channels (Etxeberria et al., 2004). Thus, the role of homomeric $K_{Na}1.2$ channel in human neurons might even be questioned if, like in CHO cells, they mediated a very small current only. Hence and apart from the gain of function mutations reported recently (Ambrosino et al., 2018), the role of $K_{Na}1.2$ and the functional consequences of the two mutants reported here would be exerted in human neurons co-expressing $K_{Na}1.1$ and $K_{Na}1.2$.

In the present study, we did not investigate the cellular mechanisms that would account for the effects of the two mutations. First, we showed that both mutant subunits failed to generate significant current. This was expected for $K_{Na}1.2^{L48Qfs43}$ as the mutant subunit would not contain a pore domain—if not degraded. This was also not surprising for $K_{Na}1.2^{K564*}$ as the truncated part of the C-terminal domain includes the RCK2 domain which contains coordination motif for Na^+ interaction (Thomson et al., 2015). Second, cells co-transfected with plasmids encoding $K_{Na}1.1$ and either of the mutant $K_{Na}1.2$ subunits in a homozygous state exhibited whole-cell currents that were similar to the currents measured in cells transfected with the $K_{Na}1.1$ plasmid alone. This suggested either that the mutant subunits are rapidly degraded or lead to a non-functional heteromeric channel, or that the mutations prevented the assembly of $K_{Na}1.2$ with $K_{Na}1.1$. Indeed, the N-terminal domain of $K_{Na}1.1$ plays a key role in heteromerization and channel trafficking (Chen et al., 2009). As channel formation (assembly, stabilization, trafficking) generally involves multiple inter-subunit association sites (Deutsch, 2002), it is also possible that the lack of the C-terminal part of mutant $K_{Na}1.2$ subunits plays instrumental role.

In the $K_{Na}1.1/K_{Na}1.2^{WT}/K_{Na}1.2^{K564*}$ mutant heterozygous configuration mimicking the patient situation, global current density was intermediate between that of cells expressing $K_{Na}1.1$ alone and that of cells expressing both $K_{Na}1.1/K_{Na}1.2$ subunits. Whether the moderate alteration (∼25% decrease) of K_{Na} current density observed with the p.K564* mutation would be sufficient to cause EIFMS remains to be firmly established. Indeed, *KCNT2* does not look that intolerant to heterozygous loss of function mutations, as can be inferred from databases of control individuals. On the one hand and although very unlikely, we cannot firmly exclude that the identification of the *de novo* p.K564* mutation in an EFMIS patient was coincidental by chance only. On the other hand, nonsense mutations in other epilepsy genes (e.g., *DEPDC5*) have also been detected in control individuals, and pLI scores

should be interpreted with caution (Fuller et al., 2019). Also, different nonsense mutations in a given gene might be differently subjected to nonsense-mediated mRNA decay (NMD) which in turn sustains compensatory effects (El-Brolosy et al., 2019). Moreover, the actual impact of a deleterious ion channel mutation might be better seen in the genetic context of variants in other ion channels (Klassen et al., 2011). Interestingly, while the typical mutations of *KCNT1* leading to EIFMS are gain of function and *KCNT1* would be even more tolerant than *KCNT2* to loss-of-function variants (pLI score at 0.01 at the ExAC database, http://exac.broadinstitute.org/), a Phe932Ile loss of function variant in *KCNT1* was reported in a patient with severe epilepsy, delayed myelination and leukoencephalopathy (Vanderver et al., 2014; Evely et al., 2017), further indicating that decreased activity of K_{Na} channels can indeed be associated with severe neurological manifestations including epilepsy. The other mutation found here in *KCNT2*, p.L48Qfs43, had more dramatic effects than p.K564*: in the $K_{Na}1.1/K_{Na}1.2^{WT}/K_{Na}1.2^{L48Qfs43}$ configuration, current global density was more severely affected than with p.K564* and was similar to that of $K_{Na}1.1$ alone, consistent with a dominant-negative effect of p.L48Qfs43. Overall this indicates how important these channels are to control neuronal excitability at early developmental stages. That similar phenotypes were observed in patient B carrying the p.L48Qfs43 mutation (∼55% decrease K_{Na} current density) or in a patient carrying the gain of function p.R190P mutation (Ambrosino et al., 2018) suggests that K_{Na} channels efficiency should be tightly regulated during brain development and that any alteration, whatever its direction, would deeply impact on cortical networks activities.

There is now evidence that gain or loss of function mutations of a given ion channel may both lead to epileptic encephalopathies—although differences in phenotypes may exist (see above). This has been well documented for Kv7.2 *de novo* mutations (Miceli et al., 2013, 2015; Orhan et al., 2014; Abidi et al., 2015; Devaux et al., 2016; Mulkey et al., 2017). We now show that this is also the case for $K_{Na}1.2$ mutations. This may have practical implications as drugs inhibiting/reducing $K_{Na}1.1$ channel activity such as quinidine have been used to improve the EEG and background activity in a subset of the patients. Different hypotheses have been proposed to explain how an increase or a decrease in the function of a given ion channel may have similar consequences on network activity. Notably different sensitivity of a mutant channel in pyramidal cells and in interneurons has been suggested, creating an imbalance between excitation and inhibition or favoring neuronal synchronization (Miceli et al., 2015; Niday and Tzingounis, 2018). The development of animal models carrying loss and gain of function mutations is needed to solve this apparent paradox. This is particularly important for the $K_{Na}1.2$ subunit, whose exact role in neuronal activity remains to be addressed.

DATA AVAILABILITY STATEMENT

The raw data of WES were deposited at the Sequence Read Archive (SRA) public database at NCBI (https://www.ncbi.nlm.nih.gov/sra; accession numbers: PRJNA592898; release date 2020-01-31, and PRJNA593942, release date 2019-12-08). The KCNT2 variants were deposited at the ClinVar public database at NCBI https://www.ncbi.nlm.nih.gov/clinvar/; c.1690A>T: accession number VCV000695093.1; c.143-144 delTA: accession number VCV000695094.1).

ETHICS STATEMENT

The studies involving human participants were reviewed and approved by Ethics Committee of Hunan Provincial Maternal and Child Health Care Hospital. Written informed consent to participate in this study was provided by the participants' legal guardian/next of kin. Written informed consent was obtained from the individual(s), and minor(s)' legal guardian/next of kin, for the publication of any potentially identifiable images or data included in this article.

AUTHOR CONTRIBUTIONS

XM designed and performed clinical investigations and genetic analyzes. NB designed and performed cell biology experiments (expression constructs, cell cultures and transfections). HB participated in the electrophysiological experiments. QG, ZJ, and HW collected clinical data. HX and LS performed data analysis. PS coordinated and participated in the design of the overall study. LA designed, performed, analyzed and coordinated the electrophysiological experiments and wrote the article with the help of XM, NB, and PS.

FUNDING

This work was supported by INSERM (Institut National de la Santé et de la Recherche Médicale), by the European Union Seventh Framework Programme FP7/2007–2013 under the project DESIRE (grant agreement n°602531), by the National Natural Science Foundation of China (grant number 81801136), and by the Natural Science Foundation of Hunan Province, China (grant number 2017JJ3142).

REFERENCES

Abidi, A., Devaux, J. J., Molinari, F., Alcaraz, G., Michon, F.-X., Sutera-Sardo, J., et al. (2015). A recurrent KCNQ2 pore mutation causing early onset epileptic encephalopathy has a moderate effect on M current but alters subcellular localization of Kv7 channels. *Neurobiol. Dis.* 80, 80–92. doi: 10.1016/j.nbd.2015.04.017

Ambrosino, P., Soldovieri, M. V., Bast, T., Turnpenny, P. D., Uhrig, S., Biskup, S., et al. (2018). *De novo* gain-of-function variants in KCNT2 as a novel cause of developmental and epileptic encephalopathy. *Ann. Neurol.* 83, 1198–1204. doi: 10.1002/ana.25248

Barcia, G., Fleming, M. R., Deligniere, A., Gazula, V. R., Brown, M. R., Langouet, M., et al. (2012). *De novo* gain-of-function KCNT1 channel

mutations cause malignant migrating partial seizures of infancy. *Nat. Genet.* 44, 1255–1259. doi: 10.1038/ng.2441

Bedoyan, J. K., Kumar, R. A., Sudi, J., Silverstein, F., Ackley, T., Iyer, R. K., et al. (2010). Duplication 16p11.2 in a child with infantile seizure disorder. *Am. J. Med. Genet.* 152A, 1567–1574. doi: 10.1002/ajmg.a.33415

Berg, A. P., Sen, N., and Bayliss, D. A. (2007). TrpC3/C7 and Slo2.1 are molecular targets for metabotropic glutamate receptor signaling in rat striatal cholinergic interneurons. *J. Neurosci.* 27, 8845–8856. doi: 10.1523/JNEUROSCI.0551-07.2007

Bhattacharjee, A., Joiner, W. J., Wu, M., Yang, Y., Sigworth, F. J., and Kaczmarek, L. K. (2003). Slick (Slo2.1), a rapidly-gating sodium-activated potassium channel inhibited by ATP. *J. Neurosci.* 23, 11681–11691. doi: 10.1523/JNEUROSCI.23-37-11681.2003

Bhattacharjee, A., von Hehn, C. A. A., Mei, X., and Kaczmarek, L. K. (2005). Localization of the Na^+-activated K^+ channel slick in the rat central nervous system. *J. Comp. Neurol.* 484, 80–92. doi: 10.1002/cne.20462

Budelli, G., Hage, T. A., Wei, A., Rojas, P., Jong, Y. J., O'Malley, K., et al. (2009). Na^+-activated K^+ channels express a large delayed outward current in neurons during normal physiology. *Nat. Neurosci.* 12, 745–750. doi: 10.1038/nn.2313

Carranza Rojo, D., Hamiwka, L., McMahon, J. M., Dibbens, L. M., Arsov, T., Suls, A., et al. (2011). *De novo* SCN1A mutations in migrating partial seizures of infancy. *Neurology* 77, 380–383. doi: 10.1212/WNL.0b013e318227046d

Chen, H., Kronengold, J., Yan, Y., Gazula, V.-R., Brown, M. R., Ma, L., et al. (2009). The N-terminal domain of slack determines the formation and trafficking of slick/slack heteromeric sodium-activated potassium channels. *J. Neurosci.* 29, 5654–5665. doi: 10.1523/JNEUROSCI.5978-08.2009

Coppola, G., Plouin, P., Chiron, C., Robain, O., and Dulac, O. (1995). Migrating partial seizures in infancy: a malignant disorder with developmental arrest. *Epilepsia* 36, 1017–1024. doi: 10.1111/j.1528-1157.1995.tb00961.x

Deutsch, C. (2002). Potassium channel ontogeny. *Annu. Rev. Physiol.* 64, 19–46. doi: 10.1146/annurev.physiol.64.081501.155934

Devaux, J., Abidi, A., Roubertie, A., Molinari, F., Becq, H., Lacoste, C., et al. (2016). A Kv7.2 mutation associated with early onset epileptic encephalopathy with suppression-burst enhances Kv7/M channel activity. *Epilepsia* 57, e87–e93. doi: 10.1111/epi.13366

El-Brolosy, M. A., Kontarakis, Z., Rossi, A., Kuenne, C., Günther, S., Fukuda, N., et al. (2019). Genetic compensation triggered by mutant mRNA degradation. *Nature* 568, 193–197. doi: 10.1038/s41586-019-1064-z

Etxeberria, A., Santana-Castro, I., Regalado, M. P., Aivar, P., and Villarroel, A. (2004). Three mechanisms underlie KCNQ2/3 heteromeric potassium M-channel potentiation. *J. Neurosci.* 24, 9146–9152. doi: 10.1523/JNEUROSCI.3194-04.2004

Evely, K. M., Pryce, K. D., and Bhattacharjee, A. (2017). The Phe932Ile mutation in KCNT1 channels associated with severe epilepsy, delayed myelination and leukoencephalopathy produces a loss-of-function channel phenotype. *Neuroscience* 351, 65–70. doi: 10.1016/j.neuroscience.2017.03.035

Fuller, Z. L., Berg, J. J., Mostafavi, H., Sella, G., and Przeworski, M. (2019). Measuring intolerance to mutation in human genetics. *Nat. Genet.* 51, 772–776. doi: 10.1038/s41588-019-0383-1

Garg, P., and Sanguinetti, M. C. (2014). Intracellular ATP does not inhibit Slo2.1 K^+ channels. *Physiol. Rep.* 2:e12118. doi: 10.14814/phy2.12118

Gururaj, S., Palmer, E. E., Sheehan, G. D., Kandula, T., Macintosh, R., Ying, K., et al. (2017). A *de novo* mutation in the sodium-activated potassium channel KCNT2 alters ion selectivity and causes epileptic encephalopathy. *Cell Rep.* 21, 926–933. doi: 10.1016/j.celrep.2017.09.088

Hage, T. A., and Salkoff, L. (2012). Sodium-activated potassium channels are functionally coupled to persistent sodium currents. *J. Neurosci.* 32, 2714–2721. doi: 10.1523/JNEUROSCI.5088-11.2012

Howell, K. B., McMahon, J. M., Carvill, G. L., Tambunan, D., Mackay, M. T., Rodriguez-Casero, V., et al. (2015). SCN2A encephalopathy: a major cause of epilepsy of infancy with migrating focal seizures. *Neurology* 85, 958–966. doi: 10.1212/WNL.0000000000001926

Ishii, A., Shioda, M., Okumura, A., Kidokoro, H., Sakauchi, M., Shimada, S., et al. (2013). A recurrent KCNT1 mutation in two sporadic cases with malignant migrating partial seizures in infancy. *Gene* 531, 467–471. doi: 10.1016/j.gene.2013.08.096

Kaczmarek, L. K. (2013). Slack, slick, and sodium-activated potassium channels. *ISRN Neurosci.* 2013:354262. doi: 10.1155/2013/354262

Kaczmarek, L. K., Aldrich, R. W., Chandy, K. G., Grissmer, S., Wei, A. D., and Wulff, H. (2016). International union of basic and clinical pharmacology. C. Nomenclature and properties of calcium-activated and sodium-activated potassium channels. *Pharmacol. Rev.* 69, 1–11. doi: 10.1124/pr.116.012864

Kim, U., and McCormick, D. A. (1998). Functional and ionic properties of a slow afterhyperpolarization in ferret perigeniculate neurons *in vitro*. *J. Neurophysiol.* 80, 1222–1235. doi: 10.1152/jn.1998.80.3.1222

Klassen, T., Davis, C., Goldman, A., Burgess, D., Chen, T., Wheeler, D., et al. (2011). Exome sequencing of ion channel genes reveals complex profiles confounding personal risk assessment in epilepsy. *Cell* 145, 1036–1048. doi: 10.1016/j.cell.2011.05.025

Kumar, P., Kumar, D., Jha, S. K., Jha, N. K., and Ambasta, R. K. (2016). *Ion Channels in Neurological Disorders.* 1st Edn. Elsevier Inc.

McTague, A., Appleton, R., Avula, S., Cross, H., King, M. D., Jacques, T. S., et al. (2013). Migrating partial seizures of infancy: expansion of the electroclinical, radiological and pathological disease spectrum. *Brain* 136, 1578–1591. doi: 10.1093/brain/awt073

Miceli, F., Soldovieri, M. V., Ambrosino, P., Barrese, V., Migliore, M., Cilio, M. R., et al. (2013). Genotype-phenotype correlations in neonatal epilepsies caused by mutations in the voltage sensor of $K_v7.2$ potassium channel subunits. *Proc. Natl. Acad. Sci. U S A* 110, 4386–4391. doi: 10.1073/pnas.1216867110

Miceli, F., Soldovieri, M. V., Ambrosino, P., De Maria, M., Migliore, M., Migliore, R., et al. (2015). Early-onset epileptic encephalopathy caused by gain-of-function mutations in the voltage sensor of $K_v7.2$ and $K_v7.3$ potassium channel subunits. *J. Neurosci.* 35, 3782–3793. doi: 10.1523/JNEUROSCI.4423-14.2015

Milh, M., Falace, A., Villeneuve, N., Vanni, N., Cacciagli, P., Assereto, S., et al. (2013). Novel compound heterozygous mutations in TBC1D24 cause familial malignant migrating partial seizures of infancy. *Hum. Mutat.* 34, 869–872. doi: 10.1002/humu.22318

Mulkey, S. B., Ben-Zeev, B., Nicolai, J., Carroll, J. L., Grønborg, S., Jiang, Y. H., et al. (2017). Neonatal nonepileptic myoclonus is a prominent clinical feature of KCNQ2 gain-of-function variants R201C and R201H. *Epilepsia* 58, 436–445. doi: 10.1111/epi.13676

Niday, Z., and Tzingounis, A. V. (2018). Potassium channel gain of function in epilepsy: an unresolved paradox. *Neuroscientist* 24, 368–380. doi: 10.1177/1073858418763752

Ohba, C., Kato, M., Takahashi, S., Lerman-Sagie, T., Lev, D., Terashima, H., et al. (2014). Early onset epileptic encephalopathy caused by *de novo* SCN8A mutations. *Epilepsia* 55, 994–1000. doi: 10.1111/epi.12668

Orhan, G., Bock, M., Schepers, D., Ilina, E. I., Reichel, S. N., Löffler, H., et al. (2014). Dominant-negative effects of KCNQ2 mutations are associated with epileptic encephalopathy. *Ann. Neurol.* 75, 382–394. doi: 10.1002/ana.24080

Poduri, A., Chopra, S. S., Neilan, E. G., Elhosary, P. C., Kurian, M. A., Meyer, E., et al. (2012). Homozygous PLCB1 deletion associated with malignant migrating partial seizures in infancy. *Epilepsia* 53, e146–e150. doi: 10.1111/j.1528-1167.2012.03538.x

Poduri, A., Heinzen, E. L., Chitsazzadeh, V., Lasorsa, F. M., Elhosary, P. C., LaCoursiere, C. M., et al. (2013). SLC25A22 is a novel gene for migrating partial seizures in infancy. *Ann. Neurol.* 74, 873–882. doi: 10.1002/ana.23998

Richards, S., Aziz, N., Bale, S., Bick, D., Das, S., Gastier-Foster, J., et al. (2015). Standards and guidelines for the interpretation of sequence variants: a joint consensus recommendation of the American College of Medical Genetics and Genomics and the Association for Molecular Pathology. *Genet. Med.* 17, 405–424. doi: 10.1038/gim.2015.30

Rizzi, S., Knaus, H. G., and Schwarzer, C. (2016). Differential distribution of the sodium-activated potassium channels slick and slack in mouse brain. *J. Comp. Neurol.* 524, 2093–2116. doi: 10.1002/cne.23934

Rizzo, F., Ambrosino, P., Guacci, A., Chetta, M., Marchese, G., Rocco, T., et al. (2016). Characterization of two *de novo* KCNT1 mutations in children with malignant migrating partial seizures in infancy. *Mol. Cell. Neurosci.* 72, 54–63. doi: 10.1016/j.mcn.2016.01.004

Salkoff, L., Butler, A., Ferreira, G., Santi, C., and Wei, A. (2006). High-conductance potassium channels of the SLO family. *Nat. Rev. Neurosci.* 7, 921–931. doi: 10.1038/nrn1992

Santi, C. M., Ferreira, G., Yang, B., Gazula, V. R., Butler, A., Wei, A., et al. (2006). Opposite regulation of slick and slack K^+ channels by neuromodulators. *J. Neurosci.* 26, 5059–5068. doi: 10.1523/JNEUROSCI.3372-05.2006

Stafstrom, C. E., Schwindt, P. C., Chubb, M. C., and Crill, W. E. (1985). Properties of persistent sodium conductance and calcium conductance of layer V neurons from cat sensorimotor cortex *in vitro*. *J. Neurophysiol.* 53, 153–170. doi: 10.1152/jn.1985.53.1.153

Stödberg, T., McTague, A., Ruiz, A. J., Hirata, H., Zhen, J., Long, P., et al. (2015). Mutations in SLC12A5 in epilepsy of infancy with migrating focal seizures. *Nat. Commun.* 6:8038. doi: 10.1038/ncomms9038

Tejada, M. A., Hashem, N., Calloe, K., and Klaerke, D. A. (2017). Heteromeric Slick/Slack K^+ channels show graded sensitivity to cell volume changes. *PLoS One* 12:e0169914. doi: 10.1371/journal.pone.0169914

Thomson, S. J., Hansen, A., and Sanguinetti, M. C. (2015). Identification of the intracellular Na^+ sensor in Slo2.1 potassium channels. *J. Biol. Chem.* 290, 14528–14535. doi: 10.1074/jbc.m115.653089

Vanderver, A., Simons, C., Schmidt, J. L., Pearl, P. L., Bloom, M., Lavenstein, B., et al. (2014). Identification of a novel *de novo* p.Phe932Ile KCNT1 mutation in a patient with leukoencephalopathy and severe epilepsy. *Pediatr. Neurol.* 50, 112–114. doi: 10.1016/j.pediatrneurol.2013.06.024

Villa, C., and Combi, R. (2016). Potassium channels and human epileptic phenotypes: an updated overview. *Front. Cell. Neurosci.* 10:81. doi: 10.3389/fncel.2016.00081

Wang, J. L., Cao, L., Li, X. H., Hu, Z. M., Li, J. D., Zhang, J. G., et al. (2011). Identification of PRRT2 as the causative gene of paroxysmal kinesigenic dyskinesias. *Brain* 134, 3493–3501. doi: 10.1093/brain/awr289

Conflict of Interest: The authors declare that the research was conducted in the absence of any commercial or financial relationships that could be construed as a potential conflict of interest.

frontiers in Cellular Neuroscience

MINI REVIEW
published: 13 February 2020
doi: 10.3389/fncel.2020.00009

A Reappraisal of GAT-1 Localization in Neocortex

Giorgia Fattorini[1,2†], *Marcello Melone*[1,2†] *and Fiorenzo Conti*[1,2,3*†]

[1]*Department of Experimental and Clinical Medicine, Faculty of Medicine and Surgery, Università Politecnica delle Marche, Ancona, Italy,* [2]*Center for Neurobiology of Aging, IRCCS INRCA, Ancona, Italy,* [3]*Fondazione di Medicina Molecolare, Università Politecnica delle Marche, Ancona, Italy*

γ-Aminobutyric acid (GABA) transporter (GAT)-1, the major GABA transporter in the brain, plays a key role in modulating GABA signaling and is involved in the pathophysiology of several neuropsychiatric diseases, including epilepsy. The original description of GAT-1 as a neuronal transporter has guided the interpretation of the findings of all physiological, pharmacological, genetic, or clinical studies. However, evidence published in the past few years, some of which is briefly reviewed herein, does not seem to be consistent with a neurocentric view of GAT-1 function and calls for more detailed analysis of its localization. We therefore performed a thorough systematic assessment of GAT-1 localization in neocortex and subcortical white matter. In line with earlier work, we found that GAT-1 was robustly expressed in axon terminals forming symmetric synapses and in astrocytic processes, whereas its astrocytic expression was more diffuse than expected and, even more surprisingly, immature and mature oligodendrocytes and microglial cells also expressed the transporter. These data indicate that the era of "neuronal" and "glial" GABA transporters has finally come to a close and provide a wider perspective from which to view GABA-mediated physiological phenomena. In addition, given the well-known involvement of astrocytes, oligodendrocytes, and microglial cells in physiological as well as pathological conditions, the demonstration of functional GAT-1 in these cells is expected to provide greater insight into the phenomena occurring in the diseased brain as well as to prompt a reassessment of earlier findings.

Keywords: GAT-1, GABA transporters, astrocytes, oligodendrocytes, microglia

OPEN ACCESS

Edited by:
Eleonora Palma,
Sapienza University of Rome, Italy

Reviewed by:
Annalisa Scimemi,
University at Albany, United States
Enrico Cherubini,
European Brain Research Institute, Italy

***Correspondence:**
Fiorenzo Conti
f.conti@univpm.it

[†]***ORCID***
Giorgia Fattorini
orcid.org/0000-0002-2497-2942
Marcello Melone
orcid.org/0000-0003-4173-0774
Fiorenzo Conti
orcid.org/0000-0001-5853-1566

Received: *29 November 2019*
Accepted: *13 January 2020*
Published: *13 February 2020*

Citation:
Fattorini G, Melone M and Conti F (2020) A Reappraisal of GAT-1 Localization in Neocortex. Front. Cell. Neurosci. 14:9. doi: 10.3389/fncel.2020.00009

INTRODUCTION

γ-Aminobutyric acid (GABA) transporter (GAT)-1 is a highly conserved molecule that is encoded by *SLC6A1* and transports GABA in a high-affinity, Na^+- and Cl^--dependent manner (Kanner, 1978; Guastella et al., 1990; Borden, 1996). As the major GABA transporter in the brain, it plays a key role in modulating GABA signaling (Cherubini and Conti, 2001; Scimemi, 2014). Besides being involved in a broad range of brain functions (Cherubini and Conti, 2001; Bragina et al., 2008; Conti et al., 2011; Kinjo et al., 2013; Scimemi, 2014; Savtchenko et al., 2015; Zafar and Jabeen, 2018), GAT-1 has also been implicated in the pathophysiology of a number of neuropsychiatric disorders including anxiety, depression, epilepsy, Alzheimer's disease, and schizophrenia (Lai et al., 1998; Nägga et al., 1999; Pierri et al., 1999;

Sundman-Eriksson and Allard, 2002; Conti et al., 2004; Lewis and Gonzalez-Burgos, 2006; Cope et al., 2009; Bitanihirwe and Woo, 2014; Carvill et al., 2015; Gong et al., 2015; Fuhrer et al., 2017; Mattison et al., 2018).

GABA uptake by GAT-1 is heavily inhibited by cis-3-aminocyclohexane carboxylic acid (ACHC) and, to a lower extent, by 2,4-diaminobutyric acid, but not by β-alanine (Guastella et al., 1990; Keynan et al., 1992; Liu et al., 1993), two features that have often been considered typical of "neuronal" transporters. This view has been bolstered by the demonstration that GAT-1 is strongly expressed in axon terminals (Minelli et al., 1995; Conti et al., 1998)—despite the fact that the same studies also clearly documented an astrocytic localization—and is still widely used to interpret physiological, pharmacological, genetic, and clinical investigations. However, the findings of several studies published in the past few years call for a more detailed analysis of GAT-1 localization.

RECENT STUDIES SUGGEST A LESS SIMPLISTIC SCENARIO

After reports of *SLC6A1* variants in patients with myoclonic atonic epilepsy (Dikow et al., 2014; Carvill et al., 2015; Mattison et al., 2018; Cai et al., 2019; Posar and Visconti, 2019), clinical, neurophysiological, and genetic examination of a relatively large cohort of subjects (n = 34) bearing *SLC6A1* mutations demonstrated that 97% of them exhibited varying degrees of intellectual disability (ID) and that 91% had been diagnosed with epilepsy (absence, myoclonic, or atonic) based on EEG patterns characterized by irregular, high, ample, generalized spikes, and wave discharges (Johannesen et al., 2018). Notably, more than 60% of these subjects had suffered from moderate or significant ID before epilepsy onset, whereas in a limited number of cases, the ID was not accompanied by epilepsy. Although genetic analysis of the *SLC6A1* variants suggested that the probable disease mechanism was loss of GAT-1 function, assessment of the clinical characteristics associated to them disclosed a wide phenotypic spectrum where the dominant sign, ID, is not quite a "pure" neuronal disorder (Di Marco et al., 2016; Iwase et al., 2017; Maglorius Renkilaraj et al., 2017).

Earlier this year, Inaba et al. (2019) used a model of chronic brain hypoperfusion to assess the protective effects conferred by the anticonvulsant levetiracetam (LEV) on the white matter of mice subjected to bilateral common carotid artery stenosis (BCAS). They found that LEV: (i) did confer protection against learning and memory impairment and white matter injury; (ii) induced PKA/CREB activation; (iii) raised the number of (GFAP-labeled) astrocytes in a time-dependent manner; (iv) reduced Iba-1-positive (+) microglial cells; and (v) increased oligodendrocytes and their precursor cells (Inaba et al., 2019). According to the evidence published to date, synaptic vesicle protein SV2A is the sole receptor for LEV (Lynch et al., 2004). However, an earlier report that LEV increases GAT-1 expression (Ueda et al., 2007), presumably through protein–protein interactions—as recently shown for other vesicular proteins (Marcotulli et al., 2017)—suggests that at least some of the effects described by Inaba et al. (2019) might be mediated through GAT-1.

In 1990, Braestrup and colleagues reported that tiagabine [(3R)-1-[4,4-bis(3-methylthiophen-2-yl)but-3-en-1-yl]piperidine-3-carboxylic acid] nipecotic acid] binds GAT-1 with high affinity (Braestrup et al., 1990). Subsequently, after GAT-1 cloning and functional characterization (Guastella et al., 1990), tiagabine was demonstrated to interact specifically with it (Borden et al., 1994; Borden, 1996) and to be a clinically effective antiepileptic drug (Suzdak and Jansen, 1995; Schousboe and White, 2009; Froestl, 2011). The selectivity of tiagabine for GAT-1 confines its action to those regions of the central nervous system where the transporter plays a large role (neocortex, cerebellum, and hippocampus; Jasmin et al., 2004). Tiagabine has also been found to exert antinociceptive, anxiolytic-like, sedative, and antidepressant-like actions (Jasmin et al., 2004; Sałat et al., 2015). Finally, tiagabine monotherapy appears to improve the performance of epilepsy patients on a number of neuropsychological tests (Dodrill et al., 1998), an effect that seems to relate to the report that heterozygous mice show greater learning and memory compared to wild-type and homozygous *GAT-1*$^{-/-}$ mice (Shi et al., 2012).

In 2015, two articles revived the interest in the effects of tiagabine. In a study of cerebellar GABA signaling using a mouse model of diffuse white matter injury (DWMI), a severe neurological syndrome characterized by hypomyelination and disruption of subcortical white matter development and involving behavioral, cognitive, and motor deficits, Zonouzi et al. (2015) demonstrated that tiagabine enhances the progression of NG2 (oligodendrocyte precursor) cells and promotes oligodendrogenesis and myelination. The same year, Liu and coworkers documented that in a methyl-4-phenyl-1,2,3,6-tetrahydropyridine (MPTP) mouse model of Parkinson's disease, tiagabine pretreatment attenuates microglial activation, it confers partial protection on the nigrostriatal axis, and it alleviates motor deficits, but its protective function is abolished in GAT-1 knockout mice challenged with MPTP. The authors also found that tiagabine suppresses microglial activation in mice treated by intranigral lipopolysaccharide infusion, an alternative model of Parkinson's disease (Liu et al., 2015). Although neither study clarified the mechanism(s) underlying tiagabine's action, it is conceivable that the effects described by Zonouzi et al. (2015) and Liu et al. (2015) depend on a direct action on GAT-1 expression by microglial cells and oligodendrocytes, which may go some way toward explaining the findings of the two groups.

EVIDENCE FOR A WIDESPREAD CELLULAR EXPRESSION OF GAT-1

Some years ago, while investigating GAT-1 immunoreactivity in subcortical white matter, we detected GAT-1 cells of different sizes and morphologies (**Figure 1**). Some were small and round with small processes (**Figure 1A**), and others were medium-sized, rounded or oval with regular profiles; some medium-sized cells had a pyramidal shape with long and intensely stained processes, whereas other

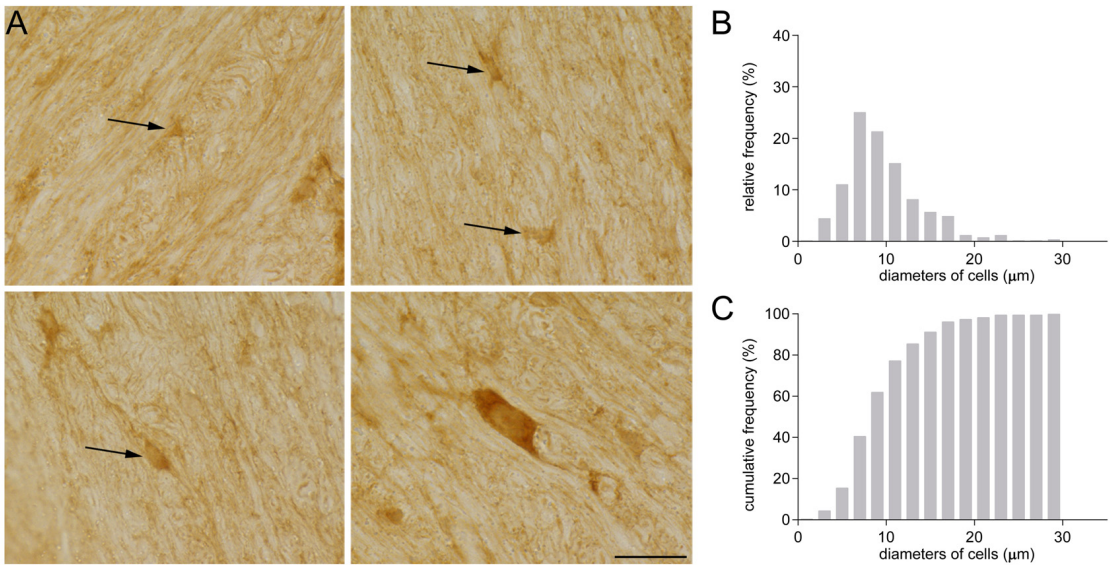

FIGURE 1 | (A) GAT-1 immunoreactivity in the subcortical white matter reveals the presence of numerous cells of small and medium size (arrows) and of different morphology. **(B)** Frequency and **(C)** cumulative frequency distribution of the diameter of GAT-1-positive cells. Bar: 20 μm (modified from Fattorini et al., 2017).

cells were large and elongated. The frequency distribution of their diameter is reported in **Figure 1B**. The broad difference in the size and morphology of these subcortical white matter cells suggested to us that they might belong to different types. We therefore set up a study to examine them in detail.

In line with earlier work (Minelli et al., 1995; Conti et al., 1998), electron microscopic (EM) observation demonstrated that GAT-1 was robustly expressed in axon terminals forming symmetric synapses and in astrocytic processes. However, its astrocytic expression was more diffuse than expected and, even more surprisingly, immature and mature oligodendrocytes and microglial cells also expressed the transporter (**Figure 2**).

Astrocytes

Recently, quantitative EM analysis, performed in our laboratory, disclosed hitherto unknown features of astrocytic GAT-1 localization in rat cerebral cortex; in particular, we found that: (i) approximately 43% of GAT-1+ profiles in the cortical neuropil are astrocytic processes; (ii) at synaptic loci, GAT-1+ astrocytic processes lie close to the pre- and postsynaptic elements of symmetric as well as asymmetric synapses; and (iii) astrocytic GAT-1 expression at symmetric synapses is not homogeneous, since in ∼15% of cases it is associated to GAT-1+ axon terminals and in ∼22% of cases it is exclusively localized in astrocytic processes associated to symmetric synapses (i.e., not expressing GAT-1 in axon terminals). The latter fraction of astrocytic GAT-1 increases to up to ∼38% in GABAergic synapses targeting distal dendrites and spines, where GAT-1+ axon terminals are less numerous (Melone et al., 2014). Immunogold EM demonstrated that the density of GAT-1 molecules in astrocytic process membranes was ∼3.5 times higher than in axon terminals and displayed a continuous distribution from perisynaptic to extrasynaptic regions (respectively within and over 300 nm from the borders of the symmetric synapse specializations), with peaks of concentration at ∼950 nm; in contrast, GAT-1 molecules in the membranes of axon terminals showed a preferential perisynaptic localization (Melone et al., 2015).

Oligodendrocytes

EM analysis revealed GAT-1 immunoreactivity in immature and mature oligodendrocytes both in gray matter and in subcortical white matter. Co-localization studies of GAT-1 and specific oligodendrocyte markers (NG2 and RIP) demonstrated that approximately 12% of GAT-1+ cells in white matter were immature oligodendrocytes and that about 15% were mature oligodendrocytes. Studies of radiolabeled GABA uptake, performed to establish whether GAT-1 localized in oligodendrocytes was functional, demonstrated significant inhibition of Na+-dependent GABA uptake in the presence of tiagabine, indicating that GABA uptake in oligodendrocytes is driven by GAT-1 (Fattorini et al., 2017).

Microglial Cells

EM analysis also demonstrated GAT-1 immunoreactivity in the soma of microglial cells in subcortical white matter and cortical gray matter as well as in microglial processes, where GAT-1 was localized predominantly in the proximal portion. To quantify GAT-1 protein in microglial cells, we measured the volume of the cells containing the GAT-1 protein signal (in cx3cr1+/gfp animals) and found that it was ∼3% in subcortical white matter and ∼8% in cortical gray matter. We also established that Na+-dependent GABA uptake was significantly inhibited by NNC-711, a potent GABA uptake inhibitor with high affinity

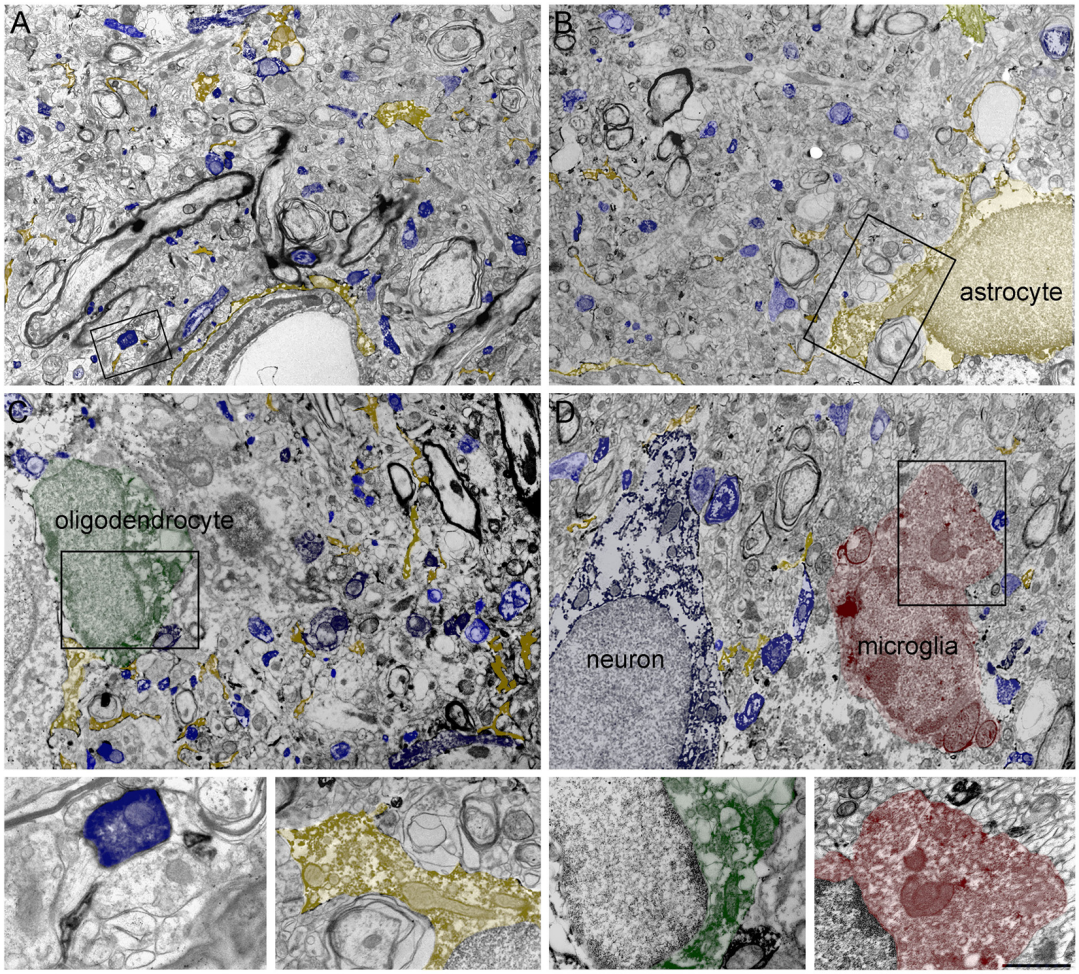

FIGURE 2 | (A–D) Four low-magnification electron microscopic (EM) fields showing GAT-1 immunoreactivity in cerebral neocortex (layers II–III of rat parietal cortex). Colored profiles code for different GAT-1-positive cell types and/or profiles: blue, axon terminals, axon, and neuron; yellow, astrocyte and astrocytic processes; green, oligodendrocyte; red, microglial cell. Framed regions in **(A–D)** are reproduced and enlarged, in the lowest portion of the figure. Bar: 2.5 μm for **(A–D)**; 0.8 and 1 μm for enlarged frames of **(A)** and **(B–D)**, respectively (modified from Melone et al., 2015; Fattorini et al., 2017, 2020).

and selectivity for GAT-1 (Borden et al., 1994). In addition, we documented that, like neurons, microglial cells can regulate the membrane expression of GAT-1 in a syntaxin1A-dependent manner (Deken et al., 2000), since syntaxin1A-specific cleavage by botulin toxin C1 (Schiavo et al., 1995; Deken et al., 2000) completely blocks GAT-1-dependent modulation of GABA uptake (Fattorini et al., 2020).

DISCUSSION

The notion that GAT-1 is not an exclusively "neuronal" transporter appears to be gaining momentum. Indeed, quantitative analysis of GAT-1 in the cerebral cortex, performed in our laboratory, showed that 54% of GAT-1 + profiles were neuronal and that no less than 42% were astrocytic (Melone et al., 2015). More recently, we reported significant GAT-1 expression in oligodendrocytes and microglia (Fattorini et al., 2017, 2020; **Figure 2**). In this connection, it is worth noting that GAT-3, a putative "glial" transporter (see Minelli et al., 1996 for the neocortex), also seems to be expressed in brainstem and cortical neurons, at least in certain experimental conditions (Clark et al., 1992; Melone et al., 2003, 2005, 2015), and that GAT-2, another putative "glial" transporter, is expressed in epithelial cells and, although at a very low level, also in neurons (Conti et al., 1999). It therefore seems that the era of "neuronal" and "glial" GABA transporters has finally come to a close.

The demonstration that all major brain cells express GAT-1 will conceivably contribute to generate a wider framework through which to assess (and indeed reassess) numerous cerebral GABA-mediated phenomena that occur in physiological conditions. This requires tackling first the issue of the physiological role of GAT-1 in oligodendrocytes and microglial cells. Given the well-established involvement of astrocytes, oligodendrocytes, and microglial cells in pathophysiological conditions (Verkhratsky and Butt, 2013), the demonstration

of functional GAT-1 in these cells is expected to provide greater insight into the phenomena occurring in the diseased brain and to prompt a reappraisal of earlier findings. Notably, one of the studies that stimulated the present reassessment (Zonouzi et al., 2015) can now be interpreted as showing that the contribution of GAT-1 to the pathophysiology of DWMI may be mediated by oligodendrocytes, and a similar situation may well arise for the ID seen in some forms of epilepsy. Also, the findings reported by Liu et al. (2015) could simply be interpreted as indicating that GAT-1 expression by microglia may be the direct mechanism by which the transporter contributes to the pathophysiology of Parkinson's disease.

AUTHOR CONTRIBUTIONS

GF, MM, and FC discussed the project, realized the figures, and wrote the article.

FUNDING

This work was supported by Ministero dell'Istruzione, dell'Università e della Ricerca (MIUR; 2015H4K2CR_002) and Università Politecnica delle Marche (PSA2018). We are indebted to the colleagues who collaborated in the original studies and to NC Brecha (Los Angeles, CA, USA) for providing the GAT-1 antibody.

REFERENCES

Bitanihirwe, B. K. Y., and Woo, T. U. W. (2014). Transcriptional dysregulation of γ-aminobutyric acid transporter in parvalbumin-containing inhibitory neurons in the prefrontal cortex in schizophrenia. *Psychiatry Res.* 220, 1155–1159. doi: 10.1016/j.psychres.2014.09.016

Borden, L. A. (1996). GABA transporter heterogeneity: pharmacology and cellular localization. *Neurochem. Int.* 29, 335–356. doi: 10.1016/0197-0186(95)00158-1

Borden, L. A., Dhar, T. G. M., Smith, K. E., Weinshank, R. L., Branchek, T. A., and Gluchowski, C. (1994). Tiagabine, SK & F 89976-A, CI-966, and NNC-711 are selective for the cloned GABA transporter GAT-1. *Eur. J. Pharmacol.* 269, 219–224. doi: 10.1016/0922-4106(94)90089-2

Braestrup, C., Nielsen, E. B., Sonnewald, U., Knutsen, L. J. S., Andersen, K. E., Jansen, J. A., et al. (1990). (R)-N-[4,4-bis(3-methyl-2-thienyl)but-3-en-yl]nipecotic acid binds with high affinity to the brain gamma-aminobutyric acid uptake carrier. *J. Neurosci.* 54, 639–647. doi: 10.1111/j.1471-4159.1990.tb01919.x

Bragina, L., Marchionni, I., Omrani, A., Cozzi, A., Pellegrini-Giampietro, D. E., Cherubini, E., et al. (2008). GAT-1 regulates both tonic and phasic $GABA_A$ receptor-mediated inhibition in the cerebral cortex. *J. Neurochem.* 105, 1781–1793. doi: 10.1111/j.1471-4159.2008.05273.x

Cai, K., Wang, J., Eissman, J., Wang, J., Nwosu, G., Shen, W., et al. (2019). A missense mutation in SLC6A1 associated with Lennox–Gastaut syndrome impairs GABA transporter 1 protein trafficking and function. *Exp. Neurol.* 320:112973. doi: 10.1016/j.expneurol.2019.112973

Carvill, G. L., McMahon, J. M., Schneider, A., Zemel, M., Myers, C. T., Saykally, J., et al. (2015). Mutations in the GABA transporter SLC6A1 cause epilepsy with myoclonic-atonic seizures. *Am. J. Hum. Genet.* 96, 808–815. doi: 10.1016/j.ajhg.2015.02.016

Cherubini, E., and Conti, F. (2001). Generating diversity at GABAergic synapses. *Trends Neurosci.* 24, 155–162. doi: 10.1016/s0166-2236(00)01724-0

Clark, J. A., Deutch, A. Y., Gallipoli, P. Z., and Amara, S. G. (1992). Functional expression and CNS distribution of a β-alanine-sensitive neuronal GABA transporter. *Neuron* 9, 337–348. doi: 10.1016/0896-6273(92)90172-a

Conti, F., Melone, M., De Biasi, S., Minelli, A., Brecha, N. C., and Ducati, A. (1998). Neuronal and glial localization of GAT-1, a high-affinity γ-aminobutyric acid plasma membrane transporter, in human cerebral cortex: with a note on its distribution in monkey cortex. *J. Comp. Neurol.* 396, 51–63. doi: 10.1002/(sici)1096-9861(19980622)396:1<51::aid-cne5>3.0.co;2-h

Conti, F., Melone, M., Fattorini, G., Bragina, L., and Ciappelloni, S. (2011). A role for GAT-1 in presynaptic GABA homeostasis? *Front. Cell. Neurosci.* 5:2. doi: 10.3389/fncel.2011.00002

Conti, F., Minelli, A., and Melone, M. (2004). GABA transporters in the mammalian cerebral cortex: localization, development and pathological implications. *Brain Res. Rev.* 45, 196–212. doi: 10.1016/j.brainresrev.2004.03.003

Conti, F., Zuccarello, L. V., Barbaresi, P., Minelli, A., Brecha, N. C., and Melone, M. (1999). Neuronal, glial, and epithelial localization of γ-aminobutyric acid transporter 2, a high-affinity γ-aminobutyric acid plasma membrane transporter, in the cerebral cortex and neighboring structures. *J. Comp. Neurol.* 409, 482–494. doi: 10.1002/(SICI)1096-9861(19990705)409:3<482::AID-CNE11>3.0.CO;2-O

Cope, D. W., Di Giovanni, G., Fyson, S. J., Orbán, G., Errington, A. C., Lrincz, M. L., et al. (2009). Enhanced tonic $GABA_A$ inhibition in typical absence epilepsy. *Nat. Med.* 15, 1392–1398. doi: 10.1038/nm.2058

Deken, S. L., Beckman, M. L., Boos, L., and Quick, M. W. (2000). Transport rates of GABA transporters: regulation by the N-terminal domain and syntaxin 1A. *Nat. Neurosci.* 3, 998–1003. doi: 10.1038/79939

Di Marco, B., M. Bonaccorso, C., Aloisi, E., D'Antoni, S., and V. Catania, M. (2016). Neuro-inflammatory mechanisms in developmental disorders associated with intellectual disability and autism spectrum disorder: a neuro-immune perspective. *CNS Neurol. Disord. Drug Targets* 15, 448–463. doi: 10.2174/1871527315666160321105039

Dikow, N., Maas, B., Karch, S., Granzow, M., Janssen, J. W. G., Jauch, A., et al. (2014). 3p25.3 microdeletion of GABA transporters SLC6A1 and SLC6A11 results in intellectual disability, epilepsy and stereotypic behavior. *Am. J. Med. Genet. A* 164A, 3061–3068. doi: 10.1002/ajmg.a.36761

Dodrill, C. B., Arnett, J. L., Shu, V., Pixton, G. C., Lenz, G. T., and Sommerville, K. W. (1998). Effects of tiagabine monotherapy on abilities, adjustment, and mood. *Epilepsia* 39, 33–42. doi: 10.1111/j.1528-1157.1998.tb01271.x

Fattorini, G., Catalano, M., Melone, M., Serpe, C., Bassi, S., Limatola, C., et al. (2020). Microglial expression of GAT-1 in the cerebral cortex. *Glia* 68, 646–655. doi: 10.1002/glia.23745

Fattorini, G., Melone, M., Sánchez-Gómez, M. V., Arellano, R. O., Bassi, S., Matute, C., et al. (2017). GAT-1 mediated GABA uptake in rat oligodendrocytes. *Glia* 65, 514–522. doi: 10.1002/glia.23108

Froestl, W. (2011). An historical perspective on GABAergic drugs. *Future Med. Chem.* 3, 163–175. doi: 10.4155/fmc.10.285

Fuhrer, T. E., Palpagama, T. H., Waldvogel, H. J., Synek, B. J. L., Turner, C., Faull, R. L., et al. (2017). Impaired expression of GABA transporters in the human Alzheimer's disease hippocampus, subiculum, entorhinal cortex and superior temporal gyrus. *Neuroscience* 351, 108–118. doi: 10.1016/j.neuroscience.2017.03.041

Gong, X., Shao, Y., Li, B., Chen, L., Wang, C., and Chen, Y. (2015). γ-aminobutyric acid transporter-1 is involved in anxiety-like behaviors and cognitive function in knockout mice. *Exp. Ther. Med.* 10, 653–658. doi: 10.3892/etm.2015.2577

Guastella, J., Nelson, N., Nelson, H., Czyzyk, L., Keynan, S., Miedel, M. C., et al. (1990). Cloning and expression of a rat brain GABA transporter. *Science* 249, 1303–1306. doi: 10.1126/science.1975955

Inaba, T., Miyamoto, N., Hira, K., Ueno, Y., Yamashiro, K., Watanabe, M., et al. (2019). Protective role of levetiracetam against cognitive impairment and brain white matter damage in mouse prolonged cerebral hypoperfusion. *Neuroscience* 414, 255–264. doi: 10.1016/j.neuroscience.2019.07.015

Iwase, S., Bérubé, N. G., Zhou, Z., Kasri, N. N., Battaglioli, E., Scandaglia, M., et al. (2017). Epigenetic etiology of intellectual disability. *J. Neurosci.* 37, 10773–10782. doi: 10.1523/jneurosci.1840-17.2017

Jasmin, L., Wu, M. V., and Ohara, P. T. (2004). GABA puts a stop to pain. *Curr. Drug Targets CNS Neurol. Disord.* 3, 487–505. doi: 10.2174/1568007043336716

Johannesen, K. M., Gardella, E., Linnankivi, T., Courage, C., de Saint Martin, A., Lehesjoki, A.-E., et al. (2018). Defining the phenotypic spectrum of SLC6A1 mutations. *Epilepsia* 59, 389–402. doi: 10.1111/epi.13986

Kanner, B. I. (1978). Active transport of γ-aminobutyricacid by membrane vesicles isolated from rat brain. *Biochemistry* 17, 1207–1211. doi: 10.1021/bi00600a011

Keynan, S., Suh, Y. J., Kanner, B. I., and Rudnick, G. (1992). Expression of a cloned γ-aminobutyric acid transporter in mammalian cells. *Biochemistry* 31, 1974–1979. doi: 10.1021/bi00122a011

Kinjo, A., Koito, T., Kawaguchi, S., and Inoue, K. (2013). Evolutionary history of the GABA transporter (GAT) group revealed by marine invertebrate GAT-1. *PLoS One* 8:e82410. doi: 10.1371/journal.pone.0082410

Lai, C. T., Tanay, V. A. M. I., Charrois, G. J. R., Baker, G. B., and Bateson, A. N. (1998). Effects of phenelzine and imipramine on the steady-state levels of mRNAs that encode glutamic acid decarboxylase (GAD67 and GAD65), the GABA transporter GAT-1 and GABA transaminase in rat cortex. *Naunyn. Schmiedebergs Arch. Pharmacol.* 357, 32–38. doi: 10.1007/pl00005135

Lewis, D. A., and Gonzalez-Burgos, G. (2006). Pathophysiologically based treatment interventions in schizophrenia. *Nat. Med.* 12, 1016–1022. doi: 10.1038/nm1478

Liu, J., Huang, D., Xu, J., Tong, J., Wang, Z., Huang, L., et al. (2015). Tiagabine protects dopaminergic neurons against neurotoxins by inhibiting microglial activation. *Sci. Rep.* 5:15720. doi: 10.1038/srep15720

Liu, Q. R., López-Corcuera, B., Mandiyan, S., Nelson, H., and Nelson, N. (1993). Molecular characterization of four pharmacologically distinct γ-aminobutyric acid transporters in mouse brain. *J. Biol. Chem.* 268, 2106–2112.

Lynch, B. A., Lambeng, N., Nocka, K., Kensel-Hammes, P., Bajjalieh, S. M., Matagne, A., et al. (2004). The synaptic vesicle protein SV2A is the binding site for the antiepileptic drug levetiracetam. *Proc. Natl. Acad. Sci. U S A* 101, 9861–9866. doi: 10.1073/pnas.0308208101

Maglorius Renkilaraj, M. R. L., Baudouin, L., Wells, C. M., Doulazmi, M., Wehrlé, R., Cannaya, V., et al. (2017). The intellectual disability protein PAK3 regulates oligodendrocyte precursor cell differentiation. *Neurobiol. Dis.* 98, 137–148. doi: 10.1016/j.nbd.2016.12.004

Marcotulli, D., Fattorini, G., Bragina, L., Perugini, J., and Conti, F. (2017). Levetiracetam affects differentially presynaptic proteins in rat cerebral cortex. *Front. Cell. Neurosci.* 11:389. doi: 10.3389/fncel.2017.00389

Mattison, K. A., Butler, K. M., Inglis, G. A. S., Dayan, O., Boussidan, H., Bhambhani, V., et al. (2018). SLC6A1 variants identified in epilepsy patients reduce γ-aminobutyric acid transport. *Epilepsia* 59, e135–e141. doi: 10.1111/epi.14531

Melone, M., Barbaresi, P., Fattorini, G., and Conti, F. (2005). Neuronal localization of the GABA transporter GAT-3 in human cerebral cortex: a procedural artifact? *J. Chem. Neuroanat.* 30, 45–54. doi: 10.1016/j.jchemneu.2005.04.002

Melone, M., Ciappelloni, S., and Conti, F. (2014). Plasma membrane transporters GAT-1 and GAT-3 contribute to heterogeneity of GABAergic synapses in neocortex. *Front. Neuroanat.* 8:72. doi: 10.3389/fnana.2014.00072

Melone, M., Ciappelloni, S., and Conti, F. (2015). A quantitative analysis of cellular and synaptic localization of GAT-1 and GAT-3 in rat neocortex. *Brain Struct. Funct.* 220, 885–897. doi: 10.1007/s00429-013-0690-8

Melone, M., Cozzi, A., Pellegrini-Giampietro, D. E., and Conti, F. (2003). Transient focal ischemia triggers neuronal expression of GAT-3 in the rat perilesional cortex. *Neurobiol. Dis.* 14, 120–132. doi: 10.1016/s0969-9961(03)00042-1

Minelli, A., Brecha, N. C., Karschin, C., DeBiasi, S., and Conti, F. (1995). GAT-1, a high-affinity GABA plasma membrane transporter, is localized to neurons and astroglia in the cerebral cortex. *J. Neurosci.* 15, 7734–7746. doi: 10.1523/jneurosci.15-11-07734.1995

Minelli, A., DeBiasi, S., Brecha, N. C., Zuccarello, L. V., and Conti, F. (1996). GAT-3, a high-affinity GABA plasma membrane transporter, is localized to astrocytic processes and it is not confined to the vicinity of GABAergic synapses in the cerebral cortex. *J. Neurosci.* 16, 6255–6264. doi: 10.1523/jneurosci.16-19-06255.1996

Nägga, K., Bogdanovic, N., and Marcusson, J. (1999). GABA transporters (GAT-1) in Alzheimer's disease. *J. Neural Transm.* 106, 1141–1149. doi: 10.1007/s007020050230

Pierri, J. N., Chaudry, A. S., Woo, T. U. W., and Lewis, D. A. (1999). Alterations in chandelier neuron axon terminals in the prefrontal cortex of schizophrenic subjects. *Am. J. Psychiatry* 156, 1709–1719. doi: 10.1176/ajp.156.11.1709

Posar, A., and Visconti, P. (2019). Mild phenotype associated with *SLC6A1* gene mutation: a case report with literature review. *J. Pediatr. Neurosci.* 14, 100–102. doi: 10.4103/jpn.jpn_2_19

Sałat, K., Podkowa, A., Kowalczyk, P., Kulig, K., Dziubina, A., Filipek, B., et al. (2015). Anticonvulsant active inhibitor of GABA transporter subtype 1, tiagabine, with activity in mouse models of anxiety, pain and depression. *Pharmacol. Rep.* 67, 465–472. doi: 10.1016/j.pharep.2014.11.003

Savtchenko, L., Megalogeni, M., Rusakov, D. A., Walker, M. C., and Pavlov, I. (2015). Synaptic GABA release prevents GABA transporter type-1 reversal during excessive network activity. *Nat. Commun.* 6:6597. doi: 10.1038/ncomms7597

Schiavo, G., Shone, C. C., Bennett, M. K., Scheller, R. H., and Montecucco, C. (1995). Botulinum neurotoxin type C cleaves a single Lys-Ala bond within the carboxyl-terminal region of syntaxins. *J. Biol. Chem.* 270, 10566–10570. doi: 10.1074/jbc.270.18.10566

Schousboe, A., and White, H. S. (2009). "Glial modulation of excitability *via* glutamate and GABA transporters," in *Encyclopedia of Basic Epilepsy Research*, ed. P. A. Scheartzkroin (Oxford: Academic Press), 397–401.

Scimemi, A. (2014). Structure, function, and plasticity of GABA transporters. *Front. Cell. Neurosci.* 8:161. doi: 10.3389/fncel.2014.00161

Shi, J., Cai, Y., Liu, G., Gong, N., Liu, Z., Xu, T., et al. (2012). Enhanced learning and memory in GAT1 heterozygous mice. *Acta Biochim. Biophys. Sin.* 44, 359–366. doi: 10.1093/abbs/gms005

Sundman-Eriksson, I., and Allard, P. (2002). [^{3}H]Tiagabine binding to GABA transporter-1 (GAT-1) in suicidal depression. *J. Affect. Disord.* 71, 29–33. doi: 10.1016/s0165-0327(01)00349-4

Suzdak, P. D., and Jansen, J. A. (1995). A review of the preclinical pharmacology of tiagabine: a potent and selective anticonvulsant GABA uptake inhibitor. *Epilepsia* 36, 612–626. doi: 10.1111/j.1528-1157.1995.tb02576.x

Ueda, Y., Doi, T., Nagatomo, K., Tokumaru, J., Takaki, M., and Willmore, L. J. (2007). Effect of levetiracetam on molecular regulation of hippocampal glutamate and GABA transporters in rats with chronic seizures induced by amygdalar FeCl3 injection. *Brain Res.* 1151, 55–61. doi: 10.1016/j.brainres.2007.03.021

Verkhratsky, A., and Butt, A. (2013). *Glial Physiology and Pathophysiology*. Oxford: John Wiley & Sons.

Zafar, S., and Jabeen, I. (2018). Structure, function and modulation of γ-aminobutyric, acid transporter 1 (GAT1) in neurological disorders: a pharmacoinformatic prospective. *Front. Chem.* 6:397. doi: 10.3389/fchem.2018.00397

Zonouzi, M., Scafidi, J., Li, P., McEllin, B., Edwards, J., Dupree, J. L., et al. (2015). GABAergic regulation of cerebellar NG2 cell development is altered in perinatal white matter injury. *Nat. Neurosci.* 18, 674–682. doi: 10.1038/nn.3990

Conflict of Interest: The authors declare that the research was conducted in the absence of any commercial or financial relationships that could be construed as a potential conflict of interest.

frontiers in Cellular Neuroscience

MINI REVIEW
published: 13 March 2020
doi: 10.3389/fncel.2020.00039

Emerging Role of the Autophagy/Lysosomal Degradative Pathway in Neurodevelopmental Disorders With Epilepsy

Anna Fassio[1,2*†], *Antonio Falace*[3†], *Alessandro Esposito*[1,4], *Davide Aprile*[1,4], *Renzo Guerrini*[3,5] *and Fabio Benfenati*[2,4]

[1]*Department of Experimental Medicine, University of Genoa, Genoa, Italy,* [2]*IRCCS Ospedale Policlinico San Martino, Genoa, Italy,* [3]*Pediatric Neurology, Neurogenetics and Neurobiology Unit and Laboratories, Children's Hospital A. Meyer—University of Florence, Florence, Italy,* [4]*Center for Synaptic Neuroscience and Technology, Istituto Italiano di Tecnologia, Genoa, Italy,* [5]*IRCCS Fondazione Stella Maris, Pisa, Italy*

Autophagy is a highly conserved degradative process that conveys dysfunctional proteins, lipids, and organelles to lysosomes for degradation. The post-mitotic nature, complex and highly polarized morphology, and high degree of specialization of neurons make an efficient autophagy essential for their homeostasis and survival. Dysfunctional autophagy occurs in aging and neurodegenerative diseases, and autophagy at synaptic sites seems to play a crucial role in neurodegeneration. Moreover, a role of autophagy is emerging for neural development, synaptogenesis, and the establishment of a correct connectivity. Thus, it is not surprising that defective autophagy has been demonstrated in a spectrum of neurodevelopmental disorders, often associated with early-onset epilepsy. Here, we discuss the multiple roles of autophagy in neurons and the recent experimental evidence linking neurodevelopmental disorders with epilepsy to genes coding for autophagic/lysosomal system-related proteins and envisage possible pathophysiological mechanisms ranging from synaptic dysfunction to neuronal death.

Keywords: epilepsy, autophagy, lysosome, neuron development, synapse

OPEN ACCESS

Edited by:
Eleonora Palma, Sapienza University of Rome, Italy

Reviewed by:
Alexander Dityatev, German Center for Neurodegenerative Diseases (DZNE), Germany
Elisabetta Catalani, Università degli Studi della Tuscia, Italy

***Correspondence:**
Anna Fassio
afassio@unige.it

†These authors have contributed equally to this work

Received: *09 December 2019*
Accepted: *10 February 2020*
Published: *13 March 2020*

Citation:
Fassio A, Falace A, Esposito A, Aprile D, Guerrini R and Benfenati F (2020) Emerging Role of the Autophagy/Lysosomal Degradative Pathway in Neurodevelopmental Disorders With Epilepsy. Front. Cell. Neurosci. 14:39. doi: 10.3389/fncel.2020.00039

INTRODUCTION

Macroautophagy (henceforth autophagy) is a highly conserved cellular process that tackles dysfunctional proteins, lipids, and organelles to lysosomes for degradation. Substrates are initially isolated by a double membrane, the phagophore, which subsequently elongates and surrounds the substrates with a membranous structure, the autophagosome (AP; Dikic and Elazar, 2018). APs are transient organelles destined to fuse with the lysosome for the degradation of their contents. Autophagy is virtually active in all cell types to ensure homeostasis and has been implicated in protein and organelle quality control, development and differentiation, aging, and immunity. Autophagy is modulated by nutrients and growth factors and levels of AMP/ATP sensed by mammalian target of rapamycin complex1 (mTORC1) and AMP-dependent protein kinase (AMPK), respectively (Menzies et al., 2017). A scheme of the autophagy pathway is reported in **Figure 1**.

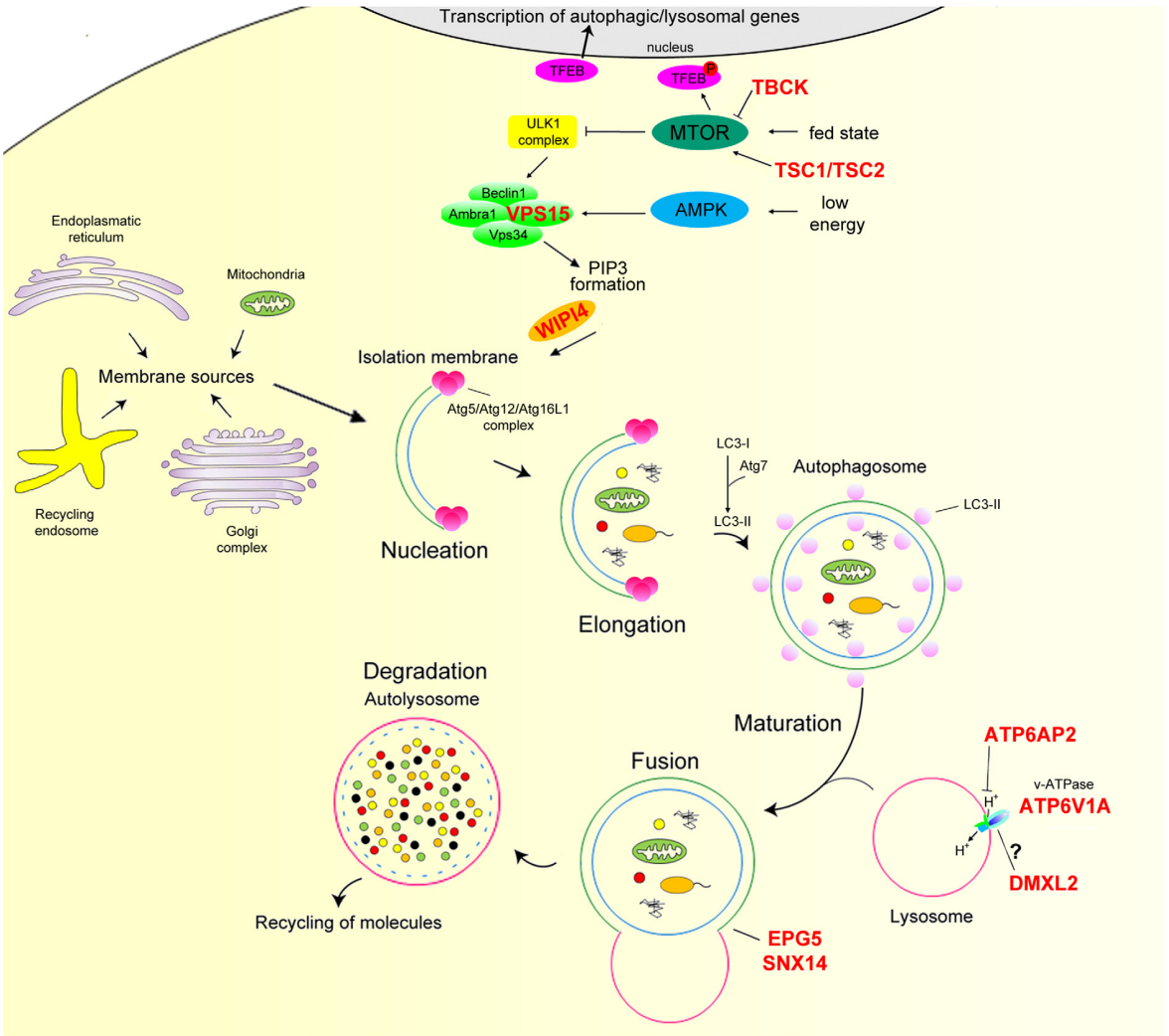

FIGURE 1 | Overview of the mammalian autophagy pathway. In nutrient-rich conditions (fed state) mTOR phosphorylates TFEB preventing its nuclear translocation. In nutrient depletion or low-energy state, mTOR is inactive, and TFEB translocates to the nucleus leading to the transcription of many autophagy and lysosomal genes. mTOR inhibition together with AMPK activation positively regulate the ULK1 complex. Induction of this complex regulates the recruitment of the Beclin1/Ambta1/VSP34/VPS15 complex to the phagophore and, hence, the production of PI3P and downstream autophagy effectors Atg5/Atg12/Atg16L1 *via* the binding of WIPI proteins. This step is essential for the conversion of LC3-I to LC3-II through Atg7 and its conjugation to phagophore membrane. The membranes of these structures appear to have multiple sources, such as the endoplasmic reticulum, Golgi apparatus and trans-Golgi network, endosomal compartment, and mitochondria. LC3-II attracts components of the autophagy machinery and is required for elongation and closure of the phagophore membrane. Mature autophagosome finally fuses with the lysosome, forming the autolysosome, where autophagic cargo is degraded and then released back to the cytoplasm to be re-used by the cell. The proton gradient imposed by the lysosomal v-ATPase is essential for proteolysis as hydrolase activity strictly relies on acidic pH. Autophagy genes mutated in neurodevelopmental disorders with epilepsy are marked in red. AMPK, AMP-dependent protein kinase; mTORC1, mammalian target of rapamycin complex 1; TFEB, transcription factor EB; ULK, mammalian homologs of the *Caenorhabditis elegans* uncoordinated-51 kinase.

Dysfunctional autophagy has been associated with several pathologies and most neurodegenerative diseases. Neurons appear to be particularly dependent on autophagy since their post-mitotic nature makes them highly sensitive to the accumulation of toxic proteins and damaged organelles. The complex and polarized neuronal architecture poses specific challenges for an efficient cargo recycling. In neurons, APs are preferentially formed at synaptic terminals, and are transported to the cell soma, where they fuse to lysosomes for degradation. Here, we review the physiological role of autophagy in neurons and discuss recent experimental evidence linking neurodevelopmental disorders with epilepsy to genes of the autophagy/lysosomal systems (**Table 1**).

AUTOPHAGY AND NEURODEGENERATION

The central nervous system (CNS) requires autophagy to maintain its homeostasis. Since the ubiquitous deletion of core autophagy genes is lethal at the embryonic or perinatal stages,

TABLE 1 | List autophagy/lysosomal genes involved in neurodevelopmental disorders with epilepsy.

Disorder	Gene	Inheritance	Molecular defect	Key clinical features	Clinical references
Tuberous sclerosis-1 (OMIM # 191100) Tuberous sclerosis-2 (OMIM # # 613254)	***TSC1*** ***TSC2***	AD	Autophagy induction	• DD/ID • Epilepsy • Hamartomas in multiple organ systems • Renal failure	Lipton and Sahin (2014)
TBCK encephaloneuronopathy (OMIM #616900)	***TBCK***	AR	Autophagy induction	• DD/ID • Regression and cognitive decline • Neuronopathy • Epilepsy	Bhoj et al. (2016), Chong et al. (2016) and Ortiz-González et al. (2018)
Cortical atrophy/dysplasia and epilepsy	***VPS15***	AR	Autophagosome formation	• DD/ID • Cortical dysplasia • Ataxia • Hearing deficits • Epilepsy	Gstrein et al. (2018)
Beta-propeller protein-associated neurodegeneration (OMIM #300894)	***WDR45***	X-linked	Autophagosome elongation	• DD/ID • Encephalopathy with epilepsy • Rett-like stereotypies • Dystonia	Haack et al. (2012), Saitsu et al. (2013), Hayflick et al. (2018) and Carvill et al. (2018)
Vici syndrome (OMIM #242840)	***EPG5***	AR	Autophagosome–lysosome fusion	• Hypopigmentation (skin, hair, retina) • Agenesis of the corpus callosum • Epilepsy • Bilateral cataracts • Cardiomyopathy • Combined immunodeficiency • Microcephaly • DD • Failure to thrive	Dionisi Vici et al. (1988), Byrne et al. (2016) and Ebrahimi-Fakhari et al. (2016)
Spinocerebellar ataxia20 (OMIM #616354)	***SNX14***	AR	Autophagosome–lysosome fusion	• DD/ID • Ataxia • Coarse facial features • Epilepsy • Sensorineural hearing loss • Hepatosplenomegaly	Thomas et al. (2014) and Akizu et al. (2015)
Developmental encephalopathy with epilepsy	***ATP6V1A***	AD	v-ATPase function	• DD/ID • Encephalopathy with epilepsy • Quadriparesis	Van Damme et al. (2017) and Fassio et al. (2018)
X-linked ID, epilepsy and fulminant neurodegeneration	***ATP6AP2***	X-linked	v-ATPase function	• Cortical atrophy • DD/ID • Dysmorphic features • Early-onset neurodegeneration • Epilepsy	Hirose et al. (2019)
Ohtahara syndrome with progressive course	***DMXL2***	AR	v-ATPase function	• Profound DD • Cortical atrophy • Encephalopathy with epilepsy • Severe epilepsy • Failure to thrive • Dysmorphic features • Quadriparesis • Sensorineural hearing loss • Severe hypotonia	Esposito et al. (2019)

Note. AD, autosomal dominant; AR, autosomal recessive; DD, developmental delay; ID, intellectual disability.

several nervous system-specific knockout mouse models have been developed to explore the roles of autophagy in CNS. Removal of Atg5 and Atg7 in neuronal precursor cells (NPCs) leads to the accumulation of cytoplasmic inclusion bodies, with neurodegeneration and progressive motor deficits, further pointing to autophagy as a key quality control system in neurons

over their lifespan (Hara et al., 2006; Komatsu et al., 2006). In subsequent models, generated by targeting distinct genes of the core autophagic pathway (Fimia et al., 2007; Liang et al., 2010; Joo et al., 2016), similarly reduced survival and early-onset, progressive neurodegeneration occurred, although the underlying pathophysiological basis varied according to the specific gene targeted. Altogether these models emphasize autophagy as a major cellular process protecting against neurodegeneration, in line with the evidence that in human defective autophagy underlies the accumulation of protein aggregates in several neurodegenerative disorders (Rubinsztein et al., 2005; Kiriyama and Nochi, 2015).

AUTOPHAGY AND NEUROGENESIS

Balanced differentiation, proliferation, and cell death rates in the developing brain are essential for neurogenesis. The autophagy machinery interacts with developmental signals involved in cell fate decisions, including Wnt, Sonic hedgehog, TGFB, and FGF (Kiyono et al., 2009; Gao et al., 2010; Jimenez-Sanchez et al., 2012; Zhang et al., 2012). Studies in animal models have disclosed the pivotal role of autophagy in neuronal proliferation and in sustaining the post-natal pool of NPCs. Loss of Ambra1, a Beclin1 activator, resulted in severe defects of the neural tube development, ubiquitinated protein accumulation, unbalanced cell proliferation, and excessive apoptosis, as a consequence of autophagy impairment (Fimia et al., 2007). In this model, impairment of basal autophagy induced hyperproliferation as indirect consequence of misregulated recycling of transcriptional factors (Cecconi et al., 2007; Fimia et al., 2007). Notch signaling is a master regulator of neurogenesis and neuronal development (Bray, 2006; Ables et al., 2011). Autophagy regulates Notch degradation and defects in the autophagy machinery impact on NPC fate (Wu et al., 2016). Impairing AP formation by *in utero* knockdown of *Atg5* harms β-Catenin stability, thus, leading to inhibited differentiation and increased proliferation of NPCs in the developing cortex (Lv et al., 2015). These *in vivo* findings suggest that a multi-level interaction between autophagy, cell proliferation, and cell death occurs during mammalian neural development. As reviewed elsewhere, an important role for autophagy in adult neurogenesis has also emerged (Dhaliwal et al., 2017; Menzies et al., 2017).

AUTOPHAGY AND NEURONAL POLARITY

Neurons have a uniquely polarized morphology characterized by extended and highly elaborated axonal and dendritic arborizations, and neuronal homeostasis is critical for establishment and maintenance of their polarized structures (Lee et al., 2013; Maday, 2016). From the earlier phases of neurodevelopment, a highly efficient autophagy is required to allow membrane trafficking events, axonal guidance, and establishment of brain connectivity (Dragich et al., 2016). Axonal APs undergo robust retrograde motility toward the soma, driven by the active motor dynein. Moreover, mutations in autophagy genes cause pathological processes associated with long-range white matter defects.

While autophagy in axonal development and homeostasis has been extensively studied, recent findings have also pointed out the key role of autophagy in ciliogenesis. In neurons, cilia are involved in cortical patterning, neurogenesis, neuronal maturation, and cerebellar development (Lee and Gleeson, 2010). The autophagy impairment due to somatic-activating mutations in *MTOR* leads to abnormal accumulation of the OFD1 protein at centriolar satellites and disruption of neuronal ciliogenesis. Impaired ciliogenesis abrogates Wnt signaling, which is required for neuronal polarization, and underlies cortical dyslamination reported in patients (Park et al., 2018).

AUTOPHAGY AND SYNAPTIC FUNCTION

Autophagy not only regulates early neuronal development but also plays specific, multiple, and largely unexplored roles at synapses. As recently reviewed, dysfunctional autophagy at both pre- and post-synaptic sites leads to aging and neurodegeneration (Nikoletopoulou et al., 2015; Vijayan and Verstreken, 2017; Azarnia Tehran et al., 2018; Liang and Sigrist, 2018). Degradation of postsynaptic neurotransmitter receptors involves trafficking in autophagosomal structures (Rowland, 2006; Shehata et al., 2012, 2018; Hui et al., 2019). At dopaminergic presynaptic sites, autophagy shapes synapse ultrastructure and modulates neurotransmitter release, while at glutamatergic synapses mTOR-regulated autophagy promotes spine pruning during development (Hernandez et al., 2012; Tang et al., 2014). The presynaptic proteins endophilin and its partner synaptojanin, known to regulate synaptic vesicle (SV) endocytosis and recycling, turned out to positively regulate synaptic autophagy, suggesting a functional link between SV cycling and autophagy. Endophilin induces the membrane curvature that recruits Atg3 and Atg8 to initiate synaptic AP generation (Murdoch et al., 2016; Soukup et al., 2016). Synaptojanin promotes synaptic autophagy by removing Atg18 from preautophagosomal structures necessary for AP maturation (George et al., 2014; Vanhauwaert et al., 2017). Conversely, the active zone protein Bassoon has been proposed to inhibit autophagy (Okerlund et al., 2017). At presynaptic sites, a role for autophagy in the degradation of SV proteins has been suggested, and the small GTPase Rab26 was reported to cluster SVs and direct them to preautophagosomal structures for degradation (Binotti et al., 2015; Lüningschrör et al., 2017). In addition, endosomal microautophagy, a chaperone-mediated form of autophagy, which directly targets proteins to the endo-lysosomal system, has been described to degrade misfolded synaptic proteins and regulate neurotransmission at the *Drosophila* neuromuscular junction (Uytterhoeven et al., 2015). The biogenesis of APs occurs in nerve terminals (Katsumata et al., 2010; Shehata et al., 2012), and synaptic APs retrogradely transport endocytosed elements to the neuronal soma for signaling (Wang et al., 2015). Whether SV cycling and synaptic autophagy are reciprocally regulated and how they crosstalk with somatic autophagy is a matter of investigation. In a recent article, selective induction of autophagy at the presynaptic site has been shown to specifically target damaged proteins, thus

maintaining synapse integrity and function (Hoffmann et al., 2019). The discovery that neuronal autophagy and formation of APs at synapses are activity dependent (Shehata et al., 2018) suggests that synaptic autophagy may be regulated by long-term synaptic plasticity underlying learning and memory formation. However, whether autophagy stimulates or suppresses memory processes and its relationship with nutrient signaling pathways is still controversial. Fasting has been shown to induce autophagy in the hypothalamus, but to inhibit it in the hippocampus and cerebral cortex, where memory formation and consolidation occur. BDNF-mediated suppression of autophagy is required for the growth factor effects on synaptic plasticity and memory enhancement both *in vitro* and *in vivo* (Nikoletopoulou et al., 2017). Glatigny and coworkers recently showed that, in hippocampal neurons, autophagy is induced by synaptic plasticity paradigms and necessary for novel memory formation (Glatigny et al., 2019). These recent data suggest that autophagy is involved in the regulation of synaptic strength and that its dysregulation may impact on the plasticity of the network and on the excitation/inhibition balance.

AUTOPHAGY AND NEURODEVELOPMENTAL DISORDER WITH EPILEPSY

In the last decade, several single-gene disorders of the autophagy pathway—defined as "congenital disorders of autophagy"—have been identified through next-generation sequencing. Genetic defects affect a range of functional steps from early phases of autophagy induction to autolysosome formation. The associated disorders, which are clinically heterogeneous, mainly affect the central and peripheral nervous systems, but often cause multi-systemic involvement (Ebrahimi-Fakhari et al., 2016). Structural brain abnormalities, developmental delay, intellectual disability, severe epilepsy, and progressive impairment in relation to neurodegeneration are common features of this class of disorders. Members of the autophagy process involved in neurodevelopmental disorders with epilepsy are highlighted in **Figure 1** and discussed below.

A direct link between autophagy and epileptogenesis was first supported by studies showing that rapamycin, an inhibitor of the mTOR pathway and a powerful autophagy inducer, strongly modulates seizures in several models (Giorgi et al., 2015). Germline and somatic mutations in genes of the mTOR pathway have been identified in patients with various epileptic disorders (Parrini et al., 2016), and a direct contribution of defective autophagy has been confirmed (Yasin et al., 2013; Park et al., 2018). Hypofunctional mutations in ***TSC1*** or ***TSC2*** in tuberous sclerosis result in the uncontrolled activation of the mTORC1 pathway (Lipton and Sahin, 2014) and subsequent inhibition of autophagy directly linked to epileptogenesis in a forebrain-specific conditional *TSC1* mouse model (McMahon et al., 2012).

Mutations in ***TBCK*** cause a neurodevelopmental syndrome with intellectual disability, coarse face, congenital hypotonia, leukoencephalopathy, progressive motor neuronopathy, and seizures (Bhoj et al., 2016; Chong et al., 2016; Ortiz-González et al., 2018). As suggested by bioinformatic analysis, *TBCK* encodes a putative Rab GTPase-activating protein, although its function remains elusive. Loss-of-function mutations in *TBCK* lead to inhibition of mTORC1 and, thus, to uncontrolled autophagy induction in patient-derived fibroblasts (Bhoj et al., 2016; Ortiz-González et al., 2018). In this model, loss of TBCK results in increased number of APs accompanied by an augmented autophagic flux insensitive to pro-autophagic stimuli (Ortiz-González et al., 2018). Glycosylated proteins were not properly degraded in TBCK patients' fibroblasts, and storage of lipofuscin was observed in patient's neurons (Beck-Wödl et al., 2018; Ortiz-González et al., 2018), suggesting that dysregulated autophagy leads to a storage disease phenotype (Teinert et al., 2020).

The signaling pathway adapting the autophagic response to nutrients and energy levels focuses on the phosphorylation of the ULK1 complex, a process which controls the recruitment of the VPS34/VPS15/Ambra1/Beclin1 complex to the phagophore and the formation of PI3P and downstream autophagy effectors through the binding of WD-repeat phosphoinositide-interacting (WIPI) proteins (Menzies et al., 2017; **Figure 1**). Gstrein et al. (2018) identified a recessive homozygous mutation in ***VSP15*** (L1224R) in a single patient with severe cortical atrophy and dysplasia, optic nerve atrophy, intellectual disability, spasticity, ataxia, muscle wasting, and seizures. The L1224R mutation leads to an accumulation of autophagy substrates in patient's fibroblasts. In the same study, a forebrain-specific conditional Vps15 mouse model was developed revealing that loss of Vps15 resulted in severe cortical atrophy accompanied by autophagic impairment and progressive degeneration of the hippocampus and cortex (Gstrein et al., 2018).

Mutations in X-linked gene ***WDR45***, encoding WIPI4, cause beta-propeller protein-associated neurodegeneration (BPAN; Haack et al., 2012; Saitsu et al., 2013). BPAN is a variant of neurodegeneration with brain iron accumulation spectrum (Hayflick et al., 2018) and is characterized by a bi-phasic development. After an initial epileptic encephalopathy in the childhood, progressive neurodegeneration and Parkinsonism develop in adulthood (Carvill et al., 2018). Studies in *WDR45* patients' fibroblasts and neurons derived from their reprogramming showed that loss of WDR45 leads to higher levels of cell iron and oxidative stress, accompanied by mitochondrial abnormalities, autophagic impairment, and dysfunctional lysosomes (Seibler et al., 2018). In mice, deletion of *Wdr45* in the brain results in axonal pathology and accumulation of autophagy substrates in neurons (Zhao et al., 2015).

Biallelic ***EPG5*** mutations in the Vici syndrome, together with recessive ***SNX14*** variants in cerebellar ataxia and intellectual disability syndrome, affect the late stages of autophagy. Vici syndrome is a severe progressive neurodevelopmental multisystem disorder featuring agenesis of the corpus callosum, bilateral cataracts, hypertrophic and/or dilated cardiomyopathy, combined immunodeficiency, and hypopigmentation (Dionisi

Vici et al., 1988; Byrne et al., 2016; Ebrahimi-Fakhari et al., 2016). Profound developmental delay, progressive microcephaly, and failure to thrive are common features and suggest a neurodegenerative component following the prominent neurodevelopmental defect. Two-thirds of patients develop seizures, often evolving as epileptic encephalopathy (Byrne et al., 2016). The EPG5 protein acts as a tethering factor that determines the fusion specificity of APs with late endosomes/lysosomes (Wang et al., 2016), and *in vivo* loss of EPG5 results in block of the autophagic pathway, progressive motor deficit, and neurodegeneration (Zhao et al., 2013). Bi-allelic mutations in *SNX14* are the cause of autosomal-recessive childhood-onset spinocerebellar ataxia 20 (Thomas et al., 2014; Akizu et al., 2015). Patients showed progressive cerebellar neurodegeneration, developmental delay, intellectual disability, and seizures (Akizu et al., 2015). *SNX14* encodes a protein, of the sorting nexin family and binds lysosomal membrane phosphatidylinositol residues, that is enriched in AP-containing cell fraction where it mediates lysosome–AP fusion (Mas et al., 2014). In SNX14 patient-derived neurons, lysosomal enlargement and autophagic dysfunction were reported. This phenotype was also observed in the *Snx14*-zebrafish model, where it leads to progressive Purkinje cell degeneration, suggesting that impaired autophagy finally results in neuronal cell death (Akizu et al., 2015). In cultured mouse neurons, loss of Snx14 decreases intrinsic excitability and impairs both excitatory and inhibitory synaptic transmission (Huang et al., 2014).

The vacuole H^+-adenosine triphosphatases (v-ATPase) is a proton pump responsible for acidification of intracellular organelles and secretory granules that regulates several cellular processes such as protein trafficking, maturation, and degradation (Forgac, 2007). Acidification of lysosomes by v-ATPase is essential for autophagy progression, and inhibiting v-ATPase activity is a widely used treatment to mimic a block of autophagy. In neurons, v-ATPase is expressed by SVs and allows neurotransmitter loading and SV trafficking (Bodzęta et al., 2017). V-ATPase is a multimeric complex composed by a cytosolic domain (v_1), responsible for ATP hydrolysis, and a transmembrane domain (v_0), responsible for H^+ transport. Recessive mutations in ***ATP6V1A***, coding for the "A" subunit of the v_1 sub-complex, have been first described in patients with cutis laxa, dysmorphic features, and seizures in the context of a severe condition with premature lethality (Van Damme et al., 2017). Subsequently, we described *de novo* heterozygous mutations in *ATP6V1A* in four patients with developmental delay and epilepsy with variable of severity, ranging from mild intellectual disability and epilepsy to early-onset epileptic encephalopathies accompanied by myelination defects and brain atrophy. Pathogenic mutations affect lysosomal homeostasis in patients' cells and impair neurite development and synaptic contacts when expressed in murine neurons. The mutations associated with the severe phenotype result in loss of function and autophagy impairment (Fassio et al., 2018). On the contrary, covalent targeting of ATP6V1A has been recently shown to activate autophagy by increasing v-ATPase catalytic activity and inhibiting mTORC1 activation (Chung et al., 2019).

A *de novo* deletion variant of the v-ATPase accessory protein ***ATP6AP2*** has been found in a patient with neurodevelopmental disorder characterized by fulminant degeneration (Hirose et al., 2019). This patient exhibited mild facial dysmorphisms, early-onset intractable seizures, and spasticity. Sequential MRI scans documented progressive brain shrinkage with thin corpus callosum and hypomyelination. The authors, by employing both patient's iPSC-derived neural cells and murine knockdown models, demonstrated that ATP6AP2 is a key regulator of v-ATPase function in the CNS, and that its loss results in lysosomal and autophagic defects. In these models, the loss of ATP6AP2 impairs stem cell self-renewal and neuronal survival with a strong dependence on the dosage of the transcripts.

In addition to ATP6AP2, v-ATPase assembly and activity relies on several parameters, including kinase activity, nutrient and stress levels, extra- and intra-cellular pH, and accessory proteins that interact with v0 and v1 components (McGuire et al., 2017). We recently demonstrated that ***DMXL2***, a member of WD40 protein family known to regulate v-ATPase trafficking and activity (Yan et al., 2009; Einhorn et al., 2012; Tuttle et al., 2014), is mutated in children with severe developmental and epileptic encephalopathy, associating Ohtahara syndrome, and profound developmental delay with a progressive course leading to premature mortality. MRI scans in these patients showed thin corpus callosum, hypomyelination, and progressive brain shrinkage. Loss of DMXL2 protein in patients' fibroblasts results in impaired autophagy, and modeling DMXL2 loss in murine neurons recapitulates defective autophagy and affects neurite development and synaptic connectivity (Esposito et al., 2019). While the complete loss of *Dmxl2* is embryonically lethal in mice (Tata et al., 2014; Gobé et al., 2019), heterozygous *Dmxl2* mice show macrocephaly and corpus callosum dysplasia, confirming the DMXL2 role in brain development (Kannan et al., 2017).

Altogether, these pieces of evidence support a primary role of autophagy dysregulation in epileptogenesis and suggest that severity of the clinical manifestations variably evolving in a neurodegenerative disorder might depend on different timing and specificity of molecular events underlying epilepsy and neurodegeneration. Defects altering early stages of neuronal development and, therefore, synaptic activity could underlie pro-epileptogenic changes in neuronal circuitries followed by progressive accumulation of autophagy substrates and consequent neuronal stress and degeneration. Our hypothesis is that the spectrum of phenotypes and clinical severities of the epileptic syndromes associated with mutations of autophagy genes primarily derive from an initial synaptic dysfunction, with structural and functional synaptic alterations that, depending on gene dosage and/or severity of the pathogenic mutations, may turn into neuronal damage with degeneration and death. Future work on disease murine models and/or patient-derived neurons needs to be performed to unravel the cellular and molecular mechanisms linking autophagy failure to brain hyperexcitability, seizures, and fulminant neurodegeneration and to evaluate the ability of autophagy inducers as novel therapeutic strategies for these intractable disorders.

AUTHOR CONTRIBUTIONS

AFas and AFal wrote the manuscript and prepared the table and the figure. AE, DA, and RG revised the manuscript. FB coordinated the preparation of the review and revised the manuscript for submission.

FUNDING

This work was supported by Fondazione Telethon, GGP19120 2019 and ERA-NET-NEURON SNAREOPATHIES 2017 to FB; IRCCS San Martino 5x100 2016 to AFas.

REFERENCES

Ables, J. L., Breunig, J. J., Eisch, A. J., and Rakic, P. (2011). Not(ch) just development: notch signalling in the adult brain. *Nat. Rev. Neurosci.* 12, 269–283. doi: 10.1038/nrn3024

Akizu, N., Cantagrel, V., Zaki, M. S., Al-Gazali, L., Wang, X., Rosti, R. O., et al. (2015). Biallelic mutations in SNX14 cause a syndromic form of cerebellar atrophy and lysosome-autophagosome dysfunction. *Nat. Genet.* 47, 528–534. doi: 10.1038/ng.3256

Azarnia Tehran, D., Kuijpers, M., and Haucke, V. (2018). Presynaptic endocytic factors in autophagy and neurodegeneration. *Curr. Opin. Neurobiol.* 48, 153–159. doi: 10.1016/j.conb.2017.12.018

Beck-Wödl, S., Harzer, K., Sturm, M., Buchert, R., Rieß, O., Mennel, H.-D., et al. (2018). Homozygous TBC1 domain-containing kinase (*TBCK*) mutation causes a novel lysosomal storage disease—a new type of neuronal ceroid lipofuscinosis (CLN15)? *Acta Neuropathol. Commun.* 6:145. doi: 10.1186/s40478-018-0646-6

Bhoj, E. J., Li, D., Harr, M., Edvardson, S., Elpeleg, O., Chisholm, E., et al. (2016). Mutations in *TBCK*, encoding TBC1-domain-containing kinase, lead to a recognizable syndrome of intellectual disability and hypotonia. *Am. J. Hum. Genet.* 98, 782–788. doi: 10.1016/j.ajhg.2016.03.016

Binotti, B., Pavlos, N. J., Riedel, D., Wenzel, D., Vorbrüggen, G., Schalk, A. M., et al. (2015). The GTPase Rab26 links synaptic vesicles to the autophagy pathway. *Elife* 4:e05597. doi: 10.7554/eLife.05597

Bodzęta, A., Kahms, M., and Klingauf, J. (2017). The presynaptic v-ATPase reversibly disassembles and thereby modulates exocytosis but is not part of the fusion machinery. *Cell Rep.* 20, 1348–1359. doi: 10.1016/j.celrep.2017.07.040

Bray, S. J. (2006). Notch signalling: a simple pathway becomes complex. *Nat. Rev. Mol. Cell Biol.* 7, 678–689. doi: 10.1038/nrm2009

Byrne, S., Jansen, L., U-King-Im, J.-M., Siddiqui, A., Lidov, H. G. W., Bodi, I., et al. (2016). *EPG5*-related Vici syndrome: a paradigm of neurodevelopmental disorders with defective autophagy. *Brain* 139, 765–781. doi: 10.1093/brain/awv393

Carvill, G. L., Liu, A., Mandelstam, S., Schneider, A., Lacroix, A., Zemel, M., et al. (2018). Severe infantile onset developmental and epileptic encephalopathy caused by mutations in autophagy gene *WDR45*. *Epilepsia* 59, e5–e13. doi: 10.1111/epi.13957

Cecconi, F., Di Bartolomeo, S., Nardacci, R., Fuoco, C., Corazzari, M., Giunta, L., et al. (2007). A novel role for autophagy in neurodevelopment. *Autophagy* 3, 505–507. doi: 10.4161/auto.4616

Chong, J. X., Caputo, V., Phelps, I. G., Stella, L., Worgan, L., Dempsey, J. C., et al. (2016). Recessive inactivating mutations in *TBCK*, encoding a Rab GTPase-activating protein, cause severe infantile syndromic encephalopathy. *Am. J. Hum. Genet.* 98, 772–781. doi: 10.1016/j.ajhg.2016.01.016

Chung, C. Y.-S., Shin, H. R., Berdan, C. A., Ford, B., Ward, C. C., Olzmann, J. A., et al. (2019). Covalent targeting of the vacuolar H^+-ATPase activates autophagy *via* mTORC1 inhibition. *Nat. Chem. Biol.* 15, 776–785. doi: 10.1038/s41589-019-0308-4

Dhaliwal, J., Trinkle-Mulcahy, L., and Lagace, D. C. (2017). Autophagy and adult neurogenesis: discoveries made half a century ago yet in their infancy of being connected. *Brain Plast.* 3, 99–110. doi: 10.3233/bpl-170047

Dikic, I., and Elazar, Z. (2018). Mechanism and medical implications of mammalian autophagy. *Nat. Rev. Mol. Cell Biol.* 19, 349–364. doi: 10.1038/s41580-018-0003-4

Dionisi Vici, C., Sabetta, G., Gambarara, M., Vigevano, F., Bertini, E., Boldrini, R., et al. (1988). Agenesis of the corpus callosum, combined immunodeficiency, bilateral cataract, and hypopigmentation in two brothers. *Am. J. Med. Genet.* 29, 1–8. doi: 10.1002/ajmg.1320290102

Dragich, J. M., Kuwajima, T., Hirose-Ikeda, M., Yoon, M. S., Eenjes, E., Bosco, J. R., et al. (2016). Autophagy linked FYVE (Alfy/WDFY3) is required for establishing neuronal connectivity in the mammalian brain. *Elife* 5:e14810. doi: 10.7554/eLife.14810

Ebrahimi-Fakhari, D., Saffari, A., Wahlster, L., Lu, J., Byrne, S., Hoffmann, G. F., et al. (2016). Congenital disorders of autophagy: an emerging novel class of inborn errors of neuro-metabolism. *Brain* 139, 317–337. doi: 10.1093/brain/awv371

Einhorn, Z., Trapani, J. G., Liu, Q., and Nicolson, T. (2012). Rabconnectin3 promotes stable activity of the H^+ pump on synaptic vesicles in hair cells. *J. Neurosci.* 32, 11144–11156. doi: 10.1523/JNEUROSCI.1705-12.2012

Esposito, A., Falace, A., Wagner, M., Gal, M., Mei, D., Conti, V., et al. (2019). Biallelic DMXL2 mutations impair autophagy and cause Ohtahara syndrome with progressive course. *Brain* 142, 3876–3891. doi: 10.1093/brain/awz326

Fassio, A., Esposito, A., Kato, M., Saitsu, H., Mei, D., Marini, C., et al. (2018). *De novo* mutations of the ATP6V1A gene cause developmental encephalopathy with epilepsy. *Brain* 141, 1703–1718. doi: 10.1093/brain/awy092

Fimia, G. M., Stoykova, A., Romagnoli, A., Giunta, L., Di Bartolomeo, S., Nardacci, R., et al. (2007). Ambra1 regulates autophagy and development of the nervous system. *Nature* 447, 1121–1125. doi: 10.1038/nature05925

Forgac, M. (2007). Vacuolar ATPases: rotary proton pumps in physiology and pathophysiology. *Nat. Rev. Mol. Cell Biol.* 8, 917–929. doi: 10.1038/nrm2272

Gao, C., Cao, W., Bao, L., Zuo, W., Xie, G., Cai, T., et al. (2010). Autophagy negatively regulates Wnt signalling by promoting Dishevelled degradation. *Nat. Cell Biol.* 12, 781–790. doi: 10.1038/ncb2082

George, A. A., Hayden, S., Holzhausen, L. C., Ma, E. Y., Suzuki, S. C., and Brockerhoff, S. E. (2014). Synaptojanin 1 is required for endolysosomal trafficking of synaptic proteins in cone photoreceptor inner segments. *PLoS One* 9:e84394. doi: 10.1371/journal.pone.0084394

Giorgi, F. S., Biagioni, F., Lenzi, P., Frati, A., and Fornai, F. (2015). The role of autophagy in epileptogenesis and in epilepsy-induced neuronal alterations. *J. Neural Transm.* 122, 849–862. doi: 10.1007/s00702-014-1312-1

Glatigny, M., Moriceau, S., Rivagorda, M., Ramos-Brossier, M., Nascimbeni, A. C., Lante, F., et al. (2019). Autophagy is required for memory formation and reverses age-related memory decline. *Curr. Biol.* 29, 435.e8–448.e8. doi: 10.1016/j.cub.2018.12.021

Gobé, C., Elzaiat, M., Meunier, N., André, M., Sellem, E., Congar, P., et al. (2019). Dual role of DMXL2 in olfactory information transmission and the first wave of spermatogenesis. *PLoS Genet.* 15:e1007909. doi: 10.1371/journal.pgen.1007909

Gstrein, T., Edwards, A., Přistoupilová, A., Leca, I., Breuss, M., Pilat-Carotta, S., et al. (2018). Mutations in Vps15 perturb neuronal migration in mice and are associated with neurodevelopmental disease in humans. *Nat. Neurosci.* 21, 207–217. doi: 10.1038/s41593-017-0053-5

Haack, T. B., Hogarth, P., Kruer, M. C., Gregory, A., Wieland, T., Schwarzmayr, T., et al. (2012). Exome sequencing reveals *de novo WDR45* mutations causing a phenotypically distinct, X-linked dominant form of NBIA. *Am. J. Hum. Genet.* 91, 1144–1149. doi: 10.1016/j.ajhg.2012.10.019

Hara, T., Nakamura, K., Matsui, M., Yamamoto, A., Nakahara, Y., Suzuki-Migishima, R., et al. (2006). Suppression of basal autophagy in neural cells causes neurodegenerative disease in mice. *Nature* 441, 885–889. doi: 10.1038/nature04724

Hayflick, S. J., Kurian, M. A., and Hogarth, P. (2018). "Neurodegeneration with brain iron accumulation," in *Handbook of Clinical Neurology*, eds D. H. Geschwind, H. L. Paulson and C. Klein (New York, NY: Elsevier), 293–305.

Hernandez, D., Torres, C. A., Setlik, W., Cebrián, C., Mosharov, E. V., Tang, G., et al. (2012). Regulation of presynaptic neurotransmission by macroautophagy. *Neuron* 74, 277–284. doi: 10.1016/j.neuron.2012.02.020

Hirose, T., Cabrera-Socorro, A., Chitayat, D., Lemonnier, T., Féraud, O., Cifuentes-Diaz, C., et al. (2019). ATP6AP2 variant impairs CNS development and neuronal survival to cause fulminant neurodegeneration. *J. Clin. Invest.* 129, 2145–2162. doi: 10.1172/jci79990

Hoffmann, S., Orlando, M., Andrzejak, E., Bruns, C., Trimbuch, T., Rosenmund, C., et al. (2019). Light-activated ROS production induces synaptic autophagy. *J. Neurosci.* 39, 2163–2183. doi: 10.1523/JNEUROSCI.1317-18.2019

Huang, H.-S., Yoon, B.-J., Brooks, S., Bakal, R., Berrios, J., Larsen, R. S., et al. (2014). Snx14 regulates neuronal excitability, promotes synaptic transmission, and is imprinted in the brain of mice. *PLoS One* 9:e98383. doi: 10.1371/journal.pone.0098383

Hui, K. K., Takashima, N., Watanabe, A., Chater, T. E., Matsukawa, H., Nekooki-Machida, Y., et al. (2019). GABARAPs dysfunction by autophagy deficiency in adolescent brain impairs $GABA_A$ receptor trafficking and social behavior. *Sci. Adv.* 5:eaau8237. doi: 10.1126/sciadv.aau8237

Jimenez-Sanchez, M., Menzies, F. M., Chang, Y.-Y., Simecek, N., Neufeld, T. P., and Rubinsztein, D. C. (2012). The Hedgehog signalling pathway regulates autophagy. *Nat. Commun.* 3:1200. doi: 10.1038/ncomms2212

Joo, J. H., Wang, B., Frankel, E., Ge, L., Xu, L., Iyengar, R., et al. (2016). The noncanonical role of ULK/ATG1 in ER-to-golgi trafficking is essential for cellular homeostasis. *Mol. Cell* 62, 491–506. doi: 10.1016/j.molcel.2016.04.020

Kannan, M., Bayam, E., Wagner, C., Rinaldi, B., Kretz, P. F., Tilly, P., et al. (2017). WD40-repeat 47, a microtubule-associated protein, is essential for brain development and autophagy. *Proc. Natl. Acad. Sci. U S A* 114, E9308–E9317. doi: 10.1073/pnas.1713625114

Katsumata, K., Nishiyama, J., Inoue, T., Mizushima, N., Takeda, J., and Yuzaki, M. (2010). Dynein- and activity-dependent retrograde transport of autophagosomes in neuronal axons. *Autophagy* 6, 378–385. doi: 10.4161/auto.6.3.11262

Kiriyama, Y., and Nochi, H. (2015). The function of autophagy in neurodegenerative diseases. *Int. J. Mol. Sci.* 16, 26797–26812. doi: 10.3390/ijms161125990

Kiyono, K., Suzuki, H. I., Matsuyama, H., Morishita, Y., Komuro, A., Kano, M. R., et al. (2009). Autophagy is activated by TGF-β and potentiates TGF-β-mediated growth inhibition in human hepatocellular carcinoma cells. *Cancer Res.* 69, 8844–8852. doi: 10.1158/0008-5472.can-08-4401

Komatsu, M., Waguri, S., Chiba, T., Murata, S., Iwata, J., Tanida, I., et al. (2006). Loss of autophagy in the central nervous system causes neurodegeneration in mice. *Nature* 441, 880–884. doi: 10.1038/nature04723

Lee, J. H., and Gleeson, J. G. (2010). The role of primary cilia in neuronal function. *Neurobiol. Dis.* 38, 167–172. doi: 10.1016/j.nbd.2009.12.022

Lee, K.-M., Hwang, S.-K., and Lee, J.-A. (2013). Neuronal autophagy and neurodevelopmental disorders. *Exp. Neurobiol.* 22, 133–142. doi: 10.5607/en.2013.22.3.133

Liang, C.-C., Wang, C., Peng, X., Gan, B., and Guan, J.-L. (2010). Neural-specific deletion of FIP200 leads to cerebellar degeneration caused by increased neuronal death and axon degeneration. *J. Biol. Chem.* 285, 3499–3509. doi: 10.1074/jbc.m109.072389

Liang, Y., and Sigrist, S. (2018). Autophagy and proteostasis in the control of synapse aging and disease. *Curr. Opin. Neurobiol.* 48, 113–121. doi: 10.1016/j.conb.2017.12.006

Lipton, J. O., and Sahin, M. (2014). The neurology of mTOR. *Neuron* 84, 275–291. doi: 10.1016/j.neuron.2014.09.034

Lüningschrör, P., Binotti, B., Dombert, B., Heimann, P., Perez-Lara, A., Slotta, C., et al. (2017). Plekhg5-regulated autophagy of synaptic vesicles reveals a pathogenic mechanism in motoneuron disease. *Nat. Commun.* 8:678. doi: 10.1038/s41467-017-00689-z

Lv, X., Jiang, H., Li, B., Liang, Q., Wang, S., Zhao, Q., et al. (2015). The crucial role of Atg5 in cortical neurogenesis during early brain development. *Sci. Rep.* 4:6010. doi: 10.1038/srep06010

Maday, S. (2016). Mechanisms of neuronal homeostasis: autophagy in the axon. *Brain Res.* 1649, 143–150. doi: 10.1016/j.brainres.2016.03.047

Mas, C., Norwood, S. J., Bugarcic, A., Kinna, G., Leneva, N., Kovtun, O., et al. (2014). Structural basis for different phosphoinositide specificities of the PX domains of sorting nexins regulating G-protein signaling. *J. Biol. Chem.* 289, 28554–28568. doi: 10.1074/jbc.m114.595959

McGuire, C., Stransky, L., Cotter, K., and Forgac, M. (2017). Regulation of V-ATPase activity. *Front. Biosci.* 22, 609–622. doi: 10.2741/4506

McMahon, J., Huang, X., Yang, J., Komatsu, M., Yue, Z., Qian, J., et al. (2012). Impaired autophagy in neurons after disinhibition of mammalian target of rapamycin and its contribution to epileptogenesis. *J. Neurosci.* 32, 15704–15714. doi: 10.1523/JNEUROSCI.2392-12.2012

Menzies, F. M., Fleming, A., Caricasole, A., Bento, C. F., Andrews, S. P., Ashkenazi, A., et al. (2017). Autophagy and neurodegeneration: pathogenic mechanisms and therapeutic opportunities. *Neuron* 93, 1015–1034. doi: 10.1016/j.neuron.2017.01.022

Murdoch, J. D., Rostosky, C. M., Gowrisankaran, S., Arora, A. S., Soukup, S.-F., Vidal, R., et al. (2016). Endophilin-A deficiency induces the Foxo3a-Fbxo32 network in the brain and causes dysregulation of autophagy and the ubiquitin-proteasome system. *Cell Rep.* 17, 1071–1086. doi: 10.1016/j.celrep.2016.09.058

Nikoletopoulou, V., Papandreou, M.-E., and Tavernarakis, N. (2015). Autophagy in the physiology and pathology of the central nervous system. *Cell Death Differ.* 22, 398–407. doi: 10.1038/cdd.2014.204

Nikoletopoulou, V., Sidiropoulou, K., Kallergi, E., Dalezios, Y., and Tavernarakis, N. (2017). Modulation of autophagy by BDNF underlies synaptic plasticity. *Cell Metab.* 26, 230.e5–242.e5. doi: 10.1016/j.cmet.2017.06.005

Okerlund, N. D., Schneider, K., Leal-Ortiz, S., Montenegro-Venegas, C., Kim, S. A., Garner, L. C., et al. (2017). Bassoon controls presynaptic autophagy through Atg5. *Neuron* 93, 897.e7–913.e7. doi: 10.1016/j.neuron.2017.01.026

Ortiz-González, X. R., Tintos-Hernández, J. A., Keller, K., Li, X., Foley, A. R., Bharucha-Goebel, D. X., et al. (2018). Homozygous boricua *TBCK* mutation causes neurodegeneration and aberrant autophagy. *Ann. Neurol.* 83, 153–165. doi: 10.1002/ana.25130

Park, S. M., Lim, J. S., Ramakrishina, S., Kim, S. H., Kim, W. K., Lee, J., et al. (2018). Brain somatic mutations in MTOR disrupt neuronal ciliogenesis, leading to focal cortical dyslamination. *Neuron* 99, 83.e7–97.e7. doi: 10.1016/j.neuron.2018.05.039

Parrini, E., Conti, V., Dobyns, W. B., and Guerrini, R. (2016). Genetic basis of brain malformations. *Mol. Syndromol.* 7, 220–233. doi: 10.1159/000448639

Rowland, A. M. (2006). Presynaptic terminals independently regulate synaptic clustering and autophagy of $GABA_A$ receptors in *Caenorhabditis elegans*. *J. Neurosci.* 26, 1711–1720. doi: 10.1523/JNEUROSCI.2279-05.2006

Rubinsztein, D. C., DiFiglia, M., Heintz, N., Nixon, R. A., Qin, Z.-H., Ravikumar, B., et al. (2005). Autophagy and its possible roles in nervous system diseases, damage and repair. *Autophagy* 1, 11–22. doi: 10.4161/auto.1.1.1513

Saitsu, H., Nishimura, T., Muramatsu, K., Kodera, H., Kumada, S., Sugai, K., et al. (2013). De novo mutations in the autophagy gene *WDR45* cause static encephalopathy of childhood with neurodegeneration in adulthood. *Nat. Genet.* 45, 445–449. doi: 10.1038/ng.2562

Seibler, P., Burbulla, L. F., Dulovic, M., Zittel, S., Heine, J., Schmidt, T., et al. (2018). Iron overload is accompanied by mitochondrial and lysosomal dysfunction in *WDR45* mutant cells. *Brain* 141, 3052–3064. doi: 10.1093/brain/awy230

Shehata, M., Abdou, K., Choko, K., Matsuo, M., Nishizono, H., and Inokuchi, K. (2018). Autophagy enhances memory erasure through synaptic destabilization. *J. Neurosci.* 38, 3809–3822. doi: 10.1523/JNEUROSCI.3505-17.2018

Shehata, M., Matsumura, H., Okubo-Suzuki, R., Ohkawa, N., and Inokuchi, K. (2012). Neuronal stimulation induces autophagy in hippocampal neurons that is involved in AMPA receptor degradation after chemical long-term depression. *J. Neurosci.* 32, 10413–10422. doi: 10.1523/JNEUROSCI.4533-11.2012

Soukup, S.-F., Kuenen, S., Vanhauwaert, R., Manetsberger, J., Hernández-Díaz, S., Swerts, J., et al. (2016). A LRRK2-dependent endophilina phosphoswitch is critical for macroautophagy at presynaptic terminals. *Neuron* 92, 829–844. doi: 10.1016/j.neuron.2016.09.037

Tang, G., Gudsnuk, K., Kuo, S.-H., Cotrina, M. L., Rosoklija, G., Sosunov, A., et al. (2014). Loss of mTOR-dependent macroautophagy causes autistic-like synaptic pruning deficits. *Neuron* 83, 1131–1143. doi: 10.1016/j.neuron.2014.07.040

Tata, B., Huijbregts, L., Jacquier, S., Csaba, Z., Genin, E., Meyer, V., et al. (2014). Haploinsufficiency of Dmxl2, encoding a synaptic protein, causes infertility

associated with a loss of GnRH neurons in mouse. *PLoS Biol.* 12:e1001952. doi: 10.1371/journal.pbio.1001952

Teinert, J., Behne, R., Wimmer, M., and Ebrahimi-Fakhari, D. (2020). Novel insights into the clinical and molecular spectrum of congenital disorders of autophagy. *J. Inherit. Metab. Dis.* 43, 51–62. doi: 10.1002/jimd.12084

Thomas, A. C., Williams, H., Setó-Salvia, N., Bacchelli, C., Jenkins, D., O'Sullivan, M., et al. (2014). Mutations in SNX14 cause a distinctive autosomal-recessive cerebellar ataxia and intellectual disability syndrome. *Am. J. Hum. Genet.* 95, 611–621. doi: 10.1016/j.ajhg.2014.10.007

Tuttle, A. M., Hoffman, T. L., and Schilling, T. F. (2014). Rabconnectin-3a regulates vesicle endocytosis and canonical Wnt signaling in zebrafish neural crest migration. *PLoS Biol.* 12:e1001852. doi: 10.1371/journal.pbio.1001852

Uytterhoeven, V., Lauwers, E., Maes, I., Miskiewicz, K., Melo, M. N., Swerts, J., et al. (2015). Hsc70–4 deforms membranes to promote synaptic protein turnover by endosomal microautophagy. *Neuron* 88, 735–748. doi: 10.1016/j.neuron.2015.10.012

Van Damme, T., Gardeitchik, T., Mohamed, M., Guerrero-Castillo, S., Freisinger, P., Guillemyn, B., et al. (2017). Mutations in ATP6V1E1 or ATP6V1A cause autosomal-recessive cutis laxa. *Am. J. Hum. Genet.* 100, 216–227. doi: 10.1016/j.ajhg.2016.12.010

Vanhauwaert, R., Kuenen, S., Masius, R., Bademosi, A., Manetsberger, J., Schoovaerts, N., et al. (2017). The SAC1 domain in synaptojanin is required for autophagosome maturation at presynaptic terminals. *EMBO J.* 36, 1392–1411. doi: 10.15252/embj.201695773

Vijayan, V., and Verstreken, P. (2017). Autophagy in the presynaptic compartment in health and disease. *J. Cell Biol.* 216, 1895–1906. doi: 10.1083/jcb.201611113

Wang, T., Martin, S., Papadopulos, A., Harper, C. B., Mavlyutov, T. A., Niranjan, D., et al. (2015). Control of autophagosome axonal retrograde flux by presynaptic activity unveiled using botulinum neurotoxin type A. *J. Neurosci.* 35, 6179–6194. doi: 10.1523/JNEUROSCI.3757-14.2015

Wang, Z., Miao, G., Xue, X., Guo, X., Yuan, C., Wang, Z., et al. (2016). The vici syndrome protein *EPG5* is a Rab7 effector that determines the fusion specificity of autophagosomes with late endosomes/lysosomes. *Mol. Cell* 63, 781–795. doi: 10.1016/j.molcel.2016.08.021

Wu, X., Fleming, A., Ricketts, T., Pavel, M., Virgin, H., Menzies, F. M., et al. (2016). Autophagy regulates Notch degradation and modulates stem cell development and neurogenesis. *Nat. Commun.* 7:10533. doi: 10.1038/ncomms10533

Yan, Y., Denef, N., and Schüpbach, T. (2009). The vacuolar proton pump, V-ATPase, is required for notch signaling and endosomal trafficking in *Drosophila*. *Dev. Cell* 17, 387–402. doi: 10.1016/j.devcel.2009.07.001

Yasin, S. A., Ali, A. M., Tata, M., Picker, S. R., Anderson, G. W., Latimer-Bowman, E., et al. (2013). mTOR-dependent abnormalities in autophagy characterize human malformations of cortical development: evidence from focal cortical dysplasia and tuberous sclerosis. *Acta Neuropathol.* 126, 207–218. doi: 10.1007/s00401-013-1135-4

Zhang, J., Liu, J., Liu, L., McKeehan, W. L., and Wang, F. (2012). The fibroblast growth factor signaling axis controls cardiac stem cell differentiation through regulating autophagy. *Autophagy* 8, 690–691. doi: 10.4161/auto.19290

Zhao, Y. G., Sun, L., Miao, G., Ji, C., Zhao, H., Sun, H., et al. (2015). The autophagy gene *Wdr45/Wipi4* regulates learning and memory function and axonal homeostasis. *Autophagy* 11, 881–890. doi: 10.1080/15548627.2015.1047127

Zhao, H., Zhao, Y. G., Wang, X., Xu, L., Miao, L., Feng, D., et al. (2013). Mice deficient in *Epg5* exhibit selective neuronal vulnerability to degeneration. *J. Cell Biol.* 200, 731–741. doi: 10.1083/jcb.201211014

Conflict of Interest: The authors declare that the research was conducted in the absence of any commercial or financial relationships that could be construed as a potential conflict of interest.

frontiers in Cellular Neuroscience

ORIGINAL RESEARCH
published: 17 March 2020
doi: 10.3389/fncel.2020.00053

Granule Cell Dispersion in Human Temporal Lobe Epilepsy: Proteomics Investigation of Neurodevelopmental Migratory Pathways

*Joan Y. W. Liu[1,2,3], Natasha Dzurova[3], Batoul Al-Kaaby[1], Kevin Mills[4], Sanjay M. Sisodiya[2,5] and Maria Thom[1,2]**

[1]Division of Neuropathology, National Hospital for Neurology and Neurosurgery, London, United Kingdom, [2]Department of Clinical and Experimental Epilepsy, UCL Queen Square Institute of Neurology, London, United Kingdom, [3]School of Life Sciences, University of Westminster, London, United Kingdom, [4]Biological Mass Spectrometry Centre, UCL Great Ormond Street Institute of Child Health, University College London, London, United Kingdom, [5]Chalfont Centre for Epilepsy, Chalfont St Peter, United Kingdom*

Granule cell dispersion (GCD) is a common pathological feature observed in the hippocampus of patients with Mesial Temporal Lobe Epilepsy (MTLE). Pathomechanisms underlying GCD remain to be elucidated, but one hypothesis proposes aberrant reactivation of neurodevelopmental migratory pathways, possibly triggered by febrile seizures. This study aims to compare the proteomes of basal and dispersed granule cells in the hippocampus of eight MTLE patients with GCD to identify proteins that may mediate GCD in MTLE. Quantitative proteomics identified 1,882 proteins, of which 29% were found in basal granule cells only, 17% in dispersed only and 54% in both samples. Bioinformatics analyses revealed upregulated proteins in dispersed samples were involved in developmental cellular migratory processes, including cytoskeletal remodeling, axon guidance and signaling by Ras homologous (Rho) family of GTPases ($P < 0.01$). The expression of two Rho GTPases, RhoA and Rac1, was subsequently explored in immunohistochemical and *in situ* hybridization studies involving eighteen MTLE cases with or without GCD, and three normal post mortem cases. In cases with GCD, most dispersed granule cells in the outer-granular and molecular layers have an elongated soma and bipolar processes, with intense RhoA immunolabeling at opposite poles of the cell soma, while most granule cells in the basal granule cell layer were devoid of RhoA. A higher percentage of cells expressing RhoA was observed in cases with GCD than without GCD ($P < 0.004$). In GCD cases, the percentage of cells expressing RhoA was significantly higher in the inner molecular layer than the granule cell layer ($P < 0.026$), supporting proteomic findings. *In situ* hybridization studies using probes against *RHOA* and *RAC1* mRNAs revealed fine peri- and nuclear puncta in granule cells of all cases.

OPEN ACCESS

Edited by:
Eleonora Aronica, Amsterdam University Medical Center, Netherlands

Reviewed by:
Sang Ryong Kim, Kyungpook National University, South Korea
Angelika Mühlebner, Academic Medical Center, Netherlands

***Correspondence:**
Maria Thom
m.thom@ucl.ac.uk

Received: *30 October 2019*
Accepted: *21 February 2020*
Published: *17 March 2020*

Citation:
Liu JYW, Dzurova N, Al-Kaaby B, Mills K, Sisodiya SM and Thom M (2020) Granule Cell Dispersion in Human Temporal Lobe Epilepsy: Proteomics Investigation of Neurodevelopmental Migratory Pathways. Front. Cell. Neurosci. 14:53. doi: 10.3389/fncel.2020.00053

Abbreviations: CA, cornu ammonis; GCD, granule cell dispersion; GCL, granule cell layer; HS ILAE, Type 1 hippocampal sclerosis Type 1 according to International League Against Epilepsy classification system; MOL, molecular layer; MTLE, Mesial Temporal Lobe Epilepsy.

The density of cells expressing *RHOA* mRNAs was significantly higher in the inner molecular layer of cases with GCD than without GCD (P = 0.05). In summary, our study has found limited evidence for ongoing adult neurogenesis in the hippocampus of patients with MTLE, but evidence of differential dysmaturation between dispersed and basal granule cells has been demonstrated, and elevated expression of Rho GTPases in dispersed granule cells may contribute to the pathomechanisms underpinning GCD in MTLE.

Keywords: proteome, dentate gyrus, epilepsy, Rho GTPases, migration

INTRODUCTION

Temporal lobe epilepsy is the most common form of pharmacoresistant epilepsy in adults (Engel, 1998). Up to 80% of patients with a mesial form of temporal lobe epilepsy (MTLE) have structural abnormalities in the hippocampus (de Tisi et al., 2011; Blumcke et al., 2017). Over 60% of patients with MTLE and hippocampal pathologies remained seizure-free for at least a year after surgical resection of the hippocampus as treatment for their epilepsy (de Tisi et al., 2011; Engel et al., 2012; Blumcke et al., 2017), suggesting that the hippocampus is the primary site for epileptogenesis.

Hippocampal Sclerosis ILAE Type 1 (HS Type 1) is the most common pathology observed in patients with pharmacoresistant MTLE, and it is primarily characterized by segmental loss of pyramidal neurons in cornu ammonis subfields CA1, 3, and 4 (Blumcke et al., 2017). Over half of the MTLE patients with HS Type 1 also have abnormalities affecting dentate granule cells (DGCs) including granule cell dispersion (GCD) and mossy fiber sprouting (Wieser, 2004; Blümcke et al., 2009; Thom et al., 2010; Da Costa Neves et al., 2013). In the normal human hippocampus, DGCs are organized into a compact layer of up to ten cells thick or $\leq$120 μm (Houser, 1990; Wieser, 2004). In GCD, ectopic DGCs in clusters or rows disperse to the inner and outer molecular layers of the sclerotic hippocampus, widening the granule cell layer to up to 400 μm in thickness (Blümcke et al., 2009). The presence, severity, and extent of GCD along the hippocampal body is highly variable amongst patients with MTLE (Thom et al., 2010; Blümcke et al., 2013) and there is no confirmed grading scheme for GCD in MTLE. The exact cause of GCD in human MTLE is unknown; however, animal models of MTLE with or without hippocampal sclerosis have shown that seizures can displace the migration of newly-generated (Parent et al., 2006; Hester and Danzer, 2013) and mature DGCs to CA4 and molecular layer (Murphy and Danzer, 2011; Koyama et al., 2012; Chai et al., 2014). Reelin is an extracellular matrix glycoprotein secreted by Cajal-Retzius cells during neurodevelopment to regulate the correct layering of migrating cells (Frotscher, 1998). Low levels of reelin transcript and protein have been reported in the hippocampus of patients with MTLE (Haas et al., 2002; Haas and Frotscher, 2010) and animal models of MTLE (Heinrich et al., 2006), possibly as a consequence of elevated methylation at the promotor region of *RELN* (Kobow et al., 2009) or loss of reelin-synthesizing neurons in hippocampus (Haas et al., 2002; Orcinha et al., 2016). The loss of reelin in MTLE is believed to lead to the "over-running" of DGCs into the molecular layer. Past studies have shown that pharmacological inhibition of mammalian target of rapamycin (mTOR) pathway can prevent the development of the mossy fiber sprouting (Buckmaster et al., 2009) and reduce the severity of GCD in animal models of MTLE (Lee et al., 2018), suggesting that the mTOR pathway may have a role in the pathomechanisms of these abnormalities. In patients with MTLE, most astroglial cells strongly expressed markers of mTOR signaling activation such as phospho-S6 ribosomal protein in the sclerotic hippocampus, whereas DGCs showed minimal immunohistochemical evidence of mTOR activation (Sha et al., 2012; Sosunov et al., 2012; Liu et al., 2014). Clinicopathological studies reported that the presence of GCD in patients with MTLE was associated with a history of early onset of epilepsy and febrile seizures (<4 years) and longer duration of epilepsy (Lurton et al., 1998; Blümcke et al., 2009) suggesting that GCD may be a consequence of seizures or brain trauma acquired during the first decade of life where dentate neurogenesis is still active. Although it is unclear whether the presence of GCD is associated with positive surgical outcomes for patients with pharmacoresistant MTLE based on existing literature (Blümcke et al., 2009; Thom et al., 2010; Da Costa Neves et al., 2013), there is supportive evidence from animal studies to show that ectopic DGCs increase hippocampal excitability by having a lower activation threshold, forming excess dendritic axonal connections and receiving more excitatory and fewer inhibitory synaptic inputs than normal cells (Zhan et al., 2010; Murphy and Danzer, 2011; Althaus et al., 2019). In patients with MTLE, GCD is often observed in conjunction with mossy fiber sprouting, where mossy fibers of DGCs form excitatory synaptic contact with apical dendrites and spines of neighboring DGCs in the molecular layer (Sutula et al., 1989; Cavazos et al., 2003), thus potentially creating an internal, pro-epileptogenic circuit.

DGCs are functionally important for cognition and memory since they filter the main inputs into the hippocampus, and propagate signals by innervating pyramidal neurons in CA subfields. Electrophysiological *in vivo* animal studies have demonstrated that DGCs normally have low-excitability, and only a small, spatially-defined population of DGCs would fire to allow the execution of fine and spatially-complex activities such as pattern separation, novelty detection and spatial discrimination (Kahn et al., 2019). Stimulated DGCs release vesicles containing glutamate to activate the population firing of interconnected CA3 pyramidal cells (Miles and Wong,

1983; Scharfman and MacLusky, 2014). Consequently, many stimulated DGCs would enhance hippocampal excitability, thus increasing the chances of seizures (Overstreet-Wadiche et al., 2006; Hester and Danzer, 2013), and reducing the ability to perform fine, spatial discrimination tasks (Kahn et al., 2019). Silencing DGCs using ontogenetic manipulation can reduce seizure frequency and reverse cognitive impairments in animal models of MTLE (Krook-Magnuson et al., 2015).

In view of the important role DGCs play in cognition and promoting hyperexcitability, it is important to understand mechanisms and substrates driving abnormal displacement of DGCs in patients with MTLE. The proteome of the human hippocampus has been studied in normal (Edgar et al., 1999a; Föcking et al., 2012; Koopmans et al., 2018), and diseased post mortem human brains, including in the context of schizophrenia (Edgar et al., 1999b), Alzheimer's disease (Edgar et al., 1999b; Sultana et al., 2007; Begcevic et al., 2013; Hondius et al., 2016), and non-CNS malignancies (Yang et al., 2004a). In epilepsy, the proteomes of surgically-resected hippocampi from patients with refractory TLE (Czech et al., 2004; Yang et al., 2004b, 2006; Persike et al., 2012, 2018; Mériaux et al., 2014) or temporal cortex (Eun et al., 2004; He et al., 2006; Keren-Aviram et al., 2018) have been studied. Most of these past studies investigated the whole hippocampus rather than specific hippocampal subregions, and information about structural hippocampal pathology was not disclosed in three studies (Czech et al., 2004; Persike et al., 2012, 2018). None of the previous human proteomic studies discussed GCD in their samples. We aimed to investigate the proteomes of DGCs located in the basal and dispersed regions of the granule and molecular layers of patients with HS Type 1 and GCD, and to identify the molecular substrates that mediate GCD. Ectopic DGCs are potential substrates for recurrent excitation, and they may be the key to understanding MTLE with hippocampal sclerosis and GCD, and its comorbidities including cognitive and memory impairments.

MATERIALS AND METHODS

Cases

Patients with refractory MTLE who had undergone surgical resection of the hippocampus as a treatment for their epilepsy between 2005 and 2016 were identified from the records of UCL Epilepsy Society Brain and Tissue Bank (**Table 1**). All patients provided written informed consent for the use of tissue in research studies in accordance with the Declaration of Helsinki, and the study has obtained ethical approval. Eight cases with age at surgery ranged from 20 to 60 years were submitted to proteomic analysis. All cases had HS Type 1 with marked GCD pathology as confirmed by an experienced neuropathologist.

At the initial neuropathological assessment, two 5 mm-thick blocks from each case were coronally sampled from the middle of the hippocampus (2 cm from anterior tip) to ensure that the dentate gyrus was presented for assessment and subsequent experiments. One block of the sampled hippocampus was snap-frozen in liquid nitrogen, stored in −70 freezers and later retrieved for proteomic studies, while the other block was fixed in 10% neutral-buffered formalin, processed and embedded in paraffin wax for histological staining and immunohistochemistry.

Laser Capture Microdissection

Fourteen sections of 14 μm thickness were sectioned from each frozen hippocampal sample, and sections were collected onto polyethylene terephthalate metal frame slides for laser capture microdissection (Leica, Milton Keynes, UK). Two additional sections were collected onto a microscopic slide (VWR International, UK) and stained briefly in 0.1% toluidine blue (pH 4.5) solution for 5 s to visualize the granule cell layer. Laser capture microdissection (LCM 700; Leica, Milton Keynes, UK) was then carried out along the entire length of the GCL of multiple sections per case to capture basal and dispersed DGCs (**Figure 2A**). Basal samples included DGCs in the granule cell layer closest to CA4, while the dispersed samples included ectopic DGCs in the outer-granular layer and inner and outer molecular layers. A total tissue area of 9 ± 1 mm^2 was dissected for each case, and submitted for proteomic analysis.

Proteomic and Bioinformatics Analyses

Samples were denatured using in-solution trypsin digestion and prepared for MSe label-free quantitative proteomics as described previously (Heywood et al., 2013; Manwaring et al., 2013; Liu et al., 2016). Data were processed using ProteinLynx GlobalServer version 2.5. Protein identifications were obtained by searching the UniProt reference human proteomes with the sequence of porcine trypsin (P00761) added. Protein identification from the low/high collision spectra for each sample was processed using a hierarchical approach where more than three fragment ions per peptide, seven fragment ions per protein, and more than two peptides per protein had to be matched. Peptide identification was accepted if they could be established at 95% or greater probability. Statistical analyses of group means were performed using *t*-test in SPSS (v25; IBM, USA) to identify significantly differentially expressed proteins between dispersed and basal samples, or younger and older cohorts ($P < 0.05$). The younger cohort consisted of four cases with an age at surgery ranging from 20 to 34 years, and the older cohort included four cases with an age at surgery ranging from 51 to 60 years. For volcano plots, fold change between groups was transformed using base 2 logarithmic transformations and plotted against the negative logarithmic transformation of *P*-value. List of differentially expressed proteins in Basal, Dispersed, Younger and Older clusters included proteins found only in the respective samples, and proteins that were significantly different between comparison group (fold change >1.5, $P < 0.05$). Enriched lists were analyzed using bioinformatics resources, Database for Annotation, Visualization and Integrated Discovery (DAVID; version 6.8; Huang da et al., 2009a,b) and Enrichr (Chen et al., 2013; Kuleshov et al., 2016), to obtain information regarding biological, cellular and molecular functions of proteins. Interactions between proteins were investigated using STRING analysis[1], and proteins in functional

[1]https://string-db.org/

TABLE 1 | Clinical details of cases studied.

Age at surgery	Cases	Relevant clinical history under age of 4 years	Age of onset (years)	Antiepileptic medications	Neuro-psychometric findings	DG pathology laterality (other pathology)	Type of studies proteomic (*n* = 8) RhoA IHC (*n* = 17) RhoA ISH (*n* = 10) Rac1 ISH (*n* = 15)
Between 20–30 years	E1	FS	13	Carb, Lam, Lev, Mid, Val	No remarkable cognitive deficits	HS Type 1. Left. GCD. MFS	All studies
	E20	FS, meningitis	12	Carb	Average intellectual abilities and language functions	HS Type 1. Left. GCD. MFS (TS)	RhoA IHC
	E2	FS	14	Carb, Lev, Ox, Val	Weak verbal and recognition functions	HS Type 1. Right. GCD. MFS (TS)	All studies
	E122	none	14	Carb, Lam, Preg	Weak working and verbal memory	HS Type 1. Right. GCD. MFS.	All except proteomics
	E123	FS	1.5	Carb, Lam, Val	Average intellectual abilities and memory. Weak visuospatial processing abilities	HS Type 3 (OH)	All studies except proteomic
	E16	None	9	Lam, Lev	Average cognition and memory functions	HS Type 3. Right	Rac1-ISH
	E3	Head trauma	11	Carb, Lev, Zon	Weak verbal intelligence and verbal and visual memory	HS Type 1. Left. GCD. MFS	Proteomic, RhoA-IHC
	E12	None	15	Lam, Zon	Weak verbal memory	HS Type 3. Left.	Rac1-ISH
Between 31–40 years	E4	None	10	Carb, Lev	Average cognition and memory functions	HS Type 1. Right. GCD. MFS	Proteomic, Rac1-ISH
	E14	B cell non-Hodgkin's lymphoma	8	Carb, Lev, Dia	Weak verbal and working memory Depression. Psychosis.	HS Type 1. Left. GCD. MFS	All except proteomics
	E13	FS	1	Val, Clob, Carb	Average cognition and memory functions.	HS Type 1. Right. GCD. MFS	All except proteomics
Between 41–50 years	E5P	None	2	Lev, Carb	Weak visual memory	HS Type 3. Right.	All except proteomic
	E11	None	8	Clonazepam, Ox	Weak cognition and visual memory. Depression, Paranoia	HS Type 1. Right. GCD. MFS	All except proteomics
Between 51–60 years	E5	Head trauma	16	Carb, Lam, Pheny	Weak verbal intelligence and working memory. Anxiety. Depression	HS Type 1. Right. GCD. MFS	Proteomic
	E6	FS	Late 30s	Carb, Ox, Lev, Lam, Pheno	Weak verbal and non-verbal memory. Psychosis	HS Type 1. Left. GCD. MFS.	All except RhoA-ISH
	E7	n/a	11	Val, Preg, Carb	Weak verbal memory and spatial recognition. Paranoia	HS Type 1. Left. GCD. MFS	All studies
	E1P	FS	22	Carb, Clob	Impaired intellectual ability and visual and verbal memory	HS Type 1. Left. GCD. MFS	All except proteomic
	E8	Head trauma	8	Carb, Gaba, Lam, Prim	Poor verbal memory	HS Type 1. Left. GCD. MFS	All studies
29	PM44	COD: sudden death	n/a	None	None	None	RhoA-IHC, qualitative only
35	PM45	COD: cardiac arrest	n/a	None	None	None	RhoA-IHC, qualitative only
57	PM46	COD: no notes available	n/a	None	None	None	RhoA-IHC, qualitative only

Eight cases with Hippocampal Sclerosis Type I [according to the International League Against Epilepsy (ILAE) classification system] and granule cell dispersion were analyzed using proteomics (E1–8, in gray). In addition to these cases, another ten surgical cases with MTLE and three post mortem normal cases were included in RhoA and Rac1 immunohistochemical and/or in situ hybridization studies. In situ hybridization studies using probes against CDC42, or RELN transcripts were performed on four cases (E1P, E122, E1, E3). Abbreviations: Carb, carbamazepine; COD, cause of death; Clob, clobazam; Dia, diazepam; Gaba, Gabapentin; GCD, granule cell dispersion; GG, ganglioglioma; HS, hippocampal sclerosis; Lam, Lamotrigine; Lev, Levetiracetam; MCD, malformation of cortical development; MFS, mossy fiber sprouting; OH, oligodendroglial hyperplasia in white matter; Ox, Oxcarbazepine; Pheny, Phenytoin; Pheno, Phenobarbitone; Preg, Pregabalin; Prim, Primidone; TS, temporal sclerosis; Tem, temapazem; Top, topiramate; Val, Sodium valproate; Zon, Zonisamide.

pathways were explored in established pathway databases, Kyoto Encyclopaedia of Genes and Genomes (KEGG), Reactome, and Wikipathways. *P*-values and adjusted *P*-values (corrected according to Bonferroni's method and false discovery rate)

were calculated by bioinformatics resources. For gene ontology annotation and enriched pathway analyses, the stringency of the criteria was set to high, and *P*-value cut-off was set at 0.01 and only pathways with four proteins of interests or more were presented. The dendrogram was constructed using Morpheus (Broad Institute[2]) and included hierarchical clustering based on Pearson correlation coefficient, and average linkage clustering (Meunier et al., 2007).

Other clinical details, including patients' epilepsy history and psychometry, were also reviewed and analyzed with proteomic data. Pre-operative MRI sequences, PET, EEG, video-telemetry, and psychometry had been carried out according to the epilepsy surgical protocols at the National Hospital of Neurology and Neurosurgery, and clinical findings were reviewed for each case.

Immunohistochemistry

Eighteen cases were included in RhoA, Rac1, and Cdc42 immunohistochemistry and/or *in situ* hybridization studies. Cases included eight MTLE cases submitted for proteomics, an additional six surgical MTLE with hippocampal sclerosis and GCD, four surgical MTLE with hippocampal sclerosis but no GCD, and three postmortem healthy controls (**Table 1**).

Five micrometer-thick formalin-fixed, paraffin-embedded sections from selected cases were examined histologically with Haematoxylin and Eosin, and Luxol Fast Blue stains. Routine automated and manual immunochemistry was performed using antibodies against neuronal nuclei (NeuN), glial fibrillary acidic protein (GFAP), non/phosphorylated neurofilament (SMI32, SMI31), myelin basic protein (SMI94), microtubule associated protein 2 (MAP2), zinc transporter 3 (ZnT3) calbindin, nestin (**Table 2**). Additional immunohistochemistry using anti-RhoA was performed manually using pretreatment and incubation procedures described in **Table 2**, and breast carcinoma tissue was used as a positive control (Ma et al., 2010). Negative controls where primary antibodies were omitted showed no specific labeling. A number of commercially-available antibodies against RhoA, RhoB and Cdc42 (Santa Cruz Biotechnology, Germany), RhoC and pan-Rac1 (Cell Signalling Biotechnology, UK) were also tested using formalin-fixed, paraffin-embedded human brain tissue, but no specific immunolabeling was obtained after applying a number of different antigen retrieval methods. These antibodies were excluded from further immunohistochemical studies.

In situ Hybridization

Five micrometer-thick formalin-fixed, paraffin-embedded sections from selected surgical cases were processed for *in situ* hybridization following supplier's instructions (Wang et al., 2019). Probes against human *RHOA, RAC1, CDC42*, and *RELN* mRNAs were used in conjunction with ready-to-use reagents from RNAscope® 2.5 HD Reagent Brown and Duplex kits (**Table 2**; Bio-Techne, Abingdon, UK). Positive probe control, *UBC*, and negative probe control, *dapB* transcripts, were performed on Hela cell tissue (positive tissue control) and formalin-fixed, paraffin-embedded surgical human brain tissue to ensure specificity of labeling prior to final studies. Labeled sections were counterstained with Gills I hematoxylin solution (VWR, UK) before coverslipped.

Image Analysis

Labeled sections were assessed qualitatively using a brightfield microscope (Nikon Eclipse 80i) and subsequently scanned at 40x magnification using the whole slide scanner, AxioScan.Z1 (Zeiss, Germany) to obtain high-quality digital images for quantitative analysis and data interpretation. All images were viewed and analyzed using the image analysis software, QuPath (Bankhead et al., 2017). Criteria for GCD: at present, there are no strict criteria to evaluate GCD, or to identify the boundaries amongst the granule cell layer and inner and outer molecular layers. In this study, the extent of GCD in each case was assessed by measuring the thickness of the granule cell layer along with the external and internal limbs on hematoxylin and eosin-stained, whole-slide images at 2.8x magnification. The curved region joining the internal and external limbs of GCL was not included. An average of 19 ± 2 measurements (mean ± SEM) with a mean interval of 400 ± 3 μm were made along the entire length of GCL in each case. Each line measurement was taken from the basal granule cell layer closest to CA4 to the furthest dispersed DGCs in the outer molecular layer. The length of each line was then divided into three groups: ≤120 μm (no GCD, DGCs within granule cell layer as previously reported in Blümcke et al., 2009), between 121 and 215 μm (moderate GCD, scattered DGCs in the inner molecular layer) and ≥216 μm (severe GCD, scattered, clusters or rows of DGCs in the outer molecular layer). The threshold of 215 μm was taken from the longest line measurement to the most dispersed cell minus 120 μm (granule cell layer) to get the thickness of the molecular layer and then divided by two to derive a mid-point to divide the inner and outer molecular layer (**Supplementary Material S1**). The frequency of lines in each measurement group was used to categorize the extent of GCD in each case.

Automated quantification of RhoA immunopositive labeling, and RhoA and Rac1-positive puncta from *in situ* hybridization studies were performed using QuPath. First, granule cell layer, inner and outer molecular layers spanning 120, 215 and 310 μm from the basal granule cell layer were annotated. The software was then trained to recognize hematoxylin-stained nuclei, positive labeled cells and puncta using positive cell and subcellular detection modules (Bankhead et al., 2017). The number of cells with RhoA-positive labeling and RhoA/ Rac1-positive puncta per μm^2, and the percentage of cells detected with RhoA immunolabeling and RhoA/ Rac1-positive puncta were recorded and compared between MTLE cases with or without GCD, three dentate regions and younger or older cohorts using non-parametric Mann–Whiney or Kruskal–Wallis tests in SPSS (IBM, USA; $P < 0.05$). Spearman correlations were performed to examine the relationship between quantitative measures and thickness of granule cell layer, age of onset or age at surgery ($P < 0.01$).

[2]https://software.broadinstitute.org/morpheus

TABLE 2 | Antibodies and protocols for RNA and immunohistochemical studies.

Antibodies/Probes Clone, Code	Immunogen or target epitope	Labeled cell or protein type	Pre-treatment (mins)	Antibody supplier, dilution, incubation time (mins) and temperature
Anti-NeuN A60, MAB377	Purified cell nuclei from mouse brain	Nuclei of most neurons, some proximal dendrites	ER1 (20)	Millipore; 1:2K, 15, RT
SMI31 801601	Phosphorylated epitope in neurofilament H and M	Neurons	H-3301 (12)	Sternberger; 1:500, ov, 4°C
SMI32 801707	Non-phosphorylated epitope in neurofilament H	Neurons	H-3301 (12)	Sternberger; 1:500, ov, 4°C
Anti-MAP2 HM-2, M4403	Rat microtubule-associated proteins	Neurons	H-3301 (12)	Sigma; 1:1,500, ov, 4°C
Anti-Calbindin D-28K, 300	Calbindin D-28k	Calbindin-expressing interneurons	H-3301 (12)	Swant; 1:10K, ov, 4°C
Anti-ZnT3 197–003	Recombinant protein of mouse ZnT3 (aa. 2–75)	Synaptic vesicle located zinc-transporter	H-3301 (12)	Synaptic Systems; 1:10K, ov, 4°C
SMI 94 SMI-94R	70–89 aa of human myelin basic protein	Myelinated fiber in white matter	ENZ1 (10)	DAKO; 1:2,000, 20, RT
Anti-Nestin 10C2, AB22035	150 aa recombinant fragment from human nestin conjugated to GST	Immature progenitors, glia, endothelial cells	H-3301 (12)	Abcam; 1:1K, ov, 4°C
Anti-GFAP Z0334	GFAP isolated from cow spinal cord	Astrocytes, some ependymal cells	ENZ1 (10)	DAKO; 1:2.5K, 20, RT
Anti-RhoA OSR00266W	A synthetic peptide from human Transforming protein RhoA conjugated to an immunogenic carrier protein	Small GTPase protein that regulates actin cytoskeleton in the formation of stress fibers, and cell division. Expressed in the cytoplasm of cells undergoing structural changes in preparation for migration	Protease (20, 37°C)	Thermo; 1:500, ov, 4°C
RHOA mRNA 416291	NM_001664.2. Probe region from 135 to 1796	Pretreatment 2 and 3*	BioTechne; 120, 40°C	
RAC1 mRNA 419851	NM_006908.4 Probe region from 1194 to 2256		Pretreatment 2 and 3*	BioTechne; 120, 40°C
CDC42 mRNA 502651	NM_044472.2 Probe region from 2 to 1091	Pretreatment 2 and 3*	BioTechne; 120, 40°C	
RELN mRNA 413051	NM_173054.2 Probe region from 4401 to 5340	Glycoprotein expressed by Cajal-Retzius cells	Pretreatment 2 and 3*	BioTechne; 120, 40°C

*Automated immunohistochemistry was performed using the Bond Max automated immunostainer and reagents (Leica, Milton Keynes, UK). *RNA detection was performed using the RNAscope patent assays system following the supplier's instruction. Abbreviations: aa, amino acids; Cdc42, Cell division control protein 42 homolog; GFAP, glial fibrillary acidic protein; K, thousands; MAP, microtubule-associated protein; NeuN, neuronal nuclei; ov, overnight; Rac1, Ras-Related C3 Botulinum Toxin Substrate 1; RhoA, Transforming protein RhoA or Ras homolog family member A; RT, room temperature. Antigen retrieval buffers: ENZ1, Leica Bond enzyme concentrate, and diluent; ER1, Leica Bond citrate-based buffer; ER2, Leica Bond EDTA-based buffer; H-3301, Vector's Tris-based buffer pH 9.0; H-3300, Vector's citrate-based buffer pH 6.0; SC, Sodium citrate buffer, pH 6.0. Suppliers: Abcam plc., Cambridge, UK; BD Transduction Lab., Oxford, UK; Bio-Techne, Abingdon, UK; DAKO, Cambridgeshire, UK; Millipore, Watford, UK; Sternberger, Maryland, US; Swant, Marly, Switzerland; Thermo Fisher Scientific, Hemel Hempstead, UK; Synaptic Systems, Goettingen, Germany.*

RESULTS

Granule Cell Pathology Observed in Cases Submitted for Proteomics

In MTLE cases with GCD, a thick band of NeuN-positive cells was observed in the dentate granule cell layer (**Figure 1A**). Two morphologies of NeuN-positive DGCs were noted: the basal population of DGCs located closer to CA4 was round and tightly packed with neighboring DGCs (basal DGCs), and a dispersed population of NeuN-positive DGCs with round or elongated soma with uni- or bipolar processes located in outer-granular and molecular layers of the hippocampus (dispersed DGCs). In the case of E6, the bilamination of the granule cell layer was observed, and a gap of approximately 130 μm measured from the bottom of the basal layer to the top of the dispersed layer was noted. No marked difference in NeuN-positive immunolabeling was noted between younger and older cohorts. In contrast, the granule cell layer in the hippocampus of four MTLE cases with no GCD (**Figure 1F**) and healthy post mortem controls contained round, tightly packed NeuN-positive cells, and no immunopositive cells were observed in the molecular layer. Quantitative measures of granule cell layer revealed a significantly thicker granule cell layer in MTLE cases with GCD than cases without GCD or healthy controls (P = 0.004; mean ± SEM, range; *cases with GCD* 133 ± 11 μm, 71–213 μm; *cases without GCD* 64 ± 10 μm, 34–82 μm; *healthy controls*; 70 ± 4 μm, 63–76 μm).

MAP2-positive cells were observed in the granule cell layer of all MTLE cases (**Figures 1B,G**). Numerous MAP2-positive processes were observed in the granule and molecular layers. Random short MAP2-positive processes were observed in the CA4 around a few large densely-labeled MAP2-positive cells. Calbindin-positive cells expression was observed in DGCs scattered throughout the outer-granule cell layer and molecular

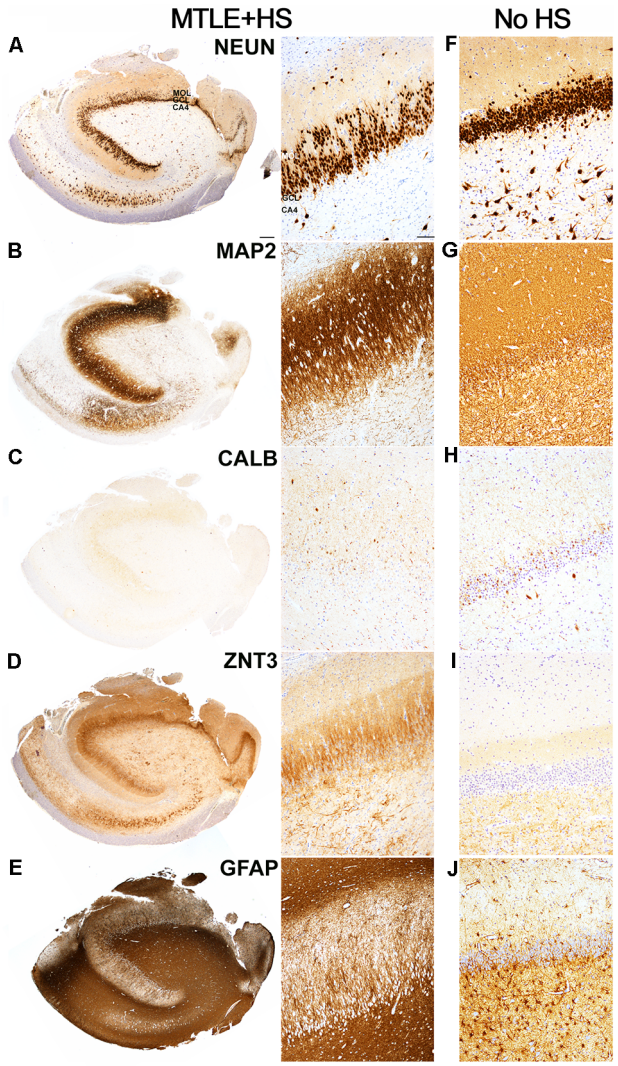

FIGURE 1 | Hippocampal pathology observed in an Mesial Temporal Lobe Epilepsy (MTLE) patient with Hippocampal Sclerosis and Granule Cell Dispersion. **(A)** NeuN-positive granule cells were observed in the granule cell layer of the hippocampal dentate gyrus. The number of dentate granule cells (DGCs) remained abundant despite marked loss of pyramidal neurons in the cornu ammonis (CA) 1, 3 and 4 subfields, which are typical features of Hippocampal Sclerosis Type 1 based on classification scheme established by the task force of International League against Epilepsy (ILAE; Blümcke et al., 2013). However, the majority of the NeuN-positive DGCs appeared to scatter in rows or clusters to the outer-granular layer and molecular layer (MOL), which is consistent with granule cell dispersion pathology. NeuN-positive pyramidal neurons were still observed in the CA2 region. **(B)** I MAP2-positive DGCs were observed in the granule cell layer. MAP2-positive DGCs had immunopositive fibers projected towards the molecular layer, and MAP2-positive labeling appeared to be stronger in the molecular layer than in the basal granule cell layer. MAP2-positive fibers of various lengths and a small number of MAP2-positive cells were observed in the CA4 region. **(C)** Calbindin immunoreactivity was observed in most, but not all, dispersed and elongated DGCs in the granule and molecular layer. In contrast, small, round basal DGCs were immunonegative for calbindin. An intense blush of granular calbindin-positive labeling was also observed in the molecular layer. **(D)** Intense ZnT3-positive labeling was observed in the molecular layer, particularly in the inner molecular layer. This is consistent with mossy fiber

(*Continued*)

FIGURE 1 | Continued
sprouting pathology in MTLE. Clusters of ZnT3-positive fibers were observed predominantly in the CA4 region. **(E)** The dense matrix of GFAP-positive fibers was observed in all CA regions. GFAP-positive radially-directed fibers extended between DGCs in the granule cell layer, and GFAP-positive cells were visible in the molecular layer. **(F–J)** Images showing the immunoreactivities of NeuN, MAP2, calbindin, ZnT3, and GFAP in the hippocampus of an MTLE patient with no remarkable hippocampal pathologies. Scale bars in **(A)** left 500 μm, and **(A)** right 50 μm.

layer of MTLE cases with GCD (**Figure 1C**). In cases with GCD, calbindin-positive dispersed DGCs had round cell bodies, and occasionally, calbindin-positive cells with long processes extending into the molecular layer were noted. Not all DGCs in the outer-granular layer were calbindin-positive, and the majority of basal DGCs in the sclerotic hippocampus were devoid of calbindin immunolabeling. In contrast, calbindin-positive DGCs were often observed in the granule cell layer of cases without GCD (**Figure 1H**). ZnT3-positive processes were observed in between DGCs in the granule cell layer and in the molecular layer and CA4 subfield of cases with GCD (**Figure 1D**). In cases without GCD, ZnT3 immunolabeling was primarily observed in CA4 (**Figure 1I**). GFAP immunolabeling was observed throughout the hippocampus of all cases, with more intense labeling detected in MTLE cases with GCD (**Figure 1E**) compared to cases without hippocampal sclerosis or GCD (**Figure 1J**), and healthy controls. DGCs in the granule cell layer were not immunopositive for GFAP, but GFAP-positive processes extended between DGCs in the granule cell layer, and individual GFAP-positive cells were observed in the molecular layer of cases with GCD. In cases with GCD, a very dense matrix of GFAP processes was observed in the CA4. In contrast, distinctive GFAP-positive cells were seen in the CA4 of cases without GCD (**Figure 1J**) and in healthy postmortem controls.

Proteomic Analysis

One-thousand eight-hundred and eighty-two proteins were identified in the proteomic analysis of eight patients with HS Type 1 and GCD (**Table 1**, E1–8). 29% of the extracted proteins were observed in the basal samples only, 17% in the dispersed samples only, and 54% of the proteins were observed in both samples (**Figure 2B**). 19% of identifiable proteins were observed in the younger cohort only, 28% in older samples only and the remaining proteins were found in both younger and older samples. Some similar changes in protein expression were observed between two cases in the younger cohort (E1 and E2), and amongst three older cases, E5, E6, E8 based on hierarchical clustering (**Figure 2C**).

Common neuronal markers such as MAP2, calbindin, and calretinin were detected in MTLE samples (**Figure 2D**). The protein abundance of MAP2, calretinin, and calbindin was significantly higher in dispersed and younger samples than basal and older samples. The quantity of MAP2 detected was higher than calbindin and calretinin in all samples as expected based on earlier immunohistochemical studies (**Figures 1B,C**). Astroglial (GFAP, vimentin, S100-B) and oligodendroglial

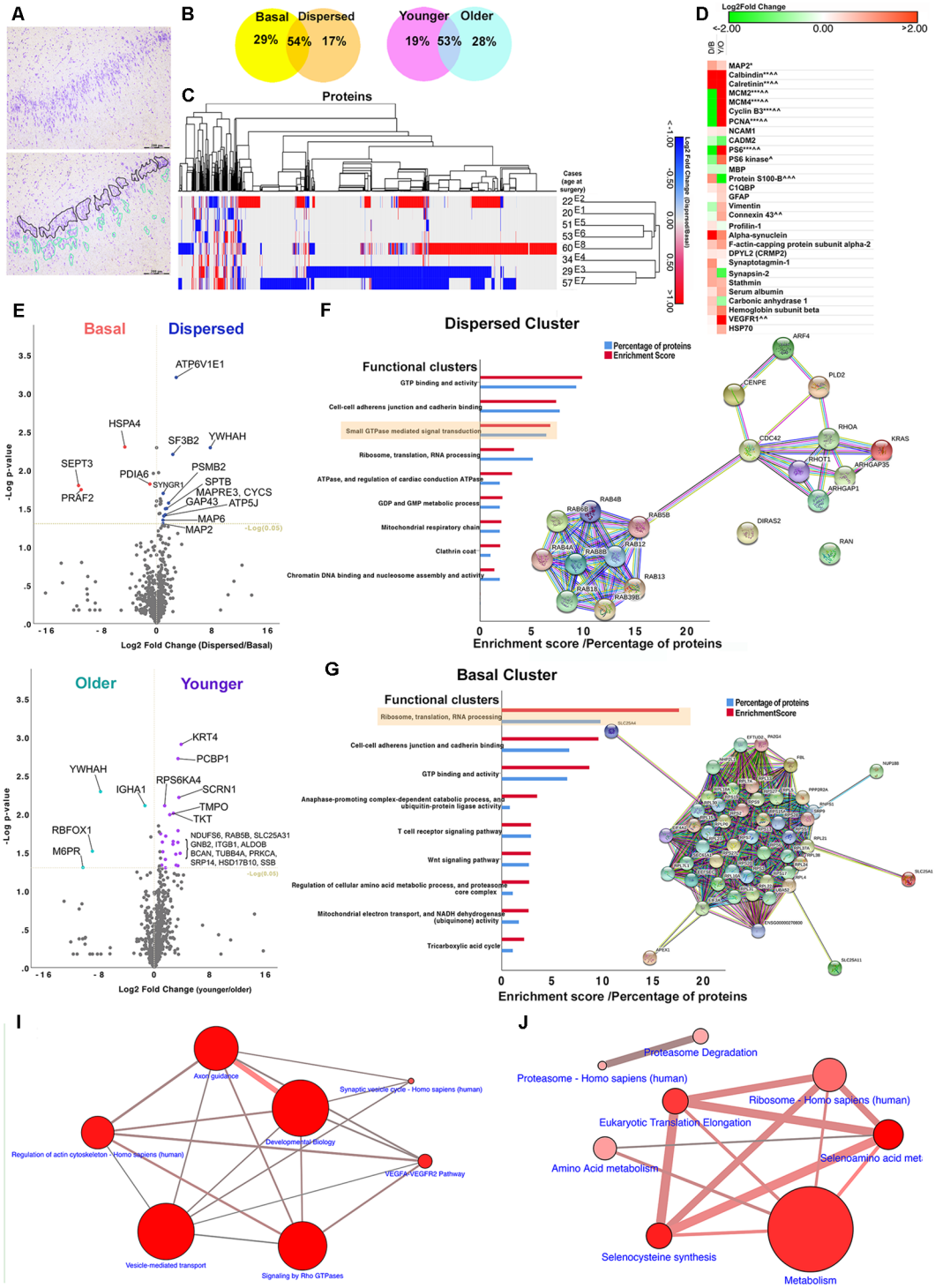

FIGURE 2 | Bioinformatics analyses. **(A)** An image of a toluidine-stained hippocampal tissue section showing marked granule cell dispersion pathology (top). DGCs were extracted from frozen hippocampal tissue sections during laser microdissection. Extracted DGCs (including nuclei and ~10 μm-perinuclear rim as cytoplasm) were divided into either basal or dispersed samples per case based on their location within the dentate gyrus. Basal samples contained DGCs located in the basal layer of the granule cell layer (black outline). These round DGCs were closely situated to neighboring DGCs, and they were aligned along the border of CA4 and granule cell layer. Dispersed samples contained a mixture of round and elongated DGCs located ectopically, in rows or clusters in the outer-granular, inner and outer molecular layers (green outline). Individual, small, round nuclei scattered in the dentate gyrus, sometimes in close proximity to DGCs, were likely to glial cells, and therefore these cells were avoided where possible. **(B)** Finding from proteomic studies show that more than 50% of the identified proteins were shared between

(*Continued*)

FIGURE 2 | Continued
basal and dispersed samples and between younger (<35 years) and older cohorts (<50 years). Less than one-third of the identified proteins were uniquely detected in basal, dispersed, younger and older samples. **(C)** A dendrogram showing hierarchical clustering of all differentially expressed proteins in eight MTLE cases with GCD. The pattern of protein changes between dispersed and basal samples was more similar between cases E1 and E2 (younger cohort) and E5, E6, and E8 (older cohort). **(D)** Heat map showing logarithmic-2 fold change between dispersed and basal samples (D/B), or younger and older cohorts (Y/O) of selected proteins expressed in neuronal (MAP2, calbindin, calretinin), glial (GFAP, S100-B, MBP, connexion 43), vascular (VEGFR), immature cell (vimentin) and proliferative populations (MCM2, MCM4, PCNA, cyclin B3), or are proteins associated with cytoskeletal (profiling-1, alpha-synuclein, f-actin capping protein, DPYL2, stathmin) and synapse remodeling (synaptotagmin-1, synapsin-2), mTOR pathway (PS6, PS6 kinase), neurogenic niches (NCAM1, CADM2), vascular changes (carbonic anhydrase 1, hemoglobin) and inflammation (C1QBP, HSP70). Keys: * or ^ significantly overexpressed proteins ($P < 0.05$), **proteins found in dispersed samples of GCD cases only, ***proteins found in basal samples of GCD cases only, ^^proteins only found in younger cohort only, ^^^proteins found in older cohort only. Abbreviations: C1QBP, complement component 1Q subcomponent-binding protein; DPYL2, dihydropyrimidinase-related protein 2; GFAP, glial fibrillary acidic protein; HSP70, heat shock proteins; MAP2, microtubule-associated protein 2; MBP myelin binding protein; MCM2, minichromosomal maintenance 2; NCAM1, neural cell adhesion molecule 1; PCNA, proliferating cell nuclear antigen; PS6 ribosomal protein S6; VEGFR vascular endothelial growth factor receptors. **(E,H)** Volcano plots showing logarithmic-2 fold change against –log *P*-value for proteins that were expressed in both dispersed and basal samples **(E)** or in both younger and older cohorts **(H)**. Significantly differentially expressed proteins that showed over the 1.5-fold change were highlighted in the plots ($P < 0.05$). **(F,G)** The abundance of each protein was compared between basal and dispersed samples, and between younger and older cohorts. Proteins that were uniquely expressed in one group only, and proteins that were significantly expressed by 1.5-fold than comparative group (fold change >1.5, $P < 0.05$) generated the Dispersed, Basal, Younger and Older clusters. Each cluster was submitted to bioinformatics platforms for Gene Ontology and Pathways analyses. Top functional annotation clusters based on Gene Ontology, Uniprot keywords, and sequences and INTERPRO terms for proteins in the Dispersed **(F)** and Basal clusters **(G)** were listed ($P < 0.01$; also refer to **Supplementary Material S3**). The enrichment scores generated by bioinformatics platforms and the percentage of proteins submitted that were associated with each functional annotation cluster are illustrated. Network maps show the connections between proteins in small GTPase mediated signal transduction **(F)** and ribosomes annotation clusters **(G)**. **(I,J)** Proteins in the Dispersed and Basal clusters were significantly involved in a number of pathways ($P < 0.01$; also refer to **Supplementary Material S4**). The size of the circle represents the number of proteins submitted that were involved in the pathways. The thickness of connections refers to the number of proteins that belongs to both connecting pathways.

markers (Myelin Basic Protein, MBP) were also detected in all samples, consistent with immunohistochemical findings (**Figure 1E**). The expression of GFAP was comparable between basal and dispersed samples and was slightly higher in younger than older samples; of interest, the expression of vimentin, expressed in immature astrocytes, was predominantly observed in basal and younger samples (**Figure 2D**) in keeping with our previous studies (Liu et al., 2018). The expression of connexion 43, a gap junction protein expressed in astrocytes, was similar to the expression of GFAP. Common microglial-specific proteins including TREM2, LST1, HLA-DRA, SP11, MMP9 were not found in our samples, but complement component 1q subcomponent binding protein (C1QBP), a protein found to be highly expressed in microglia around site of lesion in a recent animal study (Barna et al., 2019), was found to be expressed in both dispersed and basal samples. We did not detect common markers of neural progenitors or neuroblasts including SOX2, PAX6, TBR1, TBR2, and DCX; however, a higher abundance of cell adhesion molecule 2 (CADM2), a synapse-associated protein found in subventricular neurogenic niche (Lee et al., 2012; Frese et al., 2017), as well as a number of cell cycle markers (MCM2, PCNA, Cyclin B3) were found in higher amount in the basal DGCs than dispersed DGCs in cases with GCD (**Figure 2D**). Neural cell adhesion molecule 1 (NCAM) was also detected in dispersed samples of cases with GCD. Together these findings suggest that apart from DGCs and astroglial cell types, minimal level of microglia and neural progenitor cells were included in our capture. A number of proteins involved in actin and cytoskeleton remodeling including profilin-1 and 2, alpha-synuclein, f-actin capping proteins, dihydropyrimidinase-related protein 2 (also known as CRMP2), and synapse proteins such as synaptotagmin-1 and synapsin-2, were identified in dispersed and younger samples at a higher level than in basal and older samples. The detection of serum albumin, carbonic anhydrase 1 and hemoglobin subunits was noted in all samples, possibly due to increased permeability of blood brain barrier in the hippocampus of patients with MTLE.

Volcano plots in **Figures 2E,H** highlighted the most significantly differentially-expressed proteins between dispersed and basal samples, and between younger and older cohorts respectively. Proteins uniquely expressed in dispersed samples, and proteins significantly displaying over 1.5-fold change in dispersed compared to basal samples (**Figure 2E**; **Supplementary Material S2**) were first submitted to gene ontology and pathway bioinformatics analyses (Dispersed cluster, 330 proteins). The top functional annotation clustering based on Gene Ontology, Uniprot keywords, and sequences, and INTERPRO terms were GTP-binding and activity (enrichment score, 10; $P = 3.67 \times 10^{-8}$), cell to cell adhesion (enrichment score, 7; $P = 2.61 \times 10^{-6}$), and small GTPase-mediated signal transduction (enrichment score, 7; $P = 5.60 \times 10^{-4}$); **Figure 2F** and **Supplementary Material S3**). Under the functional clustering of small GTPase-mediated signal transduction, a number of proteins in the Ras homolog (Rho) GTPase families such as RhoA, Rac1, Cdc42 and ARGAP1, and ARGAP35 were identified (**Table 3** and **Supplementary Material S5**). Key pathways associated with differential proteins in the Dispersed cluster were related to cellular migration and actin cytoskeletal remodeling, including signaling by Rho GTPases pathway (R-HSA194315; $P = 1.02 \times 10^{-6}$), axon guidance (R-HSA422475; $P = 1.25 \times 10^{-6}$), regulation of actin cytoskeleton (K-HSA04810; $P = 1.01 \times 10^{-4}$), and vesicle-mediated transport (R-HSA5653656, $P = 9.29 \times 10^{-7}$; **Figure 2I** and **Supplementary Material S4**). Rho GTPases are small GTPases that regulate cytoskeletal dynamics and cell migration, which maybe of relevance to abnormal migration of DGCs in GCD. The signaling by Rho GTPases pathway shared common proteins with other pathways related to cytoskeletal dynamics as illustrated in **Figure 2I**. Proteins detected in basal samples only, and proteins that were significantly overexpressed in basal samples by at

TABLE 3 | Proteins in the Dispersed cluster that were involved in signaling by the Rho GTPases pathway (Reactome, R-HSA194315; $P = 4.68 \times 10^{-9}$).

Entry ID	Gene	Protein
P60953	CDC42	Cell division control protein 42 homolog
E7EVJ5	CYFIP2	Cytoplasmic FMR1-interacting protein 2
Q7L576	CYFIP1	Cytoplasmic FMR1-interacting protein 1
F8W7L3	A2M	Alpha-2-macroglobulin
Q12802	AKAP13	A-kinase anchor protein 13
H0YE29	ARHGAP1	Rho GTPase-activating protein 1
Q9NRY4	ARHGAP35	Rho GTPase-activating protein 35
I3L4C2	BAIAP2	Brain-specific angiogenesis inhibitor associated protein 2
P11274	BCR	Breakpoint cluster region protein
A0A087X0P0	CENPE	Kinesin-like protein Dispersed
G3XAM7	CTNNA1	Catenin-alpha-1
P78352	DLG4	Disks large homolog 4
Q99880	HIST1H2BL	Histone H2B type 1-L
Q15691	MAPRE1	Microtubule-associated protein RP/EB family member 1
Q9Y2A7	NCKAP1	Nck-associated protein 1
Q9NZQ3	NCKIPSD	NCK-interacting protein with SH3 domain
P35080	PFN2	Profilin-2
P62140	PPP1CB	Serine/threonine-protein phosphatase PP1-beta catalytic
C9J9C1	PPP2R1A	Serine/threonine-protein phosphatase 2A 65 kDa regulatory subunit A
P63000	RAC1	Ras-related C3 botulinum toxin substrate 1
C9JNR4	RHOA	Transforming protein RhoA/ Ras homologous family member A
P62745	RHOB	Rho-related GTP-binding protein RhoB
Q8IXI2	RHOT1	Mitochondrial Rho GTPase 1
P31947	SFN	14–3–3 protein sigma
O43295	SRGAP3	SLIT-ROBO Rho GTPase-activating protein 3
A2IDB2	YWHAH	14–3–3 protein eta

least 1.5-fold compared to dispersed samples (**Figure 2E** and **Supplementary Material S2**) were subsequently submitted to gene ontology and pathway enrichment analyses (Basal cluster; 555 proteins). The top functional annotation clustering included proteins involved in ribosomes, translation and RNA processing (enrichment score, 18; $P = 1.79 \times 10^{-14}$), cell-cell adherens (enrichment score, 10; $P = 1.93 \times 10^{-8}$), GTP binding (enrichment score, 9; $P = 4.31 \times 10^{-7}$), ubiquitin-protein ligase activity (enrichment score, 4; $P = 4.926 \times 10^{-2}$), and regulation of amino acid metabolic processes and proteasome activity (enrichment score, 3; $P = 2.07 \times 10^{-2}$; **Figure 2G** and **Supplementary Material S3**). The interactions between proteins clustered under ribosomes, translation and RNA processing are shown as a network map in **Figure 2G**. Pathways associated with Basal cluster were predominantly related to metabolism (R-HSA1430728, $P = 2.53 \times 10^{-26}$), including amino acid (WP3925, $P = 234 \times 10^{-5}$) and selenocysteine metabolisms (H-HSA2408557, $P = 1.71 \times 10^{-24}$), and electron transport chain (WP111, $P = 4.73 \times 10^{-3}$), and ribosomes (K-HSA03010, $P = 5.00 \times 10^{-13}$), translational mechanisms (R-HSA156842, $P = 2.90 \times 10^{-24}$), and proteasomal degradation (WP111, $P = 4.73 \times 10^{-3}$; **Figure 2J** and **Supplementary Material S4**).

Immunohistochemical and *in situ* Hybridization Using Markers Against Rho GTPases

Bioinformatics analyses revealed a number of proteins in the signaling by Rho GTPases pathway either uniquely expressed or upregulated in dispersed samples of MTLE cases with GCD. To further investigate the expression of Rho GTPases, immunohistochemistry and *in situ* hybridization using antibodies and probes against RhoA, Rac1 and Cdc42 protein and mRNAs respectively were performed on surgical, formalin-fixed, paraffin-embedded, hippocampal tissue from cases submitted to proteomics, and additional surgical MTLE cases with or without GCD. Post mortem hippocampal tissue from three healthy donors was also included for qualitative assessment.

In cases without GCD, the majority of DGCs in the granule cell layer were immunonegative for RhoA (**Figures 3A,A′**). In contrast, cases with GCD had numerous RhoA-immunopositive DGCs in the outer-granule and molecular layers. RhoA-immunopositive DGCs in the granule cell layer generally had a large, round nucleus surrounded by a thin, perinuclear "ring" of immunopositive labeling, or a "cone" of localized RhoA immunolabeling at one end of the cell soma, usually facing either towards the molecular layer or CA4 region (**Figures 3B,3B′,3C,3C′**). Occasionally, RhoA-positive cells in single-chain formation near vascular structures were observed (**Figures 3C,C′**). Most RhoA-positive cells in the molecular layer had an elongated cell soma with protruding uni- or bipolar processes. In a case with a bilaminar granule cell layer (E6), most DGCs in the basal granule cell layer were devoid of RhoA immunolabeling (**Figure 3D**), while most DGCs in the second granule cell layer had distinct RhoA immunoreactivities in one or bipolar ends of the cell soma (**Figures 3D′,D″**). Quantitative studies revealed a significantly higher density of RhoA-positive cells and a higher percentage of cells expressing RhoA in the granule and molecular layer of MTLE cases with GCD than without GCD (mean ± s.e.m; *GCL*, GCD 44 ± 3%, no GCD 23 ± 6%, $P = 0.035$; *IML*, GCD 56 ± 3%, no GCD 14 ± 3%, $P = 0.001$; *OML* GCD 27 ± 5%, no GCD 10 ± 3%, $P = 0.008$; **Figure 3E** and data in **Supplementary Material S6**). In cases with GCD, a higher percentage of cells expressing RhoA were detected in the inner molecular cell layer than the granule cell layer and the outer molecular layer (IML-GCL, $P = 0.026$; IML-OML, $P = 0.003$; **Figure 3E**). In contrast, the percentage of RhoA-positive cells detected were not significantly different between regions in cases without GCD. No significant difference in density or percentage of cells expressing RhoA was noted between younger and older cohorts. A probable relationship was observed between the percentage of cells expressing RhoA and age of surgery ($r_s = 0.390$, $P = 0.014$; **Figure 3F**), and the mean thickness of granule cell layer ($r_s = 0.675$, $P < 0.001$; **Figure 3G**).

In situ hybridization studies using probes against *RHOA* and *RAC1* mRNA sequences revealed fine nuclear and perinuclear puncta in DGCs in the granule and molecular layers of all cases (**Figures 4A–D**). *RHOA*-positive and *RAC1*-positive puncta were also observed in the neuropil, likely representing processes of DGC which were not visible in the sections. In cases with GCD,

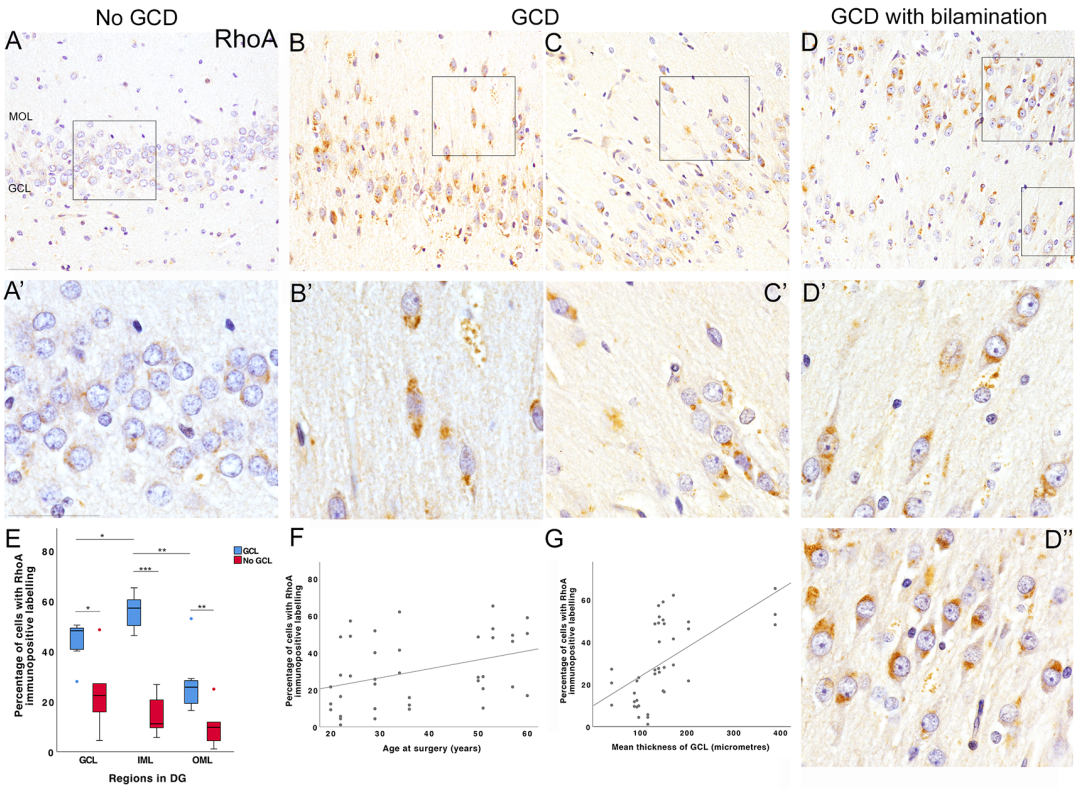

FIGURE 3 | RhoA immunohistochemical studies. **(A)** Most DGCs were immunonegative for RhoA in the granule cell layer of an MTLE case without GCD (E5P). Occasionally, weak perinuclear RhoA-positive labeling was observed in a few DGCs (**A'**, *higher magnification of area outlined in* **A**). No DGCs were observed in the molecular layer of cases without GCD. **(B,C)** Numerous DGCs with intense RhoA immunolabeling were observed in the granule and molecular cell layer of two MTLE cases with GCD (E14, **B**; E3, **C)**. In some DGCs, RhoA immunolabeling was detected in one polar end of the DGC soma directed towards the CA4 or molecular layer. A number of RhoA-positive cells in the outer-granular and molecule layer had elongated soma with uni- or bipolar processes **(B',C')**. In bipolar DGCs, RhoA immunolabeling was observed at one or both apices of cell soma. Occasionally, RhoA-positive DGCs were found to align single line formation near blood vessels **(C')**. In contrast, most basal DGCs closest to the CA4 border had no or minimal RhoA immunolabeling. **(D)** Bilamination of the granule cell layer was observed in a case with MTLE and GCD E6. In this case, most DGCs in the basal granule cell layer appeared to be devoid of RhoA immunolabeling. In contrast, nearly all DGCs in the outer-granule layer **(D')** and second granule cell layer expressed RhoA **(D")** either in one or both ends of the cell. The majority of RhoA-positive cells in the second granule cell layer had stronger and distinct RhoA immunoreactivities at the end directed towards the molecular layer. **(E)** A boxplot showing that the percentage of cells with RhoA-positive labeling in the dentate gyrus of MTLE cases with GCD (blue) or without GCD (red). A significantly higher percentage of cells expressing RhoA was observed in granule and molecular layers of cases with GCD than cases without GCD (GCL, $P = 0.035$; IML, $P = 0.001$; OML, $P = 0.008$; see **Supplementary Material S6**). In cases with GCD, the percentage of cells with RhoA immunolabeling was significantly higher in the inner molecular layer than the granule cell ($P = 0.026$) and outer molecular layer ($P = 0.003$). **(F,G)** The percentage of cells expressing RhoA in the dentate gyrus weakly correlated with the age at surgery of MTLE patients ($r_S = 0.390$, $P = 0.014$; **F**) and the mean thickness of granule cell layer ($r_S = 0.675$, $P < 0.001$; **G**). Abbreviations: DG, dentate gyrus; GCL, granule cell layer; IML, inner molecular layer; OML, outer molecular layer. Scale bars, 50 μm. $^*P \leq 0.05$, $^{**}P \leq 0.01$, $^{***}P \leq 0.001$.

a high number of *RHOA*-positive and *RAC1*-positive puncta clustered at the polar ends of the DGC soma, particularly in DGCs situated in the molecular layer (**Figures 4B,D**). Some smaller hematoxylin-stained glial cells were associated with none or only a few numbers of *RHOA*-positive or *RAC1*-positive puncta. Further immunohistochemical and *in situ* hybridization double-label studies showed that glutamine synthetase-labeled astrocytes did not have *RHOA*-positive or *RAC1*-positive puncta (**Supplementary Material S7**).

Quantitative analyses showed that a higher density of cells with *RAC1*-positive puncta than *RHOA* was observed in MTLE with GCD (mean ± SEM, *RAC1* $2.05 \times 10^{-3} \pm 2.15 \times 10^{-4}$ per μm^2; *RHOA* $1.74 \times 10^{-3} \pm 2.71 \times 10^{-4}$; $P = 0.017$), which was not observed in cases without GCD (*RAC1* $1.72 \times 10^{-3} \pm 2.27 \times 10^{-4}$ per μm^2; *RHOA* $1.25 \times 10^{-3} \pm 1.81 \times 10^{-4}$; $P > 0.05$). In all cases, a significantly higher density of cells with *RHOA*-positive puncta was observed in the granule cell layer than outer molecular layer (GCD, GCL $2.83 \times 10^{-3} \pm 5.61 \times 10^{-4}$ per μm^2, OML $8.97 \times 10^{-4} \pm 1.01 \times 10^{-4}$, $P = 0.004$ (blue bars); no GCD, GCL $2.11 \times 10^{-3} \pm 2.23 \times 10^{-4}$ per μm^2, OML $7.24 \times 10^{-4} \pm 6.94 \times 10^{-5}$, $P = 0.004$ (red bars); **Figure 4E** and **Supplementary Material S6**). A significantly higher density of *RHOA*-positive puncta was observed in the granule cell layer than inner molecular layer in cases without GCD (GCL $2.11 \times 10^{-3} \pm 2.23 \times 10^{-4}$ per μm^2, IML $9.25 \times 10^{-4} \pm 9.15 \times 10^{-5}$, $P = 0.023$), but not in cases with GCD (GCL $2.83 \times 10^{-3} \pm 5.61 \times 10^{-4}$ per μm^2, IML

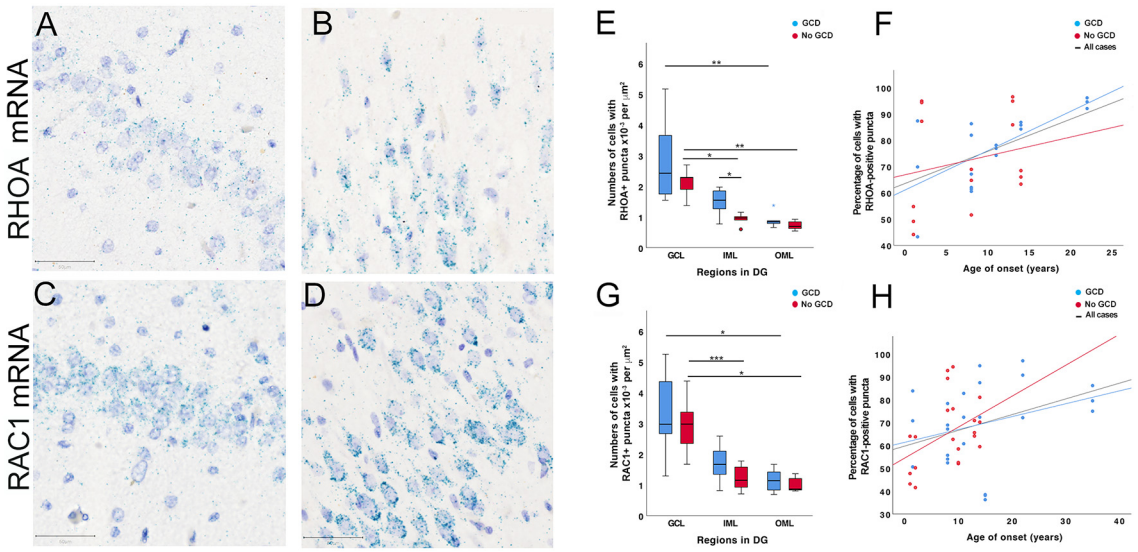

FIGURE 4 | *RHOA* and *RAC1 in situ* hybridization studies. **(A–D)** *RHOA* and *RAC1*-positive puncta (cyan) were observed in the dentate gyrus of MTLE cases without GCD **(A,C)** and cases with GCD **(B,D)**. The majority of positive puncta were found in or around hematoxylin-stained nuclei (purple) in the granule and molecular cell layers. In MTLE cases with GCD, most *RHOA* and *RAC1*-positive puncta were localized peri-nuclearly and at opposite ends of each nucleus **(B,D)**. Many *RAC1*-positive puncta were also observed in the proximal portion of uni- or bipolar processes **(D)**. A number of *RHOA* and *RAC1*-positive puncta were also observed in the neuropil. **(E,G)** In cases without GCD, the density of cells with *RHOA and RAC1*-positive puncta was higher in the granule cell layer than inner (*RHOA* $P = 0.023$; *RAC1* $P = 0.001$) and outer molecular layer (*RHOA* $P = 0.004$; *RAC*1 P = 0.018). In cases with GCD, significantly higher densities of cells with *RHOA* and *RAC1*-positive puncta were observed in the granule than outer molecular layers (*RHOA* $P = 0.004$; *RAC1* $P = 0.017$), but not in the inner molecular layer ($P > 0.05$). The density of cells expressing *RHOA* mRNAs in the inner molecular layer was significantly higher in cases with GCD than cases without GCD ($P = 0.05$), but this difference was not observed in the granule cell layer or outer molecular layer ($P > 0.05$). **(F,H)** The percentage of cells with *RHOA* or *RAC1*-positive puncta weakly correlated with age of onset in patients with GCD (*RHOA*, $r_s = 0.439$, $P = 0.011$; *RAC1*, $r_s = 0.295$, $P = 0.049$), but not in patients without GCD. Abbreviations: DG, dentate gyrus; GCL, granule cell layer; IML, inner molecular layer; OML, outer molecular layer. Scale bars, 50 µm. $^*P \leq 0.05$, $^{**}P \leq 0.01$, $^{***}P \leq 0.001$.

$1.49 \times 10^{-3} \pm 1.84 \times 10^{-4}$, $P > 0.05$), indicating that the level of *RHOA* gene expression was more similar between granule and inner molecular layers in cases with GCD than in cases without GCD. A significantly higher density of *RHOA*-positive puncta was observed in the inner molecular layer of cases with GCD than without GCD (GCL $1.49 \times 10^{-3} \pm 1.84 \times 10^{-4}$ per μm^2 IML; no GCD IML $9.25 \times 10^{-4} \pm 9.15 \times 10^{-5}$, $P = 0.05$). In all cases, the densities of cells with *RAC1*-positive puncta were higher in granule cell layer than the outer molecular layer (GCD, $3.31 \times 10^{-3} \pm 4.47 \times 10^{-4}$ per μm^2 GCL, $1.14 \times 10^{3} \pm 1.24 \times 10^{-4}$ OML, $P = 0.017$; no GCD, $2.92 \times 10^{-3} \pm 3.47 \times 10^{-4}$ per μm^2 GCL, $1.01 \times 10^{-4} \pm 8.99 \times 10^{-5}$ OML, $P = 0.018$, **Figure 4G**). A significantly higher density of *RAC1*-positive puncta was noted in the granule cell later compared to inner molecular layer in cases without GCD (GCL $2.92 \times 10^{-3} \pm 3.47 \times 10^{-4}$ per μm^2, IML $1.23 \times 10^{-3} \pm 1.62 \times 10^{-4}$, $P = 0.001$), but not in cases with GCD (GCL $3.31 \times 10^{-3} \pm 4.47 \times 10^{-4}$ per μm^2, IML $1.70 \times 10^{-3} \pm 2.06 \times 10^{-4}$, $P > 0.05$). The percentage of cells with *RHOA*-positive and *RAC1*-positive puncta weakly correlate with the age of onset (*RHOA*, $r_s = 0.439$, $P = 0.011$, **Figure 4F**; *RAC1*, $r_s = 0.294$, $p = 0.049$, **Figure 4H**).

In situ hybridization using probes against *CDC42* and *RELN* mRNAs were also performed on surgical cases, and labeling was qualitatively assessed as only four cases were investigated. The regional distribution and density of cells with *CDC42*-positive puncta were similar to *RHOA*-positive and *RAC1*-positive positive labeling. *RELN*-positive puncta were not observed in any of these cases.

DISCUSSION

We investigated the proteome of basal and dispersed DGCs in the dentate gyrus of pharmacoresistant MTLE patients with hippocampal sclerosis to explore the neurodevelopmental pathomechanisms of GCD. We have identified differences in the proteomes between basal and dispersed populations of DGCs in the hippocampus of patients with MTLE and GCD. Specifically, dispersed DGCs in cases with GCD highly expressed mature neuronal markers, MAP2, calbindin, and calretinin as well as a number of Rho GTPases and proteins associated with cell migration, cytoskeleton, and synapse remodeling. These results were further supported by findings from immunohistochemical and *in situ* hybridization studies, where a significantly higher density and percentage of cells expressing RhoA mRNA and protein was observed in the dentate gyrus of cases with GCD than cases without GCD. The expression of RhoA protein was localized to the opposite ends of uni- or bipolar of DGCs in the molecular layer of cases with GCD. Consistently, the mRNAs of *RHOA, RAC1*, and *CDC42* were also found in the same intracellular region of DGCs, while *RAC1* mRNA was also detected in the proximal portion of processes. These

findings provide evidence supportive of DGCs undergoing neurodevelopment processes relating to cellular migration, which may contribute to the abnormal dispersion of DGCs in patients with MTLE.

Comparison With Previous Human Proteomics Studies

The current study reported on proteins identified from the dentate gyrus of eight patients with refractory MTLE and HS Type I and GCD (or Type II granule cell pathology according to Blümcke et al., 2009) using protocols established in our previous proteomic study (Liu et al., 2016). There is no specific marker for DGCs in the human brain (unlike Prox1 or NeuroD in rat brains), but other neuronal markers such as MAP2 and calbindin, which are expressed by granule cells, were detected at high levels in our immunohistochemical and proteomic studies. Our samples did not capture microglial cell contaminants, but astroglial markers (GFAP, S100-B) and myelin basic protein were detected, and this is consistent with the intimate intermingling of radial glial and myelinated axons in the dentate gyrus in MTLE with hippocampal sclerosis.

Our proteomic studies did not include surgical or post mortem healthy controls as seen in most previous human proteomic studies of MTLE. This is because (i) surgically-resected "normal" hippocampal tissue from healthy individuals is not available for research; (ii) the process of protein extraction for proteomic analyses is different for surgical and post mortem brain tissue so one standardized protocol cannot be applied to both type of tissue; and (iii) autopsy tissue is likely to be affected by post mortem processes such as rapid protein degradation (especially for tubulins, intermediate filaments, high motility group box protein-1, proapolioprotein, hemoglobin and mutant derivative (He et al., 2006) which may influence our findings. In view of these arguments, we compared the protein profile of basal and dispersed DGCs as well as between younger (<35 years) and older groups (>50 years) to avoid the detection of changes associated with tissue type.

The differential expression of certain proteins in our study is generally consistent with findings from previous human MTLE studies. There is good agreement amongst human TLE proteomics studies that most proteins related to metabolism are significantly upregulated in epilepsy compared to archival normal brain hippocampal samples (Eun et al., 2004; Yang et al., 2006; Persike et al., 2012, 2018). This may be because the generation of epileptiform activity, or response to such activity, consumes a large amount of energy, and rapid glycolysis and oxidative phosphorylation are necessary to fulfill energy demands in the epileptic human brain (Kovac et al., 2017). Consistently, we found 15% of proteins extracted from our epilepsy samples were involved in metabolic processes, and up to 8% of proteins in the Basal cluster were involved in the tricyclic acid cycle and mitochondrial electron chain (**Figure 2G** and **Supplementary Material S4**).

A key finding in this study is the identification of proteins in dispersed DGCs of cases with GCD specifically involved in axonal guidance (including beta-spectrin, growth-associated protein 43, postsynaptic density protein 95, profilins), regulation of actin cytoskeleton (cytoplasmic FMR1-interacting proteins, WAVE complex proteins), cytoskeletal and synaptic remodeling (DPYL2, alpha-synuclein, synaptotagmin 1, synapsin II, and stathmin1), as well as Rho GTPases, signaling (RhoA, Cdc42, Rac1, brain-specific angiogenesis inhibitor, Rho GTPases activating proteins; **Table 3**). These processes are active during neurodevelopment and in neurogenic niches in the adult mammalian brain (Lee et al., 2012; Frese et al., 2017). Our findings are consistent with previous human proteomic studies which have reported increased expression of DPYL2 (also known as collapsing response mediator protein 2, CRMP2), a cytoplasmic phosphoprotein that binds microtubules and promotes neurite outgrowth during neurogenesis and neuronal migration (Inagaki et al., 2001; Fukata et al., 2002), in the hippocampus of MTLE patients compared to controls (Persike et al., 2012, 2018; Keren-Aviram et al., 2018). The CRMP2 antagonist, lacosamide, is an antiepileptic drug often used in patients with drug-resistant epilepsy (Kelemen and Peter, 2010).

GCD and Neurogenesis: Evidence?

During neurodevelopment, new DGCs migrate from the dentate ventricular zone to the granule cell layer to form an "outside-in" dentate gyrus, where the outer-granular cells are the oldest (and showing earliest NeuN immunoreactivity), and DGCs located in the inner layer (basal granule cells) are the youngest (Altman and Bayer, 1990; Seress et al., 2001). A secondary dentate matrix is formed at gestation week (GW) 10–11 which will later become the subgranular zone that supports ongoing neurogenesis that continues to adulthood so there is also an outside-in gradient for neurogenesis (Cipriani et al., 2017). Previous studies have reported that the dentate neurogenesis is still active postnatally at 1 year of age, but proliferative and neurogenic activities decline sharply between 7–13 years and argued to be minimally detected in adulthood (Sorrells et al., 2018) even in the brains of adult patients with MTLE (Blümcke et al., 2001; Cipriani et al., 2017). The level of hippocampal neurogenesis in the normal and diseased adult human brain is still controversial because the detection of neural progenitor cells and new neurons in adult human brains depends on tissue quality and the immunohistochemical protocols employed in studies (Sorrells et al., 2018; Moreno-Jiménez et al., 2019). Considering that the level of neurogenesis is lower in adults than children, it is more plausible that new DGCs born in early childhood contributes to GCD. Although our current findings did not capture immature neural progenitor cell proteins (SOX1, SOX2, TBR1, TBR2, PAX6), or neuroblast proteins (DCX), even in the youngest MTLE patients with age at surgery of 20 and 22 years, we did detect a number of proliferative cell cycle proteins, minichromosome maintenance protein 2 (MCM2), proliferative cell nuclear antigen (PCNA) and cyclin B3, and immature glial progenitor protein, vimentin, in the basal DGCs of younger MTLE cases and not in the dispersed DGCs, thus providing some supporting evidence of neuroplasticity. Our previous immunohistochemical study found a number of proliferative cells expressing MCM2 in the granule cell layer of patients with MTLE (Thom et al., 2005). In addition, we detected

a high abundance of neural cell adhesion molecule 1 in dispersed DGCs of younger MTLE cases. In adult animal neurogenesis studies, calretinin is transiently expressed in newborn DGCs before calbindin (Brandt et al., 2003). Calretinin was detected in the dispersed samples of this study, however as we know marked re-organization of calretinin neurons and networks occurs in the hippocampus of patients with MTLE and hippocampal sclerosis (Thom et al., 2012), calretinin may not be a reliable marker of adult neurogenesis in this context. Calbindin D28K was only detected in dispersed DGCs in our study, which is consistent with previous studies that reported reduced expression of calbindin in basal granule cell layer of patients with MTLE (Maglóczky et al., 1997; Arellano et al., 2004; Abrahám et al., 2009, 2011; Martinian et al., 2012).

We did not detect reelin, a glycoprotein secreted by Cajal-Retzius cells to regulate the migration of DGCs during neurodevelopment, in our samples. This is confirmed in subsequent *in situ* hybridization studies using a probe against *RELN* mRNA, where no positive labeling was observed in the hippocampus of MTLE cases with GCD. This finding is consistent with previous studies that have reported low levels of *RELN* mRNA in MTLE patients with hippocampal sclerosis and GCD (Haas et al., 2002; Frotscher et al., 2003; Kobow et al., 2009). In those studies, reelin was detected in the CA1, 3 and 4, and we did not sample those areas.

Rho GTPases and Mechanisms for Migration or GCD

Due to the observation of Rho GTPases in the dispersed DGCs, these proteins have become the focus of further investigation as to their role in pathomechanisms underlying GCD.

The main finding in this study is the upregulation of proteins involved in the Rho GTPase signaling pathway in dispersed DGCs of patients with MTLE and GCD. Rho GTPases belong to the Rho family of GTPases, which is a subgroup of the Ras family of small GTP binding protein (Heasman and Ridley, 2008). Ras homologous member A (RhoA), Ras-related C3 (Rac1) and cell division cycle 42 (Cdc42) are the three most-studied Rho GTPases, and the activated form of these Rho GTPases bind with a number of effector molecules (Dia, ROCK, myosin light chain, phosphatase and kinase, WAVE, Arp2/3, PAK, LIMK, Cofilin-P, Mec-3, WASP; see **Supplementary Material S5**) to regulate actin polymerization, microtubule stabilization, and actomyosin contractility during neurodevelopment when cells undergo active morphogenesis and participate in migratory, proliferative, and survival activities (Heasman and Ridley, 2008; Zarco et al., 2019). Data from the Human Brain Transcriptome project has reported continuous gene expression of *RHOA, RAC1* and *CDC42* in the human hippocampus from embryonic and early fetal periods to adulthood (4 post-conceptional weeks to 60 years of age; **Supplementary Material S8**; Kang et al., 2011). Similarly, we observed a high number of DGCs expressing *RHOA, RAC1* and *CDC42* mRNAs in the brains of adult MTLE patients with and without GCD, with age at surgery spanning 20–60 years. Whether the protein expression of these Rho GTPases is continuously expressed in DGCs from development to adulthood in the normal and MTLE human brain remain to be investigated as there is currently limited information. In this study, we found significantly higher protein expression of RhoA in uni- or bipolar ends of DGCs in cases with GCD than without GCD, particularly in displaced DGCs in the outer-granule and molecular layers. RhoA was absent in most DGCs located in the basal granule cell layer of MTLE cases. Considering the established role of RhoA in polarized cell migration in neurogenic niches, it is plausible that RhoA has a role in the mismigration of DGCs in cases with DGCs. The distinct localization of RhoA to the apices of dispersed DGC soma may be suggestive of proximal cytoplasmic bulging, a characteristic feature of cells undergoing saltatory migratory during neurodevelopment and in neurogenic zones of adult mammalian brains (Schaar and McConnell, 2005; Wang et al., 2019). During saltatory migration, the centrosome of the migrating cell moves forward to form a transient swelling in the proximal leading process and then the cell body and nucleus move towards the centrosome then pause and this process is repeated again. Previous *in vitro* morphodynamic studies have found spatiotemporal changes to the expression of RhoA in migrating cells as they undergo saltatory migration (Fritz et al., 2013; Martin et al., 2016; Kaneko et al., 2017). These studies detected RhoA initially at the transient swelling of the leading proximal process where RhoA interacted with effector proteins to regulate f-actin and myosin II in the actomyosin contraction to allow cell soma to translocate forward (Solecki et al., 2009; Ota et al., 2014). As the cell moved forward then stalled, RhoA expression was reduced in the front and gradually increased at the rear of the cell to facilitate retraction of cell soma and back processes, allowing the entire cell to move forward. Thus, RhoA expression may be detected at either or both ends of the cell soma depending on the cell's migratory state. In agreement, we observed varying numbers of DGCs with RhoA accumulation in one or both ends of the cell soma in cases with GCD. Rho GTPase-mediated cell migration is a well-coordinated process during neurodevelopment, tightly regulated by a number of guanine nucleotide exchange factors and dissociation inhibitors, and GTPase-activating proteins to ensure new neurons arrive timely at a specific location (Schmidt and Hall, 2002). Genetic knockout of Rho GTPase-activating proteins, such as Gimp, in animal studies, can lead to the appearance of ectopic cells (Ota et al., 2014). In this study, Gimp was not detected in our samples, but other GTPase-activating proteins, such as ARGAP1, ARGAP35, A-kinase anchor protein 13, SLIT-ROBO Rho GTPase-activating protein 3 were detected, and further studies are needed to investigate their cellular expression and role in regulating DGC migration in MTLE. In our study, a number of *RHOA* and *RAC1*-positive puncta were observed in the neuropil of MTLE cases. It is possible that some of these positive puncta maybe transcripts localized to the processes of DGCs. Previous studies have demonstrated the protein expression of Rac1 and Rho GTPases-exchange factors at the tip of leading processes of migrating cells (Shinohara et al., 2012; Hikita et al., 2014). It is also plausible that *RHOA* and *RAC1* mRNAs are expressed in surrounding glial cells in the granule and molecular layers, although our initial double labeling experiments did not detect *RHOA* and *RAC1* transcripts in astroglial cells expressing glutamine synthetase.

Other modes of cellular migration involving Rho GTPases include "frog leap" and "vessel-based" migrations. Using live imaging techniques, a study reported that 50% of the adult-born new DGCs had leading process pointed tangentially in the subgranular zone of the hippocampal granule cell layer, and these cells underwent lateral migration in small clusters coupled by connexin 43 before migrating radially into the deeper granule cell layer (Wang et al., 2019). During this migratory process, the leading cells in the migratory cluster changed repeatedly (akin to leapfrog), hovering forward and backward as the cluster moved towards their final destination. Other animal studies have also reported that gap junctions are important for neuronal dispersion in the embryonic cortex (Elias et al., 2007, 2010; Yu et al., 2012). In our study, expression of connexin 43 was observed in dispersed DGCs of cases with GCD and we did observe a number of dispersed DGCs in single line formation in outer-granule and molecular layers of cases with GCD, sometimes in close proximity to vascular structures. In microvessel-based migration, DGCs are postulated to migrate tangentially along blood vessels, followed by limited radial migration into the granule cell layer (Sun et al., 2015). In developing animals, it is known that large plexuses of vasculature are developed in the molecular layer and CA4 during postnatal days 0–7, while only short bridges of blood vessels are found to extend through the granule cell layer (Pombero et al., 2018).

CONCLUSION

In conclusion, we have shown limited evidence to support ongoing adult neurogenesis in the hippocampus of patients with MTLE, but evidence of differential dysmaturation between dispersed and basal DGCs has been shown. We have provided evidence from proteomic and immunohistochemical studies to demonstrate that DGCs contribute to ongoing structural and synaptic changes in the MTLE human brain, and expression of Rho GTPases in these cells may support abnormal cellular migratory activities that are linked to GCD pathology. Further studies are required to assess the possible contribution of DGCs expressing Rho GTPases to seizure generation and cognitive impairments.

DATA AVAILABILITY STATEMENT

Peptide identification and quantification data analyzed in this study can be found in the **Supplementary Material S9**. Any further queries related to data availability should be directed to Professor MT (m.thom@ucl.ac.uk).

ETHICS STATEMENT

The studies involving human participants were reviewed and approved by Epilepsy Society Brain and Tissue Bank (NRES 17/SC/0573). Informed written consents were obtained from all tissue donors.

AUTHOR CONTRIBUTIONS

JL, MT, and SS planned and designed the study. KM and this team performed the proteomics analyses. ND and BA-K conducted experiments using *in situ* hybridization and immunohistochemistry, respectively. JL performed bioinformatics and quantitative analyses. All authors contributed to the writing and reviewing of the manuscript.

FUNDING

This work was supported by Medical Research Council (MRC MR/J0127OX/1), European Union Seventh Framework Programme (FP7/2007–2013) under grant agreement EPITARGET (#602102), and through Epilepsy Society from the Horne Family Charitable Foundation. This work was undertaken at the University of Westminster and UCLH/UCL who received a proportion of funding from the Department of Health's NIHR Biomedical Research Centres funding scheme. Proteomics was performed by Mills Research Group at the Biological Mass Spectrometry Centre, UCL Great Ormond Street Institute of Child Health. JL received funding from the EPITARGET (#602102), and Research Starter Fund from the University of Westminster. The Epilepsy Society Brain and Tissue Bank at UCL was funded by the Epilepsy Society.

ACKNOWLEDGMENTS

We would like to thanks patients who donated their brain tissue to the Epilepsy Society Brain and Tissue Bank and consented for the use of their valuable tissue in research. We would like to acknowledge Houda Aljibouri for her assistance with optimizing conditions for double-label *in situ* hybridization and immunohistochemical experiments.

SUPPLEMENTARY MATERIAL

The Supplementary Material for this article can be found online at: https://www.frontiersin.org/articles/10.3389/fncel.2020.00053/full#supplementary-material.

REFERENCES

Abrahám, H., Richter, Z., Gyimesi, C., Horváth, Z., Janszky, J., Dóczi, T., et al. (2011). Degree and pattern of calbindin immunoreactivity in granule cells of the dentate gyrus differ in mesial temporal sclerosis, cortical malformation- and tumor-related epilepsies. *Brain Res.* 1399:66. doi: 10.1016/j.brainres.2011.05.010

Abrahám, H., Veszprémi, B., Kravják, A., Kovács, K., Gömöri, É., and Seress, L. (2009). Ontogeny of calbindin immunoreactivity in the human hippocampal formation with a special emphasis on granule cells of the dentate gyrus. *Int. J. Dev. Neurosci.* 27, 115–127. doi: 10.1016/j.ijdevneu.2008.12.004

Althaus, A. L., Moore, S. J., Zhang, H., Du Plummer, X., Murphy, G. G., and Parent, J. M. (2019). Altered synaptic drive onto birthdated dentate granule cells in experimental temporal lobe epilepsy. *J. Neurosci.*, 7604–7614. doi: 10.1523/jneurosci.0654-18.2019

Altman, J., and Bayer, S. A. (1990). Mosaic organization of the hippocampal neuroepithelium and the multiple germinal sources of dentate granule cells. *J. Comp. Neurol.* 301, 325–342. doi: 10.1002/cne.903010302

Arellano, J. I., Muoz, A., BallesterosYez, I., Sola, R. G., and DeFelipe, J. (2004). Histopathology and reorganization of chandelier cells in the human epileptic sclerotic hippocampus. *Brain* 127, 45–64. doi: 10.1093/brain/awh004

Bankhead, P., Loughrey, M. B., Fernández, J. A., Dombrowski, Y., McArt, D. G., Dunne, P. D., et al. (2017). QuPath: open source software for digital pathology image analysis. *Sci. Rep.* 7:16878. doi: 10.1038/s41598-017-17204-5

Barna, J., Dimén, D., Puska, G., Kovács, D., Csikós, V., Oláh, S., et al. (2019). Complement component 1q subcomponent binding protein in the brain of the rat. *Sci. Rep.* 9:4597. doi: 10.1038/s41598-019-40788-z

Begcevic, I., Kosanam, H., Martínez-Morillo, E., Dimitromanolakis, A., Diamandis, P., Kuzmanov, U., et al. (2013). Semiquantitative proteomic analysis of human hippocampal tissues from Alzheimer's disease and age-matched control brains. *Clin. Proteomics* 10:5. doi: 10.1186/1559-0275-10-5

Blümcke, I., Kistner, I., Clusmann, H., Schramm, J., Becker, A. J., Elger, C. E., et al. (2009). Towards a clinico-pathological classification of granule cell dispersion in human mesial temporal lobe epilepsies. *Acta Neuropathol.* 117:535. doi: 10.1007/s00401-009-0512-5

Blümcke, I., Schewe, J.-C., Normann, S., Brüstle, O., Schramm, J., Elger, C. E., et al. (2001). Increase of nestin-immunoreactive neural precursor cells in the dentate gyrus of pediatric patients with early-onset temporal lobe epilepsy. *Hippocampus* 11, 311–321. doi: 10.1002/hipo.1045

Blumcke, I., Spreafico, R., Haaker, G., Coras, R., Kobow, K., Bien, C. G., et al. (2017). Histopathological findings in brain tissue obtained during epilepsy surgery. *N. Engl. J. Med.* 377, 1648–1656. doi: 10.1056/NEJMoa1703784

Blümcke, I., Thom, M., Aronica, E., Armstrong, D. D., Bartolomei, F., Bernasconi, A., et al. (2013). International consensus classification of hippocampal sclerosis in temporal lobe epilepsy: a task force report from the ILAE commission on diagnostic methods. *Epilepsia* 54, 1315–1329. doi: 10.1111/epi.12220

Brandt, M. D., Jessberger, S., Steiner, B., Kronenberg, G., Reuter, K., Bick-Sander, A., et al. (2003). Transient calretinin expression defines early postmitotic step of neuronal differentiation in adult hippocampal neurogenesis of mice. *Mol. Cell. Neurosci.* 24, 603–613. doi: 10.1016/s1044-7431(03)00207-0

Buckmaster, P. S., Ingram, E. A., and Wen, X. (2009). Inhibition of the mammalian target of rapamycin signaling pathway suppresses dentate granule cell axon sprouting in a rodent model of temporal lobe epilepsy. *J. Neurosci.* 29, 8259–8269. doi: 10.1523/jneurosci.4179-08.2009

Cavazos, J. E., Zhang, P., Qazi, R., and Sutula, T. P. (2003). Ultrastructural features of sprouted mossy fiber synapses in kindled and kainic acid-treated rats. *J. Comp. Neurol.* 458, 272–292. doi: 10.1002/cne.10581

Chai, X., Münzner, G., Zhao, S., Tinnes, S., Kowalski, J., Häussler, U., et al. (2014). Epilepsy-induced motility of differentiated neurons. *Cereb. Cortex* 24, 2130–2140. doi: 10.1093/cercor/bht067

Chen, E. Y., Tan, C. M., Kou, Y., Duan, Q., Wang, Z., Meirelles, G. V., et al. (2013). Enrichr: interactive and collaborative HTML5 gene list enrichment analysis tool. *BMC Bioinformatics* 14, 128–128. doi: 10.1186/1471-2105-14-128

Cipriani, S., Journiac, N., Nardelli, J., Verney, C., Delezoide, A.-L., Guimiot, F., et al. (2017). Dynamic expression patterns of progenitor and neuron layer markers in the developing human dentate gyrus and fimbria. *Cereb. Cortex* 27, 358–372. doi: 10.1093/cercor/bhv223

Czech, T., Yang, J. W., Csaszar, E., Kappler, J., Baumgartner, C., and Lubec, G. (2004). Reduction of hippocampal collapsin response mediated protein-2 in patients with mesial temporal lobe epilepsy. *Neurochem. Res.* 29, 2189–2196. doi: 10.1007/s11064-004-7025-3

Da Costa Neves, R. S., Jardim, A. P., Caboclo, L. O., Lancellotti, C., Marinho, T. F., Hamad, A. P., et al. (2013). Granule cell dispersion is not a predictor of surgical outcome in temporal lobe epilepsy with mesial temporal sclerosis. *Clin. Neuropathol.* 32:24. doi: 10.5414/np300509

de Tisi, J., Bell, G. S., Peacock, J. L., McEvoy, A. W., Harkness, W. F., Sander, J. W., et al. (2011). The long-term outcome of adult epilepsy surgery, patterns of seizure remission and relapse: a cohort study. *Lancet* 378, 1388–1395. doi: 10.1016/S0140-6736(11)60890-8

Edgar, P. F., Douglas, J. E., Knight, C., Cooper, G. J., Faull, R. L., and Kydd, R. (1999a). Proteome map of the human hippocampus. *Hippocampus* 9, 644–650. doi: 10.1002/(sici)1098-1063(1999)9:6<644::aid-hipo5>3.0.co;2-s

Edgar, P. F., Schonberger, S. J., Dean, B., Faull, R. L., Kydd, R., and Cooper, G. J. (1999b). A comparative proteome analysis of hippocampal tissue from schizophrenic and Alzheimer's disease individuals. *Mol. Psychiatry* 4, 173–178. doi: 10.1038/sj.mp.4000463

Elias, L. A. B., Turmaine, M., Parnavelas, J. G., and Kriegstein, A. R. (2010). Connexin 43 mediates the tangential to radial migratory switch in ventrally derived cortical interneurons. *J. Neurosci.* 30, 7072–7072. doi: 10.1523/jneurosci.5728-09.2010

Elias, L. A. B., Wang, D. D., and Kriegstein, A. R. (2007). Gap junction adhesion is necessary for radial migration in the neocortex. *Nature* 448, 901–907. doi: 10.1038/nature06063

Engel, J. Jr. (1998). Etiology as a risk factor for medically refractory epilepsy: a case for early surgical intervention. *Neurology* 51, 1243–1244. doi: 10.1212/wnl.51.5.1243

Engel, J., McDermott, M. P., Wiebe, S., Langfitt, J. T., Stern, J. M., Dewar, S., et al. (2012). Early surgical therapy for drug-resistant temporal lobe epilepsy: a randomized trial. *JAMA* 307, 922–930. doi: 10.1001/jama.2012.220

Eun, J.-P., Choi, H.-Y., and Kwak, Y.-G. (2004). Proteomic analysis of human cerebral cortex in epileptic patients. *Exp. Mol. Med.* 36, 185–191. doi: 10.1038/emm.2004.26

Föcking, M., Chen, W.-Q., Dicker, P., Dunn, M. J., Lubec, G., and Cotter, D. R. (2012). Proteomic analysis of human hippocampus shows differential protein expression in the different hippocampal subfields. *Proteomics* 12, 2477–2481. doi: 10.1002/pmic.201200031

Frese, C. K., Mikhaylova, M., Stucchi, R., Gautier, V., Liu, Q., Mohammed, S., et al. (2017). Quantitative map of proteome dynamics during neuronal differentiation. *Cell Rep.* 18, 1527–1542. doi: 10.1016/j.celrep.2017.01.025

Fritz, R. D., Letzelter, M., Reimann, A., Martin, K., Fusco, L., Ritsma, L., et al. (2013). A versatile toolkit to produce sensitive FRET biosensors to visualize signaling in time and space. *Sci. Signal.* 6, rs12–rs12. doi: 10.1126/scisignal.2004135

Frotscher, M. (1998). Cajal-retzius cells, Reelin and the formation of layers. *Curr. Opin. Neurobiol.* 8, 570–575. doi: 10.1016/s0959-4388(98)80082-2

Frotscher, M., Haas, C. A., and Förster, E. (2003). Reelin controls granule cell migration in the dentate gyrus by acting on the radial glial scaffold. *Cereb. Cortex* 13, 634–640. doi: 10.1093/cercor/13.6.634

Fukata, Y., Itoh, T. J., Kimura, T., Ménager, C., Nishimura, T., Shiromizu, T., et al. (2002). CRMP-2 binds to tubulin heterodimers to promote microtubule assembly. *Nat. Cell Biol.* 4, 583–591. doi: 10.1038/ncb825

Haas, C. A., Dudeck, O., Kirsch, M., Huszka, C., Kann, G., Pollak, S., et al. (2002). Role for reelin in the development of granule cell dispersion in temporal lobe epilepsy. *J. Neurosci.* 22, 5797–5802. doi: 10.1523/jneurosci.22-14-05797.2002

Haas, C., and Frotscher, M. (2010). Reelin deficiency causes granule cell dispersion in epilepsy. *Exp. Brain Res.* 200, 141–149. doi: 10.1007/s00221-009-1948-5

He, S., Wang, Q., He, J., Pu, H., Yang, W., and Ji, J. (2006). Proteomic analysis and comparison of the biopsy and autopsy specimen of human brain temporal lobe. *Proteomics* 6, 4987–4996. doi: 10.1002/pmic.200600078

Heasman, S. J., and Ridley, A. J. (2008). Mammalian Rho GTPases: new insights into their functions from *in vivo* studies. *Nat. Rev. Mol. Cell Biol.* 9, 690–701. doi: 10.1038/nrm2476

Heinrich, C., Nitta, N., Flubacher, A., Müller, M., Fahrner, A., Kirsch, M., et al. (2006). Reelin deficiency and displacement of mature neurons, but not neurogenesis, underlie the formation of granule cell dispersion in the epileptic hippocampus. *J. Neurosci.* 26, 4701–4713. doi: 10.1523/JNEUROSCI.5516-05.2006

Hester, M. S., and Danzer, S. C. (2013). Accumulation of abnormal adult-generated hippocampal granule cells predicts seizure frequency and severity. *J. Neurosci.* 33, 8926–8936. doi: 10.1523/jneurosci.5161-12.2013

Heywood, W. E., Mills, P., Grunewald, S., Worthington, V., Jaeken, J., Carreno, G., et al. (2013). A new method for the rapid diagnosis of protein n-linked congenital disorders of glycosylation. *J. Proteome Res.* 12, 3471–3479. doi: 10.1021/pr400328g

Hikita, T., Ohno, A., Sawada, M., Ota, H., and Sawamoto, K. (2014). Rac1-mediated indentation of resting neurons promotes the chain migration of new neurons in the rostral migratory stream of post-natal mouse brain. *J. Neurochem.* 128, 790–797. doi: 10.1111/jnc.12518

Hondius, D. C., van Nierop, P., Li, K. W., Hoozemans, J. J. M., van der Schors, R. C., van Haastert, E. S., et al. (2016). Profiling the human hippocampal proteome at all pathologic stages of Alzheimer's disease. *Alzheimers Dement.* 12, 654–668. doi: 10.1016/j.jalz.2015.11.002

Houser, C. R. (1990). Granule cell dispersion in the dentate gyrus of humans with temporal lobe epilepsy. *Brain Res.* 535, 195–204. doi: 10.1016/0006-8993(90)91601-c

Huang da, W., Sherman, B. T., and Lempicki, R. A. (2009a). Bioinformatics enrichment tools: paths toward the comprehensive functional analysis of large gene lists. *Nucleic Acids Res.* 37, 1–13. doi: 10.1093/nar/gkn923

Huang da, W., Sherman, B. T., and Lempicki, R. A. (2009b). Systematic and integrative analysis of large gene lists using DAVID bioinformatics resources. *Nat. Protoc.* 4, 44–57. doi: 10.1038/nprot.2008.211

Inagaki, N., Chihara, K., Arimura, N., Ménager, C., Kawano, Y., Matsuo, N., et al. (2001). CRMP-2 induces axons in cultured hippocampal neurons. *Nat. Neurosci.* 4, 781–782. doi: 10.1038/90476

Kahn, J. B., Port, R. G., Yue, C., Takano, H., and Coulter, D. A. (2019). Circuit-based interventions in the dentate gyrus rescue epilepsy-associated cognitive dysfunction. *Brain* 142, 2705–2721. doi: 10.1093/brain/awz209

Kaneko, N., Sawada, M., and Sawamoto, K. (2017). Mechanisms of neuronal migration in the adult brain. *J. Neurochem.* 141, 835–847. doi: 10.1111/jnc.14002

Kang, H. J., Kawasawa, Y. I., Cheng, F., Zhu, Y., Xu, X., Li, M., et al. (2011). Spatio-temporal transcriptome of the human brain. *Nature* 478, 483–489. doi: 10.1038/nature10523

Kelemen, A., and Peter, H. (2010). Lacosamide for the prevention of partial onset seizures in epileptic adults. *Neuropsychiatr. Dis. Treat.* 6, 465–471. doi: 10.2147/ndt.s7967

Keren-Aviram, G., Dachet, F., Bagla, S., Balan, K., Loeb, J. A., and Dratz, E. A. (2018). Proteomic analysis of human epileptic neocortex predicts vascular and glial changes in epileptic regions. *PLoS One* 13:e0195639. doi: 10.1371/journal.pone.0195639

Kobow, K., Jeske, I., Hildebrandt, M., Hauke, J., Hahnen, E., Buslei, R., et al. (2009). Increased reelin promoter methylation is associated with granule cell dispersion in human temporal lobe epilepsy. *J. Neuropathol. Exp. Neurol.* 68, 356–364. doi: 10.1097/nen.0b013e31819ba737

Koopmans, F., Pandya, N. J., Franke, S. K., Phillippens, I. H. C. M. H., Paliukhovich, I., Li, K. W., et al. (2018). Comparative hippocampal synaptic proteomes of rodents and primates: differences in neuroplasticity-related proteins. *Front. Mol. Neurosci.* 11:364. doi: 10.3389/fnmol.2018.00364

Kovac, S., Dinkova Kostova, A. T., Herrmann, A. M., Melzer, N., Meuth, S. G., and Gorji, A. (2017). Metabolic and homeostatic changes in seizures and acquired epilepsy—mitochondria, calcium dynamics and reactive oxygen species. *Int. J. Mol. Sci.* 18:1935. doi: 10.3390/ijms18091935

Krook-Magnuson, E., Armstrong, C., Bui, A., Lew, S., Oijala, M., and Soltesz, I. (2015). *In vivo* evaluation of the dentate gate theory in epilepsy. *J. Physiol.* 593, 2379–2388. doi: 10.1113/JP270056

Kuleshov, M. V., Jones, M. R., Rouillard, A. D., Fernandez, N. F., Duan, Q., Wang, Z., et al. (2016). Enrichr: a comprehensive gene set enrichment analysis web server 2016 update. *Nucleic Acids Res.* 44:W90. doi: 10.1093/nar/gkw377

Lee, J. M., Hong, J., Moon, G. J., Jung, U. J., Won, S.-Y., and Kim, S. R. (2018). Morin prevents granule cell dispersion and neurotoxicity *via* suppression of mTORC1 in a kainic acid-induced seizure model. *Exp. Neurobiol.* 27, 226–237. doi: 10.5607/en.2018.27.3.226

Lee, C., Hu, J., Ralls, S., Kitamura, T., Loh, Y. P., Yang, Y., et al. (2012). The molecular profiles of neural stem cell niche in the adult subventricular zone. *PLoS One* 7:e50501. doi: 10.1371/journal.pone.0050501

Liu, J. Y. W., Reeves, C., Diehl, B., Coppola, A., Al-Hajri, A., Hoskote, C., et al. (2016). Early lipofuscin accumulation in frontal lobe epilepsy. *Ann. Neurol.* 80, 882–895. doi: 10.1002/ana.24803

Liu, J., Reeves, C., Jacques, T., McEvoy, A., Miserocchi, A., Thompson, P., et al. (2018). Nestin-expressing cell types in the temporal lobe and hippocampus: morphology, differentiation and proliferative capacity. *Glia* 66, 62–77. doi: 10.1002/glia.23211

Liu, J., Reeves, C., Michalak, Z., Coppola, A., Diehl, B., Sisodiya, S. M., et al. (2014). Evidence for mTOR pathway activation in a spectrum of epilepsy-associated pathologies. *Acta Neuropathol. Commun.* 2:71. doi: 10.1186/2051-5960-2-71

Lurton, D., El Bahh, B., Sundstrom, L., and Rougier, A. (1998). Granule cell dispersion is correlated with early epileptic events in human temporal lobe epilepsy. *J. Neurol. Sci.* 154, 133–136. doi: 10.1016/s0022-510x(97)00220-7

Ma, L., Liu, Y.-P., Geng, C.-Z., Wang, X.-L., Wang, Y.-J., and Zhang, X.-H. (2010). Over expression of RhoA is associated with progression in invasive breast duct carcinoma. *Breast J.* 16, 105–107. doi: 10.1111/j.1524-4741.2009.00860.x

Maglóczky, Z., Halász, P., Vajda, J., Czirják, S., and Freund, T. F. (1997). Loss of Calbindin-D 28K immunoreactivity from dentate granule cells in human temporal lobe epilepsy. *Neuroscience* 76, 377–385. doi: 10.1016/s0306-4522(96)00440-x

Manwaring, V., Heywood, W. E., Clayton, R., Lachmann, R. H., Keutzer, J., Hindmarsh, P., et al. (2013). The identification of new biomarkers for identifying and monitoring kidney disease and their translation into a rapid mass spectrometry-based test: evidence of presymptomatic kidney disease in pediatric fabry and type-i diabetic patients. *J. Proteome Res.* 12, 2013–2021. doi: 10.1021/pr301200e

Martin, K., Reimann, A., Fritz, R. D., Ryu, H., Jeon, N. L., and Pertz, O. (2016). Spatio-temporal co-ordination of RhoA, Rac1 and Cdc42 activation during prototypical edge protrusion and retraction dynamics. *Sci. Rep.* 6:21901. doi: 10.1038/srep21901

Martinian, L., Catarino, C. B., Thompson, P., Sisodiya, S. M., and Thom, M. (2012). Calbindin D28K expression in relation to granule cell dispersion, mossy fibre sprouting and memory impairment in hippocampal sclerosis: a surgical and post mortem series. *Epilepsy Res.* 98, 14–24. doi: 10.1016/j.eplepsyres.2011.08.011

Mériaux, C., Franck, J., Park, D. B., Quanico, J., Kim, Y. H., Chung, C. K., et al. (2014). Human temporal lobe epilepsy analyses by tissue proteomics. *Hippocampus* 24, 628–642. doi: 10.1002/hipo.22246

Meunier, B., Dumas, E., Piec, I., Béchet, D., Hébraud, M., and Hocquette, J.-F. (2007). Assessment of hierarchical clustering methodologies for proteomic data mining. *J. Proteome Res.* 6, 358–366. doi: 10.1021/pr060343h

Miles, R., and Wong, R. K. (1983). Single neurones can initiate synchronized population discharge in the hippocampus. *Nature* 306, 371–373. doi: 10.1038/306371a0

Moreno-Jiménez, E. P., Flor-García, M., Terreros-Roncal, J., Rábano, A., Cafini, F., Pallas-Bazarra, N., et al. (2019). Adult hippocampal neurogenesis is abundant in neurologically healthy subjects and drops sharply in patients with Alzheimer's disease. *Nat. Med.* 25, 554–560. doi: 10.1038/s41591-019-0375-9

Murphy, B. L., and Danzer, S. C. (2011). Somatic translocation: a novel mechanism of granule cell dendritic dysmorphogenesis and dispersion. *J. Neurosci.* 31, 2959–2964. doi: 10.1523/jneurosci.3381-10.2011

Orcinha, C., Münzner, G., Gerlach, J., Kilias, A., Follo, M., Egert, U., et al. (2016). Seizure-induced motility of differentiated dentate granule cells is prevented by the central reelin fragment. *Front. Cell. Neurosci.* 10:183. doi: 10.3389/fncel.2016.00183

Ota, H., Hikita, T., Sawada, M., Nishioka, T., Matsumoto, M., Komura, M., et al. (2014). Speed control for neuronal migration in the postnatal brain by Gmip-mediated local inactivation of RhoA. *Nat. Commun.* 5:4532. doi: 10.1038/ncomms5532

Overstreet-Wadiche, L. S., Bromberg, D. A., Bensen, A. L., and Westbrook, G. L. (2006). Seizures accelerate functional integration of adult-generated granule cells. *J. Neurosci.* 26, 4095–4103. doi: 10.1523/jneurosci.5508-05.2006

Parent, J. M., Elliott, R. C., Pleasure, S. J., Barbaro, N. M., and Lowenstein, D. H. (2006). Aberrant seizure-induced neurogenesis in experimental temporal lobe epilepsy. *Ann. Neurol.* 59, 81–91. doi: 10.1002/ana.20699

Persike, D., Lima, M., Amorim, R., Cavalheiro, E., Yacubian, E., Centeno, R., et al. (2012). Hippocampal proteomic profile in temporal lobe epilepsy. *J. Epilepsy Clin. Neurophysiol.* 18, 53–56. doi: 10.1590/S1676-26492012000200007

Persike, D. S., Marques-Carneiro, J. E., Stein, M. L. D. L., Yacubian, E. M. T., Centeno, R., Canzian, M., et al. (2018). Altered proteins in the hippocampus of patients with mesial temporal lobe epilepsy. *Pharmaceuticals* 11:E95. doi: 10.3390/ph11040095

Pombero, A., Garcia-Lopez, R., Estirado, A., and Martinez, S. (2018). Vascular pattern of the dentate gyrus is regulated by neural progenitors. *Brain Struct. Funct.* 223, 1971–1987. doi: 10.1007/s00429-017-1603-z

Koyama, R., Tao, K., Sasaki, T., Ichikawa, J., Miyamoto, D., Muramatsu, R., et al. (2012). GABAergic excitation after febrile seizures induces ectopic granule cells and adult epilepsy. *Nat. Med.* 18, 1271–1278. doi: 10.1038/nm.2850

Schaar, B. T., and McConnell, S. K. (2005). Cytoskeletal coordination during neuronal migration. *Proc. Natl. Acad. Sci. U S A* 102, 13652–13657. doi: 10.1073/pnas.0506008102

Scharfman, H. E., and MacLusky, N. J. (2014). Differential regulation of BDNF, synaptic plasticity and sprouting in the hippocampal mossy fiber pathway of male and female rats. *Neuropharmacology* 76, 696–708. doi: 10.1016/j.neuropharm.2013.04.029

Schmidt, A., and Hall, A. (2002). Guanine nucleotide exchange factors for Rho GTPases: turning on the switch. *Genes Dev.* 16, 1587–1609. doi: 10.1101/gad.1003302

Seress, L., Ábrahám, H., Tornóczky, T., and Kosztolányi, G. (2001). Cell formation in the human hippocampal formation from mid-gestation to the late postnatal period. *Neuroscience* 105, 831–843. doi: 10.1016/s0306-4522(01)00156-7

Sha, L.-Z., Xing, X.-L., Zhang, D., Yao, Y., Dou, W.-C., Jin, L.-R., et al. (2012). Mapping the spatio-temporal pattern of the mammalian target of rapamycin (mTOR) activation in temporal lobe epilepsy. *PLoS One* 7:e39152. doi: 10.1371/journal.pone.0039152

Shinohara, R., Thumkeo, D., Kamijo, H., Kaneko, N., Sawamoto, K., Watanabe, K., et al. (2012). A role for mDia, a Rho-regulated actin nucleator, in tangential migration of interneuron precursors. *Nat. Neurosci.* 15, 373–380. doi: 10.1038/nn.3020

Solecki, D. J., Trivedi, N., Govek, E.-E., Kerekes, R. A., Gleason, S. S., and Hatten, M. E. (2009). Myosin II motors and F-actin dynamics drive the coordinated movement of the centrosome and soma during CNS glial-guided neuronal migration. *Neuron* 63, 63–80. doi: 10.1016/j.neuron.2009.05.028

Sorrells, S. F., Paredes, M. F., Cebrian-Silla, A., Sandoval, K., Qi, D., Kelley, K. W., et al. (2018). Human hippocampal neurogenesis drops sharply in children to undetectable levels in adults. *Nature* 555, 377–381. doi: 10.1038/nature25975

Sosunov, A. A., Wu, X., McGovern, R. A., Coughlin, D. G., Mikell, C. B., Goodman, R. R., et al. (2012). The mTOR pathway is activated in glial cells in mesial temporal sclerosis. *Epilepsia* 53, 78–86. doi: 10.1111/j.1528-1167.2012.03478.x

Sultana, R., Boyd-Kimball, D., Cai, J., Pierce, W. M., Klein, J. B., Merchant, M., et al. (2007). Proteomics analysis of the Alzheimer's disease hippocampal proteome. *J. Alzheimers Dis.* 11, 153–164. doi: 10.3233/jad-2007-11203

Sun, G. J., Zhou, Y., Stadel, R. P., Moss, J., Yong, J. H. A., Ito, S., et al. (2015). Tangential migration of neuronal precursors of glutamatergic neurons in the adult mammalian brain. *Proc. Natl. Acad. Sci. U S A* 112, 9484–9489. doi: 10.1073/pnas.1508545112

Sutula, T., Cascino, G., Cavazos, J., Parada, I., and Ramirez, L. (1989). Mossy fiber synaptic reorganization in the epileptic human temporal lobe. *Ann. Neurol.* 26, 321–330. doi: 10.1002/ana.410260303

Thom, M., Liagkouras, I., Elliot, K. J., Martinian, L., Harkness, W., McEvoy, A., et al. (2010). Reliability of patterns of hippocampal sclerosis as predictors of postsurgical outcome. *Epilepsia* 51, 1801–1808. doi: 10.1111/j.1528-1167.2010.02681.x

Thom, M., Liagkouras, I., Martinian, L., Liu, J., Catarino, C. B., and Sisodiya, S. M. (2012). Variability of sclerosis along the longitudinal hippocampal axis in epilepsy: a post mortem study. *Epilepsy Res.* 102, 45–59. doi: 10.1016/j.eplepsyres.2012.04.015

Thom, M., Martinian, L., Williams, G., Stoeber, K., and Sisodiya, S. M. (2005). Cell proliferation and granule cell dispersion in human hippocampal sclerosis. *J. Neuropathol. Exp. Neurol.* 64, 194–201. doi: 10.1093/jnen/64.3.194

Wang, J., Shen, J., Kirschen, G. W., Gu, Y., Jessberger, S., and Ge, S. (2019). Lateral dispersion is required for circuit integration of newly generated dentate granule cells. *Nat. Commun.* 10:3324. doi: 10.1038/s41467-019-11206-9

Wieser, H.-G., and ILAE Commission on Neurosurgery of Epilepsy. (2004). ILAE Commission Report. Mesial temporal lobe epilepsy with hippocampal sclerosis. *Epilepsia* 45, 695–714. doi: 10.1111/j.0013-9580.2004.09004.x

Yang, J. W., Czech, T., Felizardo, M., Baumgartner, C., and Lubec, G. (2006). Aberrant expression of cytoskeleton proteins in hippocampus from patients with mesial temporal lobe epilepsy. *Amino Acids* 30, 477–493. doi: 10.1007/s00726-005-0281-y

Yang, J. W., Czech, T., and Lubec, G. (2004a). Proteomic profiling of human hippocampus. *Electrophoresis* 25, 1169–1174. doi: 10.1002/elps.200305809

Yang, J. W., Czech, T., Yamada, J., Csaszar, E., Baumgartner, C., Slavc, I., et al. (2004b). Aberrant cytosolic acyl-CoA thioester hydrolase in hippocampus of patients with mesial temporal lobe epilepsy. *Amino Acids* 27, 269–275. doi: 10.1007/s00726-004-0138-9

Yu, Y.-C., He, S., Chen, S., Fu, Y., Brown, K. N., Yao, X.-H., et al. (2012). Preferential electrical coupling regulates neocortical lineage-dependent microcircuit assembly. *Nature* 486, 113–117. doi: 10.1038/nature10958

Zarco, N., Norton, E., Quiñones-Hinojosa, A., and Guerrero-Cázares, H. (2019). Overlapping migratory mechanisms between neural progenitor cells and brain tumor stem cells. *Cell. Mol. Life Sci.* 76, 3553–3570. doi: 10.1007/s00018-019-03149-7

Zhan, R., Timofeeva, O., and Nadler, J. V. (2010). High ratio of synaptic excitation to synaptic inhibition in hilar ectopic granule cells of pilocarpine-treated rats. *J. Neurophysiol.* 104, 3293–3304.

Conflict of Interest: The authors declare that the research was conducted in the absence of any commercial or financial relationships that could be construed as a potential conflict of interest.

frontiers in Cellular Neuroscience

ORIGINAL RESEARCH
published: 20 March 2020
doi: 10.3389/fncel.2020.00054

Paroxysmal Discharges in Tissue Slices From Pediatric Epilepsy Surgery Patients: Critical Role of $GABA_B$ Receptors in the Generation of Ictal Activity

*Simon Levinson[1], Conny H. Tran[1], Joshua Barry[1], Brett Viker[1], Michael S. Levine[1], Harry V. Vinters[2,3], Gary W. Mathern[1,4] and Carlos Cepeda[1]**

[1] IDDRC, Semel Institute for Neuroscience and Human Behavior, David Geffen School of Medicine, University of California, Los Angeles, Los Angeles, CA, United States, [2] Section of Neuropathology, Department of Pathology and Laboratory Medicine, David Geffen School of Medicine, University of California, Los Angeles, Los Angeles, CA, United States, [3] Department of Neurology, David Geffen School of Medicine, University of California, Los Angeles, Los Angeles, CA, United States, [4] Department of Neurosurgery, David Geffen School of Medicine, University of California, Los Angeles, Los Angeles, CA, United States

OPEN ACCESS

Edited by:
Eleonora Palma,
Sapienza University of Rome, Italy

Reviewed by:
Laurent Venance,
INSERM U1050 Centre Interdisciplinaire de Recherche en Biologie, France
Silvia Di Angelantonio,
Sapienza University of Rome, Italy

***Correspondence:**
Carlos Cepeda
ccepeda@mednet.ucla.edu;
ccepeda@ucla.edu

Specialty section:
This article was submitted to Cellular Neurophysiology, a section of the journal Frontiers in Cellular Neuroscience

Received: 14 November 2019
Accepted: 24 February 2020
Published: 20 March 2020

Citation:
Levinson S, Tran CH, Barry J, Viker B, Levine MS, Vinters HV, Mathern GW and Cepeda C (2020) Paroxysmal Discharges in Tissue Slices From Pediatric Epilepsy Surgery Patients: Critical Role of $GABA_B$ Receptors in the Generation of Ictal Activity. Front. Cell. Neurosci. 14:54. doi: 10.3389/fncel.2020.00054

In the present study, we characterized the effects of bath application of the proconvulsant drug 4-aminopyridine (4-AP) alone or in combination with $GABA_A$ and/or $GABA_B$ receptor antagonists, in cortical dysplasia (CD type I and CD type IIa/b), tuberous sclerosis complex (TSC), and non-CD cortical tissue samples from pediatric epilepsy surgery patients. Whole-cell patch clamp recordings in current and voltage clamp modes were obtained from cortical pyramidal neurons (CPNs), interneurons, and balloon/giant cells. In pyramidal neurons, bath application of 4-AP produced an increase in spontaneous synaptic activity as well as rhythmic membrane oscillations. In current clamp mode, these oscillations were generally depolarizing or biphasic and were accompanied by increased membrane conductance. In interneurons, membrane oscillations were consistently depolarizing and accompanied by bursts of action potentials. In a subset of balloon/giant cells from CD type IIb and TSC cases, respectively, 4-AP induced very low-amplitude, slow membrane oscillations that echoed the rhythmic oscillations from pyramidal neurons and interneurons. Bicuculline reduced the amplitude of membrane oscillations induced by 4-AP, indicating that they were mediated principally by $GABA_A$ receptors. 4-AP alone or in combination with bicuculline increased cortical excitability but did not induce seizure-like discharges. Ictal activity was observed in pyramidal neurons and interneurons from CD and TSC cases only when phaclofen, a $GABA_B$ receptor antagonist, was added to the 4-AP and bicuculline solution. These results emphasize the critical and permissive role of $GABA_B$ receptors in the transition to an ictal state in pediatric CD tissue and highlight the importance of these receptors as a potential therapeutic target in pediatric epilepsy.

Keywords: pediatric epilepsy, 4-aminopyridine, phaclofen, ictal activity, cortical dysplasia, slices

INTRODUCTION

There are two major GABA receptor subtypes in the central nervous system, type A (including the A-ρ subfamily) and type B (Olsen and Sieghart, 2009). The ionotropic GABA$_A$ receptor mediates fast inhibitory neurotransmission and is preferentially localized in postsynaptic membranes. When the neurotransmitter binds the multimeric GABA$_A$ receptor, it allosterically opens a chloride ion channel leading, in most cases, to membrane hyperpolarization (Olsen and Sieghart, 2009). In contrast, the metabotropic GABA$_B$ receptor is a G protein-coupled receptor present at both pre- and post-synaptic membranes where it regulates neurotransmitter release and slow, prolonged inhibitory responses, respectively. GABA$_B$ receptors function via multiple mechanisms including inwardly rectifying K^+ channels, voltage-gated Ca^{2+} channels, and adenylyl cyclase, all of which result in either reduced neurotransmitter release or hyperpolarization of the neuron (Newberry and Nicoll, 1984; Thompson and Gahwiler, 1992; Bowery et al., 2002; Bettler et al., 2004; Frangaj and Fan, 2018). Reduced function of GABA$_A$ receptors is traditionally thought to contribute to a breakdown in inhibitory neurotransmission. Thus, GABA$_A$ receptor antagonists have been used to mimic some features of epileptic activity. However, the role of GABA$_B$ receptors in epileptogenesis, especially in humans, is less well understood.

Spontaneous paroxysmal discharges, ictal or interictal, are rarely observed in *ex vivo* slices from pediatric or adult epilepsy surgery tissue samples resected for the treatment of pharmacoresistant epilepsy. This is probably due to the elimination of long-range excitatory inputs. In our cohort of approximately 300 cases examined thus far (Cepeda et al., 2003, 2005a,b, 2006, 2012; Abdijadid et al., 2015), epileptic activity in the form of paroxysmal depolarizing shifts or spontaneous bursting was only seen in about 2% of cases and ictal activity was never recorded in cortical pyramidal neurons (CPNs). However, fast-spiking interneurons were more prone to display ictal-like activity (Cepeda et al., 2019). Also, cytomegalic interneurons in cases of severe cortical dysplasia (CD), i.e., CD type II, may generate spontaneous paroxysmal depolarizations (Andre et al., 2007). In order to induce paroxysmal discharges in tissue slices, the ionic concentrations of the bathing solution have been manipulated (e.g., Mg^{2+} removal or increased K^+ concentration), or proconvulsant agents such as GABA$_A$ receptor antagonists (bicuculline, BIC, or picrotoxin) and K^+-channel blockers [4-aminopyridine (4-AP)] have been used (Avoli et al., 1999, 2003; D'Antuono et al., 2004; Avoli and Jefferys, 2016). Of particular interest is the fact that human CD tissue is exquisitely sensitive to the proconvulsant effects of 4-AP, as this drug induces spontaneous seizures in about 50% of slices from CD, but not from mesial temporal lobe epilepsy cases (Avoli et al., 1999; D'Antuono et al., 2004).

4-Aminopyridine is an isomeric amine of pyridine and has been widely used to characterize K^+ channel subtypes. It is a powerful epileptogenic agent that acts by blocking type A/D K^+ channels (Traub et al., 1995; Mitterdorfer and Bean, 2002; Szente et al., 2002). It increases neurotransmitter release by prolonging action potential duration (Bostock et al., 1981) and in hippocampal and cortical tissue slices it also induces membrane oscillations which depend on synchronous activation of GABA receptors and facilitation of gap junctional current and/or permeability (Traub et al., 2001).

In the present study, the sensitivity of neocortical pyramidal and non-pyramidal neurons to proconvulsants 4-AP and BIC, alone or in conjunction, was tested in slices from tissue resected surgically for the treatment of refractory epilepsy in pediatric surgery patients. Pathologies included CD type I and type II, tuberous sclerosis complex (TSC, a genetic form of severe CD), and non-CD etiologies (e.g., perinatal stroke, tumor). Normal and abnormal cell types, including normal-appearing CPNs and interneurons, cytomegalic and immature pyramidal neurons, and balloon/giant cells were studied. In addition, we examined the modulatory effects of GABA$_B$ receptors on paroxysmal discharges induced by 4-AP. Taken together, the present study supports the idea that GABA$_B$ receptors play a key role in the transition from interictal to ictal activity, especially in CD cases.

MATERIALS AND METHODS

Cohort and Standard Protocol Approvals

The Institutional Review Board at the University of California Los Angeles (UCLA) approved the use of human subjects for research purposes, and parents or responsible persons signed written informed consents and HIPAA authorizations. Children undergoing resective surgery with the UCLA Pediatric Epilepsy Program to help control their medically refractory focal epilepsy were sequentially recruited from December 2002 to October 2016. For the present study, cortical tissue samples from four groups of etiologies were included; CD type I, CD type IIa/b (Blumcke et al., 2011; Guerrini et al., 2015), TSC, and non-CD etiologies including tumor, infarct, Sturge–Weber syndrome (SWS), polymicrogyria, multicystic encephalopathy, Aicardi syndrome, and three cases with mild, undetermined cortical pathology.

Electrocorticography and Surgical Resection

The site and margin of the surgical resection were based on recommendations from a multidisciplinary meeting after careful consideration of the presurgical evaluation of each patient, as previously described (Cepeda et al., 2003, 2005b, 2014, 2019). For the four groups of etiologies, our goal was complete resection of the epileptogenic zone primarily defined by non-invasive testing (Lerner et al., 2009; Hemb et al., 2010), including video-EEG capturing ictal events, high-resolution magnetic resonance imaging (MRI), and ^{18}-fluorodeoxyglucose positron emission tomography (FDG-PET), as well as magnetic source imaging and co-registration of MRI and FDG-PET when the initial battery of tests was inconclusive (Salamon et al., 2008).

Slice Preparation and Electrophysiological Recordings

After surgical resection, the tissue samples were immediately immersed in ice-cold artificial cerebrospinal fluid (ACSF)

enriched with sucrose for better preservation and then expeditiously hand-carried out of the operating room and transported directly to the laboratory within 5–10 min. The high sucrose-based slicing solution contained (in mM): 208 sucrose, 10 glucose, 26 $NaHCO_3$, 1.25 NaH_2PO_4, 2.5 KCl, 1.3 $MgCl_2$, 8 $MgSO_4$. Coronal slices (300 μm) were cut and transferred to an incubating chamber containing ACSF (in mM): 130 NaCl, 3 KCl, 1.25 NaH_2PO_4, 26 $NaHCO_3$, 2 $MgCl_2$, 2 $CaCl_2$, and 10 glucose) oxygenated with 95% O_2–5% CO_2 (pH 7.2–7.4, osmolality 290–310 mOsm/L, 32–34°C). In selected experiments, the ACSF solution was modified to reduce the amount of glucose and introduce additional energy substrates, i.e., ketones and pyruvate, more akin to those used by developing brains (Holmgren et al., 2010; Zilberter et al., 2010). This bathing solution, also known as enriched ACSF (eACSF) contained (in mM): 130 NaCl, 3 KCl, 1.25 NaH_2PO_4, 26 $NaHCO_3$, 2 $MgCl_2$, 2 $CaCl_2$, 5 glucose, 5 Na pyruvate, 2 Na 3-hydroxybutyrate (BHB). Slices were allowed to recover for an additional 60 min at room temperature prior to recording. All recordings were performed at room temperature using an upright microscope (Olympus BX51WI) equipped with infrared-differential interference contrast (IR-DIC) optics.

Whole-cell patch clamp recordings in voltage- or current-clamp modes were obtained from different cell types (layers II–V) visualized with IR-DIC (Cepeda et al., 2012). The patch pipette (3–5 MΩ resistance) contained a cesium-based internal solution (in mM): 125 Cs-methanesulfonate, 4 NaCl, 1 $MgCl_2$, 5 MgATP, 9 EGTA, 8 HEPES, 1 GTP-Tris, 10 phosphocreatine, and 0.1 leupeptin (pH 7.2 with CsOH, 270–280 mOsm/L) for voltage clamp recordings. K-gluconate-based solution containing (in mM): 112.5 K-gluconate, 4 NaCl, 17.5 KCl, 0.5 $CaCl_2$, 1 $MgCl_2$, 5 ATP, 1 NaGTP, 5 EGTA, 10 HEPES, pH 7.2 (270–280 mOsm/L) was used for current clamp recordings. After breaking the seal, basic cell membrane properties (capacitance, input resistance, decay time constant) were recorded while holding the membrane potential (V_h) at −70 mV. Electrode access resistances during whole-cell recordings were less than 25 MΩ (range 8–25 MΩ). Electrodes also contained 0.2% biocytin in the internal solution to label recorded cells. Proconvulsant drugs included 4-AP (100 μM), BIC (10–20 μM), and the GABA$_B$ receptor antagonist phaclofen (6–25 μM). In voltage and current clamp modes, the latency, frequency, and amplitude of 4-AP oscillations were measured using the Clampfit software (v 10.3). As all slices were treated with 4-AP, alone or in combination with other drugs, the number of cells recorded is equivalent to the number of slices.

Statistics

In the text and figures, results are expressed as mean ± SEM. For group comparisons, we used one-way ANOVA (with Bonferroni correction) or if normality failed the Kruskal–Wallis ANOVA on Ranks with pairwise multiple comparisons (Dunn or Holm–Sidak methods) was used. For simple comparisons between two groups, we used the Student's *t*-test and for comparisons between proportions the Chi-square test was used. SigmaStat (3.5) software was used for all statistical analyses. Differences were deemed statistically significant if $p < 0.05$.

RESULTS

Cohort

The number of cases included in the present study, their pathologies, and the number of cells recorded separated by type are shown, in abridged form, in **Table 1**. The average age of the pediatric population examined, regardless of pathology, was 3 ± 0.43 years (n = 80, 45 male and 35 female). There was a strong trend for CD patients to be younger than patients with TSC or non-CD pathologies, but the difference did not reach statistical significance (p = 0.056). Similarly, the average age of CD type I (2.5 ± 0.26 year, n = 18, 13 male and five female) and type II (2.4 ± 0.26 year, n = 28, 13 male and 15 female) cases or the TSC (3.6 ± 0.43 year, n = 18, 11 male and seven female) and non-CD (3.9 ± 0.35 year, n = 16, eight male and eight female) cases were not significantly different between them. In all cases, histopathological analyses confirmed initial clinical and imaging diagnoses. At the time of surgery, patients were taking antiepileptic drugs (AEDs) to control seizures. AEDs included topiramate, clonazepam, phenobarbital, lamotrigine, zonisamide, carbamazepine, or adrenocorticotropic hormone.

Pathological Findings

In patients with CD type I and type II histopathological analyses confirmed changes consistent with the ILAE consensus classification of FCDs (Blumcke et al., 2011). In CD type I these included moderate to severe neuronal disorganization, heterotopic neurons in the white matter, mild neuronal crowding and, in some cases, blurring of the gray–white matter junction. In patients with CD type II, in addition to neuronal disorganization, dysmorphic, cytomegalic neurons (IIa) and balloon cells (IIb) also occurred. TSC cases displayed giant cells and dysmorphic cytomegalic neurons. Severe neuronal disorganization and heterotopic neurons in the white matter were also observed. Non-CD pathologies included; six infarct cases, two patients had a cystic infarct with gliosis, one patient had multiple cortical and subcortical white matter infarcts with marked neuronal loss, two other patients had some neuronal crowding but no evidence of dyslamination, while the remaining patient had some scattered heterotopic neurons in the white matter. The two SWS cases showed pronounced leptomeningeal angiomatosis, with predominantly thin-walled, venous channels. The tumor case had a small oligodendroglial hamartoma. Additionally, one case presented with multicystic encephalopathy, one with Aicardi syndrome without evidence of CD, and two cases presented with

TABLE 1 | Pediatric epilepsy cohort.

Pathology (cases)	Age (years)	Pyramidal cells	Interneurons	Balloon/ giant cells
CD type I (n = 18)	2.9 ± 0.6	59	5	–
CD type II (n = 28)	2.5 ± 0.4	66	10	4
TSC (n = 18)	3.1 ± 0.6	45	1	6
Non-CD (n = 16)	3.6 ± 0.6	44	5	–
Total (n = 80)	3.0 ± 0.3	214	21	10

polymicrogyria and pachygyria. Finally, in three cases, there was no definitive histopathological diagnosis. The first two showed varying amounts of heterotopic neurons in the white matter, and the third had a right ventricular cyst and showed gliosis of the ventricular wall and nodular gray matter but no signs of dysplastic changes.

Cell Types and Basic Membrane Properties

All cells (n = 245) were recorded using the whole-cell patch clamp configuration in both current clamp (n = 69) and voltage clamp (n = 176) modes. Basic membrane properties, including cell capacitance, input resistance, and decay time constant were determined in voltage clamp mode. Cells were recorded in layers II/V from frontal, parietal, and temporal areas. As expected, the most abundant cell type in our cohort was normal-appearing CPNs (n = 182). In CD types I and IIa/b and in TSC cases, additional cell types were observed including dysmorphic/cytomegalic pyramidal neurons (n = 17), immature-looking pyramidal neurons (n = 15), and balloon/giant cells (n = 4 in CD type IIb and n = 6 in TSC cases) (Blumcke et al., 2011; Guerrini et al., 2015). Giant cells have morphological and electrophysiological properties that are similar to those of balloon cells (Cepeda et al., 2003; Jozwiak et al., 2006; Grajkowska et al., 2008; Abdijadid et al., 2015). Balloon/giant cells appear to be enlarged astrocytes but in the cerebral cortex, they can also express neuronal markers (Cepeda et al., 2003, 2010; Jozwiak et al., 2006). A small number of interneurons were observed across the different pathologies (n = 21, including one cytomegalic interneuron in a CD type IIb case with associated hemimegalencephaly) (**Table 1**).

Statistically significant differences in basic cell membrane properties were observed among the different cell types ($p < 0.001$, one-way ANOVA on Ranks, see details in **Figure 1** legend). In particular, normal-appearing CPNs had larger capacitance and lower input resistance than cortical interneurons. Similarly, cytomegalic CPNs had larger capacitance and lower input resistance than normal-appearing and immature CPNs. The Resting Membrane Potential (RMP) was calculated in a subset of cells recorded in current clamp mode. Significant differences were found among the main cell types (p = 0.001, one-way ANOVA followed by pairwise multiple comparison procedures, Holm–Sidak method). The RMP of cortical interneurons (−60 ± 1.1 mV, n = 12) was more depolarized than that of normal-appearing CPNs (−66.3 ± 1.2 mV, n = 52) (p = 0.02). In addition, the RMP of balloon/giant cells (−76.8 ± 3.9 mV, n = 5) was more hyperpolarized than that of both CPNs (p = 0.015) and interneurons ($p < 0.001$).

4-AP Oscillations in Different Cortical Cell Types in CD, TSC, and Non-CD Cases

Bath application of 4-AP (100 μM) initially increased the frequency of spontaneous glutamatergic and GABAergic synaptic events. The magnitude of this increase in frequency was calculated in a small sample of CPNs using the MiniAnalysis software (Synaptosoft). At a holding potential of −70 mV (to isolate glutamatergic events), the frequency of spontaneous glutamatergic events increased from 1.5 ± 0.3 to 5.7 ± 0.9 Hz (p = 0.001, n = 7 CPNs), whereas at + 10 mV (to isolate GABAergic events) it increased from 4.2 ± 0.5 to 8.5 ± 0.6 Hz ($p < 0.001$, n = 25 CPNs). After a latency of about 2–3 min 4-AP induced large-amplitude, rhythmic membrane oscillations. It has been postulated that 4-AP oscillations are the result of synchronous activation of GABA receptors and facilitation of gap junctional currents and/or permeability (Traub et al., 2001). Without ruling out completely the contribution of gap junctions, we found that 4-AP oscillations were synaptically mediated as blockade of Na^+ channels with tetrodotoxin (TTX, 1 μM) or blockade of Ca^{2+} channels with cadmium (100 μM) abolished these membrane oscillations (**Supplementary Figure S1**).

Almost all CPNs and interneurons (n = 221) displayed 4-AP oscillations of variable frequency and amplitude. A small subset of neurons (n = 14) did not display oscillations or they were negligible. These cells occurred generally in the youngest cases (three CD type I, five CD type II, two TSC, and two non-CD; mean age 1.2 ± 0.3 year, range 0.3–3 year). Most were normal-appearing CPNs (n = 8), four were immature pyramidal neurons, and two were interneurons based on electrophysiological and morphological properties.

In current clamp mode (K-gluconate in the patch pipette), CPNs displayed three main types of 4-AP oscillations at RMP (**Figure 2**). Provided CPNs had an RMP more negative than the chloride reversal potential, the oscillation was purely depolarizing (n = 20 cells). The average depolarization amplitude was 10.8 ± 1 mV and if the depolarization was large enough it could elicit scattered action potentials. A few CPNs (n = 10) displayed small amplitude oscillations that were hyperpolarizing (average amplitude −5.1 ± 1 mV). At more depolarized potentials (around −60 mV) CPNs displayed biphasic responses (n = 13), equally divided between depolarization followed by hyperpolarization, or vice versa. In contrast, 4-AP oscillations in cortical interneurons (n = 13, including three FSI, nine non-FSI, and one cytomegalic interneuron) were consistently depolarizing and, in almost all cases, accompanied by bursts of action potentials. These bursts were also seen in voltage clamp mode (V_h = −70 mV). This suggests that 4-AP oscillations in CPNs are primarily triggered by rhythmic bursting of cortical interneurons.

In CD type IIb (n = 4) and TSC (n = 5) cases 10 balloon/giant (n = 4 and 6, respectively) cells were recorded. As previously described, these cells share similar morphological and electrophysiological properties including lack of inward Na^+ or Ca^{2+} currents and no synaptic inputs but prominent K^+ currents (Cepeda et al., 2003). We tested the effects of 4-AP on these cells. Most cells did not display any obvious effect. However, four cells (three from two CD type IIb cases and one from a TSC case) displayed very slow (3.75 ± 0.3/min), low-amplitude membrane depolarizations (2.1 ± 0.4 mV in current clamp) or inward currents (8.3 ± 2 pA in voltage clamp) (**Supplementary Figure S2**), suggesting they could be sensing K^+ elevations induced by 4-AP. The function of these oscillations remains unknown, but it is possible that they may be buffering increases

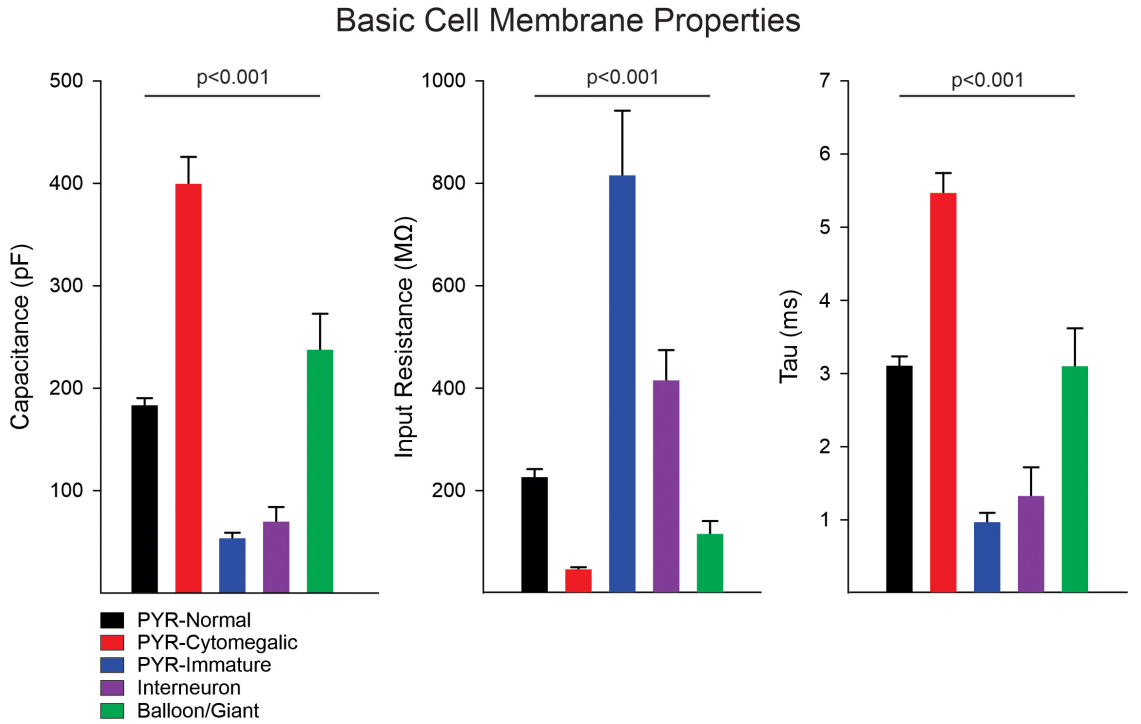

FIGURE 1 | Membrane properties of the different cell types. Measurement of basic cell membrane properties (capacitance, input resistance, and time constant) in voltage clamp mode demonstrated statistically significant differences among cell groups ($p < 0.001$, one-way ANOVA on Ranks). The cell capacitance of cytomegalic pyramidal neurons was significantly larger than that of normal CPNs, immature pyramidal neurons, and interneurons (all at $p < 0.001$, pairwise multiple comparisons using Dunn's method), whereas it was not different from that of balloon/giant cells ($p = 0.3$). Similarly, the cell capacitance of normal CPNs and balloon/giant cells was larger than that of interneurons and immature CPNs (both at $p < 0.001$). Comparison of cell capacitance between balloon/giant cells and normal CPNs or that between interneurons and immature CPNs was not significantly different. In contrast, the membrane input resistance of cytomegalic CPNs was significantly lower than that of normal and immature CPNs, as well as interneurons (all at $p < 0.001$). The input resistance of cytomegalic and normal CPNs compared with balloon/giant cells was not significantly different (both at $p = 0.6$). Immature CPNs had significantly higher input resistance compared with that of normal CPNs and balloon/giant cells (both at $p < 0.001$) but not different from that of cortical interneurons. Finally, the input resistance of interneurons was significantly higher than that of balloon/giant cells ($p = 0.004$) and normal CPNs ($p = 0.02$). The differences in time constant were similar to those in cell capacitance, except for the comparison between cytomegalic CPNs and balloon/giant cells, which was significantly lower in the latter ($p < 0.05$).

in K^+ caused by 4-AP-induced paroxysmal activity, acting as a retardant of network synchrony.

4-AP Oscillations in CPNs and Interneurons From Different Pathologies

No significant difference was found in the frequency of 4-AP oscillations of CPNs regardless of pathology, although there was a trend for CPNs from CD type II cases to display higher frequencies (**Figure 3A**, upper graphs). The lowest frequencies were observed in CPNs from TSC cases. The frequency range among CPNs was between 2 and 29 oscillations/min. Cells with the highest frequencies ($\geq$15 oscillations/min) were consistently found in CD type I (5.3%) and II (11.5%) and TSC (4.8%) cases compared with non-CD cases (2.4%). Although overall the difference in proportions among groups was not statistically significant, the difference between the CD type II and the non-CD groups almost reached statistical significance ($p = 0.09$, Chi-square test). Interestingly, the latency to the first oscillation was significantly different among groups ($p = 0.002$, Kruskal–Wallis one-way analysis of variance on Ranks). *Post hoc* pairwise multiple comparisons showed that the latency in the CD type I group was significantly longer than that of the non-CD group ($q = 3.3$) and the TSC group ($q = 2.9$) (**Figure 3A**, lower graphs). This suggests that network synchrony requires more time when there is cortical disorganization or as a result of the presence of abnormal cells, at least for the CD type 1 and non-CD group comparison. This does not explain, however, why the latency in the TSC group was also decreased. Finally, there was no significant correlation between frequency and latency of 4-AP oscillations with age, only a small trend for frequency to increase and latency to decrease with age (**Figure 3B**).

Electrophysiological Characterization of 4-AP-Induced Membrane Oscillations in Pediatric Epilepsy Tissue Samples

4-Aminopyridine oscillations in pediatric cortical tissue are primarily mediated by activation of GABA$_A$ receptors, based on electrophysiological and pharmacological observations. In whole-cell current clamp mode (K-gluconate in the patch pipette), 4-AP oscillations in CPNs were mostly depolarizing

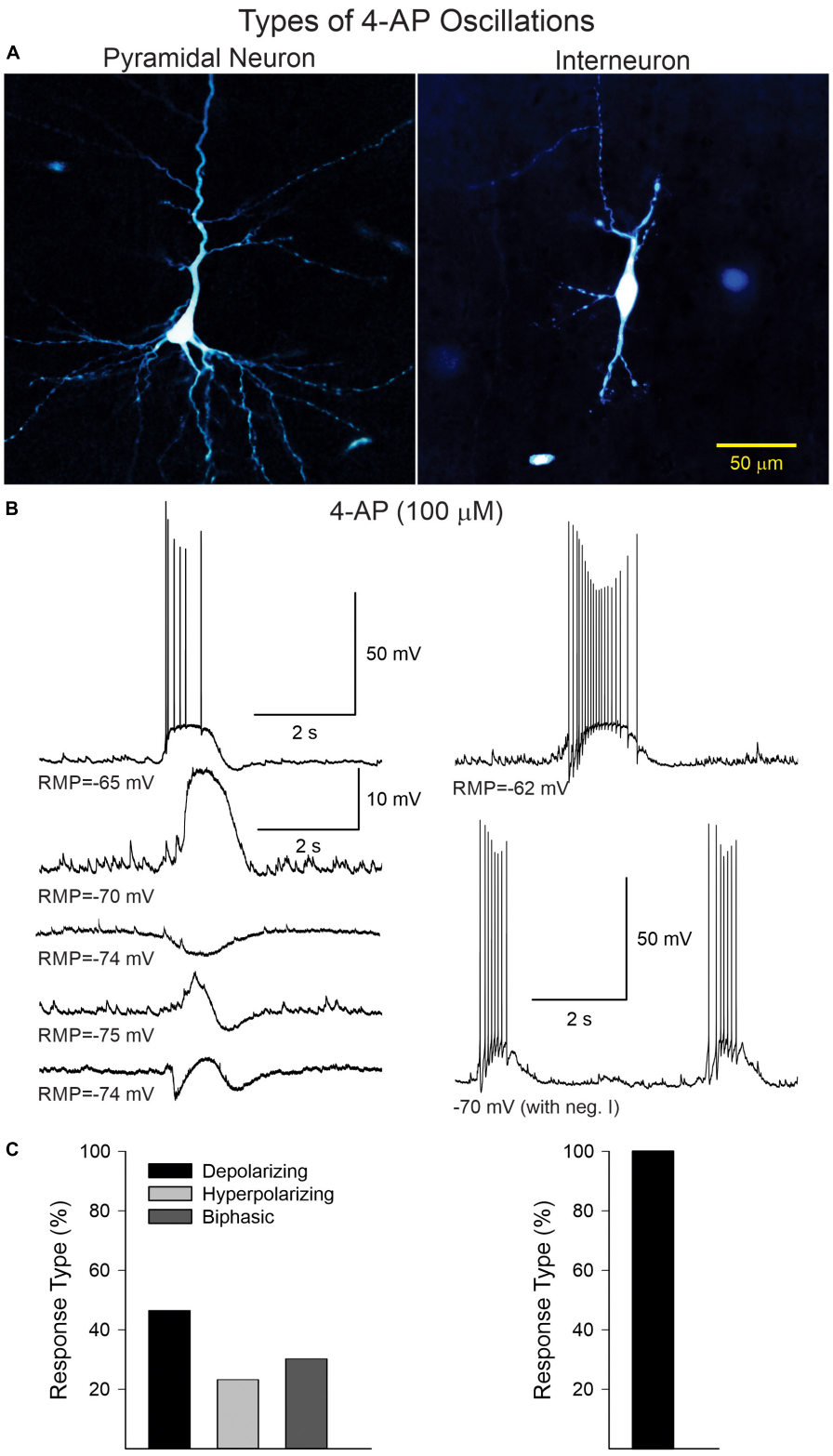

FIGURE 2 | (A) Examples of a CPN and an interneuron recorded and filled with biocytin. **(B)** Current clamp recordings illustrating the different types of 4-AP oscillations in CPNs and interneurons. In CPNs, 4-AP induced three main types of oscillations; most were depolarizing, with or without action potentials, some were mainly hyperpolarizing, and others were biphasic (depolarization followed by hyperpolarization or vice versa). In interneurons, 4-AP consistently induced membrane depolarizations accompanied by bursts of action potentials, even at hyperpolarized potentials (with negative current). **(C)** Bar graphs show the percentage of cells displaying the different types of oscillations in CPNs and interneurons.

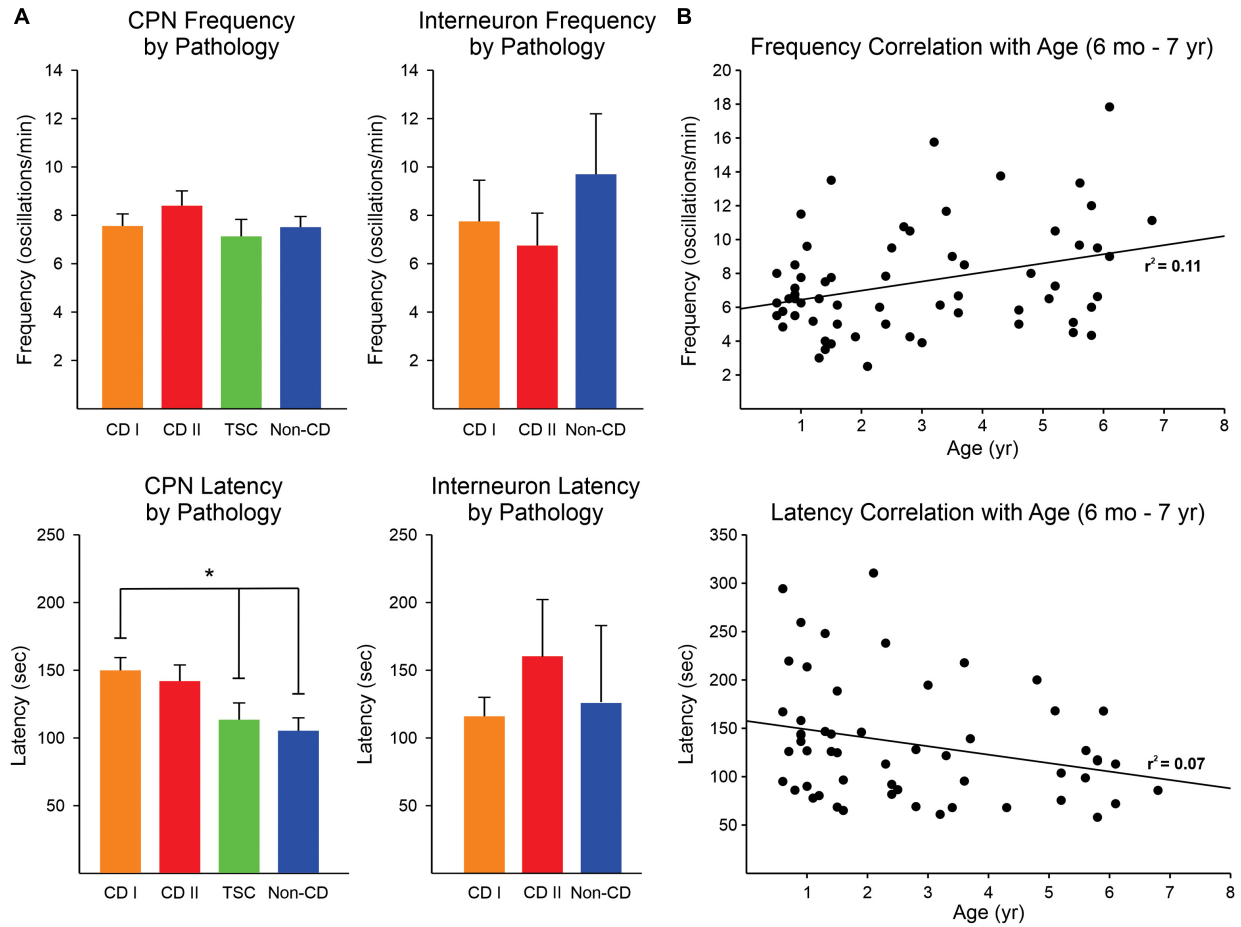

FIGURE 3 | Frequency and latency of 4-AP oscillations by pathology. **(A)** No difference was observed in the frequency of 4-AP oscillations in CPNs and interneurons among pathologies, only a trend for higher frequency of oscillations in CPNs in the CD type II group (upper panels). The latency for the first occurrence of 4-AP oscillations in CPNs was significantly increased in CD type 1 cases compared with non-CD and TSC cases (lower panels) ($p < 0.05$, one-way ANOVA with Bonferroni correction). CD type II cases also had a strong trend for longer latencies. No difference in latency among groups occurred in interneurons. In TSC, only one interneuron was recorded, so this group was not included in the graphs. **(B)** Correlations between frequency and latency of 4-AP oscillations with age. There was a minimal, non-significant correlation between age and frequency/latency of 4-AP oscillations. *$p < 0.05$.

at RMP (usually around −70 mV). However, when the membrane was more depolarized (around −54 mV or less), the oscillation became hyperpolarizing. The estimated reversal potential occurred at approximately −57 mV, which corresponds to the chloride equilibrium potential in our recording conditions. This observation was confirmed in voltage clamp recordings. At a holding potential of + 10 mV, the 4-AP oscillations in CPNs (including normal-appearing, cytomegalic, and immature) were manifested as large outward currents (mean = 904.3 ± 49 pA, n = 120). No statistically significant difference in amplitude was observed among pathologies (p = 0.8, one-way ANOVA). The amplitude of the oscillation decreased as a function of the holding potential. At −70 mV holding potential the currents were small and, in most cases, became inward (mean = −103.6 ± 12 pA, n = 31). The estimated reversal potential also was around −57 mV (**Figure 4**). This value corresponds to our previous estimates for GABA$_A$ receptor-mediated responses (Cepeda et al., 2007, 2014). Further, during the 4-AP oscillation, the cell membrane input resistance decreased, probably as a result of the shunting inhibition mediated by GABA$_A$ receptors.

Effects of BIC, a GABA$_A$ Receptor Antagonist, on 4-AP Oscillations and Cortical Excitability

Supporting the idea that 4-AP oscillations were mainly GABAergic and mediated by GABA$_A$ receptors, the addition of BIC greatly reduced their amplitude and, in some cases, it eliminated them completely (**Figure 5A**). Similarly, BIC reduced the amplitude of 4-AP oscillations and bursting observed in cortical interneurons (**Figure 5B**).

An interesting observation was that in CPNs bath application of BIC reversed the polarity of the oscillations, i.e., in current clamp mode the membrane depolarization converted into a hyperpolarization (**Supplementary Figure S3**) and in voltage

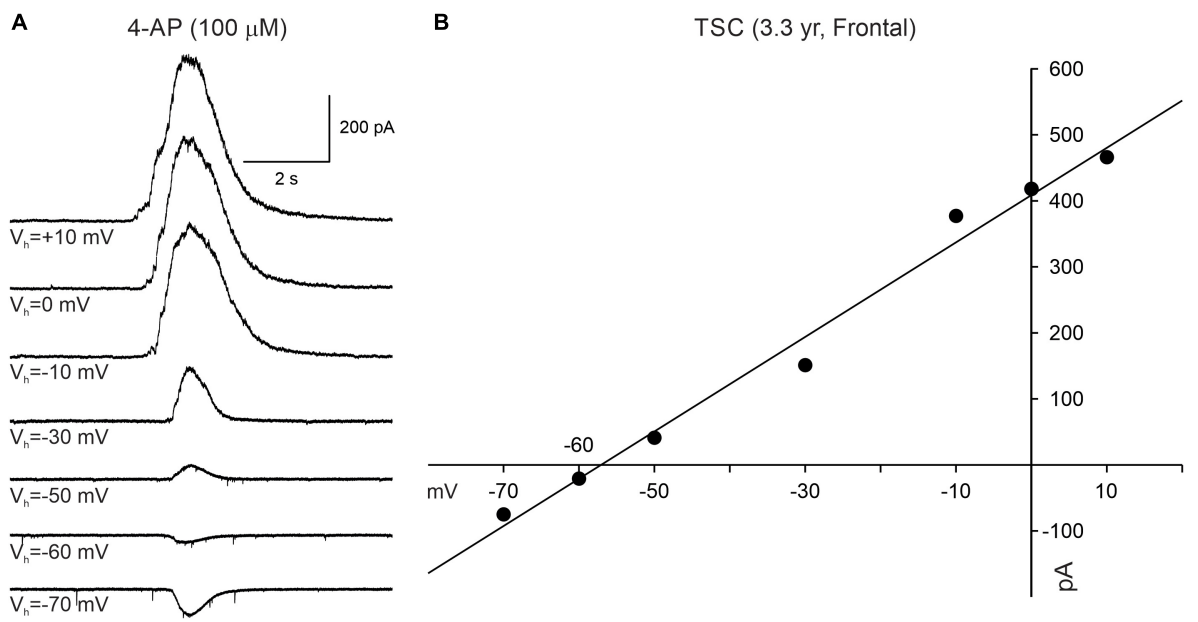

FIGURE 4 | Reversal potential of 4-AP oscillations in CPNs recorded in voltage clamp mode. **(A)** Traces show voltage clamp recordings of a CPN. After 4-AP oscillations were induced, the holding potential was changed from + 10 to −70 mV. The amplitude of the 4-AP oscillation decreased from +10 to −50 mV and reversed between −60 and −70 mV. **(B)** The IV relationship of the 4-AP oscillation determined that the equilibrium potential occurred around −57 mV, corresponding to the predicted chloride equilibrium potential based on our internal patch solution.

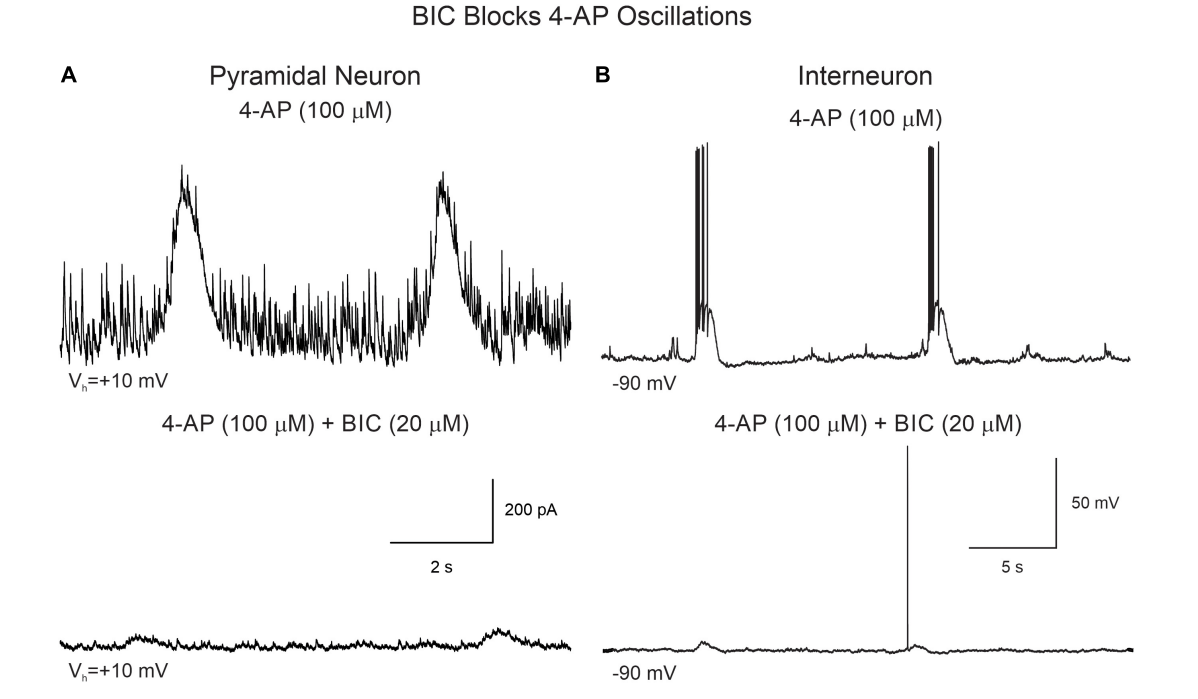

FIGURE 5 | BIC reduces the amplitude of 4-AP oscillations in CPNs and interneurons. **(A)** CPN recorded in voltage clamp mode (+10 mV holding potential). After stable 4-AP oscillations were induced (upper trace), bath application of BIC (20 μM) significantly reduced the amplitude of the oscillations (lower trace). **(B)** 4-AP oscillations and bursting were induced in this interneuron recorded in current clamp mode. The cell was hyperpolarized to −90 mV by injecting negative current to prevent spontaneous firing. After BIC application, membrane depolarization amplitude and bursting were reduced.

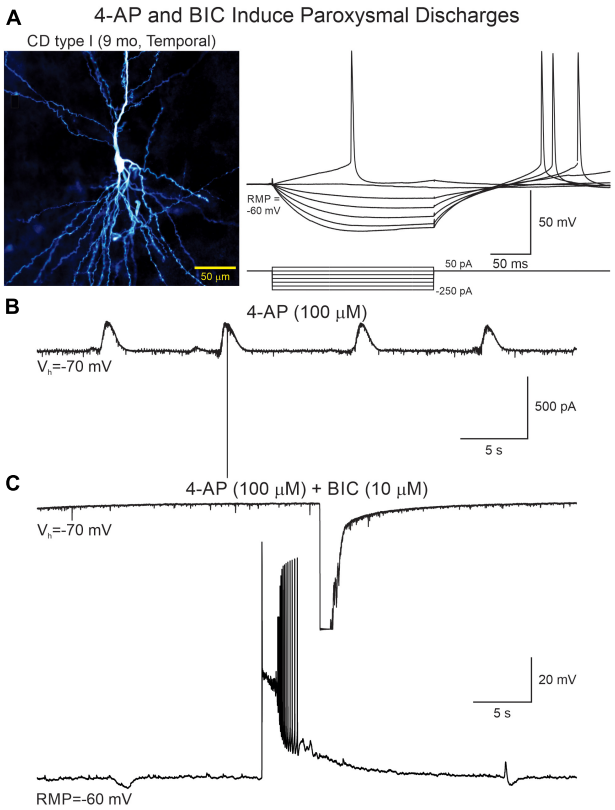

FIGURE 6 | 4-AP and BIC increase network excitability. **(A)** A CPN from a CD type I case was recorded in current and voltage clamp modes. Left panel shows the cell after biocytin processing. Right panel shows voltage changes induced by hyperpolarizing and depolarizing current pulses. **(B)** After addition of 4-AP rhythmic oscillations with scattered action potentials were seen. **(C)** Addition of BIC eliminated the 4-AP oscillations but simultaneously increased network excitability as demonstrated by the generation of paroxysmal discharges recorded in both voltage clamp (top trace, truncated due to saturation) and current clamp (lower trace).

clamp (V_h = −70 mV) the inward current became outward. This suggested there is another minor component of the 4-AP oscillation, which is not mediated by GABA$_A$ receptors. As in voltage clamp this component was outward-going, it seemed unlikely it was mediated by glutamate receptors. Further, it could occur in the presence of glutamate receptor antagonists CNQX (10 µM) and APV (50 µM). Importantly, while GABA$_A$ receptor antagonists such as BIC reduced the amplitude of 4-AP oscillations, they also increased overall network excitability as demonstrated by the sporadic occurrence of paroxysmal discharges (**Figure 6** and **Table 2**).

Effects of Phaclofen, a GABA$_B$ Receptor Antagonist, on 4-AP Oscillations and Cortical Excitability

We attempted to determine the reversal potential of the remnant current persisting after BIC application and found that its amplitude decreased as a function of cell membrane hyperpolarization until it reversed around −85 mV (**Figure 7A**),

TABLE 2 | Effects of 4AP + BIC.

Pathology	Cases	Cell type	No PDs	Isolated PDs/ bursts of APs	Repetitive PDs	Ictal-like activity
CD type I	7	Pyr (*n* = 10)	4	5	1	–
		Inter (*n* = 2)	1	1	–	–
CD type II	13	Pyr (*n* = 19)	7	11	1	–
		Inter (*n* = 4)	3	–	1	–
TSC	6	Pyr (n = 11)	4	7	–	–
		Inter (*n* = 0)	0			
Non-CD	5	Pyr (*n* = 11)	4	7	–	–
		Inter (*n* = 0)	0			
Total	31	Pyr (*n* = 51)	19	30	2	0
		Inter (*n* = 6)	4	1	1	0

PD = paroxysmal discharges. AP = action potentials. Pyr = pyramidal neuron. Inter = interneuron.

strongly indicating it was mediated by K^+ channels, in particular, inwardly rectifying K^+ channels such as those in the Kir3 family (Mott, 2015). As GABA$_B$ receptors are linked to Kir channels, this suggested that 4-AP membrane hyperpolarizations occurring after GABA$_A$ receptor antagonism could be mediated by activation of GABA$_B$ receptors. In support, the GABA$_B$ receptor antagonist phaclofen (6–10 µM) obliterated this remnant current (**Figure 7B**).

In spite of inducing interictal-like membrane oscillations and enhancing overall cortical excitability, 4-AP and BIC were not sufficient, in our recording conditions, to induce ictal activity. A previous report showed that in human CD tissue GABA$_B$ receptors play an important role in epileptogenesis as baclofen blocks paroxysmal discharges induced by 4-AP (D'Antuono et al., 2004). Thus, to confirm this observation, we tested the effects of a GABA$_B$ antagonist, phaclofen on 4-AP oscillations. This selective GABA$_B$ receptor antagonist which, as shown previously, reduced the amplitude of 4-AP oscillations, further enhanced cortical excitability and induced ictal-like activity.

Phaclofen (10–25 µM) was tested in 21 neurons (16 CPNs and five interneurons) from nine cases (three CD type I, one CD type II, four TSC, and one non-CD). At the low concentration, no enhancement of paroxysmal discharges generated by 4-AP and BIC were seen in 10 cells. In the remainder, phaclofen showed a clear proconvulsant effect. At the low concentration (10 µM), it facilitated the induction of paroxysmal discharges and/or increased burst duration (*n* = 6) (**Figure 8**). At the high concentration (20–25 µM), it induced ictal-like activity in three CPNs (**Figure 9**) and two interneurons (**Figure 10**). In those cells, 14 ictal-like episodes were captured and had an average duration of 21 ± 9 s (range 1.4–105 s). Ictal discharges were only seen in CD and TSC cases but not in the non-CD case. A comparison between the effects of combined drug application of 4-AP + BIC and 4-AP + BIC + Phaclofen demonstrated significantly higher epileptogenicity when the GABA$_B$ receptor antagonist was present (**Tables 2**, **3**). In 4-AP + BIC, 40.3% of neurons did not present with paroxysmal discharges (besides 4-AP oscillations), 54.4% showed isolated paroxysmal discharges

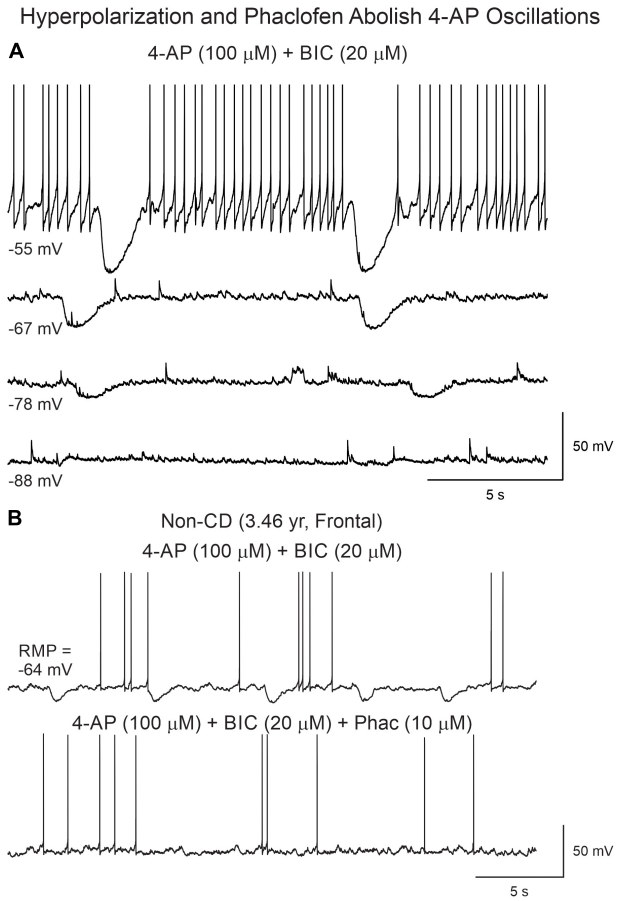

FIGURE 7 | Reversal potential of 4-AP oscillations after BIC. **(A)** With increasing membrane hyperpolarization, by injection of negative current, the amplitude of the oscillation was reduced and reversed around −85 mV, suggesting involvement of K^+ conductances, as expected if GABA$_B$ receptors were activated. **(B)** Supporting this idea, addition of the GABA$_B$ receptor antagonist phaclofen eliminated the 4-AP oscillation.

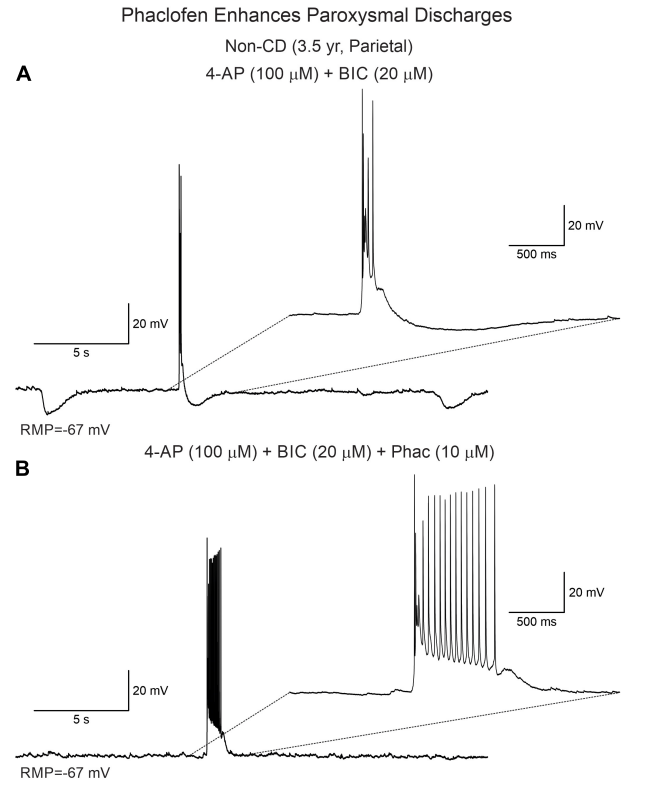

FIGURE 8 | Phaclofen enhances paroxysmal activity. **(A)** In current clamp mode, paroxysmal discharges were induced by combined application of 4-AP and BIC. **(B)** After addition of phaclofen, burst duration was increased.

or bursts of action potentials, and only 5.3% displayed repetitive paroxysmal discharges. No cells exhibited ictal-like activity. In contrast, after addition of phaclofen, all cells showed paroxysmal activity; 61.9% displayed isolated discharges or bursts of action potentials, 14.3% showed repetitive paroxysmal discharges, and 23.8% presented with ictal-like activity. The difference between groups was statistically significant ($p < 0.001$, Chi-square test).

Finally, at the low concentration, phaclofen also enhanced paroxysmal discharges induced in 0 Mg^{2+} external solution in a CPN from a CD type II case (**Supplementary Figure S4**). This provided further proof that antagonism of GABA$_B$ receptors facilitates epileptic activity, particularly in CD cases.

Effects of eACSF (BHB and Pyruvate) on 4-AP Oscillations

It has been reported that eACSF, with BHB and pyruvate added, can reduce the depolarizing/excitatory actions of GABA in early development (Holmgren et al., 2010). In consequence, we tested the effects of eACSF on 4-AP oscillations in eight cases ($n = 4$ CD type I, 1 TSC, and 3 non-CD). Surprisingly, within minutes after changing the external solution from regular ACSF to eACSF (BHB and pyruvate), the frequency and/or amplitude of 4-AP oscillations was reduced in all, except 1, CPNs tested ($n = 15$, including three immature-looking pyramidal neurons) (**Supplementary Figure S5**). This suggests that addition of these energy substrates could have antiepileptic effects.

DISCUSSION

In the present study, we used cortical tissue samples from pediatric epilepsy surgery patients to examine CPN and interneuron sensitivity to proconvulsant drugs including 4-AP, as well as GABA$_A$ and GABA$_B$ receptor antagonists. 4-AP induced membrane oscillations that were mediated primarily by synaptic activity as TTX and cadmium abolished these oscillations. Cells from cases presenting with CD or TSC displayed enhanced sensitivity to proconvulsant drugs compared with non-CD cases. We also found that a subset of balloon/giant cells from CD type IIb and TSC cases can sense K^+ surges induced by 4-AP. In addition, we demonstrate the critical and permissive role of GABA$_B$ receptors in the transition to the ictal state in CD and TSC tissue, but not in non-CD tissue. These findings emphasize

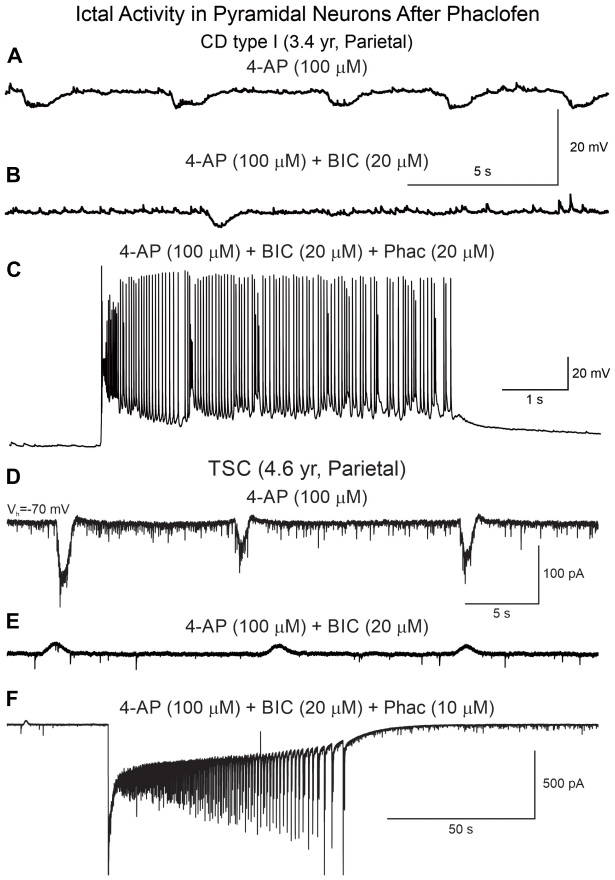

FIGURE 9 | Phaclofen favors the transition to ictal-like discharges in CPNs. **(A)** Membrane oscillations were induced by 4-AP (top trace). **(B)** After BIC, the oscillations were reduced. **(C)** Addition of phaclofen to the mix generated ictal-like discharges. **(D)** In voltage clamp mode, 4-AP induced rhythmic inward currents. **(E)** After addition of BIC, the currents became outward and the amplitude was reduced. **(F)** Phaclofen in combination with 4-AP and BIC induced ictal-like activity.

the importance of using *in vitro* slice preparations from human tissue to discern potential and selective new therapies in pediatric patients with intractable epilepsy from CD, TSC, and non-CD pathologies.

In slices from pediatric epilepsy cases, spontaneous interictal and/or ictal activities occur very rarely at the single-cell level, even when the sample is from the most epileptogenic area. This is probably due to the fact that tissue slices represent a reduced preparation lacking long-range excitatory inputs. However, in our hands, spontaneous paroxysmal discharges and ictal-like activity can be recorded from some GABAergic interneurons (Andre et al., 2007; Cepeda et al., 2019). In order to enhance CPN excitability, proconvulsant agents have been used traditionally. In particular, studies in human brain tissue have demonstrated the exquisite sensitivity of CD tissue samples to 4-AP, a K^+-channel blocker that increases neurotransmitter release by prolonging action potential duration (Buckle and Haas, 1982; Avoli et al., 2003). 4-AP produces neuronal synchrony manifested by rhythmic membrane oscillations caused by synchronous GABA release from interneurons and possibly also by increases in gap junctional currents and/or permeability (Traub et al., 1995; Traub et al., 2001; Szente et al., 2002). Here, in pediatric epilepsy cases, we confirmed the principal role of GABA$_A$ receptors in the induction of 4-AP oscillations, as blockade of these receptors with BIC greatly reduced their amplitude. However, network excitability was increased further as demonstrated by the occurrence of paroxysmal discharges, likely mediated by activation of glutamate receptors. Notably BIC, in combination with the GABA$_B$ receptor antagonist, phaclofen abolished 4-AP oscillations while simultaneously allowing the transition from an interictal to an ictal state in both CPNs and interneurons, particularly from CD and TSC cases.

GABA$_B$ receptors have been largely neglected compared to GABA$_A$ receptors in the treatment of epileptic patients. Most studies on epileptogenic mechanisms have concentrated on studying the role of GABA$_A$ receptors due to their ability to produce fast inhibition of excitatory neurons. Their potential to induce excitatory effects has also been examined profusely in developing brains (Ben-Ari, 2014, 2015). In contrast to GABA$_A$ receptors, which can mediate depolarizing and potentially excitatory actions, activation of postsynaptic GABA$_B$ receptors is always inhibitory. However, studies on the role of GABA$_B$ receptors in epileptogenesis are much more limited but their importance is becoming more and more recognized (Craig and McBain, 2014). The present study in pediatric epilepsy surgery patients confirms experimental data showing that GABA$_B$ receptors play a key role in the transition from interictal to ictal activity (Swartzwelder et al., 1987; Watts and Jefferys, 1993; Scanziani et al., 1994). They are also in line with multitude experimental studies demonstrating that antagonism of GABA$_B$ receptors is epileptogenic (Badran et al., 1997; Sutor and Luhmann, 1998; Prosser et al., 2001; Motalli et al., 2002; Uusisaari et al., 2002). In another study, it was shown that GABA$_B$ receptors also control the depolarizing response mediated by GABA$_A$ receptors as blocking GABA$_B$ receptors makes this depolarization excitatory and proconvulsant (Kantrowitz et al., 2005).

Another novel finding was that balloon/giant cells can also display membrane oscillations, suggesting that these undifferentiated cells, with variable expression of glial and neuronal markers (Cepeda et al., 2003; Jozwiak et al., 2006; Blumcke et al., 2011), can sense K^+ accumulations. The oscillations in balloon/giant cells were significantly smaller and slower than those in CPNs and interneurons. At present, it remains unknown what the function of these oscillations in balloon/giant cells might be. However, based on the fact that these cells share more resemblance to astrocytes than neurons (Cepeda et al., 2006), it can be speculated that their function is to buffer K^+ surges to prevent the occurrence of epileptic discharges. Interestingly, it has been reported that in CD type IIb, areas with balloon cells are less epileptogenic than adjacent cortex (Boonyapisit et al., 2003). Further, while ictal activity can be generated in areas with histopathologic CD type IIa, areas with CD type IIb do not show seizure activity, suggesting a possible protective role of balloon cells (Boonyapisit et al., 2003).

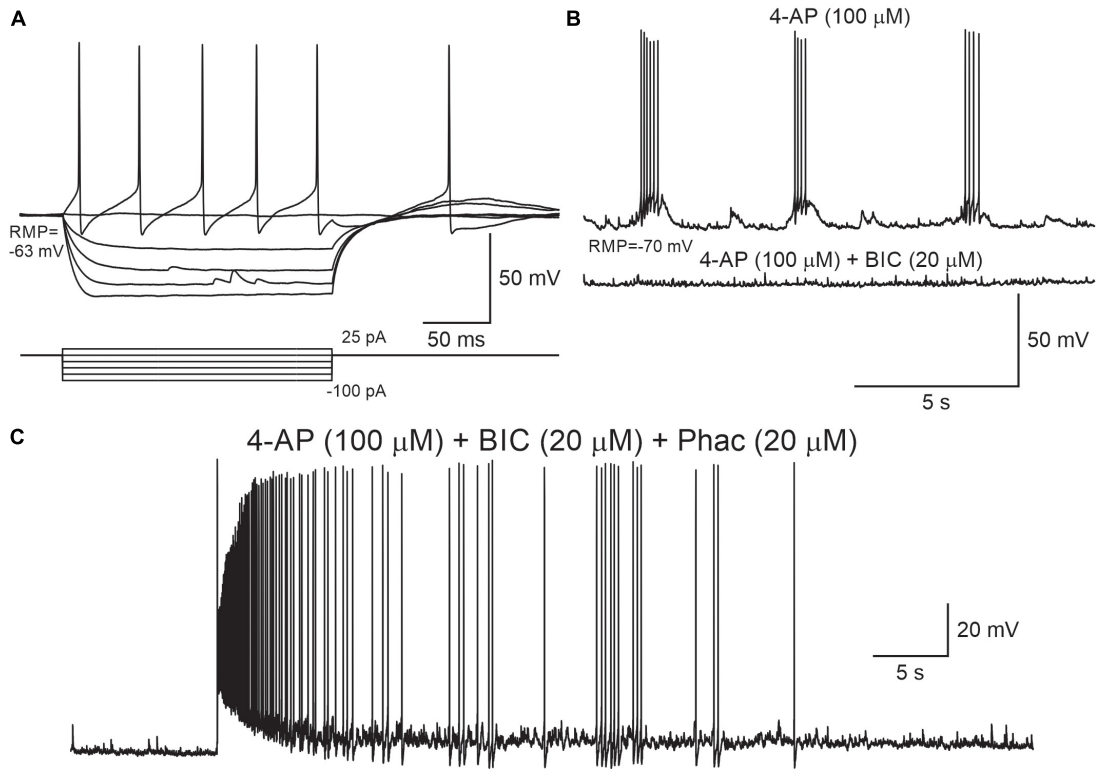

FIGURE 10 | Phaclofen induces ictal-like activity in cortical interneurons. **(A)** Current clamp recording of a cortical interneuron from a CD type I case. Depolarizing current pulses induced action potentials with very large after-hyperpolarization. **(B)** After 4-AP, rhythmic depolarizations and bursting were induced. Addition of BIC almost completely eliminated bursting. **(C)** Addition of phaclofen to the mix resulted in ictal-like discharges.

While multitude studies have emphasized that GABA interneuron synchrony jump starts focal seizures (Avoli et al., 1999, 2003; D'Antuono et al., 2004; Shiri et al., 2015; de Curtis and Avoli, 2016; Blauwblomme et al., 2018; Elahian et al., 2018), the respective role of GABA$_A$ and GABA$_B$ receptors has not been elucidated. Based on our observations, we can propose that relaxation of GABA inhibition mediated by GABA$_B$ receptors is responsible for the transition to ictal activity. In a previous study using CD tissue from mostly teenage and adult patients, D'Antuono et al. (2004) demonstrated that baclofen, a GABA$_B$ receptor agonist, stopped seizure activity induced by 4-AP and proposed that these receptors can be a target of AEDs. They also concluded that GABA$_A$ receptors lead to network synchrony and generation of ictal activity. While here we confirmed that GABA$_B$ receptors play a critical role in the modulation of seizure activity, our study also showed that GABA$_A$ receptors are not an absolute requirement for seizure generation since ictal activity was observed even after full blockade of these receptors with BIC.

TABLE 3 | Effects of 4-AP + BIC + phaclofen.

Pathology	Cases	Cell type	No PDs	Isolated PDs/ bursts of APs	Repetitive PDs	Ictal-like activity
CD I	3	Pyr (n = 5)	0	4	1	–
		Inter (n = 2)	0	1		1
CD II	1	Pyr (n = 1)	0	1	–	–
		Inter (n = 0)	0			
TSC	4	Pyr (n = 8)	0	5	–	3
		Inter (n = 1)	0	1	–	1
Non-CD	1	Pyr (n = 2)	0	1	1	–
		Inter (n = 2)	0	0	1	–
Total	9	Pyr (n = 16)	0	11	2	3
		Inter (n = 5)	0	2	1	2

What makes CD tissue particularly susceptible to proconvulsant drugs? The etiology, age of onset, and pathological substrates of pediatric epilepsy are very diverse. Thus, the sensitivity to proconvulsant and AEDs could be different depending on age and pathology. The most common substrate in epilepsy surgery patients less than 5 years of age is CD, a malformation characterized by architectural abnormalities (CD type I) of the cerebral cortex and, in severe cases, the presence of large, dysmorphic neurons and balloon cells (CD type IIa/b). The histopathology of TSC is very similar to that observed in CD

type IIb. Interestingly, in pediatric epilepsy cases, GABA synaptic activity is not reduced. On the contrary, we demonstrated that GABA$_A$ receptor-mediated synaptic activity is increased compared with glutamatergic activity (Cepeda et al., 2005b) and in some cases GABA is depolarizing (Cepeda et al., 2007). More recently, we found that areas with pathological high-frequency oscillations (HFOs) had a significant increase in spontaneous GABA synaptic activity as well as pacemaker GABA synaptic activity (PGA) (Cepeda et al., 2014, 2019). In light of the present results, it can be speculated that such an increase can be the result of enhanced GABAergic interneuron excitability and dysfunction of presynaptic GABA$_B$ receptors (D'Antuono et al., 2004). Importantly, GABA$_B$ receptors are also present postsynaptically on CPNs, are always inhibitory *via* activation of inwardly rectifying K^+ channels as well as inhibition of voltage-gated Ca^{2+} channels, and could dampen CPN excitability.

We also found that addition of a ketone body, BHB, reduced 4-AP oscillations and, presumably, cortical hyperexcitability. In pediatric epilepsy, the ketogenic diet has demonstrated beneficial effects. However, the antiepileptic mechanisms of this diet are multiple and still remain ill-defined (Rho, 2017; Simeone et al., 2017). Importantly, experimental studies have demonstrated that the ketone body BHB reduces seizure-like activity in a drosophila melanogaster model (Li et al., 2017). In the same study, it was shown that a K_{ATP} blocker or a GABA$_B$ receptor antagonist (CGP-55845) reversed BHB effects, providing conclusive evidence that the beneficial effects of the ketogenic diet are likely mediated by K_{ATP} channels and GABA$_B$ receptors. In pediatric epilepsy, a prospective study found a positive and strong correlation between measures of seizure frequency and BHB blood concentrations. Although the results did not reach statistical significance, likely due to the relatively small number of cases, a larger study is warranted (Buchhalter et al., 2017).

LIMITATIONS

We acknowledge that the present study has a number of important limitations. First and foremost, all patients were taking AEDs, some of which directly affect GABA transmission and potentially GABA$_{A/B}$ receptor function. Second, studies have shown that the slice preparation alters chloride concentrations due to trauma caused by the slicing procedure, so that more superficial cells have increased intracellular chloride and, in consequence, a more depolarized reversal potential (Dzhala et al., 2012). Third, our recordings were obtained at room temperature which, although helping preserve tissue integrity, it also decreases overall neuronal excitability (Javedan et al., 2002). Fourth, the GABA$_A$ receptor antagonist we used (BIC) also blocks the small Ca^{2+}-activated K^+ currents (Khawaled et al., 1999), which could further enhance neuronal excitability. Finally, in some experiments testing the GABA$_B$ receptor antagonist, phaclofen, we used a Cs-based internal solution. Cs^+ is known to reduce inwardly rectifying K^+ currents, which could have contributed to some of the findings. However, the same observations were confirmed using K-gluconate as the internal solution. Thus, in spite of these limitations, our work allows to reach several important conclusions.

CONCLUSION AND CLINICAL IMPLICATIONS

In conclusion, using the 4-AP model of epileptogenesis in combination with GABA$_{A/B}$ receptor antagonists, we demonstrate a critical role of GABA$_B$ receptors in the transition from interictal to ictal activity. When GABA$_B$ receptors are functional, they are able to prevent catastrophic excitation of CPNs. However, when they are disabled, ictal activity is facilitated. This implies that ensuring proper function of GABA$_B$ receptors is critical for keeping a normal balance between excitation and inhibition. Use of allosteric modulators of GABA$_B$ receptors at postsynaptic sites could hold promise as effective antiepileptic agents in cases of pediatric epilepsy not responsive to common AEDs (Morrisett et al., 1993; Ong and Kerr, 2005; Mares, 2012; Lang et al., 2014).

DATA AVAILABILITY STATEMENT

The data resulting in this publication are available from the corresponding author upon reasonable request and provided patient confidentiality is preserved.

ETHICS STATEMENT

The present study was approved by the IRB at UCLA (No. 11-000030-CR-00009). Parents or responsible persons signed written informed consents to allow use of pathological tissue samples for research purposes. No tissue was resected outside the area deemed affected by the pathology and required for seizure control.

AUTHOR CONTRIBUTIONS

GM, ML, and CC designed the study. GM resected the tissue samples. CC and JB performed slice recordings. CT, BV, SL, JB, and CC analyzed the electrophysiological data and prepared the figures. HV examined the pathological tissue samples and identified the histopathology. SL and CC co-wrote the manuscript. All the authors contributed to the final edition.

FUNDING

This study was supported by NIH grant NS38992 (GM).

ACKNOWLEDGMENTS

We deeply appreciate the patients and their parents for allowing the use of resected specimens for experimentation. We also thank the UCLA Hospital Pediatric Neurology staff for their assistance and dedication. Dr. Julia Chang and Ms. My N. Huynh performed the biocytin processing.

SUPPLEMENTARY MATERIAL

The Supplementary Material for this article can be found online at: https://www.frontiersin.org/articles/10.3389/fncel.2020.00054/full#supplementary-material

FIGURE S1 | Tetrodotoxin (TTX) and cadmium block 4-AP oscillations. **(A)** Voltage clamp recording (holding potential, Vh = +10 mV) of a pyramidal neuron from a CD type IIb case. 4-AP oscillations were completely blocked after 3 min bath application of TTX. **(B)** Current clamp recording (at RMP) of a pyramidal neuron from a CD type I case. Cadmium blocked 4-AP oscillations after 3 min bath application.

FIGURE S2 | 4-AP oscillations in balloon cells. **(A)** A balloon cell from a CD type IIb case was recorded and filled with biocytin. **(B)** Depolarizing current pulses were unable to induce action potentials (top right panel). However, bath application of 4-AP induced slow, small amplitude membrane depolarizations (bottom right panel), suggesting they might be sensing increases in K^+ concentration.

FIGURE S3 | BIC inverts the polarity of 4-AP oscillations. **(A)** In the presence of BIC, 4-AP oscillations were depolarizing and accompanied by action potentials. After addition of BIC to the bath solution, the oscillations reversed polarity and became hyperpolarizing. **(B)** In this CPN 4-AP oscillations were biphasic (hyperpolarization followed by depolarization). After BIC, the oscillation was purely hyperpolarizing and inhibitory at two membrane potentials. Notice that the action potentials in the upper panels are truncated.

FIGURE S4 | Phaclofen enhances paroxysmal discharges in the zero Mg^{2+} model. **(A)** In this CPN from a CD type II case, removal of Mg^{2+} from the external solution increased cell excitability as reflected by spontaneous firing. **(B)** Addition of BIC induced rhythmic paroxysmal discharges. **(C)** After phaclofen burst duration was significantly increased.

FIGURE S5 | Enriched ACSF (BHB and pyruvate) blocks 4-AP oscillations. **(A)** A CPN was recorded and filled with biocytin. **(B)** In voltage clamp mode, at a +10 mV holding potential, spontaneous GABA synaptic activity was observed. After 4-AP, rhythmic oscillations (outward currents) were induced. A few minutes after switching the bathing solution to eACSF, 4-AP oscillations were abated. After wash out in normal ACSF, some 4-AP oscillations returned.

REFERENCES

Abdijadid, S., Mathern, G. W., Levine, M. S., and Cepeda, C. (2015). Basic mechanisms of epileptogenesis in pediatric cortical dysplasia. *CNS Neurosci. Ther.* 21, 92–103. doi: 10.1111/cns.12345

Andre, V. M., Wu, N., Yamazaki, I., Nguyen, S. T., Fisher, R. S., Vinters, H. V., et al. (2007). Cytomegalic interneurons: a new abnormal cell type in severe pediatric cortical dysplasia. *J. Neuropathol. Exp. Neurol.* 66, 491–504. doi: 10.1097/01.jnen.0000240473.50661.d8

Avoli, M., Bernasconi, A., Mattia, D., Olivier, A., and Hwa, G. G. (1999). Epileptiform discharges in the human dysplastic neocortex: in vitro physiology and pharmacology. *Ann. Neurol.* 46, 816–826. doi: 10.1002/1531-8249(199912)46:6<816::aid-ana3>3.0.co;2-o

Avoli, M., and Jefferys, J. G. (2016). Models of drug-induced epileptiform synchronization in vitro. *J. Neurosci. Methods* 260, 26–32. doi: 10.1016/j.jneumeth.2015.10.006

Avoli, M., Louvel, J., Mattia, D., Olivier, A., Esposito, V., Pumain, R., et al. (2003). Epileptiform synchronization in the human dysplastic cortex. *Epileptic Disord.* 5 (Suppl. 2), S45–S50.

Badran, S., Schmutz, M., and Olpe, H. R. (1997). Comparative in vivo and in vitro studies with the potent GABAB receptor antagonist, CGP 56999A. *Eur. J. Pharmacol.* 333, 135–142. doi: 10.1016/s0014-2999(97)01111-4

Ben-Ari, Y. (2014). The GABA excitatory/inhibitory developmental sequence: a personal journey. *Neuroscience* 279, 187–219. doi: 10.1016/j.neuroscience.2014.08.001

Ben-Ari, Y. (2015). Commentary: GABA depolarizes immature neurons and inhibits network activity in the neonatal neocortex in vivo. *Front. Cell. Neurosci.* 9:478. doi: 10.3389/fncel.2015.00478

Bettler, B., Kaupmann, K., Mosbacher, J., and Gassmann, M. (2004). Molecular structure and physiological functions of GABA(B) receptors. *Physiol. Rev.* 84, 835–867. doi: 10.1152/physrev.00036.2003

Blauwblomme, T., Dossi, E., Pellegrino, C., Goubert, E., Gal, Iglesias B, Sainte-Rose, C., et al. (2018). GABAergic transmission underlies interictal epileptogenicity in pediatric FCD. *Ann. Neurol.* 85, 204–217. doi: 10.1002/ana.25403

Blumcke, I., Thom, M., Aronica, E., Armstrong, D. D., Vinters, H. V., Palmini, A., et al. (2011). The clinicopathologic spectrum of focal cortical dysplasias: a consensus classification proposed by an ad hoc task force of the ILAE diagnostic methods commission. *Epilepsia* 52, 158–174. doi: 10.1111/j.1528-1167.2010.02777.x

Boonyapisit, K., Najm, I., Klem, G., Ying, Z., Burrier, C., LaPresto, E., et al. (2003). Epileptogenicity of focal malformations due to abnormal cortical development: direct electrocorticographic-histopathologic correlations. *Epilepsia* 44, 69–76. doi: 10.1046/j.1528-1157.2003.08102.x

Bostock, H., Sears, T. A., and Sherratt, R. M. (1981). The effects of 4-aminopyridine and tetraethylammonium ions on normal and demyelinated mammalian nerve fibres. *J. Physiol.* 313, 301–315. doi: 10.1113/jphysiol.1981.sp013666

Bowery, N. G., Bettler, B., Froestl, W., Gallagher, J. P., Marshall, F., Raiteri, M., et al. (2002). International Union of Pharmacology. XXXIII. Mammalian gamma-aminobutyric acid(B) receptors: structure and function. *Pharmacol. Rev.* 54, 247–264. doi: 10.1124/pr.54.2.247

Buchhalter, J. R., D'Alfonso, S., Connolly, M., Fung, E., Michoulas, A., Sinasac, D., et al. (2017). The relationship between d-beta-hydroxybutyrate blood concentrations and seizure control in children treated with the ketogenic diet for medically intractable epilepsy. *Epilepsia Open* 2, 317–321. doi: 10.1002/epi4.12058

Buckle, P. J., and Haas, H. L. (1982). Enhancement of synaptic transmission by 4-aminopyridine in hippocampal slices of the rat. *J. Physiol.* 326, 109–122. doi: 10.1113/jphysiol.1982.sp014180

Cepeda, C., André, V. M., Flores-Hernández, J., Nguyen, O. K., Wu, N., Klapstein, G. J., et al. (2005b). Pediatric cortical dysplasia: correlations between neuroimaging, electrophysiology and location of cytomegalic neurons and balloon cells and glutamate/GABA synaptic circuits. *Dev. Neurosci.* 27, 59–76. doi: 10.1159/000084533

Cepeda, C., Andre, V. M., Hauptman, J. S., Yamazaki, I., Huynh, M. N., Chang, J. W., et al. (2012). Enhanced GABAergic network and receptor function in pediatric cortical dysplasia Type IIB compared with Tuberous Sclerosis Complex. *Neurobiol. Dis.* 45, 310–321. doi: 10.1016/j.nbd.2011.08.015

Cepeda, C., André, V. M., Levine, M. S., Salamon, N., Miyata, H., Vinters, H. V., et al. (2006). Epileptogenesis in pediatric cortical dysplasia: the dysmature cerebral developmental hypothesis. *Epilepsy Behav.* 9, 219–235. doi: 10.1016/j.yebeh.2006.05.012

Cepeda, C., André, V. M., Vinters, H. V., Levine, M. S., and Mathern, G. W. (2005a). Are cytomegalic neurons and balloon cells generators of epileptic activity in pediatric cortical dysplasia? *Epilepsia* 46 (Suppl. 5), 82–88. doi: 10.1111/j.1528-1167.2005.01013.x

Cepeda, C., André, V. M., Wu, N., Yamazaki, I., Uzgil, B., Vinters, H. V., et al. (2007). Immature neurons and GABA networks may contribute to epileptogenesis in pediatric cortical dysplasia. *Epilepsia* 48 (Suppl. 5), 79–85. doi: 10.1111/j.1528-1167.2007.01293.x

Cepeda, C., André, V. M., Yamazaki, I., Hauptman, J. S., Chen, J. Y., Vinters, H. V., et al. (2010). Comparative study of cellular and synaptic abnormalities in brain tissue samples from pediatric tuberous sclerosis complex and cortical dysplasia type II. *Epilepsia* 51, 160–165. doi: 10.1111/j.1528-1167.2010.02633.x

Cepeda, C., Chen, J. Y., Wu, J. Y., Fisher, R. S., Vinters, H. V., Mathern, G. W., et al. (2014). Pacemaker GABA synaptic activity may contribute to network synchronization in pediatric cortical dysplasia. *Neurobiol. Dis.* 62, 208–217. doi: 10.1016/j.nbd.2013.10.001

Cepeda, C., Hurst, R. S., Flores-Hernández, J., Hernández-Echeagaray, E., Klapstein, G. J., Boylan, M. K., et al. (2003). Morphological and electrophysiological characterization of abnormal cell types in pediatric cortical dysplasia. *J. Neurosci. Res.* 72, 472–486. doi: 10.1002/jnr.10604

Cepeda, C., Levinson, S., Nariai, H., Yazon, V. W., Tran, C., Barry, J., et al. (2019). Pathological high frequency oscillations associate with increased GABA synaptic activity in pediatric epilepsy surgery patients. *Neurobiol. Dis.* 134:104618. doi: 10.1016/j.nbd.2019.104618

Craig, M. T., and McBain, C. J. (2014). The emerging role of GABAB receptors as regulators of network dynamics: fast actions from a 'slow' receptor? *Curr. Opin. Neurobiol.* 26, 15–21. doi: 10.1016/j.conb.2013.10.002

D'Antuono, M., Louvel, J., Kohling, R., Mattia, D., Bernasconi, A., Olivier, A., et al. (2004). GABAA receptor-dependent synchronization leads to ictogenesis in the human dysplastic cortex. *Brain* 127(Pt 7), 1626–1640. doi: 10.1093/brain/awh181

de Curtis, M., and Avoli, M. (2016). GABAergic networks jump-start focal seizures. *Epilepsia* 57, 679–687. doi: 10.1111/epi.13370

Dzhala, V., Valeeva, G., Glykys, J., Khazipov, R., and Staley, K. (2012). Traumatic alterations in GABA signaling disrupt hippocampal network activity in the developing brain. *J. Neurosci.* 32, 4017–4031. doi: 10.1523/JNEUROSCI.5139-11.2012

Elahian, B., Lado, N. E., Mankin, E., Vangala, S., Misra, A., Moxon, K., et al. (2018). Low-voltage fast seizures in humans begin with increased interneuron firing. *Ann. Neurol.* 84, 588–600. doi: 10.1002/ana.25325

Frangaj, A., and Fan, Q. R. (2018). Structural biology of GABAB receptor. *Neuropharmacology* 136, 68–79. doi: 10.1016/j.neuropharm.2017.10.011

Grajkowska, W., Kotulska, K., Matyja, E., Larysz-Brysz, M., Mandera, M., Roszkowski, M., et al. (2008). Expression of tuberin and hamartin in tuberous sclerosis complex-associated and sporadic cortical dysplasia of Taylor's balloon cell type. *Folia Neuropathol.* 46, 43–48. doi:

Guerrini, R., Duchowny, M., Jayakar, P., Krsek, P., Kahane, P., Tassi, L., et al. (2015). Diagnostic methods and treatment options for focal cortical dysplasia. *Epilepsia* 56, 1669–1686. doi: 10.1111/epi.13200

Hemb, M., Velasco, T. R., Parnes, M. S., Wu, J. Y., Lerner, J. T., Matsumoto, J. H., et al. (2010). Improved outcomes in pediatric epilepsy surgery: the UCLA experience, 1986-2008. *Neurology* 74, 1768–1775. doi: 10.1212/WNL.0b013e3181e0f17a

Holmgren, C. D., Mukhtarov, M., Malkov, A. E., Popova, I. Y., Bregestovski, P., and Zilberter, Y. (2010). Energy substrate availability as a determinant of neuronal resting potential, GABA signaling and spontaneous network activity in the neonatal cortex in vitro. *J. Neurochem.* 112, 900–912. doi: 10.1111/j.1471-4159.2009.06506.x

Javedan, S. P., Fisher, R. S., Eder, H. G., Smith, K., and Wu, J. (2002). Cooling abolishes neuronal network synchronization in rat hippocampal slices. *Epilepsia* 43, 574–580. doi: 10.1046/j.1528-1157.2002.40101.x

Jozwiak, J., Kotulska, K., and Jozwiak, S. (2006). Similarity of balloon cells in focal cortical dysplasia to giant cells in tuberous sclerosis. *Epilepsia* 47:805. doi: 10.1111/j.1528-1167.2006.00531_1.x

Kantrowitz, J. T., Francis, N. N., Salah, A., and Perkins, K. L. (2005). Synaptic depolarizing GABA response in adults is excitatory and proconvulsive when GABAB receptors are blocked. *J. Neurophysiol.* 93, 2656–2667. doi: 10.1152/jn.01026.2004

Khawaled, R., Bruening-Wright, A., Adelman, J. P., and Maylie, J. (1999). Bicuculline block of small-conductance calcium-activated potassium channels. *Pflugers Arch.* 438, 314–321. doi: 10.1007/s004240050915

Lang, M., Moradi-Chameh, H., Zahid, T., Gane, J., Wu, C., Valiante, T., et al. (2014). Regulating hippocampal hyperexcitability through GABAB Receptors. *Physiol. Rep.* 2:e00278. doi: 10.14814/phy2.278

Lerner, J. T., Salamon, N., Hauptman, J. S., Velasco, T. R., Hemb, M., Wu, J. Y., et al. (2009). Assessment and surgical outcomes for mild type I and severe type II cortical dysplasia: a critical review and the UCLA experience. *Epilepsia* 50, 1310–1335. doi: 10.1111/j.1528-1167.2008.01998.x

Li, J., O'Leary, E. I., and Tanner, G. R. (2017). The ketogenic diet metabolite beta-hydroxybutyrate (beta-HB) reduces incidence of seizure-like activity (SLA) in a Katp- and GABAb-dependent manner in a whole-animal Drosophila melanogaster model. *Epilepsy Res.* 133, 6–9. doi: 10.1016/j.eplepsyres.2017.04.003

Mares, P. (2012). Anticonvulsant action of GABAB receptor positive modulator CGP7930 in immature rats. *Epilepsy Res.* 100, 49–54. doi: 10.1016/j.eplepsyres.2012.01.007

Mitterdorfer, J., and Bean, B. P. (2002). Potassium currents during the action potential of hippocampal CA3 neurons. *J. Neurosci.* 22, 10106–10115. doi: 10.1523/jneurosci.22-23-10106.2002

Morrisett, R. A., Lewis, D. V., Swartzwelder, H. S., and Wilson, W. A. (1993). Antiepileptic effects of GABAb receptor activation in area CA3 of rat hippocampus. *Brain Res.* 600, 235–242. doi: 10.1016/0006-8993(93)91378-6

Motalli, R., D'Antuono, M., Louvel, J., Kurcewicz, I., D'Arcangelo, G., Tancredi, V., et al. (2002). Epileptiform synchronization and GABA(B) receptor antagonism in the juvenile rat hippocampus. *J. Pharmacol. Exp. Ther.* 303, 1102–1113. doi: 10.1124/jpet.102.040782

Mott, D. D. (2015). "The metabotropic GABAB receptors," in *Cellular and Molecular Neurophysiology*, 4th Edn, ed. C. Hammond (Boston, MA: Academic Press), 245–267. doi: 10.1016/b978-0-12-397032-9.00011-x

Newberry, N. R., and Nicoll, R. A. (1984). Direct hyperpolarizing action of baclofen on hippocampal pyramidal cells. *Nature* 308, 450–452. doi: 10.1038/308450a0

Olsen, R. W., and Sieghart, W. (2009). GABA A receptors: subtypes provide diversity of function and pharmacology. *Neuropharmacology* 56, 141–148. doi: 10.1016/j.neuropharm.2008.07.045

Ong, J., and Kerr, D. I. (2005). Clinical potential of GABAB receptor modulators. *CNS Drug Rev.* 11, 317–334. doi: 10.1111/j.1527-3458.2005.tb00049.x

Prosser, H. M., Gill, C. H., Hirst, W. D., Grau, E., Robbins, M., Calver, A., et al. (2001). Epileptogenesis and enhanced prepulse inhibition in GABA(B1)-deficient mice. *Mol. Cell. Neurosci.* 17, 1059–1070. doi: 10.1006/mcne.2001.0995

Rho, J. M. (2017). How does the ketogenic diet induce anti-seizure effects? *Neurosci. Lett.* 637, 4–10. doi: 10.1016/j.neulet.2015.07.034

Salamon, N., Kung, J., Shaw, S. J., Koo, J., Koh, S., Wu, J. Y., et al. (2008). FDG-PET/MRI coregistration improves detection of cortical dysplasia in patients with epilepsy. *Neurology* 71, 1594–1601. doi: 10.1212/01.wnl.0000334752.41807.2f

Scanziani, M., Debanne, D., Muller, M., Gahwiler, B. H., and Thompson, S. M. (1994). Role of excitatory amino acid and GABAB receptors in the generation of epileptiform activity in disinhibited hippocampal slice cultures. *Neuroscience* 61, 823–832. doi: 10.1016/0306-4522(94)90405-7

Shiri, Z., Manseau, F., Levesque, M., Williams, S., and Avoli, M. (2015). Interneuron activity leads to initiation of low-voltage fast-onset seizures. *Ann. Neurol.* 77, 541–546. doi: 10.1002/ana.24342

Simeone, T. A., Simeone, K. A., and Rho, J. M. (2017). Ketone bodies as anti-seizure agents. *Neurochem. Res.* 42, 2011–2018. doi: 10.1007/s11064-017-2253-5

Sutor, B., and Luhmann, H. J. (1998). Involvement of GABA(B) receptors in convulsant-induced epileptiform activity in rat neocortex in vitro. *Eur. J. Neurosci.* 10, 3417–3427. doi: 10.1046/j.1460-9568.1998.00351.x

Swartzwelder, H. S., Lewis, D. V., Anderson, W. W., and Wilson, W. A. (1987). Seizure-like events in brain slices: suppression by interictal activity. *Brain Res.* 410, 362–366. doi: 10.1016/0006-8993(87)90339-8

Szente, M., Gajda, Z., Said Ali, K., and Hermesz, E. (2002). Involvement of electrical coupling in the in vivo ictal epileptiform activity induced by 4-aminopyridine in the neocortex. *Neuroscience* 115, 1067–1078. doi: 10.1016/s0306-4522(02)00533-x

Thompson, S. M., and Gahwiler, B. H. (1992). Comparison of the actions of baclofen at pre- and postsynaptic receptors in the rat hippocampus in vitro. *J. Physiol.* 451, 329–345. doi: 10.1113/jphysiol.1992.sp019167

Traub, R. D., Bibbig, R., Piechotta, A., Draguhn, R., and Schmitz, D. (2001). Synaptic and nonsynaptic contributions to giant ipsps and ectopic spikes induced by 4-aminopyridine in the hippocampus in vitro. *J. Neurophysiol.* 85, 1246–1256. doi: 10.1152/jn.2001.85.3.1246

Traub, R. D., Colling, S. B., and Jefferys, J. G. (1995). Cellular mechanisms of 4-aminopyridine-induced synchronized after-discharges in the rat hippocampal slice. *J. Physiol.* 489 (Pt 1), 127–140. doi: 10.1113/jphysiol.1995.sp021036

Uusisaari, M., Smirnov, S., Voipio, J., and Kaila, K. (2002). Spontaneous epileptiform activity mediated by GABA(A) receptors and gap junctions in the rat hippocampal slice following long-term exposure to GABA(B) antagonists. *Neuropharmacology* 43, 563–572. doi: 10.1016/s0028-3908(02)00156-9

Watts, A. E., and Jefferys, J. G. (1993). Effects of carbamazepine and baclofen on 4-aminopyridine-induced epileptic activity in rat hippocampal slices. *Br. J. Pharmacol.* 108, 819–823. doi: 10.1111/j.1476-5381.1993.tb12884.x

Zilberter, Y., Zilberter, T., and Bregestovski, P. (2010). Neuronal activity in vitro and the in vivo reality: the role of energy homeostasis. *Trends Pharmacol. Sci.* 31, 394–401. doi: 10.1016/j.tips.2010.06.005

Conflict of Interest: The authors declare that the research was conducted in the absence of any commercial or financial relationships that could be construed as a potential conflict of interest.

frontiers in Cellular Neuroscience

ORIGINAL RESEARCH
published: 08 May 2020
doi: 10.3389/fncel.2020.00122

Multimodal Analysis of STRADA Function in Brain Development

*Louis T. Dang[1,2], Katarzyna M. Glanowska[1,3], Philip H. Iffland II[4], Allan E. Barnes[4], Marianna Baybis[4], Yu Liu[1], Gustavo Patino[1], Shivanshi Vaid[1,2], Alexandra M. Streicher[1], Whitney E. Parker[5], Seonhee Kim[6], Uk Yeol Moon[6], Frederick E. Henry[3,7], Geoffrey G. Murphy[3,7], Michael Sutton[3,7], Jack M. Parent[1,8] and Peter B. Crino[4]**

[1]Department of Neurology, Michigan Medicine, Ann Arbor, MI, United States, [2]Department of Pediatrics, Michigan Medicine, Ann Arbor, MI, United States, [3]Michigan Neuroscience Institute, Michigan Medicine, Ann Arbor, MI, United States, [4]Department of Neurology, University of Maryland School of Medicine, Baltimore, MD, United States, [5]Department of Neurosurgery, Weill-Cornell Medical Center, New York, NY, United States, [6]Louis Katz School of Medicine, Temple University, Philadelphia, PA, United States, [7]Department of Molecular, and Integrative Physiology, Michigan Medicine, Ann Arbor, MI, United States, [8]Neurology Service, VA Ann Arbor Healthcare System, Ann Arbor, MI, United States

OPEN ACCESS

Edited by:
Eleonora Aronica, Amsterdam University Medical Center, Netherlands

Reviewed by:
Nicoletta Landsberger, University of Milan, Italy
Christina Gross, Cincinnati Children's Hospital Medical Center, United States

***Correspondence:**
Peter B. Crino
pcrino@som.umaryland.edu

Specialty section:
This article was submitted to Cellular Neuropathology, a section of the journal Frontiers in Cellular Neuroscience

Received: *06 December 2019*
Accepted: *14 April 2020*
Published: *08 May 2020*

Citation:
Dang LT, Glanowska KM, Iffland PH II, Barnes AE, Baybis M, Liu Y, Patino G, Vaid S, Streicher AM, Parker WE, Kim S, Moon UY, Henry FE, Murphy GG, Sutton M, Parent JM and Crino PB (2020) Multimodal Analysis of STRADA Function in Brain Development. Front. Cell. Neurosci. 14:122. doi: 10.3389/fncel.2020.00122

mTORopathies are a heterogeneous group of neurological disorders characterized by malformations of cortical development (MCD), enhanced cellular mechanistic target of rapamycin (mTOR) signaling, and epilepsy that results from mutations in mTOR pathway regulatory genes. Homozygous mutations (del exon 9–13) in the pseudokinase STE20-related kinase adaptor alpha (*STRAD*-α; *STRADA*), an mTOR modulator, are associated with Pretzel Syndrome (PS), a neurodevelopmental disorder within the Old Order Mennonite Community characterized by megalencephaly, intellectual disability, and intractable epilepsy. To study the cellular mechanisms of STRADA loss, we generated CRISPR-edited *Strada* mouse N2a cells, a germline mouse *Strada* knockout (KO−/−) strain, and induced pluripotent stem cell (iPSC)-derived neurons from PS individuals harboring the *STRADA* founder mutation. *Strada* KO *in vitro* leads to enhanced mTOR signaling and iPSC-derived neurons from PS individuals exhibit enhanced cell size and mTOR signaling activation, as well as subtle alterations in electrical firing properties e.g., increased input resistance, a more depolarized resting membrane potential, and decreased threshold for action potential (AP) generation. *Strada*−/− mice exhibit high rates of perinatal mortality and out of more than 100 litters yielding both WT and heterozygous pups, only eight *Strada*−/− animals survived past P5. *Strada*−/− mice are hypotonic and tremulous. Histopathological examination ($n = 5$ mice) revealed normal gross brain organization and lamination but all had ventriculomegaly. Ectopic neurons were seen in all five *Strada*−/− brains within the subcortical white matter mirroring what is observed in human PS brain tissue. These distinct experimental platforms demonstrate that STRADA modulates mTOR signaling and is a key regulator of cell size, neuronal excitability, and cortical lamination.

Keywords: mTOR, megalencephaly, epilepsy, iPSC, mouse, seizure

INTRODUCTION

"Pretzel syndrome" (PS) also known as polyhydramnios, megalencephaly, symptomatic epilepsy syndrome (PMSE; OMIM#611087) is an autosomal recessive neurodevelopmental disorder characterized by megalencephaly (ME), severe developmental delay, and medically intractable epilepsy in association with intrauterine polyhydramnios and renal dysfunction (Puffenberger et al., 2007). Post-mortem histopathological examination of a single brain specimen revealed enlarged brain size, enhanced cortical neuronal size, and heterotopic neurons in the subcortical white matter, with preserved gyral patterning (Puffenberger et al., 2007). In all Mennonite individuals, PS is caused by a homozygous founder deletion spanning exons 9–13 of the STE20-related kinase adaptor alpha (*STRADA*) gene (17q23.3) although additional non-Mennonite (non-founder) *STRADA* variants associated with PS have been reported e.g., a consanguineous Asian pedigree, c.842dupA, p.D281fs (Bi et al., 2016), and a consanguineous Turkish pedigree, c.891dupC; p.C298Lfs* (Evers et al., 2017), demonstrating that *STRADA* is relevant outside of the Mennonite community as an epilepsy and ME gene.

STRADA modulates the mechanistic target of rapamycin (mTOR) pathway as part of the LKB1/STRADA/MO25 complex that signals *via* AMPK (Hawley et al., 2003), to TSC1/TSC2/TBC1D7 and then to mTOR in response to many upstream cellular cues including cellular ATP levels (Crino, 2016). STRADA is a pseudokinase that augments LKB1 kinase activity when bound to LKB1 (Boudeau et al., 2003). In the absence of STRADA, LKB1 has minimal kinase activity, and thus it cannot phosphorylate one of its primary substrates, AMPK. Interestingly, knockout of *Lkb1* in mice leads to abnormal brain development (Asada et al., 2007; Barnes et al., 2007) yet variants in *LKB1* and *MO25* are not linked to human epilepsy or cortical malformations.

shRNA-mediated knockdown (KD) of *Strada* in mouse neural progenitor cells *in vitro* causes rapid activation of the mTOR signaling cascade and enhanced cell size, a phenotype commonly seen with activated mTOR pathway signaling (Orlova et al., 2010). *Strada* KD causes altered cell polarity, disorganized Golgi assembly, and altered motility, effects that can be prevented with the mTOR complex 1 (mTORC1) inhibitor rapamycin (Parker et al., 2013). *Strada* KD in fetal mouse brain by *in utero* electroporation at embryonic day 14–15 causes a cortical lamination defect with heterotopic neurons in the white matter, an effect that can be prevented with the mTOR inhibitor rapamycin. Interestingly, germline *Strada* knockout (KO) is a perinatal lethal phenotype with death on or around post-natal day 2 (Veleva-Rotse et al., 2014). These animals exhibit defects in axonogenesis but brain structure is otherwise intact. Finally, the treatment of PS individuals with rapamycin (sirolimus) can alter seizure frequency but does not affect intellectual disability (Parker et al., 2013).

To more fully define the role of STRADA in brain development, we have generated a *Strada* KO mouse strain carrying the same mutation (del exon 9–13) as humans with PS and we have generated induced pluripotent stem cells (iPSCs) from fibroblasts obtained from PS patients to derive neurons for morphological and electrophysiological analysis.

MATERIALS AND METHODS

CRISPR/Cas9 Construct Generation and Validation

Guide RNA targeting the spCas9 endonuclease to regions in the mouse genome encoding *Strada* (-AGTCGCCATTGGAAGGCCGGAGG-) were calculated *in silico* using ChopChop software (chopchop.cbu.uib.no). A scramble gRNA (-GACTACCAGAGCTAACTCA-) was used as a transfection and gRNA control. *In silico* guide RNAs were then assembled into oligonucleotides (Integrated DNA Technologies, Coralville, IA, USA), annealed using ligase buffer (Promega, Madison, WI, USA) at 98°C for 5 min. Annealed gRNA was then sub-cloned into PX330-based plasmid (addgene #48138) using Golden Gate Assembly containing a mCherry reporter linked to Cas9 *via* a T2a multicistronic element. Plasmid assembly was confirmed by Sanger sequencing (Genewiz, South Plainfield, NJ, USA).

To validate that our gRNA containing CRISPR/Cas9 plasmid created indels in our regions of interest, DNA from *Strada*, and scramble FAC-sorted cells lines (as described below) as well as wildtype (WT) N2aC was assayed for mismatched DNA pairs (EnGen Mutation Detection Kit; New England Biolabs, Ipswich, MA, USA) with PCR primers targeted towards our genomic region of interest (Integrated DNA Technologies, Coralville, IA, USA).

Cell Culture and Establishment of CRISPR KO Cell Lines

Neuro2a cells (N2aC; Sigma–Aldrich, St. Louis, MO, USA) were cultured in complete medium consisting of EMEM (Invitrogen, Carlsbad, CA, USA) supplemented with 10% FBS (Invitrogen, Carlsbad, CA, USA). To create stable CRISPR/Cas9 edited cell lines, N2aC were transfected using Lipofectamine LTX with Plus reagent (Thermo Fisher Scientific, Waltham, MA, USA) and 30 μg of plasmid diluted in 300 μl Opti-MEM (Invitrogen, Carlsbad, CA, USA) for 48 h. Co-transfection experiments were performed by using 30 μg of each plasmid. After 48 h of transfection, cells were trypsinized (0.25%), centrifuged, washed with ice-cold PBS, passed through a cell strainer into a 5 ml conical tube and assayed by flow cytometry (University of Maryland School of Medicine Flow Cytometry Core) for sorting based on mCherry (Cas9) fluorescence (BD FACSAria II cell sorter; Becton Dickinson and Company, Franklin Lakes, NJ, USA). mCherry+ sorted cells were placed into PBS containing 1% serum until re-plating. Cells were re-plated in complete media and grown to confluence.

Immunocytochemistry

N2aC were fixed in 4% PFA at room temperature (RT) for 20 min and then permeabilized in phosphate-buffered saline (PBS) containing 0.3% Triton X-100 (Thermo Fisher Scientific, Waltham, MA, USA). Cells were blocked for 2 h at RT in 5% normal goat serum (Jackson ImmunoResearch, West Grove, PA,

USA). Cells were incubated in one of the following primary antibodies in blocking solution containing 5% normal serum at 4°C overnight: rabbit monoclonal to phospho-S6 ribosomal protein (Ser235/236, 1:1,000; Cell Signaling).

Human Fibroblasts Isolation and Culture

PS patient (n = 2) and control (n = 2) human fibroblasts were obtained from skin-punch biopsies at the Clinic for Special Children (CSC) in Lancaster, PA, USA, following informed consent. Skin biopsies were performed following approved Institutional Review Board protocols at the University of Pennsylvania and Temple University (where the study was initiated), and Lancaster General Hospital (Lancaster, PA, USA). Parents provided informed consent before their child's participation.

Fibroblasts were extracted from tissue samples by incubation in 0.25% Trypsin/EDTA (Gibco) overnight at 4°C. The next day, the epidermis was removed, and dermis was digested with Collagenase P (Roche) buffered in 130 mM sodium chloride (Sigma–Aldrich), 10 mM calcium acetate (Sigma–Aldrich), and 20 mM HEPES buffer for 30 min at 37°C. Then 0.5% Trypsin/EDTA (Gibco) was added, and the mixture was incubated at 37°C for an additional 10 min before neutralization with fibroblast culturing media, composed of DMEM supplemented with 10% FBS (Sigma–Aldrich), 10 mM HEPES buffer, 1% penicillin/streptomycin (10,000 U/ml penicillin, 10 mg/ml streptomycin stock), and 1% fungizone. Fibroblasts were pelleted through centrifugation for 5 min at 1,500 rpm, and the pellet was resuspended in fibroblast culturing media to obtain the desired cells.

Fibroblast Reprogramming and iPSC Culture

Fibroblasts were cultured in DMEM, 10% FBS, 1X L-glutamine, 1 mM MEM non-essential amino acids (NEAA), 50 U/ml penicillin, and 50 μg/ml streptomycin (all from Life Technologies, Carlsbad, CA, USA) at 37°C and 5% CO_2. For retroviral reprogramming (Liu et al., 2013), viral stocks were obtained using GP2–293 packaging cells (Clontech, Mountain View, CA, USA) and retroviral vectors encoding Oct3/4, Sox2, Klf4 and c-Myc on a pMXs backbone (Addgene, Cambridge, MA). Fibroblasts plated in 6-well plates (30,000 per well) were transduced with retroviruses, followed by a second round of transduction the next day. After 4 days, fibroblasts were passaged onto mouse embryonic fibroblasts (MEFs, GlobalStem, Rockville, MD, USA) using 0.25% trypsin (Life Technologies) and switched 1 day later to a stem cell medium containing: DMEM/F12, 20% knock-out serum replacement, 1X L-glutamine, 1 mM MEM non-essential amino acids, 50 U/ml penicillin, 50 μg/ml streptomycin, 4 μg/ml FGF2 (Life Technologies) and 100 μM β-mercaptoethanol (Sigma–Aldrich, St., Louis, MO, USA). Fibroblasts from PS subject 2 were reprogrammed using an episomal method (Okita et al., 2011). Fibroblasts were electroporated with plasmids pCXLE-hOCT3/4-shp53-F, pCXLE-hSK, and pCXLE-hUL (Addgene# 27077, 27078, and 27080, respectively; gift from Shinya Yamanaka). Fibroblasts were grown in TeSR-E7 (StemCell Technologies, Vancouver, BC, USA) media for 17–21 days before picking single iPSC colonies.

iPSC colonies appeared and were manually picked and passaged onto MEFs and grown with stem cell medium or plated onto Matrigel (1:250 dilution in DMEM/F12; BD Biosciences, San Jose, CA, USA) and grown with mTeSR1 (StemCell Technologies). iPSCs were passaged weekly using either 5 mM AccuGENE EDTA (diluted 1:100 in DPBS without calcium or magnesium; Lonza, Basel, Switzerland), Versene (Life Technologies), or Dispase (Thermo Fisher Scientific, Waltham, MA, USA). For passaging with EDTA or Versene, culture medium was supplemented with 10 μM Y-27632 ROCK inhibitor (EMD Millipore, Darmstadt, Germany) for 24 h (Narumiya et al., 2000). After six passages the cells were evaluated for pluripotency by immunocytochemistry (ICC) and embryoid body differentiation. For embryoid body experiments, iPSC colonies were grown in suspension for a week, passaged onto 0.1% porcine type A gelatin (Sigma) for another week and processed for ICC. iPSC samples were karyotyped by Cell Line Genetics (Madison, WI, USA).

Neuronal Differentiation

iPSCs were dissociated with Versene or Accutase (Innovative Cell) and plated on Matrigel or CELLstart (Life Technologies). Upon reaching 95% confluence, the culture medium was switched to 3N medium (Shi et al., 2012), a 1:1 mix of N2 (DMEM/F12, 1X N2, 5 μg/ml insulin, 1 mM L-glutamine, 1X MEM NEAA, 100 μM 2-mercaptoethanol, 50 U/ml penicillin, 50 μg/ml streptomycin) and Neurobasal (with 1X B27, 1 mM L-glutamine, 50 U/ml penicillin and 50 μg/ml streptomycin) supplemented with 10 μM SB431542 and 1 μM Dorsomorphin (both from Tocris, Bristol, UK). The medium was changed daily for 12 days, then the cell monolayer was broken into aggregates of 300–500 cells with Dispase. The aggregates were resuspended in 3N media and then plated on Matrigel and grown in 3N media without supplements. Culture media was exchanged every 48 h. After neural rosettes appeared, the medium was supplemented with 20 ng/ml of FGF2 for 4 days and the aggregates were passaged with Dispase and cultured in unsupplemented 3N media. When neurons appeared at the edges of the colonies, cells were dissociated with Accutase and replated on Matrigel for immunocytochemistry.

Immunocytochemistry and Morphometric Analysis of iPSC Derived Neurons

Cells were plated on Matrigel and cultured for 1 week (for iPSCs or embryoid bodies) or 3–5 weeks (for neuronal cultures). The cells were rinsed with PBS and fixed in 4% paraformaldehyde (PFA) for 30 min, then washed twice in PBS at RT for 10 min. Cells were permeabilized in 0.2% Triton X-100 (Sigma; diluted in PBS) for 5 min at RT, and then blocked in a buffer containing 10% normal goat serum, 0.05% Triton X-100 and 1% bovine serum albumin (Sigma) diluted in PBS for 1 h at RT. Primary antibodies (**Table 1**) were resuspended in blocking buffer and incubated with the cells overnight at 4°C. After three washes (10 min each) with PBS, cells were incubated in secondary antibodies (**Table 1**) at a 1:400 dilution

TABLE 1 | Primary and secondary antibodies used for ICC.

Target	Host	Company	Catalog Number	Dilution
Primary antibodies				
NANOG	Rabbit	Abcam	ab21624	1:500
OCT3/4	Goat	Santa Cruz Biotechnology	sc-8628	1:100
SSEA4	Mouse	DSHB	MC-813–70	1:200
α Feto-protein	Rabbit	Dako/Agilent	A0008	1:500
Smooth muscle actin	Mouse	Abcam	ab5694	1:1,000
SOX2	Rabbit	Millipore	AB5603	1:1,000
p-S6 (S235/236)	Rabbit	Cell Signaling	4858	1:250
βIII-tubulin (TuJ1)	Mouse	Covance	MMS-435P	1:2,000
Cux1	Rabbit	Santa Cruz Biotechnology	Sc-13024	1:50
βIII-tubulin (TuJ1)	Mouse	Biolegend	801202	1:2,000
Doublecortin	Rabbit	Abcam	ab18723	1:500
Map2abc	Rabbit	Cell Signaling	4542S	1:500
Map2ab	Mouse	Sigma	M2320	1:500
GABA	Rabbit	Sigma	A2052	1:500
vGlut1	Guinea pig	Millipore	AB5905	1:200
GFAP	Rabbit	Dako/Agilent	Z0334	1:500
Secondary antibodies				
488 anti-rabbit IgG	Goat	Invitrogen	A-11034	1:400
488 anti-mouse IgG	Goat	Invitrogen	A-11001	1:400
488 anti-goat IgG	Donkey	Invitrogen	A-11055	1:400
594 anti-rabbit IgG	Goat	Invitrogen	A-11037	1:400
594 anti-mouse IgG	Goat	Invitrogen	A-11032	1:400
FITC anti-guinea pig IgG	Goat	Millipore	AP108F	1:200

in blocking buffer for 90 min at RT. Nuclei were stained with bisbenzamide (Invitrogen; 1:5,000 dilution in PBS) for 5 min at RT. Cells were then washed three times with PBS. Images were obtained with a Leica DMI 6000B epifluorescent microscope using the Leica Application Suite Advanced Fluorescence software (Leica Microsystems Inc., Buffalo Grove, IL, USA) and analyzed using ImageJ (NIH, Bethesda, MD, USA). For quantification of P-S6 immunoreactivity, ROIs were created around the somatic region of control and PS cells using the MAP2 channel, and average non-zero pixel intensity in the P-S6 channel was determined for each cell. Somatic P-S6 intensities for each cell were normalized to the average control value and expressed as a percent of control. Changes in P-S6 expression were analyzed using an unpaired student's *t*-test (two-tailed).

To analyze neuronal differentiation, neuronal cultures were stained for doublecortin (DCX) and neuron-specific-βIII-tubulin (TUBB3) to detect immature neurons, and microtubule-associated protein 2ab (MAP2ab) to detect mature neurons (**Table 1**). Samples stained for mature and immature neuronal markers were used for soma size measurement by tracing the soma of individual neurons in ImageJ. A calculated area was then obtained based on the scale bar value of the images.

Data Quantification and Statistical Analysis

Cell lysates were electrophoresed and probed with the following primary antibodies: rabbit monoclonal to phospho-S6 ribosomal protein (P-S6; Ser235/236, 1:1,000; Cell Signaling), rabbit polyclonal anti-LYK5 (recognizes STRADA; 1:500; Abcam), and rabbit monoclonal to GAPDH (1:1,000; Cell Signaling). At least two separate samples were taken for each cell line per differentiation and processed as described in the "Materials and Methods" section. WB films were digitized and the images analyzed using the Gel Analysis function of ImageJ. Bands for P-S6 were measured and the values normalized to the signal of GAPDH (used as a loading control) for each sample using a fixed window size. A second normalization was performed to the sample with the highest ratio in the same WB film. Average ratios per iPSC cell line were compared using ANOVA and planned contrasts, with statistical significance set at 0.05, in R Core Team (2014). For soma size measurements, 2 separate differentiations were performed per experimental group, and neuronal cultures were stained for DCX, TUBB3, and MAP2 antibodies as described above. For each differentiation and experimental group 5–10 random fields-of-view (FOV) were imaged, and 100 cells positive for each marker selected for measurement. The soma of each selected cell was traced using ImageJ and the resulting areas were pooled for each experimental group. Statistical comparisons were performed using unpaired, two-tailed Student's *t*-test. Patch-clamp recording data were analyzed for significance using unpaired, two-tailed Student's *t*-test to compare passive and active electrophysiological properties between experimental groups. The proportions of spontaneously active neurons between control and PS groups were compared using the two-tailed Chi-square test.

Whole-Cell Patch-Clamp Recordings

Neuronal cultures were plated on glass-bottom dishes (MatTek, Ashland, MA, USA) or coverslips coated with Matrigel and cultured in BrainPhys medium (Bardy et al., 2015) for 8–12 weeks before recordings were made. Immediately before electrophysiological recordings, dishes/coverslips with either patient or control neurons were transferred to a recording

chamber filled with fresh, CO_2-saturated BrainPhys and stabilized for at least 10 min. In our experience, neurons remain healthy in Hibernate A for approximately 2–3 h outside of the incubator, and all electrophysiological recordings from a given culture were completed within 1.5 h.

Recording micropipettes were pulled from capillary glass (type 7052, outer diameter/inner diameter 1.65/1.1 mm; World Precision Instruments, Sarasota, FL, USA) using a Flaming/Brown P-97 pipette puller (Sutter Instruments, Novato, CA, USA) to obtain pipettes with a resistance of 3.0–5.0 MΩ. Whole-cell recordings were made in voltage-clamp and current-clamp mode of an Axon amplifier with pClamp 10.0 software (Molecular Devices LLC, Sunnyvale, CA, USA) and digitized using a Digidata 1440A digitizer (Molecular Devices). Data were filtered at 3 kHz and digitized at 20 kHz. Neurons were visualized on an upright microscope (Olympus, Center Valley, PA, USA) under differential interference contrast using an Olympus OLY-150 IR CCD camera. Micropipettes were filled with an internal solution containing (in mM): 120 potassium gluconate, 20 KCl, 10 HEPES, 0.2 EGTA, 2 $MgCl^*6H_2O$, 4 Na2 ATP, 0.3 Tris-GTP, 7 phosphocreatine, pH adjusted to 7.25 with KOH. Passive properties (input resistance, series resistance, and capacitance) were monitored in voltage-clamp mode throughout recordings and only cells with stable properties were further analyzed.

Current-clamp recordings were performed to study intrinsic excitability and action potential (AP) firing properties. For some recordings, neuronal cultures were previously transfected with a lentiviral vector carrying a GFP reporter driven by the CaMKIIα promoter to aid in the prospective identification of mature neurons. After establishing a whole-cell configuration and measuring passive properties under voltage clamp, the recording mode was switched to current-clamp and resting membrane potential was recorded. Some neurons exhibited spontaneous AP firing while others displayed a depolarized membrane potential preventing them from generating APs, likely due to the inactivation of sodium channels. Therefore, a continuous injection of hyperpolarizing current was applied until they stopped firing and their membrane voltage reached approximately −60 to −65 mV to study their intrinsic excitability. To ensure proper comparisons between neurons resting at variable potentials and having different levels of spontaneous activity, all intrinsic excitability studies were performed on cells hyperpolarized to the same level *via* hyperpolarizing current. Neurons were initially depolarized with a brief high amplitude current injection to evoke a single AP followed by a series of 1-second-long depolarizing steps of increasing amplitude to study repetitive AP firing.

Voltage clamp recordings were performed to assess the presence of sodium and potassium conductances as well as spontaneous synaptic activity. Briefly, to record Na^+ and K^+ currents neurons were held at −60 mV and received a series of 200 ms long voltage steps from −100 to +90 mV. Spontaneous excitatory postsynaptic currents (PSCs) were recorded in a gap-free mode for 3 min at holding potential set at −60 mV.

Germline Mouse KO

An exon 9–13 deletion (6200 bp) homologous to the human PS locus (7304 bp deletion spanning exons 9–13) was engineered into C57/Bl6N mice with a *Neo* cassette and two *LoxP* sites (**Supplementary Figure S1**). Heterozygous (+/−) and homozygous (−/−) animals were bred in combination, but perinatal lethality was noted in litters following both breeding approaches; we did not generate enough viable *Strada*−/− pups for *Strada*−/− matings. Germline Strada KO (*Strada*) was confirmed by Southern blot (**Supplementary Figure S2**). Litters were monitored for behavioral abnormalities (movement, suckling, seizures) from P0-P30 by direct observation and continuous 12-h video-monitoring. Body masses (grams) were obtained for all live pups at select post-natal dates. Wildtype, *Strada*+/− and *Strada*−/− animals were sacrificed *via* ice anesthesia and intracardial perfusion (P0–P20) or by CO_2 asphyxiation followed by intracardial perfusion (P21+) with PBS. Brain specimens were fixed in 4% PFA, paraffin-embedded, and sectioned at 10 microns. The sections were probed with antibodies targeting P-S6. Slides were counterstained with DAPI and imaged on a fluorescent microscope. All animal experiments were approved by the Institutional Animal Care and Use Committee of the University of Pennsylvania School of Medicine, Temple University, Philadelphia, PA, and the University of Maryland School of Medicine, Baltimore, MD, USA (where the studies were performed).

RESULTS

Enhanced mTOR Signaling

CRISPR KO of *Strada* in mouse N2a cells resulted in enhanced S6 phosphorylation compared with wildtype N2a cells (**Figure 1**) as previously demonstrated following the shRNA knockdown of *Strada* in mouse neural progenitor cells *in vitro* and *in vivo* (Orlova et al., 2010; Parker et al., 2013). As in these previous studies, there was no change in non-phosphorylated S6 levels (data not shown) following *Strada* CRISPR editing.

iPSCs and Derived Neurons

Patient 1: fibroblasts were obtained from a 4-year-old child with PS who was non-verbal and suffered from recurrent seizures. Germline *STRADA* mutation was confirmed by Sanger sequencing. Patient 2: fibroblasts were obtained from a 3-year-old child with genotype-confirmed PS, with intractable seizures and severe intellectual disability. Fibroblasts from two separate healthy 1-year-old individuals as well as commercially available foreskin fibroblasts (GlobalStem) were used to generate control iPSCs. Fibroblasts were reprogrammed to iPSCs by retroviral transduction or episomally with plasmid electroporation of OCT3/4, KLF4, SOX2, and c-MYC (see "Materials and Methods" section). Two iPSC clones were expanded from each of the patients' fibroblasts and 2–3 from each control. All clones showed immunoreactivity for the pluripotency markers OCT3/4, SSEA4, NANOG and SOX2 (**Figures 2A–D**, and data not shown). The ability of the clones to differentiate into all three germ layer derivatives was tested with an embryoid body assay. All iPSCs were differentiated into cells expressing either

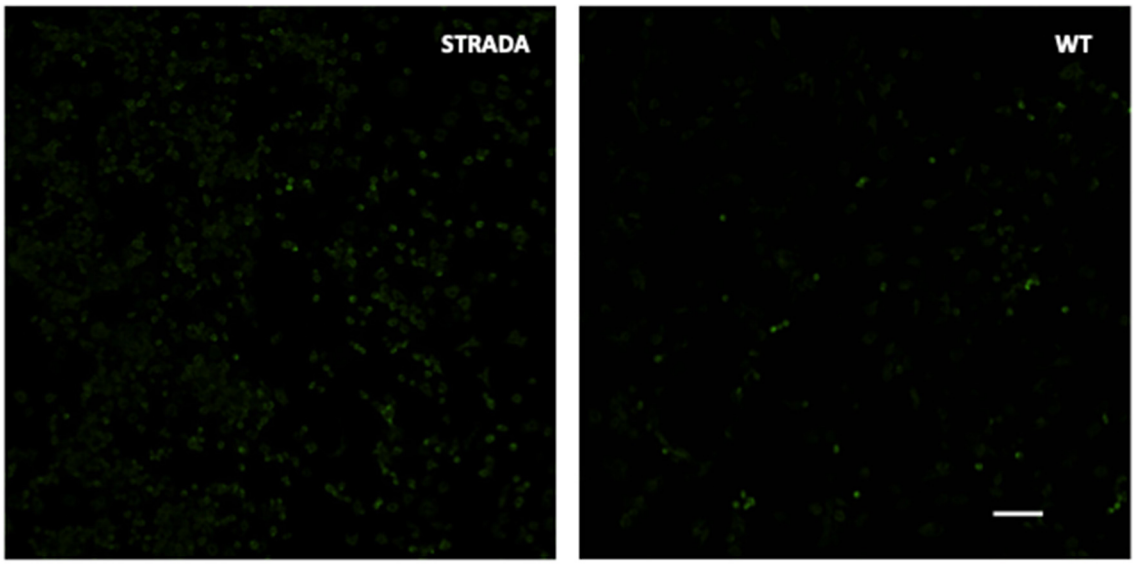

FIGURE 1 | Immunocytochemistry showing enhanced phosphorylation of ribosomal S6 protein in CRISPR-edited *Strada* N2a cells vs. wildtype (WT) cells. Scale bar, 250 microns.

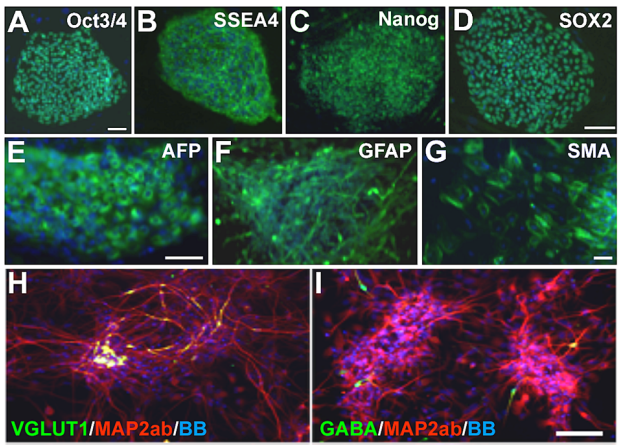

FIGURE 2 | Pretzel Syndrome (PS) induced pluripotent stem cell (iPSC) pluripotency and neuronal differentiation. **(A–D)** iPSCs obtained from reprogramming PS fibroblasts were immunostained for the pluripotency markers (in green) OCT3/4 **(A)**, SSEA4 **(B)**, NANOG **(C)** and SOX2 **(D)**. **(E–G)** Embryoid bodies differentiated from PS iPSCs contained cells from all three germinal layers (green): AFP (**E**; endoderm), GFAP (**F**; ectoderm) and SMA (**G**; mesoderm). **(H,I)** Neuronal differentiation of PS iPSCs yields mostly microtubule-associated protein 2ab (MAP2ab)/vesicular glutamate transporter type 1 (VGLUT1) double-labeled **(H)** or MAP2ab-positive and gamma-aminobutyric acid-negative **(I)** mature excitatory and rare GABA+ inhibitory cortical-like neurons. Bisbenzimide nuclear stain is in blue in all panels. Scale bars: 100 μm in **(A)** for **(A–C)** and **(G)**; 75 μm in **(D)**, in **(E)** for **(E,F)**, and in **(I)** for **(H,I)**.

α-fetoprotein (endoderm), smooth muscle actin (mesoderm) and βIII-tubulin or glial fibrillary acidic protein (GFAP; ectoderm; **Figures 2E–G** and data not shown), confirming pluripotency. The karyotype of all cell lines was normal (data not shown).

Neuronal Differentiation

iPSCs were differentiated into a neuroepithelial monolayer using dual SMAD inhibitors. Neuroepithelial cells were mechanically disrupted and passaged in a culture medium containing Neurobasal, DMEM/F12, N2, B27, and insulin to generate neural rosettes, and then differentiated into neurons. The resulting neuronal cultures contained a mixture of neural progenitors, mature and immature neurons, and astrocytes (data not shown). After 3–5 weeks of differentiation, patient and control cultures contained both glutamatergic and GABAergic neurons, with a predominance of the former (**Figures 2H,I**) as expected with the dual SMAD inhibitor differentiation protocol we used.

STRADA Deletion and Loss of *STRADA* Expression

We used PCR and Western blot to confirm the expected deletion in the *STRADA* gene and loss of protein expression in cells from PS individuals targeted PCR using primers spanning *STRADA* exons 9–11 failed to generate an amplicon from the PS fibroblasts thus confirming the deletion of exons 9–13 that is common to all Mennonite PS individuals, whereas STRADA amplicons were generated from control fibroblasts (**Figure 3C**). Amplicons for each primer set were also generated from control lymphoblasts and post-mortem control brain tissue (data not shown). Western assay did not detect STRADA protein in PS iPSCs or neurons but did detect STRADA protein in control neurons (**Figure 3D**). These data confirm the exon 9–13 deletion in the PS patient fibroblasts that were used to derive our iPSCs, and the loss of STRADA protein expression in iPSCs and derived neurons.

mTOR Activation and Cytomegaly

To assay for increased mTOR activation in PS iPSCs and neurons, we measured ribosomal S6 protein phosphorylation

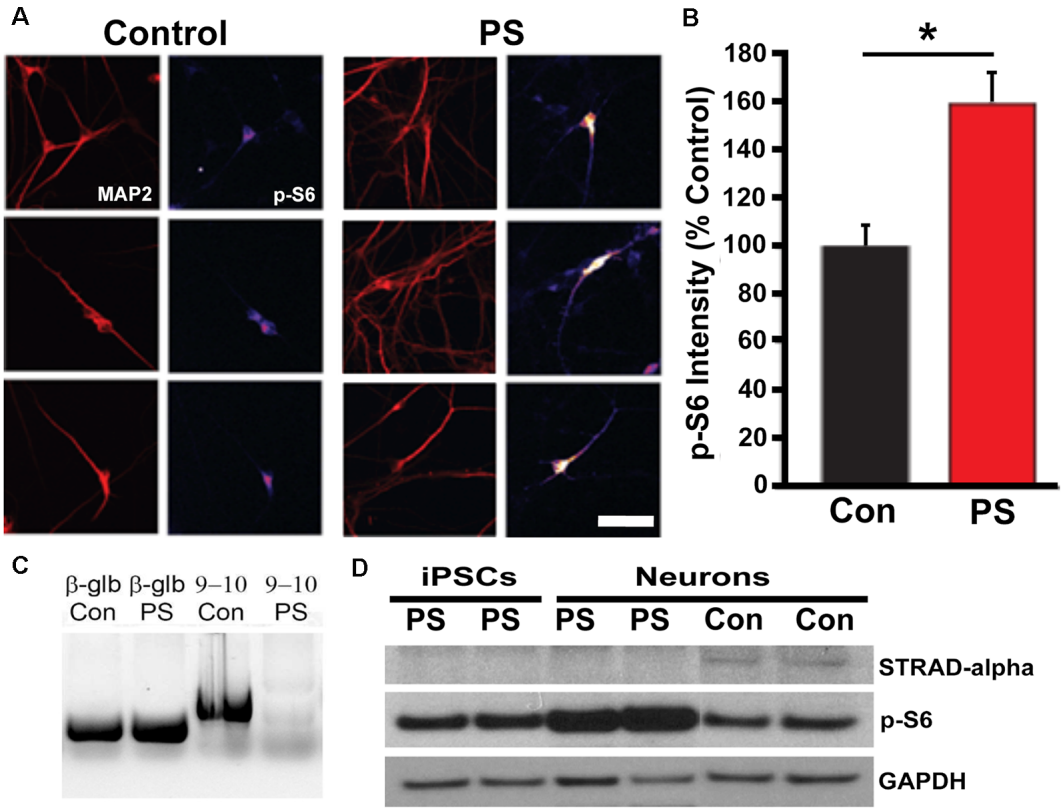

FIGURE 3 | STRADA and phosphorylated ribosomal-S6 (p-S6) expression in iPSC-derived control and PS neurons. **(A)** Immunocytochemistry for p-S6 of control vs. PS iPSC-derived neurons immunolabeled for p-S6 and MAP2abc. P-S6 signal is displayed as an intensity map (fire, NIH ImageJ), Scale bar = 40 um. **(B)** Mean p-S6 immunocytochemical signal intensity of control- vs. PS-derived MAP2+ neurons. The bar graph represents mean ± SD, with values normalized to the mean of the control samples. *$p < 0.05$ (*t*-test). **(C)** Targeted PCR using primers spanning *STRADA* exons 9–10. Lane 1, beta-globin (β-glb) detected in control (Con) individual fibroblast DNA (250 bp product); Lane 2, β-glb detected in PS fibroblast DNA; Lane 3, detection of STRADA exons 9–10 in control fibroblast genomic DNA (598 bp product); Lane 4, absence of STRADA exons 9–10 in PMSE fibroblast genomic DNA. **(D)** Western blot for: (1) STRADA protein (top row) showing absent expression in iPSCs and neurons derived from PS fibroblasts compared with control derived neurons (Con); (2) p-S6 protein (middle row) displaying increased p-S6 in PS neurons compared to PS iPSCs and control neurons; and (3) GAPDH loading control (bottom row).

(S235/236). We found increased phosphorylation of S6 in PS-derived neurons compared with control cells by both Western blot ($p = 0.02$) and ICC ($p < 0.05$; **Figures 3A,B,D**). There was no change in non-phosphorylated S6 levels (data not shown). These results indicate that the effects of STRADA deletion on mTOR signaling in our derived neurons are similar to those seen in animal models of PS, as well as human PS brain specimens and fibroblast cultures.

mTOR hyperactivity is associated with cytomegaly and cell size is enhanced in human PS brains (Puffenberger et al., 2007). To examine whether PS patient-derived cells exhibit cytomegaly, we measured soma sizes of PS and control iPSC-derived immature and mature neurons. Immature neurons were immunolabeled with either DCX or neuron-specific-βIII-tubulin (TUBB3; TuJ1 clone). We found significantly increased soma area in neurons derived from two PS patient 1 clones (PS 1a and 1b) compared to two different human control iPSC-derived neurons (**Figures 4A,B**). Mature PS iPSC-derived neurons immunolabeled for MAP2ab also exhibited significantly greater soma area compared to controls (**Figure 4C**); the differences appeared greatest in the mature neurons (note different scale bars between A/B and C in **Figure 4**). We also reproduced these results using iPSCs from PS subject #2 and an additional control iPSC line. Two neuronal differentiations were labeled with DCX, and four differentiations with TUBB3 and MAP2ab. With each differentiation, the sizes were normalized to the mean control soma size to control for batch variation. We again found increased soma size in the PS cells (**Figures 4D–F**). Taken together with the data above, these findings demonstrate that loss of *STRADA* in PS patient-derived neurons leads to cytomegaly as seen following *Strada* KD (Orlova et al., 2010) or *Strada* KO *via* CRISPR (**Figure 1**).

PS Neurons Show a Subtle Electrophysiological Phenotype

We next investigated whether *STRADA* deletion alters neuronal excitability in a manner that might explain the severe seizure phenotype seen among PS patients. We performed whole-cell patch-clamp recordings on patient and control iPSC-derived neurons to address this question. Analysis of passive neuronal

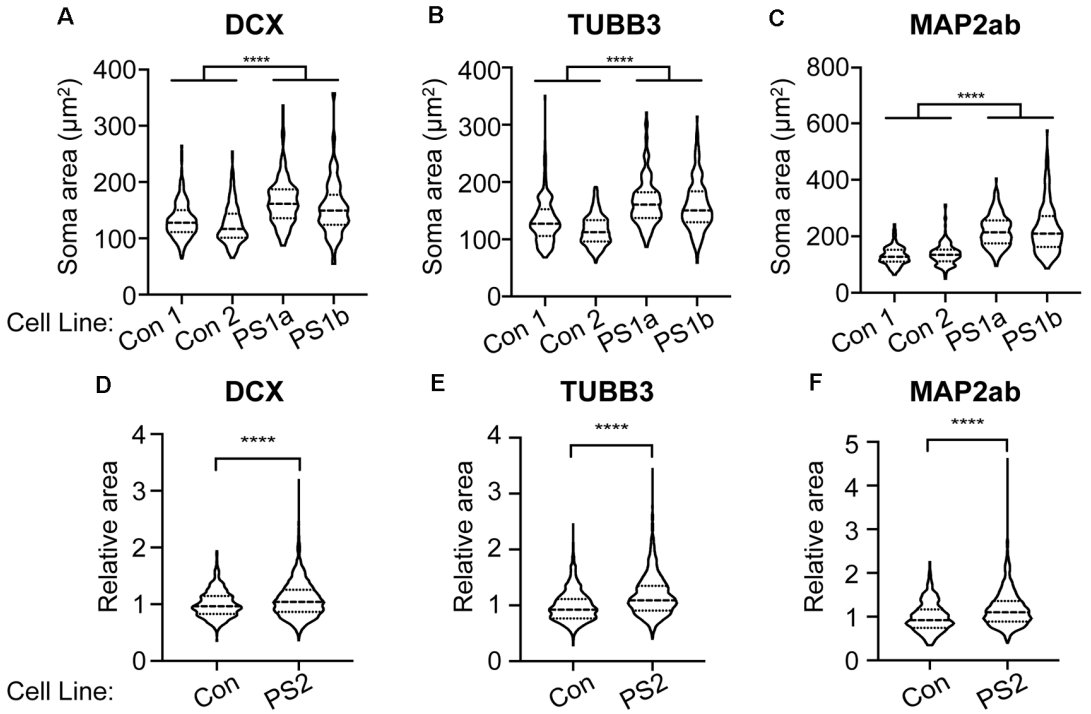

FIGURE 4 | PS iPSC-derived neurons have larger soma compared to control neurons. Soma size was measured for each experimental group using markers for immature (DCX, TUBB3) and mature (MAP2ab) neurons. Violin plots with quartiles are displayed. **(A–C)** Two control cell lines (Con) and two cell lines from PS subject 1 were quantified from two independent neuronal differentiations, and the data for each genotype were combined. **(A)** Neurons labeled for DCX. Con n = 432 PS 1: n = 438. **(B)** Neurons labeled for TUBB3. Con: n = 426, PS 1: n = 431. **(C)** Neurons labeled for MAP2ab. Con: n = 433, PS 1: n = 434. **(D–F)** Neuronal differentiations were repeated using a separate control cell line (Con) and one cell line from PS subject 2 (PS 2). For each differentiation, soma size was normalized to the control neurons to account for batch to batch variation. Two independent neuronal differentiations were quantitated for DCX **(D)** and four independent differentiations were quantitated for TUBB3 **(E)** and MAP2ab **(F)**. **(D)** Neurons labeled for DCX. Con: n = 563, PS 2: n = 1,711. **(E)** Neurons labeled for TUBB3. Con: n = 866, PS 2: n = 2,430. **(F)** Neurons labeled for MAP2ab. Con: n = 430, PS 2: n = 1,944. Statistical analysis was performed using an unpaired Student's t-test with Welch's correction. ****$p < 0.0001$.

properties from the two PS subjects and two controls showed that PS patient-derived neurons have increased input resistance and a more depolarized resting membrane potential when compared to controls (**Figures 5A,B**). Additionally, the majority of both control and patient neurons fired spontaneously *in vitro* (**Figure 5C**), although there were no statistically significant differences in tonic firing (**Figures 5D,E**). We next examined different characteristics of evoked firing including the ability of neurons to fire repetitive APs, excitability, AP threshold and maximum firing rate (**Figures 5F–H**). PS patient-derived neurons showed a statistically significantly decreased threshold for initial AP generation (**Figure 5J**), consistent with their increased input resistance and depolarized resting membrane potential. No significant differences were seen between PS and control neurons for the other measures of evoked AP firing (**Figures 5H,I,K**).

Voltage clamp experiments to study sodium and potassium conductances revealed no differences in currents between the PS patient and control neurons (**Figures 6A–D**). Interestingly, we did find a difference in spontaneous synaptic activity, with PS patient-derived cells displaying a much lower prevalence of spontaneous postsynaptic currents (sPSCs) than control cells, suggesting a delayed or altered network connectivity formation (**Figures 6E,F**). Neurons that did exhibit spontaneous synaptic activity did not differ between the two experimental groups in terms of sPSC frequency or amplitude (**Figures 6G,H**). Together, these findings indicate that PS neurons have an electrophysiological phenotype consistent with increased intrinsic excitability and decreased synaptic activity, both of which may relate to delayed neuronal maturation.

Strada KO Mouse

Previous work has shown that germline *Strada* KO is associated with a perinatal lethal phenotype with death occurring by post-natal (P) day 2 (Veleva-Rotse et al., 2014). Our C57/Bl6N *Strada*−/− strain (del exon 9–13) showed reduced survival of *Strada*−/− pups within the first five post-natal days and thus out of more than 100 litters yielding both WT and heterozygous pups, only eight *Strada*−/− animals from eight distinct litters (five females, three males) survived past P5, four into adulthood; multiple *Strada*−/− mice were never found in the same litter. The oldest living *Strada*−/− mouse in our colony is 10 months old. All heterozygous (*Strada*+/−) mice were identical in appearance and behavior to wildtype animals

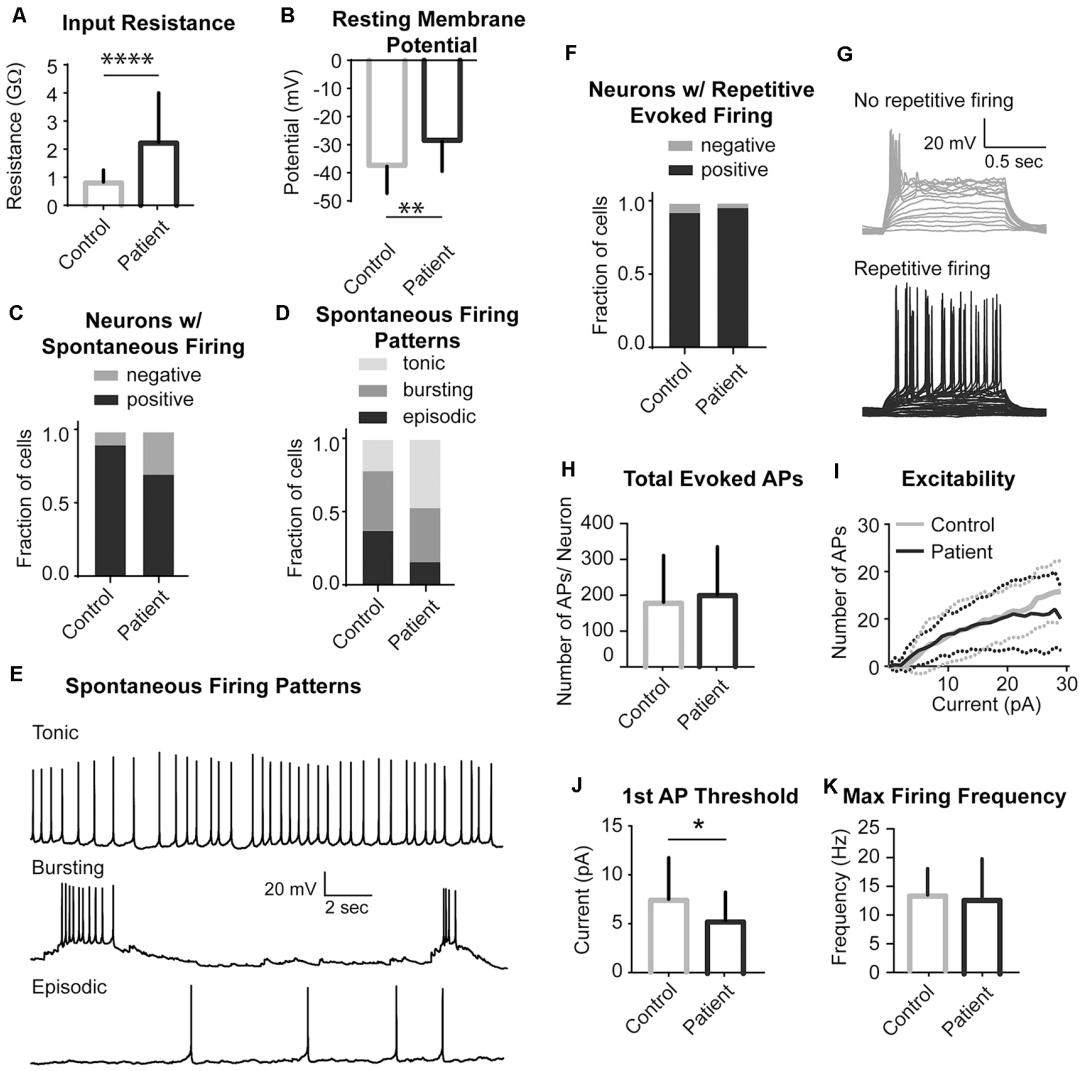

FIGURE 5 | Electrophysiological properties of PS patients and control neurons. **(A)** Summary data of Input Resistance, data represented as Mean ± SEM; sample sizes: Control (gray bar) $n = 31$, Patient (black bar) $n = 27$; Unpaired Student's t-test, ****$p < 0.0001$. **(B)** Summary data of Resting Membrane Potential, data represented as Mean ± SEM; sample sizes: Control (gray bar) $n = 31$, Patient (black bar) $n = 27$; Unpaired Student's t-test, **$p = 0.0016$. **(C)** The fraction of neurons firing spontaneously at −40 mV, data represented as a fraction of the total cell number; black bar- neurons with spontaneous firing, gray bars- neurons with no spontaneous firing; sample sizes: Control $n = 31$, Patient $n = 27$; Fisher's exact test, $p = 0.0913$ (n.s.). **(D)** Distribution of the pattern of spontaneous firing represented as fraction of total of all cells with spontaneous firing; sample sizes: Control = 28, Patient = 19; Chi-square test $\chi = 3.987$, df = 2, $p = 0.1362$ (n.s.). **(E)** Example recordings of three different spontaneous firing patterns: Tonic, Bursting and Episodic. **(F)** A fraction of neurons firing repetitive evoked action potentials (APs), data represented as a fraction of the total cell number; black bar- neurons with repetitive firing, gray bar- neurons with no repetitive firing; sample sizes: control $n = 28$, Patient $n = 26$; Fisher's exact test, $p > 0.999$ (n.s.). **(G)** Example recordings of a series of depolarizing current injections to a neuron demonstrating no repetitive firing (top gray traces) and a neuron firing repetitively (bottom black traces). **(H)** Summary data of the Total Evoked APs, data represented as Mean ± SEM; sample sizes: Control (gray bar) $n = 27$, Patient (black bar) $n = 22$; Unpaired Student's t-test, $p = 0.5634$ (n.s). **(I)** Input-Output curves characterizing excitability of neurons derived from control and mutant neurons, data represented as the mean number of APs (Y-axis) evoked with a given current injection (X-axis); sample sizes: Control (solid gray line) $n = 27$, Patient (solid black line) $n = 22$, dotted lines represent the range of SEM for each experimental group; multiple t-tests for each current step, adjusted p values n.s. **(J)** Firing threshold represented as minimum current required to evoke action potential (AP) firing, data represented as Mean ± SEM; sample sizes: Control (gray bar) $n = 26$, Patient (black bar) $n = 22$; Unpaired Student's t-test, *$p = 0.0468$. **(K)** Maximum Evoked Firing Frequency, data represented as Mean ± SEM; sample sizes: Control (gray bar) $n = 26$, Patient (black bar) $n = 22$; Unpaired Student's t-test, $p = 0.8784$ (n.s.). For all recordings, no differences were found between the two patient lines and they were pooled.

with no obvious behavioral or motor phenotype and clinical seizures were not observed in either *Strada* +/− or *Strada* −/− mice. Of note, *Strada* +/− females had either litters that were smaller than WT (<3 pups) or no litters at all, despite constant breeding. Indeed, despite heterozygous/heterozygous and heterozygous/homozygous mating attempts (we did not generate enough viable *Strada*−/− adults for matings), *Strada*−/− pups were very infrequently found.

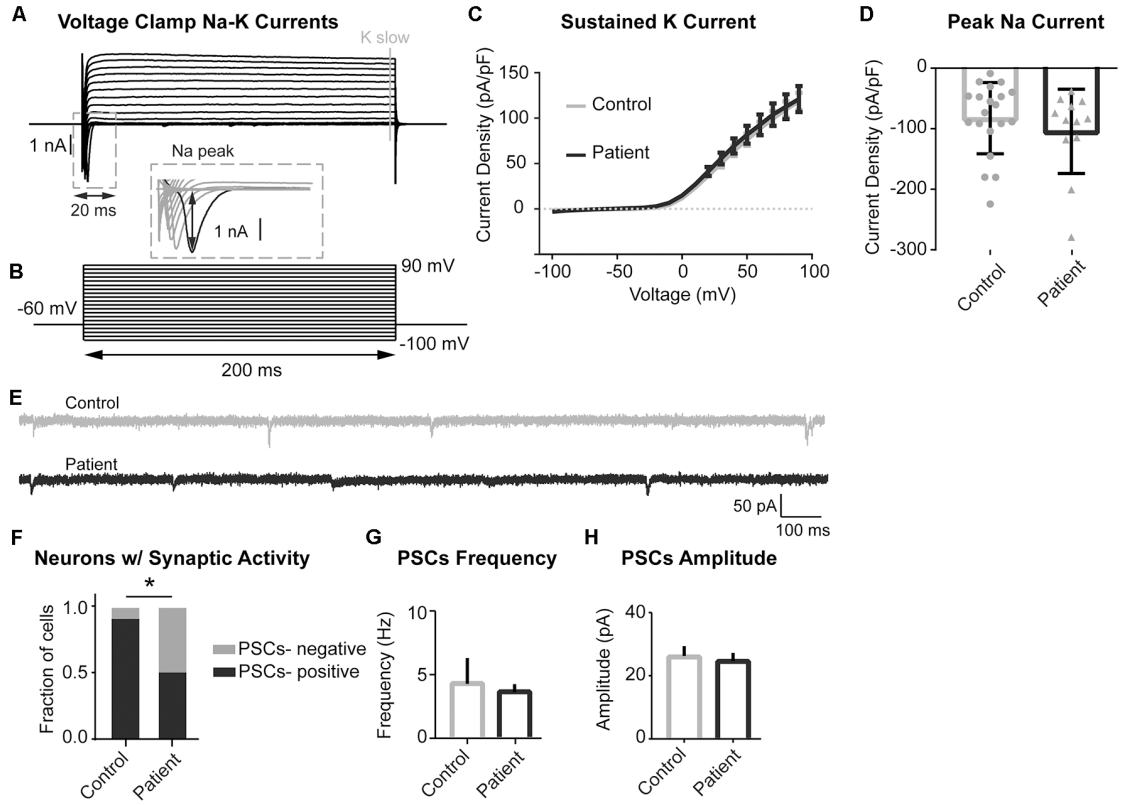

FIGURE 6 | Sodium and Potassium conductances and synaptic activity in control and mutant neurons. (**A,B**) Example recording **(A)** and voltage-clamp protocol **(B)** used to evoke voltage-gated sodium and potassium conductances. **(A)** Series of the voltage clamp traces recorded from the control neuron. Inward fast currents, expanded in the inset window, demonstrate the presence of the sodium conductances. Peak Na current is labeled with black arrowheads. Outward slow conductances measured at the end of the voltage step (labeled with gray solid line) represent slow potassium currents. **(B)** Series of 200 ms voltage steps from −100 to +90 mV at 10 mV intervals, holding potential between steps is −60 mV. **(C)** Summary data of slow potassium conductances represented as Mean ± SEM current density (Y-axis) in function of voltage (X-axis); sample sizes: Control (solid gray line) $n = 20$, Patient 2 (solid black line) $n = 12$; multiple t-tests for each current step, adjusted p values n.s. **(D)** Summary data of peak sodium currents represented as Mean ± SEM current density; sample sizes: Control (gray bar) $n = 20$, Patient 2 (black bar) $n = 12$; Unpaired Student's t-test, $F = 0.7385$, $p = 0.3526$ (n.s). **(E)** Example traces of recordings of spontaneous postsynaptic currents (PSCs) acquired in voltage-clamp mode with the membrane clamped at −60 mV. Control—gray, Patient 2–black. **(F)** Summary data of the proportion of neurons demonstrating spontaneous synaptic activity, data represented as a fraction of recorded cells with (black) and without (gray) detected PSCs; sample sizes: Control $n = 19$, Patient 2 $n = 12$; Fisher's exact test, df = 2, $^*p = 0.0316$. **(G)** Summary data of PSCs Frequency (only PSCs-positive cells), data represented as Mean ± SEM; sample sizes: Control (gray bar) $n = 17$, Patient 2 (black bar) $n = 6$; Mann–Whitney test, exact $p = 0.5069$ (n.s.). **(H)** Summary data of PSCs Amplitude (only PSCs-positive cells), data represented as Mean ± SEM; sample sizes: Control (gray bar) $n = 17$, Patient 2 (black bar) $n = 6$; Mann–Whitney test, $p = 0.2863$ (n.s.).

Overall observation of all *Strada*−/− mice revealed reduced body size compared to either *Strada*+/− or wildtype littermates. All *Strada*−/− animals had a dysmorphic skull structure with a domed appearance and malocclusion incisor teeth (**Figure 7**). The large incisors and malocclusion were seen in all eight *Strada*−/− mice and interfered with successful feeding. Veterinary medicine staff removed the incisors to facilitate feeding. *Strada*−/− mice were hypotonic with limited mobility in the cage, and when attempting to ambulate they exhibited marked tremor. Under direct observation, the pups had clear difficulties initiating and maintaining suckling in comparison with *Strada*+/− pups. All *Strada*−/− mice had properly formed anterior cruciate ligaments (ACL), unlike some PS patients who have congenital absence of the ACL (data not shown; Puffenberger et al., 2007).

Neuropathological analysis of *Strada*−/− mice ($n = 5$; ages P2–P20) demonstrated that the brains were enlarged with ventriculomegaly, but there was a normal gross structure of the hemispheres (**Figure 8**). Given our small *Strada*−/− sample size, differences in brain weights between *Strada*−/−, heterozygous, and WT animals could not be determined. There were enhanced numbers of cells immunoreactive for P-S6 (Ser 240/244) found in late embryogenesis (embryonic day 18.5; **Figure 9A**) that were also seen throughout all cortical layers, the thalamus, and hippocampus in the *Strada*−/− mice compared with *Strada*+/− and WT mice at P9 (**Figure 9B**). At P0, more Cux1 positive late-born neurons are found in the deeper layer or intermediate zone, suggesting that there may be abnormal migration of late-born neurons (**Figure 9C**). Consistently, displaced ectopic Cux1 positive neurons within the deeper layer or subcortical

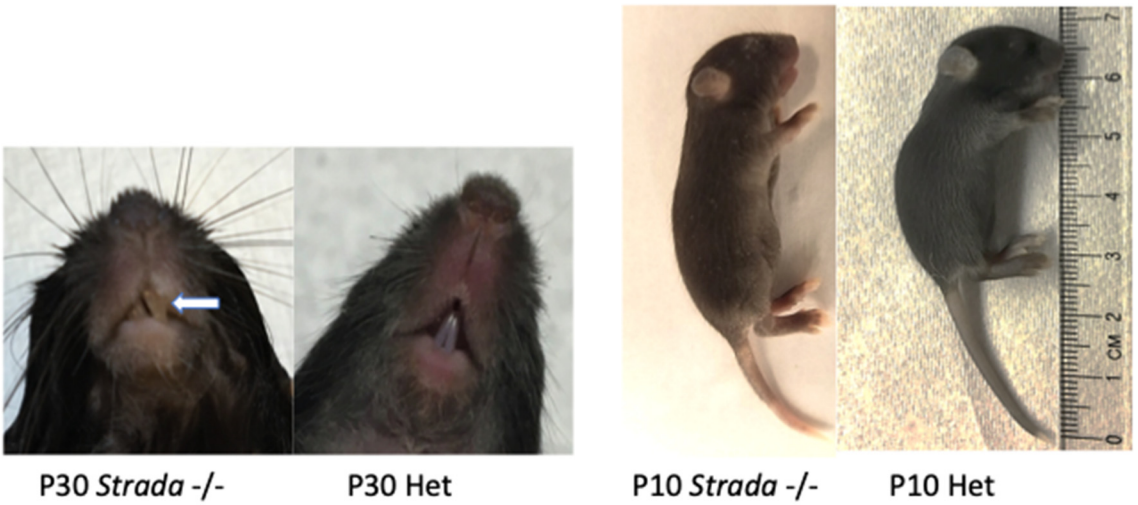

FIGURE 7 | Effects of Strada loss on development. *Strada*−/− animals had a dysmorphic skull structure with domed appearance and maloccluded incisor teeth (arrow). The animal body size was consistently smaller than either WT or heterozygous mice (Het).

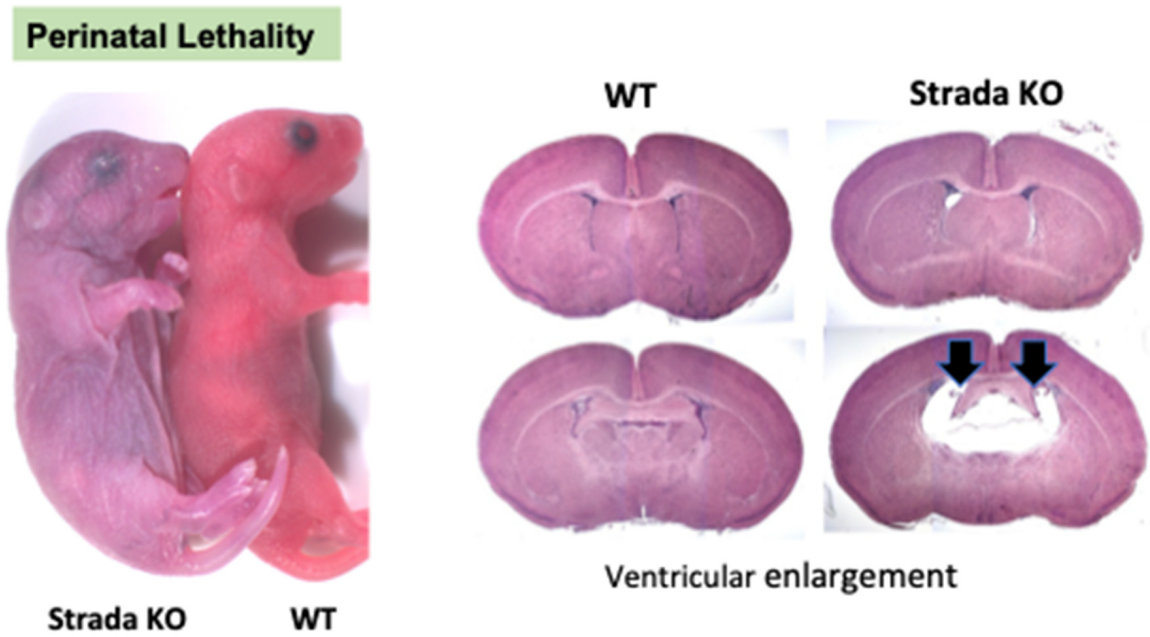

FIGURE 8 | Perinatal lethality in *Strada* −/− mice. Left, a comparison of *Strada*−/− to wildtype (WT) mouse pup. Right, evidence of ventricular enlargement (arrows) in P10 *Strada*−/− mice.

white matter were observed in *Strada*−/− brains analyzed at P9 as compared to littermate control WT (**Figure 9D**). These mirrored observations in human PS brain tissue (Puffenberger et al., 2007).

DISCUSSION

Using several model systems, we demonstrate that loss of *STRADA* in human iPSC-derived neurons and mature mouse neurons *in vivo* causes activation of mTOR pathway signaling, placing PS squarely as a mTORopathy. *STRADA* loss causes enhanced cell size in all systems studied. We show that germline KO of *Strada* effectively models many of the histological features of human PS with enlarged brain size, ventriculomegaly, and heterotopic neurons in the subcortical white matter. Finally, iPSC-derived neurons from PS patients exhibit subtle electrophysiological abnormalities including increased input resistance, a more depolarized resting

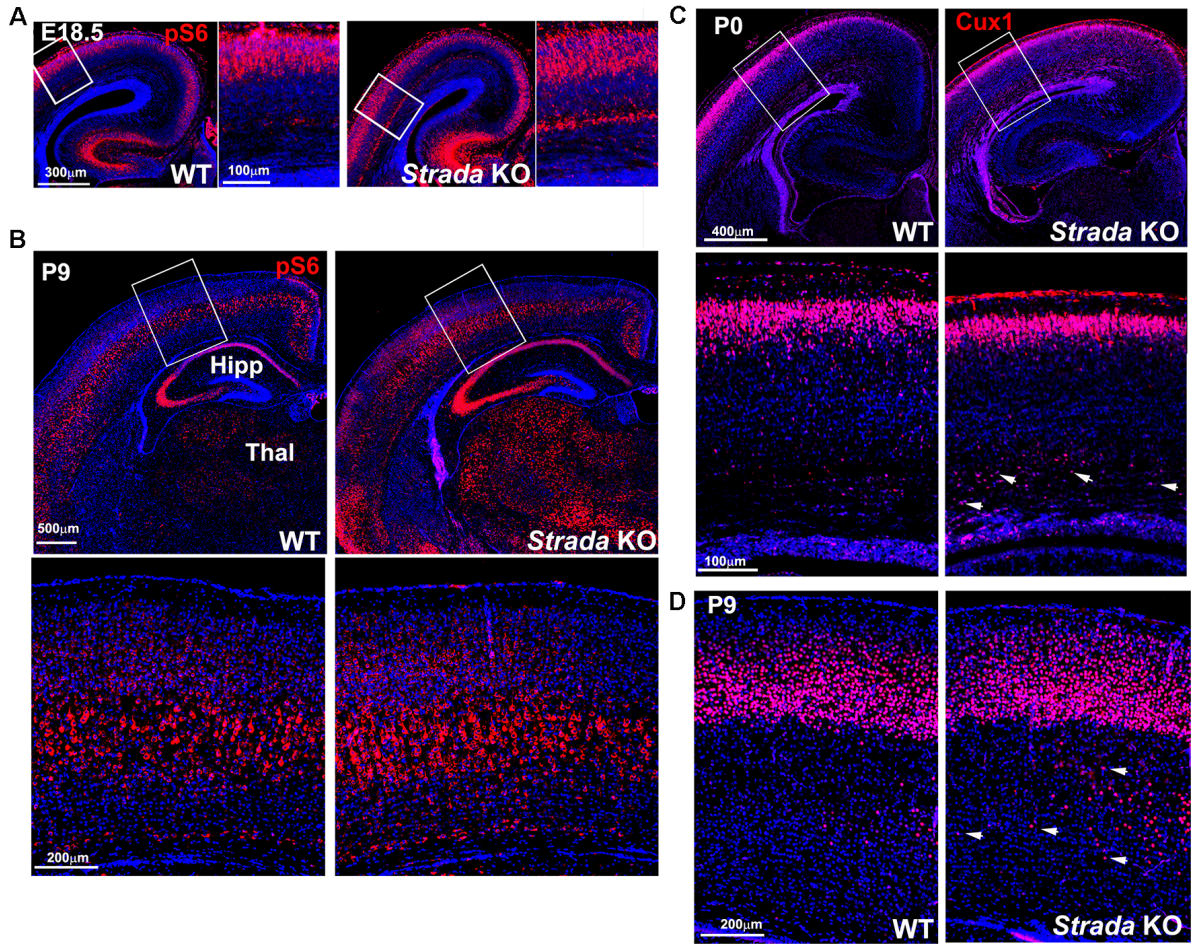

FIGURE 9 | Enhanced ribosomal S6 phosphorylation (P-S6) in *Strada*−/− mice evident at E18.5 **(A)** and P9 **(B)** compared with WT mouse. There is enhanced P-S6 immunoreactivity in the cerebral cortex deep layers, the thalamus (Thal), and the hippocampus (HIPP). Box depicts inset below, which shows P-S6 labeled neurons. **(C)** At P0, more Cux1 labeled late-born neurons (Layer II–IV) are accumulated in the intermediate zone of KO (arrows) compared with WT. **(D)** At P9, more Cux1 positive neurons are found in the deeper layer of the white matter of *Strada* KO (arrows) compared with WT.

membrane potential, and a decreased threshold for initial AP generation.

We show that the PS patient-derived iPSCs and neurons do not express STRADA and exhibit enhanced mTOR activation. These findings are consistent with our previous *in vitro* and *in vivo* mouse models, demonstrating that knockdown of STRADA leads to enhanced mTOR signaling (Orlova et al., 2010; Parker et al., 2013). Thus, these cells provide an attractive *in vitro* system to study mTORopathies. Neurons derived from PS patient iPSCs recapitulate many of the abnormal features observed in fibroblasts, lymphocytes, and fixed brain tissue from PS patients (Orlova et al., 2010; Parker et al., 2013). These iPSC and neuronal lines join a small list of lines generated from patients with a mTORopathy, including TSC and individuals with focal cortical dysplasia linked to *DEPDC5* mutations (Blair et al., 2018; Winden et al., 2019). Providing *in vitro* models of human mTORpathies is a major challenge because of the mutational mechanisms causing these disorders. Thus, an important feature of our cells is that we can generate neurons with a causative gene deletion from fibroblasts. Our PS iPSCs and neurons are unique as other identified mTORopathies result from heterozygous mutations that require the subsequent loss of heterozygosity *via* a "second hit" somatic mutations; the PS subject-derived neurons with homozygous *STRADA* loss-of-function deletions provide a unique window into mTOR activation in a homogeneous genomic background. In our studies, iPSC-derived neurons lacking STRADA show cytomegaly, likely related to mTOR hyperactivation (Orlova et al., 2010), but do not have defects in differentiation. A recent study examining hESCs with heterozygous or homozygous *TSC2* loss-of-function generated by zinc-finger nuclease-mediated gene disruption showed that homozygous loss of TSC2 produced cytomegaly as well as increased dendritic complexity (Costa et al., 2016). Thus, while a common manifestation of mTOR hyperactivation is increased cell size, other structural, phenotypic alterations may be unique to each genotype. The current results show that PS derived neurons

reflecting germline STRADA deletion provide a reproducible human cell system to study the effects of loss of STRADA on mTOR signaling.

Strada +/− mice had no phenotype. These observations parallel human heterozygous PS individuals (patient parents) who are neurologically normal (Puffenberger et al., 2007; personal clinical observations, P. Crino). A previously reported germline *Strada* knockout mouse strain exhibited subtle alterations in cortical lamination and changes in axonal outgrowth and exhibited perinatal mortality (Veleva-Rotse et al., 2014). Our *Strada*−/− mice also exhibited early lethality (from yet undefined causes) but a few animals survived to adulthood. These mice show limited mobility, tremor, and enhanced brain size. Spontaneous seizures were not observed but our sample size was too small to assess seizure phenotype. As in human PS brain histopathology, overt malformations of cortical development (MCD) was not observed in the *Strada*−/− mice, however, CUX-1 labeled heterotopic neurons were seen in the subcortical white matter which has been reported in human PS suggesting a migratory defect in the cerebral cortex. STRADA function has been implicated in the establishment of neuronal polarity and cell migration and is necessary for intact Golgi apparatus formation (Parker et al., 2013; Rao et al., 2018).

Our results suggest that STRADA loss slightly increases cell-autonomous excitability, which may contribute to an epileptic phenotype. In contrast, synaptic activity is reduced in PS neurons, consistent with a previous report of *TSC2* deletion in hESCs-derived neurons, which demonstrated decreased synaptic excitability (Costa et al., 2016). Both enhanced intrinsic excitability and a paucity of synaptic activity may reflect delayed maturation of PS-derived neurons. Ongoing research will define whether these findings relate to the severe epilepsy phenotype in PS patients. Another pertinent issue is that interneurons may be required for manifestation of the network hyperexcitability phenotype, and such a phenotype was not reflected in our *in vitro* model which consisted primarily of excitatory cortical-like neurons. Future studies should address these potential limitations by focusing on mixed excitatory and inhibitory populations in 2-D or brain organoid culture systems, the latter of which can be maintained for prolonged periods to promote maturation and also provides a 3-dimensional network architecture. These findings thus provide new and compelling evidence that STRADA loss by itself can confer a hyperexcitability phenotype, although the underlying abnormalities leading to increased spontaneous activity require further investigation. Future studies should focus on the downstream consequences of STRADA loss to uncover epilepsy mechanisms in PS that would likely apply to other mTORopathies and lead to the development of novel therapies.

DATA AVAILABILITY STATEMENT

The raw data supporting the conclusions of this article will be made available by the authors, without undue reservation, to any qualified researcher.

ETHICS STATEMENT

The studies involving human participants were reviewed and approved by University of Pennsylvania Human Subjects Committee. Written informed consent to participate in this study was provided by the participants' legal guardian/next of kin. The animal study was reviewed and approved by University of Pennsylvania Animal Care Committee. The animal study was reviewed and approved by University of Pennsylvania, Temple University, and University of Maryland School of Medicine Institutional Animal Care and Use Committees.

AUTHOR CONTRIBUTIONS

LD, YL, GM, AS, and SV: iPSC derived neurons, westerns, data analysis, and manuscript writing. AB, MB, and PI: generated CRISPR lines/validation, immunocytochemistry, and mouse KO strain work. SK and UK: mouse KO strain work. WP: identified PS patients, procured, maintained and analyzed fibroblasts for iPSCs. KG, FH, GP, and MS: electrophysiology and data analysis. PC and JP: conception of the study and experimental design, data analysis, and manuscript writing. LD, KG, PI, AB, MB, YL, GP, SV, AS, WP, SK, UK, FH, GM, MS, JP, and PC contributed to the manuscript revision, read, and approved the submitted version.

FUNDING

PC was supported by National Institute of Neurological Disorders and Stroke (NINDS) R01NS094596 and R01NS099452. PC and JP were supported by NINDS R21NS087181–01. LD was supported by NINDS K08NS109289 and a Ravitz Advancement Award from the Department of Pediatrics, Michigan Medicine.

SUPPLEMENTARY MATERIAL

The Supplementary Material for this article can be found online at: https://www.frontiersin.org/articles/10.3389/fncel.2020.00122/full#supplementary-material.

FIGURE S1 | Transgenic germline construct for generation of *Strada*$^{-/-}$ mice.

FIGURE S2 | Southern blot confirms that transformed ES cells carry the Strada transgenic construct.

REFERENCES

Asada, N., Sanada, K., and Fukada, Y. (2007). LKB1 regulates neuronal migration and neuronal differentiation in the developing neocortex through centrosomal positioning. *J. Neurosci.* 27, 11769–11775. doi: 10.1523/JNEUROSCI.1938-07.2007

Bardy, C., van den Hurk, M., Eames, T., Marchand, C., Hernandez, R. V., Kellogg, M., et al. (2015). Neuronal medium that supports basic synaptic functions and activity of human neurons *in vitro*. *Proc. Natl. Acad. Sci. U S A* 112, E2725–E2734. doi: 10.1073/pnas.1504393112

Barnes, A. P., Lilley, B. N., Pan, Y. A., Plummer, L. J., Powell, A. W., Raines, A. N., et al. (2007). LKB1 and SAD kinases define a pathway required for the

polarization of cortical neurons. *Cell* 129, 549–563. doi: 10.1016/j.cell.2007.03.025

Bi, W., Blass, I. A., Muzny, D. M., Gibbs, R. A., Eng, C. M., Yang, Y., et al. (2016). Whole exome sequencing identifies the first STRADA point mutation in a patient with polyhydramnios, megalencephaly and symptomatic epilepsy syndrome (PMSE). *Am. J. Med. Genet. A* 170, 2181–2185. doi: 10.1002/ajmg.a.37727

Blair, J. D., Hockmeyer, D., and Bateu, H. S. (2018). Genetically engineered human cortical spheroid models of tuberous sclerosis. *Nat. Med.* 24, 1568–1578. doi: 10.1038/s41591-018-0139-y

Boudeau, J., Baas, A. F., Deak, M., Morrice, N. A., Kieloch, A., Schutkowski, M., et al. (2003). MO25α/β interact with STRADα/β enhancing their ability to bind, activate and localize LKB1 in the cytoplasm. *EMBO J.* 22, 5102–5114. doi: 10.1093/emboj/cdg490

Costa, V., Aigner, S., Vukcevic, M., Sauter, E., Behr, K., Ebeling, M., et al. (2016). mTORC1 inhibition corrects neurodevelopmental and synaptic alterations in a human stem cell model of tuberous sclerosis. *Cell Rep.* 15, 86–95. doi: 10.1016/j.celrep.2016.02.090

Crino, P. B. (2016). The mTOR signalling cascade: paving new roads to cure neurological disease. *Nat. Rev. Neurol.* 12, 379–392. doi: 10.1038/nrneurol.2016.81

Evers, C., Staufner, C., Granzow, M., Paramasivam, N., Hinderhofer, K., Kaufmann, L., et al. (2017). Impact of clinical exomes in neurodevelopmental and neurometabolic disorders. *Mol. Genet. Metab.* 121, 297–307. doi: 10.1016/j.ymgme.2017.06.014

Hawley, S. A., Boudeau, J., Reid, J. L., Mustard, K. J., Udd, L., Makeeka, T. P., et al. (2003). Complexes between the LKB1 tumor suppressor, STRAD α/β and MO25 α/β are upstream kinases in the AMP-activated protein kinase cascade. *J. Biol.* 2:28. doi: 10.1186/1475-4924-2-28

Liu, Y., Lopez-Santiago, L. F., Yuan, Y., Jones, J. M., Zhang, H., O'Malley, H. A., et al. (2013). Dravet syndrome patient-derived neurons suggest a novel epilepsy mechanism. *Ann. Neurol.* 74, 128–139. doi: 10.1002/ana.23897

Narumiya, S., Ishizaki, T., and Uehata, M. (2000). Use and properties of ROCK-specific inhibitor Y-27632. *Methods Enzymol.* 325, 273–284. doi: 10.1016/s0076-6879(00)25449-9

Okita, K., Matsumura, Y., Sato, Y., Okada, A., Morizane, A., Okamoto, S., et al. (2011). A more efficient method to generate integration-free human iPS cells. *Nat. Methods* 8, 409–412. doi: 10.1038/nmeth.1591

Orlova, K. A., Parker, W. E., Heuer, G. G., Tsai, V., Yoon, J., Baybis, M., et al. (2010). STRADA deficiency results in aberrant mTORC1 signaling during corticogenesis. *J. Clin. Invest.* 120, 1591–1602. doi: 10.1172/JCI41592

Parker, W. E., Orlova, K. A., Parker, W. H., Birnbaum, J. F., Krymskaya, V. P., Goncharov, D. A., et al. (2013). Rapamycin prevents seizures after depletion of STRADA in a rare neurodevelopmental disorder. *Sci. Transl. Med.* 5:182ra53. doi: 10.1126/scitranslmed.3005271

Puffenberger, E., Strauss, K. A., Ramsey, K. E., Craig, D. W., Stephan, D. A., Robinson, D. L., et al. (2007). Syndromic cortical dysplasia caused by a homozygous 7 kilobase deletion in LYK5. *Brain* 130, 1929–1941. doi: 10.1093/brain/awm100

Rao, S., Kirschen, G. W., Szczurkowska, J., Di Antonio, A., Wang, J., Ge, S., et al. (2018). Repositioning of somatic golgi apparatus is essential for the dendritic establishment of adult-born hippocampal neurons. *J. Neurosci.* 38, 631–647. doi: 10.1523/JNEUROSCI.1217-17.2017

R Core Team (2014). R: A language and environment for statistical computing. *R Foundation for Statistical Computing*, (Vienna, Austria). Available online at: http://www.R-project.org/.

Shi, Y., Kirwan, P., and Livesey, F. J. (2012). Directed differentiation of human pluripotent stem cells to cerebral cortex neurons and neural networks. *Nat. Protoc.* 7, 1836–1846. doi: 10.1038/nprot.2012.116

Veleva-Rotse, B. O., Smart, J. L., Baas, A. F., Edmonds, B., Zhao, Z. M., Brown, A., et al. (2014). STRAD pseudokinases regulate axogenesis and LKB1 stability. *Neural Dev.* 9:5. doi: 10.1186/1749-8104-9-5

Winden, K. D., Sundberg, M., Yang, C., Wafa, S. M. A., Dwyer, S., Chen, P. F., et al. (2019). Biallelic mutations in TSC2 lead to abnormalities associated with cortical tubers in human iPSC-derived neurons. *J. Neurosci.* 39, 9294–9305. doi: 10.1523/JNEUROSCI.0642-19.2019

Conflict of Interest: The authors declare that the research was conducted in the absence of any commercial or financial relationships that could be construed as a potential conflict of interest.

Advantages of publishing in Frontiers

OPEN ACCESS
Articles are free to read for greatest visibility and readership

FAST PUBLICATION
Around 90 days from submission to decision

HIGH QUALITY PEER-REVIEW
Rigorous, collaborative, and constructive peer-review

TRANSPARENT PEER-REVIEW
Editors and reviewers acknowledged by name on published articles

Frontiers
Avenue du Tribunal-Fédéral 34
1005 Lausanne | Switzerland

Visit us: www.frontiersin.org
Contact us: info@frontiersin.org | +41 21 510 17 00

REPRODUCIBILITY OF RESEARCH
Support open data and methods to enhance research reproducibility

DIGITAL PUBLISHING
Articles designed for optimal readership across devices

FOLLOW US
@frontiersin

IMPACT METRICS
Advanced article metrics track visibility across digital media

EXTENSIVE PROMOTION
Marketing and promotion of impactful research

LOOP RESEARCH NETWORK
Our network increases your article's readership